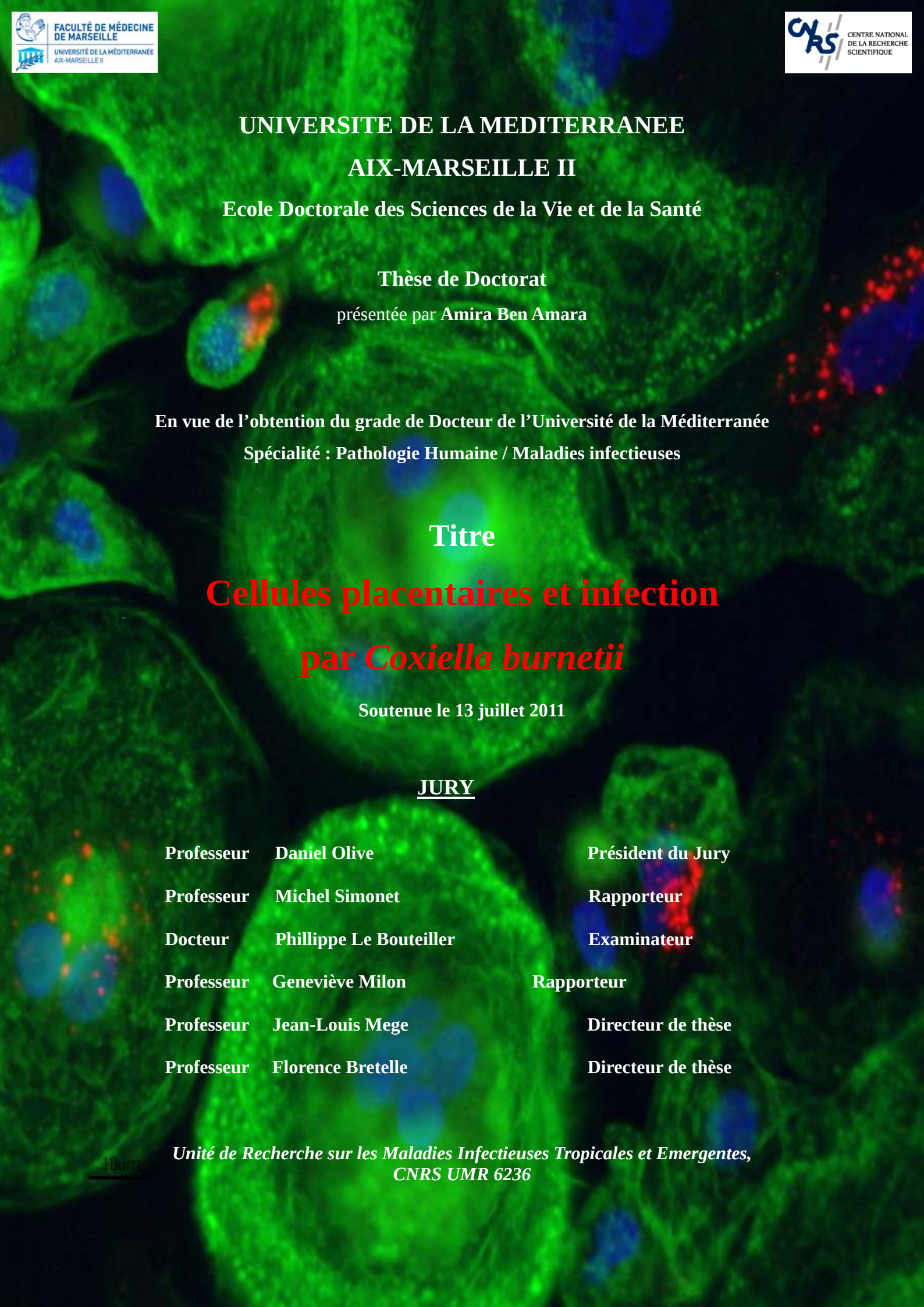

UNIVERSITE DE LA MEDITERRANEE

AIX-MARSEILLE II

Ecole Doctorale des Sciences de la Vie et de la Santé

Thèse de Doctorat

présentée par **Amira Ben Amara**

En vue de l'obtention du grade de Docteur de l'Université de la Méditerranée

Spécialité : Pathologie Humaine / Maladies infectieuses

Titre

Cellules placentaires et infection par *Coxiella burnetii*

Soutenue le 13 juillet 2011

JURY

Professeur	**Daniel Olive**	**Président du Jury**
Professeur	**Michel Simonet**	**Rapporteur**
Docteur	**Phillippe Le Bouteiller**	**Examinateur**
Professeur	**Geneviève Milon**	**Rapporteur**
Professeur	**Jean-Louis Mege**	**Directeur de thèse**
Professeur	**Florence Bretelle**	**Directeur de thèse**

Unité de Recherche sur les Maladies Infectieuses Tropicales et Emergentes, CNRS UMR 6236

Remerciements

Je remercie le Professeur Didier Raoult de m'avoir accueillie au sein de son laboratoire.

Je remercie le Professeur Jean-Louis Mege et le Docteur Eric Ghigo pour m'avoir acceptée au sein de leur équipe.

Je tiens à remercier tout particulièrement le Professeur Jean-Louis Mege pour avoir cru en moi et pour avoir guidé mes pas dans la recherche. Pour tout ce qu'il a fait pour moi en tant que directeur de thèse et également sur le plan personnel.

Je remercie le Docteur Eric Ghigo pour ses encouragements et son soutien « à sa manière ». Pour sa disponibilité en cas de besoin.

Je tiens à remercier spécialement le Docteur Christian Capo pour toutes les leçons de vie qu'il m'a données. Pour tout ce qu'il m'a appris. J'espère que je ne vous ai pas déçu et que « j'ai réussi à combler tous les trous que j'ai trouvés ». J'espère avoir été à la hauteur de vos espérances. Je remercie la vie qui vous a mis sur mon chemin. Je vous remercie pour votre disponibilité et vos conseils et toute l'aide que vous m'avez apportée. Vous avez toujours su trouver les bons mots aux bons moments et enfin j'espère que vous resterez parmi nous le plus longtemps possible. Eh oui comme vous dites j'ai presque appris à penser à moi et je ne veux pas que vous partiez à la retraite tout de suite.

Je remercie Catherine Lépolard et Virginie Trouplin pour leur aide.

Je remercie tous les étudiants de notre équipe passés ou encore présents au laboratoire. Je pense particulièrement à Marie Benoit et la remercie de m'avoir encadrée à mon arrivée au laboratoire, à Yassina qui a toujours été présente en cas de besoin. Merci pour nos longues discussions.

Je tiens à remercier Nico et Laurent d'avoir existé et de m'avoir supportée et je sais que c'est loin d'être un cadeau. Vous avez dû survivre à mes moments de folie, à mes moments de déprime et même à ma grossesse. Bravo et merci les garçons.

Merci à Adbou et à Vikram pour votre aide et je vous souhaite à tous un beau parcours et plein de bons papiers et de jolis post-doc.

Je tiens à remercier Nada qui a vécu avec moi cette thèse et qui a assisté aux plus grands événements de ma vie.

Je remercie Lina pour tous nos cafés matinaux et pour tout l'amour qu'elle me porte.

Enfin, merci à tous les Rickettssiens comprenant les étudiants, les ingénieurs et les secrétaires. Merci à toutes les personnes que j'ai connues durant ces cinq dernières années, vous m'avez tous appris quelque chose à votre manière.

Dernière pensée et pas des moindres au personnel de la maternité de l'Hôpital de la Conception et spécialement à madame Nicole Willigenes, sage-femme cadre, qui a toujours été là pour « booster» son équipe. Merci pour votre implication dans ce projet. Sans votre investissement personnel je n'aurai pas pu accomplir ce travail. Merci pour tous ces beaux placentas.

Je remercie mes parents de m'avoir fait, réussi et surtout soutenue tout au long de mes études. Merci d'avoir cru en moi. Merci d'être là. Je vous dédie cette thèse car je sais que c'est l'une de vos plus grandes fiertés.

Merci à mon mari Zied que Mr Capo a si souvent plaint. Merci d'être à mes côtés. Merci de m'avoir encouragée et soutenue en toute épreuve et bravo pour le courage que tu as pour me supporter. Merci de m'avoir donné cet enfant. Merci à ce dernier d'être bientôt là et j'espère en bonne santé. Quand tu grandiras tu comprendras pourquoi maman s'agitait à ce point. Pardon pour tout le stress que je t'ai fait subir et de t'avoir secoué dans tous les sens. A ta naissance je me rattraperai …

Je dédie ce travail à mon grand-père car c'est grâce à lui que je suis à Marseille. Il a été mon ticket d'entrée. Azizi, j'espère que tu es fier de moi.

SOMMAIRE

AVANT-PROPOS

Je suis partie du constat que l'infection en cours de grossesse par une bactérie intracellulaire telle que *Coxiella burnetii*, l'agent de la fièvre Q, a des conséquences délétères à la fois pour le fœtus et pour la mère. L'infection par *C. burnetii* présente en outre un problème socio-économique non négligeable pour l'élevage dans les pays européens puisqu'elle conduit à des avortements du cheptel bovin, ovin et caprin.
Le placenta est probablement la cible directe de *C. burnetii* puisqu'on trouve en grande quantité ces bactéries dans les produits d'avortement. Différents agents infectieux tel que des virus comme le papillomavirus, des bactéries comme *Listeria monocytogenes* et des parasites comme *Plasmodium falciparum* affectent également le placenta. A ce jour, on ignore tout de leurs cibles cellulaires et des mécanismes moléculaires impliqués dans les infections placentaires.

Nous avons dans un premier temps fait l'hypothèse que les trophoblastes, le constituant majeur du placenta, sont la cible de *C. burnetii*. Comme au début de ma thèse je ne pouvais obtenir des placentas, j'ai utilisé une lignée de trophoblastes humains, la lignée BeWo. J'ai montré d'une part que les cellules BeWo peuvent être infectées par *C. burnetii* et que les bactéries s'y répliquent. Une approche en microarray m'a permis d'élucider un certain nombre de mécanismes moléculaires: *C. burnetii* induit dans ces cellules une réponse inflammatoire atypique qui assure la réplication de la bactérie et conduit à la surexpression des gènes impliqués dans le maintien de la tolérance placentaire.

Il est donc possible que les trophoblastes humains puissent être la cible in situ de *C. burnetii*. Il est probable que les macrophages placentaires soient aussi la cible de *C. burnetii* puisque les monocytes humains et les macrophages dérivés de monocytes sont connus pour être infectés par *C. burnetii*. J'ai réussi à obtenir des placentas à terme et à isoler les trophoblastes et les macrophages sur des critères phénotypiques. Des résultats préliminaires montrent que les trophoblastes sont la cible de *C. burnetii* mais mes efforts ont essentiellement porté sur l'étude de l'infection des macrophages par *C. burnetii*.

Plusieurs problèmes se sont alors posés. Le premier est que les macrophages placentaires sont atypiques au regard de la définition classique des macrophages puisqu'ils expriment CD14, un marqueur des monocytes circulants et qu'ils n'expriment pas CD68, un marqueur classique des macrophages tissulaires. La comparaison entre monocytes circulants, macrophages placentaires et macrophages dérivés de monocytes a alors montré que les macrophages placentaires ont des

caractéristiques différentes de celles des monocytes circulants et des macrophages dérivés de monocytes.

On sait par ailleurs que l'activité microbicide des macrophages dépend de leur microenvironnement. C'est ainsi que des macrophages activés par l'interféron (IFN)-γ deviennent inflammatoires et microbicides à l'encontre de différents agents pathogènes (macrophages M1) et que les mêmes macrophages activés par l'interleukine (IL)-4 perdent leur pouvoir microbicide et deviennent régulateurs de la réponse inflammatoire (macrophages M2). Cette polarisation M1/M2 des macrophages est ainsi bien décrite pour les macrophages humains et murins. Différents arguments phénotypiques et fonctionnels suggèrent que les réponses des monocytes circulants et des macrophages pourraient être différentes. C'est la raison pour laquelle nous avons entrepris une analyse en microarray de la réponse au cours du temps des monocytes humains stimulés par l'IFN-γ ou l'IL-4. On observe effectivement une polarisation de type M1/M2 des monocytes après six heures d'incubation en présence de ces deux agonistes. En revanche, après 18 heures d'incubation, la polarisation M1 et la polarisation M2 sont perdues, ce qui montre que les études physiopathologiques effectuées sur sang total doivent tenir compte de la plasticité temporelle de la réponse monocytaire.

L'exposé bibliographique présente en première partie la fièvre Q. Je consacre la deuxième partie de cet exposé au rôle que pourrait jouer la plasticité des macrophages dans les défenses de l'organisme, la troisième partie à l'infection des macrophages par *C. burnetii* et la quatrième à l'étude du placenta et de l'infection placentaire à *C. burnetii*. Cet exposé s'accompagne d'un chapitre de livre consacré à la fièvre Q et aux réservoirs potentiels de *C. burnetii* qui pourraient expliquer la chronicisation de la fièvre Q chez certains patients.

L'exposé des travaux effectués est divisé en plusieurs parties. La première concerne un article publié en 2010 dans PLoS One et un article soumis qui étudient respectivement la réponse à l'infection par *C. burnetii* des trophoblastes de la lignée BeWo et de la lignée JEG. Le troisième article, en cours de finalisation, montre que les macrophages placentaires ont des propriétés fonctionnelles qui leur sont spécifiques et qu'en particulier ils se différencient spontanément en cellules géantes multinucléées. Le quatrième article qui a été récemment soumis concerne l'étude de la réponse des monocytes à des agonistes de la réponse M1/M2 des macrophages et montre leur plasticité temporelle. Le cinquième article récemment soumis également a porté sur l'établissement de la signature transcriptomique des endocardites infectieuses.

J’ai par ailleurs participé à différents travaux. En particulier, nous avons utilisé la spectrométrie de masse pour l’identification des cellules de mammifères y compris différents types de macrophages, ce qui a donné lieu en 2010 à un article publié dans PLoS One. Cet article est présenté en annexe 1.

EXPOSE

BIBLIOGRAPHIQUE

1. La fièvre Q

1. 1. Description

La fièvre Q est une anthropozoonose contractée par voie aérienne ou digestive. Cette zoonose est soit asymptomatique dans 40% des cas soit se présente dans 60% des cas sous une forme aiguë caractérisée par des symptômes répandus tels que fièvre, hépatite, pneumopathie ou, dans environ 1% des cas, par une méningoencéphalite (Tableau 1). Elle est en règle générale spontanément résolutive (Tableau 2). La fièvre Q aiguë peut évoluer vers un syndrome de fatigue chronique : les patients se plaignent de sueurs, de dyspnée, de troubles de la vision et d'une fatigue anormale (1). La fièvre Q peut également se présenter sous une forme chronique survenant des années après l'épisode aigu ou silencieux et dont la principale manifestation est une endocardite de pronostic sévère (2). La fièvre Q chronique est définie par une évolution clinique de plus de six mois et par la présence d'immunoglobulines (IgG et IgA dirigées contre *C. burnetii* de phase I (3). Sa présentation clinique multiforme fait de la sérologie le principal critère de diagnostic (4). C'est ainsi qu'une fièvre Q chronique a été diagnostiquée lors d'insuffisance rénale chronique, d'hépatomégalie ou de splénomégalie chronique, d'insuffisance cardiaque progressive, de décompensation cardiaque, d'augmentation des transaminases ou d'une thrombocytopénie. Les patients atteints de fièvre Q chronique diffèrent de ceux présentant une forme aiguë de la maladie : âge, conditions prédisposantes, données cliniques et biologiques les distinguent (Tableau 3). L'endocardite représente 70 à 80% de l'ensemble des cas de fièvre Q chronique et, en France, l'endocardite à *C. burnetii* correspond à 5% au moins des endocardites diagnostiquées. Le pronostic des endocardites de la fièvre Q s'est beaucoup modifié ces dernières années. En absence de traitement, le taux de mortalité peut excéder les deux tiers. Dans une étude effectuée en 1987, le taux de mortalité était de 37%. Ces dernières années, il est passé en dessous de 5% grâce à un diagnostic plus précoce, à un traitement prolongé et plus efficace et à un suivi plus attentif (5).

La grossesse constitue une situation clinique particulière. Lorsque la fièvre Q est contractée durant la grossesse, elle conduit dans la majorité des cas à une mort fœtale (48%) et/ou à une prématurité (29%). La plupart des femmes enceintes infectées présentent une fièvre pouvant être associée à un syndrome pseudo-grippal, une thrombopénie sévère ou une pneumopathie atypique. Elle peut aussi être asymptomatique (6). Environ la moitié de ces patientes présentant un profil sérologique

Tableau 1. Principaux symptômes des patients atteints de fièvre Q (d'après 2)

Manifestations cliniques	Pourcentage des cas
Infection primaire	
Asymptomatique	60
Aiguë, spontanément résolutive	38
Aiguë, patients hospitalisés	2
Aiguë, durant la grossesse	<0.5
Infection chronique	
Endocardite	78
Valvulopathie	9
Infection chronique après grossesse	5
Autres	8

Tableau 2 : Principaux signes cliniques et biologiques rencontrés dans la fièvre Q (d'après ref 2)

Clinique	Aiguë (%)	Chronique (%)
Prédisposition		
Moyenne d'âge	45 ans	57 ans
Sexe masculin	71	76
Prédisposition cardiovasculaire	ND	99
Prothèse vasculaire	ND	53
Signes cliniques		
Fièvre	91	68
Céphalées	51	ND
Pneumonie	27	ND
Insuffisance cardiaque	1	67
Méningite	1	Rare
Hépatomégalie	ND	5-56
Splénomégalie	ND	5-55
Hippocratisme digital	ND	10-37
Eruption	11	19
Eruption purpurique	ND	19
Embolie artérielle	ND	21

ND : non déterminé

d'infection chronique, la grossesse doit être considérée comme un facteur favorisant la chronicisation de la maladie (3).

Des facteurs relevant de 1'hôte tels que l'âge et le sexe semblent impliqués dans le déclenchement et le maintien de la fièvre Q. En effet, les enfants âgés de moins de 14 ans constituent 20% des sujets qui présentent des anticorps anti-*C. burnetii* mais seulement 5% des patients symptomatiques. Ils présentent en outre une expression clinique de la maladie très atténuée. La fièvre Q est plus fréquente dans la population active de 30 à 60 ans que dans les autres tranches d'âge (3). Dans un modèle expérimental d'infection à *C. burnetii*, il a été montré par notre groupe que les souris âgées de 14 mois présentent une infection splénique plus importante que les souris âgées de 1 mois (7). Le *sex ratio* des cas cliniques comme celui des infections est de 1:1 chez l'enfant (8) mais il est de 2,5 hommes pour une femme malgré une séroprévalence identique (9). Le facteur protecteur chez la femme pourrait être lié aux hormones sexuelles, comme chez la souris. En effet, les souris femelles C57BL/6 présentent une charge bactérienne plus faible que les mâles et les femelles ovariectomisées. Le traitement de ces dernières par du 17β-oestradiol ramène la charge bactérienne au niveau de celle des souris non-ovariectomisées, ce qui indique que les oestrogènes jouent un rôle protecteur dans l'infection à *C. burnetii* (10). Plus récemment, une étude transcriptomique sur génome total a montré que plus de 80% des gènes modulés en réponse à l'infection par *C. burnetii* sont différents chez les souris mâles et les souris femelles (11).

1. 2. Infection à *C. burnetii* et réponse immune

A la différence de la réponse cellulaire (voir ci-après), la réponse humorale dirigée contre *C. burnetii* semble inefficace puisque la fièvre Q chronique est caractérisée par des taux élevés d'anticorps spécifiques (3). On trouve également dans la lèpre lépromateuse des taux élevés d'anticorps sans le moindre effet microbicide (12).

Une réponse immune à médiation cellulaire efficace rend compte du pronostic favorable de la forme aiguë de la fièvre Q. Les lymphocytes périphériques des patients guéris présentent une réponse proliférative importante lorsqu'ils sont cultivés en présence de *C. burnetii*. En outre, la production d'IFN-γ par une large proportion de lymphocytes chez ces individus (13) traduit une polarisation de la réponse immune de type Th1, profil protecteur dans le cadre des infections à germes intracellulaires. La forme

chronique de la fièvre Q est, elle, caractérisée par un déficit de la réponse à médiation cellulaire, avec en particulier une absence de prolifération lymphocytaire en réponse à l'antigène et un défaut de production de 1'IFN-γ (2). On observe également chez les patients atteints d'une fièvre Q chronique une diminution du nombre de lymphocytes T $CD4^+$ et du rapport $CD4^+/CD8^+$ (14). Contrairement à ceux des patients atteints de fièvre Q aiguë ou des patients guéris, leurs lymphocytes présentent un défaut de prolifération en réponse à *C. burnetii*. Ce défaut de lymphoprolifération n'est pas associé à la lymphopénie T qui est observée aussi bien chez les patients avec une maladie active que les patients guéris (15). Par ailleurs, les lymphocytes T de personnes vaccinées avec la bactérie inactivée (vaccin Q-Vax) prolifèrent en réponse à l'antigène et produisent de l'IFN-γ (13).

La formation de granulomes en réponse à *C. burnetii* témoigne d'une réponse immune efficace. C'est ainsi que les biopsies hépatiques de patients atteints de fièvre Q aiguë, qui contrôlent l'infection à *C. burnetii*, montrent de nombreux granulomes caractéristiques en forme de beignet (*doughnut granuloma*) constitués d'une vacuole lipidique centrale et une couronne inflammatoire de fibrinogène (3). Ces granulomes sont essentiellement composés de lymphocytes, de macrophages et de cellules géantes multinucléées. Comme la lèpre lépromateuse dans laquelle les granulomes sont absents et les bactéries présentes en grand nombre (16), la fièvre Q chronique est caractérisée par une absence de granulomes, remplacés par des infiltrats macrophagiques présentant de larges vacuoles multibacillaires (3). Cette absence de granulomes témoigne de l'altération de la réponse à médiation cellulaire, altération parfois associée à des vascularites et des glomérulonéphrites. Des travaux récents de notre équipe ont montré qu'il est possible d'obtenir in vitro des structures de type granulome en utilisant des billes de Sepharose couplées à des extraits de *C. burnetii* sur lesquelles viennent adhérer les cellules mononucléées du sang périphérique (PBMCs) (17). Alors que les PBMCs de patients atteints d'une fièvre Q aiguë induisent la formation in vitro de granulomes, les PBMCs des patients atteints d'une fièvre Q chronique sont incapables d'induire la formation de granulomes (Delaby et al, manuscrit soumis).

Dans les modèles d'infection à *C. burnetii*, les mêmes caractéristiques sont retrouvées. C'est ainsi que les souris athymiques ne parviennent pas à contrôler l'infection par *C. burnetii* et présentent une infection chronique (18) et que les souris SCID succombent à l'infection par *C. burnetii* (19). L'efficacité de la réponse cellulaire est attestée par la réaction d'hypersensibilité retardée et la formation de granulomes observées chez les

cobayes et les souris infectées par *C. burnetii* (20, 21). Notre équipe a montré plus récemment que chez les souris qui surexpriment l'IL-10 dans le compartiment macrophagique sont infectées plus durablement que les souris contrôles (22), ce qui souligne le lien entre réponse immune, cytokines et infection par *C. burnetii*.

On observe également une dérégulation du réseau de cytokines au cours de la fièvre Q chronique. Les taux de CD23, un marqueur soluble d'activation des leucocytes, sont particulièrement élevés dans la fièvre Q chronique (23), ce qui pourrait indiquer une exacerbation de la réponse inflammatoire (24). La production du *Tumor Necrosis Factor* (TNF) et de l'IL-1β, deux cytokines inflammatoires, est augmentée chez les patients atteints d'une endocardite à *C. burnetii* (25), ce qui pourrait réduire l'activité bactéricide des monocytes à l'égard de *C. burnetii* (26). Enfin, l'IL-10 et le *Transforming Growth Factor* (TGF)-β sont produits en excès par les cellules mononucléées de patients souffrant d'endocardite à *C. burnetii* (27), la surproduction d'IL-10 étant associée à la survenue de rechutes (28).

Finalement, il est important de signaler que l'infection par *C. burnetii*, si elle est normalement contrôlée par la réponse cellulaire, n'est pas éradiquée puisque les sujets présentant une valvulopathie ou un déficit immunitaire peuvent subir une réactivation et voir s'installer une chronicisation de leur maladie (3). Sur le plan microbiologique, on a aussi observé la présence de *C. burnetii* dans la pulpe dentaire de cobayes apparemment guéris (29) et, chez l'homme, de l'ADN bactérien dans les monocytes circulants et la moelle osseuse plusieurs mois ou plusieurs années après un épisode infectieux (30). Des données acquises récemment dans le laboratoire suggèrent que le tissu adipeux pourrait servir de réservoir pour *C. burnetii* comme cela a été montré pour une bactérie telle que *Rickettsia prowazekii*, l'agent du typhus épidémique (31).

1. 3. *C. burnetii*, une bactérie infectant les macrophages

C. burnetii est une bactérie strictement intracellulaire mesurant 0,4 à 1 µm de long et 0,2 à 0,4 µm de large. Elle possède une membrane similaire à celle des bactéries à gram négatif. Elle ne peut cependant être colorée par la technique de Gram mais est mise en évidence par la coloration de Gimenez (32). Son cycle de développement consiste en une fission binaire et une sporulation. Les SLPs (*spore-like particles*) peuvent survivre longtemps dans l'environnement et présentent une importante résistance au stress physico-chimique. La microscopie électronique à transmission a mis en évidence deux formes morphologiques de *C. burnetii*, les SCVs (*small cell variants*) et les LCVs

(*large cell variants*) (33). Les SCVs présents dans l'environnement sont métaboliquement inactifs. Ils restent viables après un traitement thermique à 60°C pendant 30 minutes, une congélation à -20°C pendant 2 ans, une exposition aux radiations ultraviolettes ou à une pression élevée (> 3,4 x 10^5 kPa), à la fixation au formaldéhyde (à 0,5% pendant 4 jours), à l'eau de Javel à 0,5%, à une sonication de 30 minutes, à la dessiccation, au choc osmotique ou au stress oxydatif. Ils sont en revanche sensibles à l'éther, au chloroforme à 5% et à l'alcool à 70°. Le traitement par le formaldéhyde à 5% pendant 24 à 48 heures est le moyen de décontamination le plus efficace (3). Ces SCVs sont phagocytés par leurs cellules hôtes, ce qui a pour conséquence la survie des bactéries dans un phagosome acide et l'activation des enzymes bactériennes conduisant au développement des LCVs. Ces derniers sont métaboliquement actifs et, à leur tour, peuvent engendrer des spores résistantes (34).

La capacité phagocytaire des macrophages et leur longue durée de vie en font des hôtes privilégiés pour les bactéries pathogènes à développement intracellulaire telles que *Mycobacterium tuberculosis*, *Mycobacterium leprae*, *Legionella pneumophila*, *Salmonella enterica* (sérotype typhimurium) ou *L. monocytogenes*. Ainsi, de façon paradoxale, les bactéries intracellulaires résident principalement dans des cellules normalement destinées à les détruire. Pour survivre et se multiplier dans des cellules hôtes dotées d'un tel pouvoir lytique, les agents pathogènes ont donc été contraints d'élaborer divers mécanismes d'échappement à la réponse immunitaire. Les bactéries intracellulaires peuvent moduler l'activation des monocytes/ macrophages en induisant la synthèse de cytokines inhibant leurs propriétés microbicides. Elles peuvent également altérer le trafic intracellulaire et se retrouver alors dans une vacuole permettant leur développement. Enfin, un moyen efficace et peu dommageable pour l'organisme d'éliminer les bactéries est de détruire les cellules infectées en déclenchant leur mort par apoptose. Les monocytes/macrophages, des cellules hautement phagocytaires et à fort potentiel microbicide, sont connus pour être les cellules hôtes de *C. burnetii*. La survie des micro-organismes dans un environnement a priori hostile nécessite des stratégies d'évitement ou de subversion des fonctions macrophagiques. *C. burnetii* a développé une stratégie originale d'échappement partiel à la phagocytose (35). Les bactéries virulentes (dites de phase I) sont faiblement phagocytées mais survivent dans les monocytes humains tandis que les bactéries avirulentes (dites de phase II) sont plus aisément phagocytées mais sont éliminées. La phagocytose des bactéries de phase II requiert l'engagement de l'intégrine monocytaire $\alpha v\beta 3$ et de CR3 (récepteur du

complément de type 3), une intégrine β2 (CD11b/CD18), alors que celle des bactéries virulentes est assurée par la seule intégrine αvβ3. Ainsi les bactéries virulentes ont-elles mis au point une stratégie qui leur permet d'échapper à CR3, un récepteur impliqué dans la phagocytose de nombreux microorganismes, en inhibant le dialogue entre l'intégrine αvβ3 et CR3 (36). Le mécanisme conduisant à cette inhibition est complexe. Seules les bactéries de phase I induisent un remaniement du cytosquelette d'actine et la formation de pseudopodes (37) dans lesquels sont engagées des protéines tyrosine kinases de la famille src (38).

On sait depuis presque trente ans que *C. burnetii* survit dans un phagosome acide (39) et que son métabolisme est adapté à un tel pH (40). On a longtemps pensé que *C. burnetii* vivait dans un phagolysosome et que les bactéries résistaient à la dégradation lysosomiale. Il a été montré dans le laboratoire que les bactéries de phase I bloquent la maturation du phagosome au stade endosome tardif (qui exprime un marqueur tel que Lamp-1 (*lysosome-associated membrane protein*). Ce phagosome est acide mais il est incapable de fusionner avec les lysosomes puisqu'il n'exprime pas la cathepsine D, une protéase lysosomiale (41). Un défaut relatif d'acquisition de Rab7, une GTPase impliquée dans la maturation phagosomale, pourrait rendre compte du défaut de fusion des phagosomes contenant les bactéries de phase I avec les lysosomes. En revanche, les phagosomes contenant les bactéries de phase II fusionnent normalement avec les lysosomes puisqu'ils expriment Lamp-1 et la cathepsine D, cette fusion se traduisant par l'élimination des bactéries par les macrophages (42). Cette stratégie de survie mise en place par *C. burnetii* se rapproche de celle employée par *S. enterica*, à savoir l'inhibition de la voie endosomale à un stade tardif. Il semble cependant que le mécanisme en soit différent puisque le phagosome de *C. burnetii* acquiert partiellement Rab7 alors que Rab7 est pleinement recruté par celui de *Salmonella* (43). Autre point intéressant, le traitement des monocytes par l'IFN-γ, traitement connu pour induire leur activité microbicide, permet de restaurer la fusion du phagosome contenant *C. burnetii* de phase I avec les lysosomes et leur activité microbicide à l'égard de ces mêmes bactéries (42).

2. Plasticité des macrophages

Les macrophages jouent un rôle essentiel dans la mise en place de la réponse immune, étant à la fois les initiateurs et les effecteurs de la lutte anti-infectieuse. Initiateurs puisque, dès la pénétration de l'agent infectieux dans l'organisme, certaines fonctions macrophagiques sont activées: le chimiotactisme, la phagocytose et la production de cytokines. Ces fonctions, mécanismes de défense non spécifiques à l'égard de l'agent pathogène, constituent l'immunité innée. Les macrophages sont aussi initiateurs de la réponse immune spécifique puisqu'ils présentent l'antigène aux lymphocytes T. Grâce à des molécules de co-stimulation, ils activent les lymphocytes T qui acquièrent la capacité de produire des cytokines essentielles dans la lutte contre les microorganismes intracellulaires. Ces cytokines d'origine lymphocytaire, et en particulier l'IFN-γ, activent à leur tour le potentiel lytique des macrophages qui deviennent de puissants effecteurs de la lutte anti-bactérienne. Tandis que nombreux germes extracellulaires sont détruits par les macrophages avant même l'activation de l'immunité adaptative, l'élimination des microorganismes intracellulaires nécessite la coopération entre les macrophages et les lymphocytes T. Cette coopération a lieu au sein d'un granulome qui protège d'une part l'organisme de la dissémination de l'agent pathogène et d'autre part les tissus environnants du potentiel lytique des macrophages mis en œuvre au sein du granulome. Les capacités lytiques de ces macrophages activés nécessitent d'être finement régulées. Ainsi, le macrophage est en permanence soumis à l'action de cytokines activatrices et inhibitrices, de diverses origines cellulaires, agissant de façon autocrine et/ou paracrine. Ces cytokines constituent un réseau complexe qui contrôle l'état d'activation des macrophages et donc leur potentiel lytique.

La notion de macrophages recouvre une réalité bien plus complexe. Les macrophages sont définis par une origine commune, les précurseurs myéloïdes de la moelle osseuse et par une fonction commune, le pouvoir de phagocytose. Pour autant, des données déjà anciennes montrent que leurs fonctions varient non seulement selon leur localisation tissulaire et leur réponse à leur microenvironnement mais également, pour une même cellule, au cours du temps.

2. 1. Localisation tissulaire des macrophages

Les macrophages sont présents un peu partout dans l'organisme. Ils proviennent des précurseurs de la moelle osseuse qui transitent par le sang avant de se localiser dans les

tissus: ce sont les macrophages résidents. Ces macrophages peuvent changer de nom en fonction du tissu dans lequel ils résident. Les cellules de Küpffer, présentes dans le foie où elles représentent 5 à 10% du poids du foie, sont des macrophages situés dans la lumière des capillaires sinusoïdes et fixés aux intersections de leurs ramifications. Elles ont pour rôle de phagocyter les particules étrangères qui proviennent de l'intestin avant qu'elles ne gagnent la circulation générale. Les cellules de la microglie sont des macrophages ayant migré dans le cerveau. Les cellules microgliales utilisent les mécanismes phagocytaires et cytotoxiques pour détruire les corps étrangers. A l'état quiescent, elles sont dépourvues des molécules du complexe majeur d'histocompatibilité (CMH) de classe I et de classe II, de CD45 et de différents récepteurs de surface nécessaires à la présentation de l'antigène. Elles ne produisent pas (ou peu) de cytokines inflammatoires. Activées, elles contribuent à la réponse immune en agissant comme cellules présentatrices de l'antigène, en promouvant la réponse inflammatoire via la production de cytokines et des molécules de signalisation. Les ostéoclastes sont également d'origine macrophagique. Ce sont des cellules multinucléées d'un diamètre de 50 à 100 µm possédant de nombreux noyaux. Ils sont responsables de la résorption osseuse en se fixant à la matrice osseuse et en produisant en particulier des métalloprotéases (MMP). D'autres macrophages tissulaires, tels les macrophages alvéolaires gardent leur nom. Ils jouent un rôle important dans la réponse pulmonaire via la phagocytose des cellules nécrotiques et/ou apoptiques (44) mais sont des cellules faiblement présentatrices de l'antigène. Il est apparu très récemment que la notion de monocytes comme population homogène doit elle-même être revisitée. Cross et ses collaborateurs ont en effet montré qu'il est possible de définir ces monocytes comme inflammatoires ou patrouilleurs. Les monocytes qui expriment fortement CD14 mais pas CD16 sont les effecteurs de la réponse inflammatoire spécialisés dans la phagocytose et la synthèse de dérivés actifs de l'oxygène. Les monocytes qui n'expriment pas ou peu CD14 mais qui expriment CD16 sont dits patrouilleurs puisqu'ils sont impliqués dans la surveillance des tissus et qu'ils circulent le long de l'endothélium vasculaire. Ces monocytes patrouilleurs sont peu phagocytaires et ne produisent ni de dérivés actifs de l'oxygène ni de cytokines en réponse à une stimulation via les Toll-Like Récepteurs (TLRs) mais produisent du TNF, de l'IL-1β et CCL3 en réponse à des virus (45, 46).

2. 2. Microenvironnement des macrophages et fonctions macrophagiques

L'introduction d'un agent infectieux dans l'organisme stimule la réponse immune avec libération d'une variété de cytokines dont le mode d`action peut être autocrine, paracrine ou endocrine. Les monocytes/macrophages se situent au coeur de ce réseau de cytokines, étant à la fois cibles et producteurs de cytokines proinflammatoires et immunorégulatrices. Ils sont en effet la cible des cytokines de la réponse immunitaire cellulaire Th1 telles que l'IFN-γ et 1'IL-12 et de la réponse Th2 (IL-10 et IL-4) (47, 48). Ils produisent en outre des cytokines proinflammatoires telles que le TNF, l'IL-1 et l'IL-6 en réponse à de nombreux produits bactériens, en particulier le lipopolysaccharide (LPS).

L'activité microbicide des macrophages est extraordinairement sensible aux cytokines ou aux agents bactériens auxquelles ils sont exposés**.** Ainsi, I'IFN-γ augmente l'activité microbicide des macrophages dirigés contre des agents pathogènes intracellulaires aussi variés que *Mycobacterium*, *Leishmania*, *Toxoplasma* ou *Trypanosoma* via l'induction des dérivés actifs de l'oxygène et de l'azote et la production de cytokines telles que le TNF (49). Le TNF induit, lui, l'amorçage de la réponse oxydative (*oxidative burst*) tout en activant les propriétés microbicides des macrophages. A l'opposé des cytokines précédentes, 1'IL-10, l'IL-4 et le TGF-β « désactivent » les monocytes/macrophages en contrecarrant les effets de l'IFN-γ et du TNF. Ces cytokines immunorégulatrices inhibent la production des cytokines inflammatoires induites, en particulier, par le LPS ou l'IFN-γ ainsi que la production des dérivés actifs de l'oxygène et de l'azote (50). Il a été montré en outre que l'IL-10 favorise la survie de *L. pneumophila* (51), que l'IL-4 inhibe l'activité anti-leishmanienne des macrophages (52) et que le TGF-β favorise la réplication de *M. tuberculosis* (53). Cependant, dans certaines conditions, les cytokines peuvent conduire à la survie et la réplication des agents pathogènes avec une certaine sélectivité puisque, si le TGF-β favorise la réplication de *M. avium*, 1'IL-10 ne l'affecte pas (54). Par ailleurs, les agents pathogènes sont susceptibles de détourner le réseau de cytokines à leur avantage (55). Ainsi le virus d'Epstein-Barr synthétise-t-il une protéine proche de l'IL-10 humaine et les leishmanies contrôlent-elles la synthèse de diverses cytokines (IL-2, IL-3, Granulocyte Macrophage-Colony Stimulating Factor). Les souches virulentes de *Brucella abortus* induisent la synthèse d'un inhibiteur du TNF, ce qui favorise leur survie dans les macrophages humains (55).

Un concept général d'activation des macrophages est apparu ces dernières années. S'appuyant sur la dichotomie classique Th1/Th2, il porte le nom de macrophages M1/M2 (47, 56). Des études convergentes montrent que les macrophages sont polarisés en macrophages M1 ou M2 en fonction des médiateurs qu'ils rencontrent. C'est ainsi que des molécules telles que l'IFN-γ et le TNF induisent une polarisation M1 alors que des molécules immunorégulatrices induisent une polarisation M2 des macrophages. Les macrophages M1 produisent un certain nombre de molécules telles que le TNF, l'IL-6, l'IL-12 et l'IL-1β, ce qui explique leur activité inflammatoire et bactéricide. Les macrophages M2 représentent, eux, une population hétérogène quant à leurs voies d'induction, leurs caractéristiques phénotypiques et leurs propriétés. C'est ainsi que l'IL-4 et l'IL-13 induisent des macrophages dits M2a, que les complexes immuns, des agonistes des TLRs ou le récepteur de l'IL-1 induisent des macrophages dits M2 et que l'IL10 ou les hormones glucocorticoïdes induisent des macrophages dits M2c. Les macrophages M2 sont plutôt des cellules immunomodulatrices (essentiellement les macrophages M2a et M2c) et sont peu microbicides. En fait, les macrophages M2 correspondent à un continuum d'états différents (56).

2. 3. Plasticité temporelle des macrophages

Un degré de complexité supplémentaire rend l'analyse des fonctions macrophagiques difficile. On pourrait penser que la polarisation des macrophages soit stable dans le temps avec une population de macrophages M1 et une population de macrophages M2. Tel n'est pas le cas. Le potentiel lytique des monocytes/macrophages est tel qu'il impose d'être strictement contrôlé afin d'éviter l'exacerbation de la réponse inflammatoire qui pourrait nuire à l'organisme. Il doit donc être plutôt silencieux à l'état quiescent, n'être déclenché que par des signaux d'alerte adéquats puis être rapidement inhibé lorsque la nécessité ne se fait plus sentir. Il est donc nécessaire que le profil d'activation des macrophages soit transitoire et réversible (57, 58).

3. Le placenta et infection à *C. burnetii*

L'histoire naturelle de la fièvre Q indique que certains tissus sont la cible de *C. burnetii*. En effet, la chronicisation de la fièvre Q des mois ou des années après la primo-infection montre que *C. burnetii* réside au cours de la phase de latence dans un territoire qui est à ce jour inconnu. Des résultats préliminaires obtenus au sein du laboratoire montrent que le tissu adipeux serait ce réservoir même si la nature des cellules-hôtes reste à déterminer. Par ailleurs, le placenta est la cible de *C. burnetii* et c'est ce point que j'analyse plus avant.

3. 1. Le placenta

L'essentiel des informations contenues dans ce paragraphe provient des références 58 et 59.

- Organisation du placenta

Le placenta est composé des tissus embryonnaires et de la décidua ou caduque. Le placenta à terme est un disque d'environ 20 cm de diamètre et de 3 cm d'épaisseur, qui pèse approximativement 500 g, soit environ 1/6 du poids fœtal. Y circulent à la fois le sang maternel et le sang fœtal sans qu'ils entrent en contact grâce à une barrière hémato-placentaire qui assure leur séparation. Cette barrière permet aussi les échanges entre la mère et le fœtus, qu'il s'agisse de nutriments ou de substances toxiques. Le placenta à terme représente ainsi un organe autonome d'une surface totale d'échange d'environ 14 m^2 et un réseau sanguin long de 40 à 50 km, ce qui reflète l'intensité des échanges entre la mère et le fœtus au cours de la grossesse. Le placenta humain est organisé en cotylédons individualisés et qui forment sur la face externe « une galette » bien identifiable. Ces structures fonctionnelles sont fragiles et sont généralement lésées au moment de la délivrance (expulsion du placenta après l'accouchement). Quatre niveaux d'interaction sont possibles au niveau placentaire. Ce sont l'interface syncytiotrophoblaste/espace intervilleux sanguin maternel, l'interface chorion constitué de cellules du cytotrophoblaste extravilleux)/espace intervilleux sanguin maternel, l'interface cytotrophoblaste extravilleux (endovasculaire)/sang périphérique des artères spiralées maternelles et, enfin, l'interface cytotrophoblaste extravilleux (interstitiel, cellules placentaires géantes)/*decidua basalis*.

Dès la nidation qui est le phénomène au cours duquel l'œuf fécondé atteint le stade blastocyste, il s'attache à l'endomètre maternel. Le trophoblaste se différencie alors,

s'épaissit et se pluristratifie. Le cytotrophoblaste est la couche interne qui est formé de cellules de grande taille qui contiennent de grosses vacuoles. Les couches superficielles deviennent syncytiales et sont formées de grandes cellules multinucléées, les syncytiotrophoblastes. Dans un premier temps, ces syncytiotrophoblastes deviennent compacts puis se creusent de lacunes vers le neuvième jour post-conceptionnel. Ils sont responsables de l'érosion de l'épithélium et des capillaires endométriaux et participent à la formation de la barrière hémato-placentaire. Au cours de ces événements, le nombre de lymphocytes T et de lymphocytes B diminue alors que le nombre de macrophages augmente. En résumé, l'unité fonctionnelle du placenta est la villosité choriale formée d'un axe mésenchymateux parcouru par les vaisseaux sanguins fœtaux et contenant des macrophages tissulaires appelés cellules de Hofbauer. Elle est bordée d'une couche interne de cellules mononucléées, les cytotrophoblastes villeux et d'une couche externe de syncytiotrophoblastes en contact direct avec le sang maternel et qui représentent la zone privilégiée d'échanges entre la mère et le fœtus (**Tableau 3**). Ces syncytiotrophoblastes assurent des fonctions endocrines et métaboliques mais aussi des fonctions immunosuppressives et d'hémostase comparables à celles d'un endothélium. On distingue également dans la villosité des cytotrophoblastes intermédiaires à l'origine des cytotrophoblastes extravilleux qui pénètrent la décidua et migrent de façon orientée vers les artères utérines.

- Circulation placentaire

Les villosités placentaires fœtales pénètrent jusque dans les vaisseaux sanguins maternels et sont directement en contact avec le sang, ce qui permet au tissu fœtal (chorion) d'être en contact direct avec le sang maternel. Le sang artériel maternel arrive par les branches terminales des artères spiralées utérines qui s'ouvrent dans la chambre intervilleuse. La circulation sanguine est assurée par la pompe cardiaque fœtale et par les pulsations des artères autour desquelles les veines sont enroulées. Vers le terme, le volume sanguin contenu dans les vaisseaux placentaires fœtaux étant de l'ordre de 45 ml pour un flux fœto-placentaire d'environ 300 ml/min, on peut estimer que le sang fœtal est remplacé toutes les 8 à 10 secondes. L'espace sanguin fœtal est donc constitué d'un faible volume à renouvellement rapide alors que l'espace sanguin maternel présente un grand volume à renouvellement lent, ce qui favorise les échanges au niveau du sang maternel. La qualité de ces échanges dépend de ce fait de la circulation fœtale, de l'intégrité de la surface syncytiotrophoblastique et de la circulation du sang maternel dans la chambre intervilleuse.

Tableau 3. Les cellules de la villosité choriale et leurs fonctions

Cellules placentaires	**Principales fonctions**
villosités choriales	
Cytotrophoblaste villeux	Différenciation en syncytiotrophoblastes;
Syncytiotrophoblaste	Contrôle des échanges mère < fœtus; fonction endocrine et métabolique; fonction immuno-suppressive; hémostase dans la chambre intervilleuse
Mésenchyme	Structure de soutien; activité contractile
Cellule de Hofbauer	Fonction immunosuppressive
Cellule endothéliale et cellule musculaire lisse	Contrôle du flux sanguin fœtal; diffusion passive
Interface foeto-maternelle	
Cytotrophoblaste intermédiaire des colonnes	Prolifération; ancrage des villosités à l'endomètre
Cytotrophoblaste extravilleux	Migration dans la décidua; invasion contrôlée et orientée; fonction immunosuppressive; différenciation en cellules géantes
Cytotrophoblaste intravasculaire	Régulation du flux sanguin maternel

3. 2. Fonctions placentaires

Au cours de la grossesse le placenta assure plusieurs fonctions essentielles au bon déroulement de la croissance.

- Fonction d'échange du placenta

C'est la fonction première du placenta qui autorise les échanges entre la mère et le fœtus. Pour le fœtus, le placenta joue le rôle de rein, de poumon et d'intestin. Il a été longtemps considéré comme une simple membrane semi-perméable avec ses caractéristiques: libre passage de l'eau, des électrolytes, des molécules de faible poids moléculaire et blocage des composés de poids moléculaire élevé. En réalité, les échanges placentaires s'effectuent selon plusieurs modalités (**Tableau 4**). Pour l'eau, l'urée, l'oxygène et le gaz carbonique, le transfert se fait par simple diffusion du milieu à forte concentration vers le milieu à faible concentration jusqu'à atteindre l'état d'équilibre. Cependant, le transfert de l'oxygène est facilité par l'affinité de l'hémoglobine fœtale à l'égard de l'oxygène maternel. Ce type de transfert stéréospécifique est également utilisé pour le D-glucose qui représente la principale source d'énergie pour le fœtus. Le transport des acides aminés, du sodium, du calcium et du potassium nécessite, lui, un apport en énergie provenant de l'hydrolyse de l'ATP par une ATPase placentaire. Le transport de diverses protéines nécessite leur endocytose par le tissu trophoblastique via des récepteurs spécifiques situés à la surface des microvillosités. Ces récepteurs permettent, en particulier, le transfert accéléré de la mère vers le placenta de substances comme le fer et le cholestérol qui circulent sous forme liée à des protéines. Les anticorps maternels, en particulier les IgG, traversent le placenta grâce à des récepteurs spécifiques et protègent l'enfant via une immunité passive qui se prolonge quelques mois après la naissance. En revanche, le placenta est imperméable aux macroglobulines telles que les IgM et les IgA. Ainsi, leur présence dans le sérum des nouveaux-nés traduit une néosynthèse propre au bébé. Le passage transplacentaire d'agents toxiques ou pathogènes est résumé dans le **Tableau 5**. En règle générale, les molécules peu ionisées, liposolubles et de poids moléculaire inférieur à 600 daltons traversent spontanément la membrane placentaire. Leur diffusion ne dépend que des débits sanguins maternel et fœtal au niveau du placenta. Les molécules très ionisées, peu liposolubles et de poids moléculaire supérieur à 600 daltons traversent la membrane placentaire par diffusion passive. On peut signaler que des antibiotiques tels que la méthicilline et l'ampicilline, bien que ionisés, traversent facilement le placenta car très liposolubles.

Tableau 4. Mécanismes d'échange au niveau du placenta

Mère	Placenta	Fœtus
Diffusion simple: O_2, H_2O	Gradient de concentration 	CO_2, urée
Diffusion facilitée	Couplage à flux ionique Protéines vectrices 	Glucose
Transport actif	Energie dépendant ATPase 	Acides aminés
Endocytose Transferrine LDL IgG	Récepteurs spécifiques 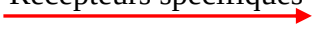	 Fer Cholestérol IgG

Tableau 5. Passage transplacentaire des agents pathogènes et toxiques par diffusion passive

Produits toxiques	- Alcool - Plomb, phosphore, mercure, iode
Médicaments	- Analgésiques (morphine, paracétamol) - Anesthésiques (thiopental, pilocaine) - Tranquillisants et hypnotiques - Diurétiques - Antibiotiques liposolubles (ampiciline, méthicilline)
Drogues	- Opiacés - LSD
Agents pathogènes	- Virus - Parasites (toxoplasme, paludisme) - Bactéries (syphilis)
Substances organiques	Poids moléculaire < 600 Da

- Fonctions métaboliques du placenta

Le placenta est un tissu en évolution continue. Il est donc actif de point de vue métabolique tout au long de la grossesse. Pour assurer ses propres besoins, il capte 60% du glucose à partir du sang maternel qu'il transforme principalement en lactate en fin de grossesse alors qu'en début de grossesse, il le stocke sous forme de glycogène au niveau des trophoblastes. Le placenta est équipé de toute la machinerie enzymatique indispensable à la synthèse des acides gras, à leur estérification en triglycérides et à leur oxydation en composés cétoniques. Il est aussi capable d'accumuler les acides aminés qui lui serviront pour la synthèse protéique. Il est cependant incapable de synthétiser le cholestérol nécessaire à la formation des membranes placentaires ou les hormones stéroïdes pour lesquels il fait appel aux apports maternels.

- Fonctions endocrines du placenta

Le placenta est un organe actif de point de vue endocrine puisqu'il est à l'origine d'une sécrétion hormonale dirigée spécifiquement soit vers la circulation maternelle et/ou fœtale. Ces hormones sont impliquées dans l'adaptation à la grossesse de la mère, le maintien de la grossesse, la croissance fœtale ou encore le mécanisme du déclanchement de l'accouchement à terme.

A partir de la huitième semaine de grossesse, le placenta est le siège d'une production accrue d'hormones stéroïdes, essentiellement de progestérone et d'oestrogènes (59). La synthèse du prégnénolone et de la progestérone par le placenta s'effectue à partir du cholestérol contenu dans les LDL *(low density lipoproteins)* plasmatiques maternelles. Contrairement à l'ovaire, le placenta est un organe endocrine dépourvu de la machinerie enzymatique indispensable pour convertir le prégnénolone en substrat des œstrogènes: cette étape est assurée par la surrénale fœtale. Les stéroïdes étant très diffusibles, leur excès pourrait avoir un effet délétère sur le fœtus, ce qui explique qu'ils sont inactivés par les tissus fœtaux et placentaires. C'est ainsi que le cortisol maternel ou fœtal peut être inactivé en cortisone par le placenta, ce qui permet un contrôle fin de la quantité de glucocorticoïdes actifs utilisables par le fœtus. En fin de grossesse, la production moyenne de progestérone est de 400 à 500 mg/jour alors que celle des œstrogènes n'est que de 50 mg/jour. Ces hormones agissent principalement sur le muscle utérin via des récepteurs spécifiques dont la synthèse est en partie contrôlée par les œstrogènes, ce qui a pour effet de supprimer les contractions utérines et donc le risque d'accouchement prématuré.

Le placenta sécrète d'autres hormones polypeptidiques (60). L'hCG (*human chorionic gonadotropin*) est sécrétée par le syncytiotrophoblaste dès la deuxième semaine de grossesse au moment de l'implantation et cette sécrétion atteint un maximum au cours du deuxième mois avant de diminuer vers le troisième mois et de rester stable jusqu'au terme. La sécrétion de l'hPL (hormone lactogène placentaire) dans le compartiment placentaire maternel est importante alors ses concentrations sont 100 fois plus faibles dans la circulation fœtale. Sa concentration est proportionnelle à la masse placentaire et évolue tout au long de la grossesse. Elle pourrait être impliquée dans l'apport de glucose au fœtus (61). Le placenta sécrète également toute une série de neuropeptides. Il s'agit d'analogues à ceux identifiés au niveau hypothalamo-hypophysaire tels que le TRH (*thyrotropin releasing hormone*), le LHRH (*luteinizing hormone releasing hormone*) et le CRH (*corticotropin releasing hormone*). Ces facteurs semblent être impliqués dans la régulation de la production hormonale au niveau placentaire (62). Le placenta est aussi connu pour donner lieu à une sécrétion accrue de facteurs de croissance et de cytokines qui assurent son développement et son bon fonctionnement, ces facteurs agissant de façon autocrine ou paracrine. On note enfin dans le placenta la présence de leptine (sécrétée par le tissu adipeux) et d'EGFR (*epidermal growth factor receptor*).

- Fonctions immunologiques du placenta

Le placenta joue le rôle d'une barrière immunologique même s'il laisse passer les anticorps de la mère vers le fœtus .L'organisme de la mère tolère, lui, le corps immunologiquement semi-étranger que représente le fœtus. C'est ainsi que le placenta bloque les effets des cellules cytotoxiques maternelles (cellules NK (*Natural Killer*) et les empêchent de s'attaquer au fœtus afin de préserver la grossesse. Dans ce contexte, plusieurs hormones stéroïdes placentaires, et plus particulièrement la progestérone, sont immunosuppressives et agissent spécifiquement sur les lymphocytes de la mère via la protéine PIBF (*Progesterone-Induced Blocking Factor*). Les molécules HLA classiques sont remplacées par des molécules HLA particulières et peu polymorphes, les HLA-G. On note également la présence de Fas-ligand sur le syncytiotrophoblaste et la déplétion locale en tryptophane, ce qui suggère que les cellules NK ne peuvent attaquer les cellules embryonnaires et le placenta. En effet, les cellules NK reconnaissent les molécules HLA-G, ce qui inhibe leur activité cytolytique et explique pourquoi le fœtus et le placenta sont épargnés par l'arsenal immunitaire de la mère quel que soit le groupe HLA paternel (63).

3. 3. Placenta et infections

Le placenta peut être la cible d'agents pathogènes divers et variés parmi lesquels on peut citer des parasites tels que *Plasmodium falciparum* (64), des virus tels que le papillomavirus (65), des bactéries telles que *Listeria monocytogenes* (66) et *Brucella abortus* (67). A l'heure actuelle, les types cellulaires dans lesquels vivent les agents pathogènes à tropisme placentaire ne sont pas identifiés probablement suite à la difficulté d'obtention des placentas humains et d'isolement des différentes populations cellulaires placentaires (68). C'est la raison pour laquelle la majeure partie des travaux relatant l'interaction placenta-agents pathogènes portent sur le bétail ou des lignées cellulaires placentaires commerciales. Cette partie sera détaillée dans la revue n°2 (revue macrophages placentaires et infections).

3. 4. Cas des infections placentaires à *C. burnetii*

La séroprévalence de la fièvre Q est élevée chez les femmes enceintes (69) pour une séroprévalence générale en France de 50 pour 100.000 personnes (3). *C. burnetii* colonise et se multiplie dans l'utérus, les glandes mammaires et le placenta (70). Une infection chronique de la mère se développe durant les premiers six mois de grossesse indépendamment du traitement. L'infection par *C. burnetii* a aussi des conséquences obstétricales puisqu'elle est à l'origine d'avortements spontanés, d'accouchements prématurés et de morts-nés (71). Dans une série de 17 femmes enceintes développant une fièvre Q, une mort fœtale est observée dans 66% des cas et une prématurité dans 30% des cas (6). Quand l'infection survient au cours du premier trimestre de la grossesse, elle induit des avortements alors que, survenant au cours du second trimestre, elle entraîne des accouchements prématurés. Un traitement antibiotique prolongé avec du co-trimoxazole prévient les avortements ainsi que la mort fœtale mais ne prévient en aucun cas la chronicisation de la maladie chez la mère. On préconise en général chez les femmes enceintes présentant une infection à *C. burnetii* une échographie cardiaque pour la recherche d'anomalies valvulaires susceptibles de favoriser la chronicisation de la fièvre Q en une endocardite infectieuse (72, 73).

CHAPITRE DE LIVRE

Immune response and *Coxiella burnetii* invasion

Amira Ben Amara, Yassina Bechah, Jean-Louis Mege

Unité de Recherche sur les Maladies Infectieuses Transmissibles et Emergentes, CNRS-IRD UMR 6236, Institut Fédératif de Recherche 48, Université de la Méditerranée, Faculté de Médecine, 13385 Marseille, France

Corresponding author. Pr J.L. Mege. Fax: (33) 4 91 38 77 72. Tel: (33) 4 91 32 45 86.

E-mail: Jean-Louis.Mege@univmed.fr

Abstract

Coxiella burnetii, the causative agent of Q fever, has evolved a wealth of mechanisms in order to persist within hosts. Two tissues, namely adipose tissue and placenta, are candidates to house *C. burnetii*, but the mechanisms governing *C. burnetii* survival in these tissues are still unknown. In contrast, monocytes and macrophages are well-known targets of *C. burnetii*. First, *C. burnetii* has developed a specific strategy of phagocytosis subversion that consists of the inhibition of integrin interplay. Second, *C. burnetii* persistence is associated with macrophage activation profiles. Indeed, monocytes (in which *C. burnetii* survives without replication) exhibit a proinflammatory M1-type response, whereas macrophages (in which *C. burnetii* slowly replicates) are polarized towards an M2-type. Third, interleukin-10 produced by monocytes is a main factor of the chronic development of Q fever, and murine models confirm the key role of interleukin-10 in *C. burnetii* persistence. Fourth, apoptotic cells may play a key role in chronic Q fever. The uptake of apoptotic cells by circulating monocytes increases *C. burnetii* replication by redirecting monocytes toward a non-protective M2 profile. In the presence of interferon-γ, apoptotic cell engulfment is inhibited and monocytes polarized toward an M1 program are able to kill *C. burnetii*; this is the situation observed in patients with uncomplicated acute Q fever. Finally, we cannot exclude that regulatory T cells may play a role in *C. burnetii* persistence because their number is increased in patients with chronic Q fever.

Keywords

Adipose tissue, apoptosis, *Coxiella burnetii*, interleukin-10, macrophage polarization, monocytes, placenta, Q fever, regulatory T cells.

1. Introduction

Persistent infections may be clinical and related to chronic infection, as observed in chronic Q fever, or subclinical and corresponding to latent infection, as found in mycobacterial and viral infections (Munz-Elias and Mc Kinney 2002). Persistent pathogens, such as *Coxiella burnetii*, have evolved a wealth of mechanisms to antagonize the bactericidal potential of the effectors of immune responses. This includes interference with the microbicidal activity of myeloid cells, dampening of inflammatory signals and inactivation of immune cells (Roy and Mocarski 2007; Sansonetti and Di Santo 2007). In this chapter, we will describe the mechanisms used by *C. burnetii* to control the immune response. This control is directly due to bacterial products that inactivate or avoid effector functions of immunocompetent cells but also indirectly due to regulatory cytokines and regulatory T cells (Belkaid and Rouse 2005). In addition, one strategy used by *C. burnetii* and already described for several viruses could rely on the choice of targeted tissues and cell types. Finally, *C. burnetii* persistence may be related to the route of infection, as some have reported for the initiation of systemic or mucosal responses (Martinoli et al. 2007).

2. The choice of niche for *C. burnetii* persistence: cells and tissues

C. burnetii must initially choose convenient cells and tissues to avoid efficient immune responses.

2.1. Cells targeted by *C. burnetii*

Monocytes and macrophages are the major targets of *C. burnetii*. As these cells have strong microbicidal activity, microorganisms have to subvert these mechanisms to create favorable conditions for survival. We have described strategies used by *C. burnetii* to make monocytes and macrophages permissive for bacterial survival. For that purpose, we have used *C. burnetii* organisms found in natural conditions (virulent organisms also called phase I organisms, here

C. burnetii) and variants obtained upon serial passages in culture (avirulent organisms also called phase II organisms). We clearly show that *C. burnetii* has developed a strategy of phagocytic subversion (Capo et al. 1999). The phagocytosis of phase I *C. burnetii* requires the engagement of αvβ3 integrin and leads to a low phagocytosis rate and intracellular survival. The phagocytosis of phase II *C. burnetii* is mediated by αvβ3 integrin and CR3 (αMβ2 integrin, CD11b/CD18), resulting in a high phagocytosis rate and bacterial elimination. The low efficiency of virulent bacteria uptake is probably critical for the persistence of *C. burnetii* in monocytes and macrophages. Inefficent uptake results from the uncoupling of the αvβ3 integrin from CR3, which is secondary to the inappropriate activation of macrophages and to actin cytoskeleton reorganization (Meconi et al. 1998; Meconi et al. 2001).

Besides low bacterial uptake, a relative deficiency in cytokine production and subsequent macrophage activation is necessary for *C. burnetii* persistence. Our initial reports have indicated that virulent *C. burnetii* organisms are less efficient than avirulent organisms at inducing the synthesis and release of tumor necrosis factor (TNF). This limited efficiency is not the consequence of poor activity of bacterial lipopolysaccharide (LPS) because purified LPS from virulent organisms is more potent than LPS from avirulent organisms at stimulating TNF release (Dellacasagrande et al. 2000b). In fact, virulent organisms, which bind poorly to monocytes, likely present fewer LPS molecules to target cells than do avirulent bacteria, which efficiently bind to monocytes (Dellacasagrande et al. 2000b). The effect of activation on uptake efficiency is strengthened by the finding that neutralizing anti-TNF antibodies decrease *C. burnetii* internalization by monocytes from patients with Q fever endocarditis but do not affect the long term survival of bacteria (Dellacasagrande et al. 2000a).

The concept of macrophage polarization illustrates their functional heterogeneity. Hence, polarized macrophages have been classified as classically activated (M1) macrophages that support microbicidal activity and alternatively activated (M2) macrophages that are not

competent to eliminate pathogens (Martinez et al. 2009; Mege et al. 2011). The identification of M1 and M2 macrophages only results from a combination of markers including membrane receptors, cytokines, chemokines and effector mediators (Benoit et al. 2008b). The activation state of monocytes and macrophages after encountering *C. burnetii* are apparently different (Figure 1). While monocytes exhibit a proinflammatory M1-type response, macrophages are polarized toward an M2-type. *C. burnetii*-infected macrophages release the M2-associated molecules interleukin (IL)-10, transforming growth factor (TGF)-β1 and CCL18, and they express mannose receptor (MR) and the active form of arginase-1. They also secrete high levels of IL-6 and CXCL8, two molecules associated with M1 polarization. However, *C. burnetii*-infected macrophages do not express the M1 molecules (TNF, IL-12, CD80 and CCR7) and fail to produce nitric oxide (NO) (Benoit et al. 2008a). These differences in macrophage activation status are associated with variations in bacterial survival because *C. burnetii* survives in monocytes without replication and slowly replicates in macrophages. We cannot exclude that the *C. burnetii* replication within macrophages is the consequence of increased uptake associated with M2 polarization (Benoit et al. 2008b).

The macrophage activation state may also affect the intracellular trafficking of *C. burnetii*. We have revisited this topic in our reports, but a lack of consensus exists among the researchers who study this aspect of the intracellular life of *C. burnetii*. This point is discussed in a dedicated chapter. The inability of naïve macrophages and monocytes from patients with chronic Q fever (in which *C. burnetii* persists) to induce phagosome-lysosome fusion makes the intracellular trafficking of *C. burnetii* a critical parameter of bacterial persistence. Intracellular trafficking is under the control of IL-10, a cytokine that is responsible for bacterial persistence and the chronic development of Q fever (Ghigo et al. 2004).

2.2. Tissues targeted by *C. burnetii*

The persistence of *C. burnetii* has been clearly documented in the bone marrow of patients who have been apparently cured of Q fever (Harris et al. 2000). It is likely that *C. burnetii* survives in bone marrow macrophages. Once differentiated, macrophages could carry the microorganisms to peripheral sites where immune control is impaired, allowing reactivation. We cannot exclude that stromal cells may be targeted by *C. burnetii* and become bacterial reservoirs. In addition to bone marrow cells, two tissues, namely adipose tissue and placenta, are candidates to house *C. burnetii*. Beyond its metabolic role, adipose tissue has recently emerged as a target for intracellular microorganisms (Desruisseaux et al. 2007). Indeed, adipose tissue is rich in cells that are highly reactive to infection, such as adipocytes and macrophages that express several features of non-microbicidal macrophages (Lumeng et al. 2007). Adipocytes have been recognized as reservoirs for *Trypanosoma cruzi* (Combs et al. 2005) and *Mycobacterium tuberculosis* (Neyrolles et al. 2006), the agents of Chagas disease and tuberculosis, respectively. We found that adipose tissue acts as a reservoir for latent *Rickettsia prowazekii*, the agent of epidemic typhus, and may account for the reactivation of *R. prowazekii* infection in a murine model of Brill-Zinsser disease (Bechah et al. 2010). We also found that *C. burnetii* is present in adipose tissue for several months following infection in mice, whereas it is absent from the blood, liver and spleen (unpublished data). The nature of the cell types that are targeted by *C. burnetii* remains to determine. Adipose tissue macrophages are the expected targets of *C. burnetii* but adipocytes may also harbor *C. burnetii*. We recently found that murine fibroblastic cells in vitro differentiated into adipocytes are permissive to *C. burnetii* infection (unpublished data). The mechanisms involved in the tropism of *C. burnetii* for adipose tissue cells are unknown but it is important to note that adipose-secreted cytokines (adipokines) have both inflammatory and immunoregulatory activities (Ouchi et al. 2011), suggesting that *C. burnetii* survival is

controlled by the microenvironment of adipose tissue. In addition, it has been recently demonstrated that the adipokine adiponectin modulates the polarization of murine peritoneal macrophages (Ohashi et al. 2010). As the polarization status of macrophages controls the intracellular fate of *C. burnetii* (see above), we can hypothesize that the polarization status of adipose tissue macrophages governs their microbicidal activity against *C. burnetii*. Hence, the imbalance in the microenvironment of adipose tissue may control or favor *C. burnetii* infection.

Placenta is also a temporary reservoir for numerous pathogens including *C. burnetii*. Pregnancy consists in the tolerance of a semi-allogeneic graft that needs the regulation of the maternal immune response. This regulation occurs through the interaction between the fetal trophoblasts and the maternal immune system essentially consisting of uterine natural killer cells, dendritic cells and macrophages. In the presence of pathogens such as *C. burnetii*, the tolerogenic phenotype of maternal immune cells is changed into a phenotype that may lead to fetal expulsion. In addition, pregnancy is considered to be an important factor for the chronic development of Q fever and its bacterial persistence (Maurin and Raoult 1999). This phenomenon has been reproduced in animal models. The infection of C57/BL6 mice followed by repeated pregnancies results in abortion, perinatal death and endocarditis in some animals (Stein et al. 2000). The placentas of the infected animals contained up to 10^9 organisms/gram of tissue, and it is likely that the heavily infected placentas contaminated the environment at the time of parturition, leading to the persistence of viable organisms in the soil for several months (Langley et al. 1988). Aerosols from the secretions and excretions of ruminants are the major source of contamination for humans (Tissot-Dupont et al. 2004). The site of *C. burnetii* replication within the placenta remains unknown. We have recently observed that *C. burnetii* infects and persists within a trophoblastic cell line. The bacteria induce an original transcriptional program that modulates genes involved in inflammatory responses and in the

maintenance of pregnancy (Ben Amara et al. 2010). It is likely that *C. burnetii*-infected trophoblasts interact with immune cells present in the placenta and interfere with fetal tolerance. In addition, the placenta is a tissue rich in macrophages and we recently found that placental macrophages harbor *C. burnetii* (unpublished data). It is possible that the tolerogenic status of pregnancy favors the polarization of placental macrophages toward a M2 phenotype unable to control *C. burnetii* infection.

3. Role of immunoregulatory cytokines in *C. burnetii* persistence

The persistence of *C. burnetii* in monocytes/macrophages and within mice and humans is related to the cytokine IL-10 (Table 1). IL-10 shares with IL-4, IL-13 and TGF-β the ability to down-modulate the microbicidal activity of macrophages and redirect their polarization status. Moreover, IL-10 has been associated with an increased susceptibility of the host to intracellular organisms and with chronic bacterial persistence (Mege et al. 2006). During the past few years, we have provided converging evidence that IL-10 is the main factor in the chronic development of Q fever. First, IL-10 is produced by mononuclear cells from patients with Q fever endocarditis and Q fever with valvulopathy who were at risk for developing chronic Q fever (Capo et al. 1996; Honstettre et al. 2003). Second, IL-10 induces *C. burnetii* replication in monocytes. IL-10 acts through the down-modulation of TNF production because TNF restores the microbicidal activity against *C. burnetii* in IL-10-treated monocytes (Ghigo et al. 2004). IL-10 also upregulates the release of type II receptors of TNF (TNF-RII). During chronic Q fever, the expression and release of monocyte TNF-RII are increased (Ghigo et al. 2000). It is likely that soluble TNF-RII interferes with TNF-stimulated microbicidal activity of monocytes, thus sustaining bacterial replication. The effect of IL-10 on *C. burnetii* replication is specific because IL-4 and TGF-β1 (two other immunoregulatory cytokines that act on monocytes) fail to induce *C. burnetii* replication (Ghigo et al. 2001).

Third, IL-10 is involved in the microbicidal defect of monocytes observed in chronic Q fever. Indeed, *C. burnetii* is eliminated in monocytes from patients with acute Q fever and low IL-10 production, whereas it replicates in monocytes from patients with chronic Q fever and high IL-10 production. The microbicidal activity of monocytes from patients with chronic Q fever is restored by neutralizing IL-10 (Ghigo et al. 2004). As the fusion of *C. burnetii*-containing phagosomes with lysosomes is a key component of the microbicidal activity of monocytes (Ghigo et al. 2002), we have studied the colocalization of *C. burnetii* with cathepsin D (a marker of phagosome-lysosome fusion) in monocytes from patients with chronic Q fever. Phagosome-lysosome fusion is impaired in these patients relative to patients with acute Q fever, and the neutralization of endogenous IL-10 reestablishes phagosome-lysosome fusion (Ghigo et al. 2002). Fourth, IL-10 affects the migration of immune cells to peripheral tissues. Indeed, the transendothelial migration of mononuclear cells is defective in patients with Q fever endocarditis, and this defect is corrected by neutralizing IL-10 (Meghari et al. 2006). Defective transendothelial migration of mononuclear cells partly accounts for the defective granuloma formation in patients with chronic Q fever (Maurin and Raoult 1999).

Murine models of *C. burnetii* infection also confirm the key role of IL-10 in bacterial persistence. Several murine models, including immunodefective mice, have permitted the reproduction of acute *C. burnetii* infection but not chronic infection or *C. burnetii* persistence (Maurin and Raoult 1999). An efficient model for chronic Q fever pathogenesis has been developed using transgenic mice that constitutively over-express IL-10 in the macrophage compartment (Meghari et al. 2008). Transgenic mice infected via an intraperitoneal injection exhibited sustained tissue infection and a strong antibody response in contrast to wild-type mice. Thus, bacterial persistence is IL-10-dependent, as in chronic Q fever. In addition, the number of granulomas is low in the spleen and liver of infected transgenic mice, as in patients with chronic Q fever. Interestingly, macrophages from transgenic mice are unable to kill *C.*

burnetii and are characterized by a non-microbicidal M2-type transcriptional program consisting of increased expression of arginase-1, MR and Ym1/2, in contrast to wild-type macrophages in which inducible NO synthase (iNOS) and inflammatory cytokines are overproduced. In the spleen and liver of transgenic mice infected with *C. burnetii*, the expression of arginase-1 is increased while the microbicidal pathway of IL-12p40, IL-23p19 and iNOS is depressed. Finally, the infection of transgenic mice through the intratracheal route, which is close to the natural route of infection, results in pulmonary lesions that consist of mixed interstitial and mild alveolar mononuclear cell pneumonia with a persistent infection of the lungs. Hence, the IL-10-mediated polarization of macrophages is necessary to increase *C. burnetii* susceptibility and persistence in host cells and tissues. There are likely multiple mechanisms leading to IL-10 repolarization of macrophages. We reported a candidate mechanism involving redox partners using vanin-1 deficient mice (Meghari et al. 2007). Vanin-1 is a membrane-anchored pantetheinase that controls tissue inflammation via local cysteamine release and control of the levels of glutathione. The lack of vanin-1 decreases the formation of granulomas in the spleen and liver and significantly affects the activation pattern of bone marrow-derived macrophages stimulated by *C. burnetii*. These macrophages exhibit decreased iNOS and CCL2 gene expression with increased IL-10 and arginase-1 expression, as found in the livers of infected mice. These results indicate that vanin-1 plays a role in granuloma formation in response to *C. burnetii* by skewing macrophage activation toward an M2 program.

The control of *C. burnetii* infection may also be related to the interaction of macrophages with T cells. In mice deficient for CD28 (a costimulatory molecule that exerts a regulatory effect on T cell responses), we observed a decreased *C. burnetii* burden in infected tissues and an impaired production of IL-10 by peritoneal macrophages (Honstettre et al. 2006). Taken

together, these results indicate that a precise regulation of macrophage activation through IL-10 controls macrophage polarization and *C. burnetii* persistence.

4. Role of apoptosis in *C. burnetii* persistence

Apoptosis plays a role in interferon (IFN)-γ-mediated immune protection against *C. burnetii* (Dellacasagrande et al. 1999), and it has been established that preventing apoptosis is a survival strategy of *C. burnetii*. Two reports have clearly documented this point. Epithelial cell lines infected with *C. burnetii* are resistant to chemical inducers of apoptosis due to interference with the intrinsic pathway of cell death (Luhrmann and Roy 2007). *C. burnetii* infection of macrophages inhibits cell apoptosis via the upregulation of c/IAP2 and A1/bfl1, which prevents the activation of caspase 3 and the BH3-only proteins (Voth et al. 2007). This mechanism of apoptosis prevention was recently analyzed: a *C. burnetii*-type IV effector system enabled proteins belonging to the ankyrin repeat family to be delivered into host cells, thus inhibiting cell apoptosis (Luhrmann et al. 2010).

The role of cellular apoptosis in *C. burnetii* persistence has recently been reevaluated (Figure 2). The engulfment of apoptotic lymphocytes by monocytes and macrophages increases both *C. burnetii* replication and the maturation of bacterial phagosomes into phago-lysosomes (Benoit et al. 2008c). *C. burnetii* replication is associated with an M2 program characterized by the upregulation of CD14, IL-10 and IL-1 receptor antagonist (IL1-ra) in monocytes and IL-10, TGF-β1, IL1-ra and MR in macrophages. The neutralization of IL-10 and TGF-β1 prevents the replication of *C. burnetii* due to the engulfment of apoptotic lymphocytes, suggesting that IL-10 and TGF-β1 are critically involved in bacterial replication. Finally, IFN-γ reverses the immune deactivation that is induced by apoptotic cells; it prevents the replication of *C. burnetii* by re-polarizing monocytes and macrophages toward an M1 program (Benoit et al. 2008c). We hypothesize that a similar mechanism may account for *C.*

burnetii persistence in endocarditis, the major manifestation of chronic Q fever that affects altered valves. Cardiac valve lesions are associated with a pathological fluid shear stress, which increases the apoptosis of neutrophils, platelets and monocytes. This association suggests that leukocyte apoptosis may be related to cardiac valvulopathy. We monitored the circulating levels of apoptotic leukocytes in patients with valvulopathy and/or Q fever. Patients with valvulopathy exhibited increased levels of circulating apoptotic leukocytes, independently of Q fever (Benoit et al. 2008c). We have hypothesized that the uptake of apoptotic cells by phagocytes may be responsible for the immune impairment observed in Q fever endocarditis, and we propose a model in which apoptotic cells play a key role in the establishment of Q fever endocarditis. The engulfment of apoptotic cells by monocytes and macrophages increases *C. burnetii* replication by redirecting their activation states toward M2 profiles that are non-protective against most pathogens. In an inflammatory context (such as that found in the presence of IFN-γ), the effect of apoptotic cell engulfment is inhibited. Monocytes and macrophages polarized toward a M1 program are able to kill *C. burnetii*, as is observed in patients with acute Q fever without valvulopathy.

5. Role of regulatory T cells in *C. burnetii* persistence

An efficient immune response requires a shaping of the immune amplitude, which can be supported by regulatory T cells. Several subsets of regulatory T cells have been described (Shevach 2006). Naturally occurring $CD4^+CD25^+$ T cells develop within the thymus early in the life and constitutively express the α-chain of the IL-2 receptor (CD25). These cells are known to be increased in chronic persistent infections such as schistosomiasis, filariasis, tuberculosis, leprosy and disseminated cutaneous leishmania (Belkaid and Rouse 2005). We studied seventy-one patients with either acute Q fever (n = 17) or Q fever endocarditis (n = 54), in addition to twenty-seven healthy subjects. We found no significant differences in the

levels of all T cell subsets in the acute Q fever patients compared to the controls. In contrast, a significant increase in Tregs expressing Foxp3 was observed in the patients with Q fever endocarditis (manuscript in preparation). It is likely that this Treg population contributes to the chronic development of Q fever and to bacterial persistence via the release of IL-10 or via an immunosuppressive process that makes macrophages permissive for *C. burnetii*.

6. Conclusions

C. burnetii establishes a survival niche within macrophages by preventing cell death and inducing an immunoregulatory loop based on IL-10 and regulatory T cells. Understanding the persistence of *C. burnetii* may provide clues for the development of chronic Q fever treatments and for reducing the risk of relapse while undergoing adapted treatment. An other problem is understanding how *C. burnetii* establishes a chronic infection that manifests as endocarditis. The immunosuppression associated with chronic Q fever is systemic and cannot account for the valvular localization of *C. burnetii*, even in the presence of valve lesions. We have recently investigated the transcriptional response in valves from infectious endocarditis patients, and we found that genes related to cell death are upregulated (Benoit et al. 2010). We suggest that valve dysfunction (mediated by the release of apoptotic cells) creates a local immunosuppressive environment that favors bacterial persistence. However, the presence of *C. burnetii* in adipose tissue may be essential for accounting for Q fever relapses, even if the presence of *C. burnetii* in human adipose tissue has yet to be reported.

References

Bechah Y, Paddock CD, Capo C, et al. (2010) Adipose tissue serves as a reservoir for recrudescent *Rickettsia prowazekii* infection in a mouse model. PLoS One 5:e8547

Belkaid Y, Rouse BT (2005) Natural regulatory T cells in infectious disease. Nat Immunol 6:353-360

Ben Amara A, Ghigo E, Le Priol Y, et al. (2010) *Coxiella burnetii*, the agent of Q fever, replicates within trophoblasts and induces a unique transcriptional response. PLoS One 5:e15315

Benoit M, Barbarat B, Bernard A, et al. (2008a) *Coxiella burnetii*, the agent of Q fever, stimulates an atypical M2 activation program in human macrophages. Eur J Immunol 38:1065-1070

Benoit M, Desnues B, Mege JL (2008b) Macrophage polarization in bacterial infections. J Immunol 181:3733-3739

Benoit M, Ghigo E, Capo C, et al. (2008c) The uptake of apoptotic cells drives *Coxiella burnetii* replication and macrophage polarization: a model for Q fever endocarditis. PLoS Pathog 4:e1000066

Benoit M, Thuny F, Le Priol Y, et al. (2010) The transcriptional programme of human heart valves reveals the natural history of infective endocarditis. PLoS One 5:e8939

Capo C, Zaffran Y, Zugun F, et al. (1996) Production of interleukin-10 and transforming growth factor beta by peripheral blood mononuclear cells in Q fever endocarditis. Infect Immun 64:4143-4147

Capo C, Lindberg FP, Meconi S, et al. (1999) Subversion of monocyte functions by *Coxiella burnetii*: impairment of the cross-talk between αvβ3 integrin and CR3. J Immunol 163:6078-6085

Combs TP, Nagajyothi, Mukherjee S, et al. (2005) The adipocyte as an important target cell for *Trypanosoma cruzi* infection. J Biol Chem 280:24085-24094

Dellacasagrande J, Capo C, Raoult D, et al. (1999) IFN-γ-mediated control of *Coxiella burnetii* survival in monocytes: the role of cell apoptosis and TNF. J Immunol 162:2259-2265

Dellacasagrande J, Ghigo E, Capo C, et al. (2000a) *Coxiella burnetii* survives in monocytes from patients with Q fever endocarditis: involvement of tumor necrosis factor. Infect Immun 68:160-164

Dellacasagrande J, Ghigo E, Hammami SM, et al. (2000b) αvβ3 integrin and bacterial lipopolysaccharide are involved in *Coxiella burnetii*-stimulated production of tumor necrosis factor by human monocytes. Infect Immun 68:5673-5678

Desruisseaux MS, Nagajyothi, Trujillo ME, et al. (2007) Adipocyte, adipose tissue, and infectious disease. Infect Immun 75:1066-1078

Ghigo E, Capo C, Amirayan N, et al. (2000) The 75-kD tumour necrosis factor (TNF) receptor is specifically up-regulated in monocytes during Q fever endocarditis. Clin Exp Immunol 121:295-301

Ghigo E, Capo C, Raoult D, et al. (2001) Interleukin-10 stimulates *Coxiella burnetii* replication in human monocytes through tumor necrosis factor down-modulation: role in microbicidal defect of Q fever. Infect Immun 69:2345-2352

Ghigo E, Capo C, Tung CH, et al. (2002) *Coxiella burnetii* survival in THP-1 monocytes involves the impairment of phagosome maturation: IFN-γ mediates its restoration and bacterial killing. J Immunol169:4488-4495

Ghigo E, Honstettre A, Capo C, et al. (2004) Link between impaired maturation of phagosomes and defective *Coxiella burnetii* killing in patients with chronic Q fever. J Infect Dis 190:1767-1772

Harris RJ, Storm PA, Lloyd A, et al. (2000) Long-term persistence of *Coxiella burnetii* in the host after primary Q fever. Epidemiol Infect 124:543-549

Honstettre A, Imbert G, Ghigo E, et al. (2003) Dysregulation of cytokines in acute Q fever: role of interleukin-10 and tumor necrosis factor in chronic evolution of Q fever. J Infect Dis 187:956-962

Honstettre A, Meghari S, Nunes JA, et al. (2006) Role for the CD28 molecule in the control of *Coxiella burnetii* infection. Infect Immun 74:1800-1808

Langley JM, Marrie TJ, Covert A, et al. (1988) Poker players' pneumonia. An urban outbreak of Q fever following exposure to a parturient cat. N Engl J Med 319:354-356

Luhrmann A, Nogueira CV, Carey KL, et al. (2010) Inhibition of pathogen-induced apoptosis by a *Coxiella burnetii* type IV effector protein. Proc Natl Acad Sci USA 107:18997-19001

Luhrmann A, Roy CR (2007) *Coxiella burnetii* inhibits activation of host cell apoptosis through a mechanism that involves preventing cytochrome c release from mitochondria. Infect Immun 75:5282-5289.

Lumeng CN, Bodzin JL, Saltiel AR (2007) Obesity induces a phenotypic switch in adipose tissue macrophage polarization. J Clin Invest 117:175-184

Martinez FO, Helming L, Gordon S (2009) Alternative activation of macrophages: an immunologic functional perspective. Annu Rev Immunol 27:451-483

Martinoli C, Chiavelli A, Rescigno M (2007) Entry route of *Salmonella typhimurium* directs the type of induced immune response. Immunity 27:975-984

Maurin M, Raoult D (1999) Q fever. Clin Microbiol Rev 12:518-553

Meconi S, Jacomo V, Boquet P, et al. (1998) *Coxiella burnetii* induces reorganization of the actin cytoskeleton in human monocytes. Infect Immun 66:5527-5533

Meconi S, Capo C, Remacle-Bonnet M, et al. (2001) Activation of protein tyrosine kinases by *Coxiella burnetii*: role in actin cytoskeleton reorganization and bacterial phagocytosis. Infect Immun 69:2520-2526

Mege JL, Meghari S, Honstettre A, et al. (2006) The two faces of interleukin 10 in human infectious diseases. Lancet Infect Dis 6:557-569

Mege JL, Mehraj V, Capo C (2011) Macrophage polarization and bacterial infections. Curr Op Infect Dis in press

Meghari S, Capo C, Raoult D, et al. (2006) Deficient transendothelial migration of leukocytes in Q fever: the role played by interleukin-10. J Infect Dis 194:365-369

Meghari S, Berruyer C, Lepidi H, et al. (2007) Vanin-1 controls granuloma formation and macrophage polarization in *Coxiella burnetii* infection. Eur J Immunol 37:24-32

Meghari S, Bechah Y, Capo C, et al. (2008) Persistent *Coxiella burnetii* infection in mice overexpressing IL-10: an efficient model for chronic Q fever pathogenesis. PLoS Pathog 4:e23

Munz-Elias EJ, Mc Kinney JD (2002) Bacterial persistence: strategies for survival in immunology of infectious diseases. In: Kaufmann SHE, Sher A, Ahmed R, editors. ASM Press, Washington., p. 331-355

Neyrolles O, Hernandez-Pando R, Pietri-Rouxel F, et al. (2006) Is adipose tissue a place for *Mycobacterium tuberculosis* persistence? PLoS One 1:e43

Ohashi K, Parker JL, Ouchi N, et al. (2010) Adiponectin promotes macrophage polarization toward an anti-inflammatory phenotype. J Biol Chem 285:6153-6160

Ouchi N, Parker JL, Lugus JJ, et al. (2011) Adipokines in inflammation and metabolic disease. Nat Rev Immunol 11:85-97

Roy CR, Mocarski ES (2007) Pathogen subversion of cell-intrinsic innate immunity. Nat Immunol 8:1179-1187

Sansonetti PJ, Di Santo JP (2007) Debugging how bacteria manipulate the immune response. Immunity 26:149-161

Shevach EM (2006) From vanilla to 28 flavors: multiple varieties of T regulatory cells. Immunity 25:195-201

Stein A, Lepidi H, Mege JL, et al. (2000) Repeated pregnancies in BALB/c mice infected with *Coxiella burnetii* cause disseminated infection, resulting in stillbirth and endocarditis. J Infect Dis 181:188-194

Tissot-Dupont H, Amadei MA, Nezri M, et al. (2004) Wind in November, Q fever in December. Emerg Infect Dis 10:1264-1269

Voth DE, Howe D, Heinzen RA (2007) *Coxiella burnetii* inhibits apoptosis in human THP-1 cells and monkey primary alveolar macrophages. Infect Immun 75:4263-4271

Table 1. Role of IL-10 in *C. burnetii* infection

Evidence	**Reference**
- IL-10 specifically increases *C. burnetii* replication in naïve monocytes	Ghigo et al. 2001
- IL-10 produced by patients with chronic Q fever	Capo et al. 1996
- IL-10 produced by patients with valvulopathy and at risk for developing chronic Q fever	Honstettre et al. 2003
- *C. burnetii* infection is controlled in patients with low IL-10 production but not in patients with high IL-10 production. Adding IL-10 to monocytes impairs *C. burnetii* killing that is restored by IL-10 neutralization	Ghigo et al. 2004
- IL-10 neutralization corrects the defective transendothelial migration of leukocytes observed in chronic Q fever	Meghari et al. 2006
- *C. burnetii* infection is persistent in mice that overexpress IL-10 in the macrophage compartment	Meghari et al. 2008

Figure 1. *C. burnetii* and polarization of myeloid cells

In circulating monocytes, *C. burnetii* stimulates an M1 profile that control bacterial replication. In macrophages, *C. burnetii* induces an atypical M2 profile that is unable to control *C. burnetii* replication, as observed during acute Q fever. The treatment of macrophages with IFN-γ reorients them toward a M1 profile.

Figure 2. Modulation of macrophage polarization and *C. burnetii* replication

M2 cytokines and the ingestion of apoptotic cells reorient the polarization of monocytes and macrophages toward a M2 phenotype that allows intense *C. burnetii* replication. This mechanism may occur during the chronic evolution of Q fever. The M2 polarization induced by the uptake of apoptotic cells is reverted by IFN-γ and/or inflammatory context.

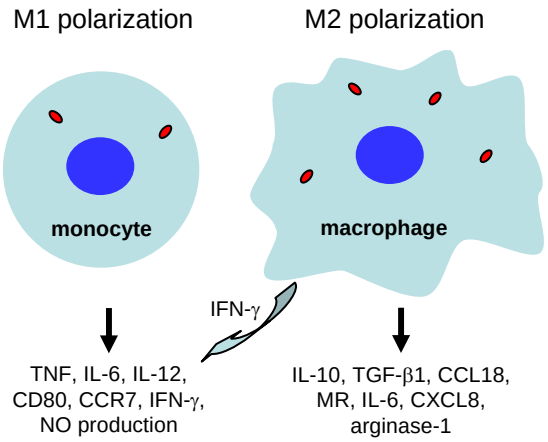
M1 polarization
M2 polarization
monocyte
macrophage
IFN-γ
TNF, IL-6, IL-12,
CD80, CCR7, IFN-γ,
NO production
IL-10, TGF-β1, CCL18,
MR, IL-6, CXCL8,
arginase-1

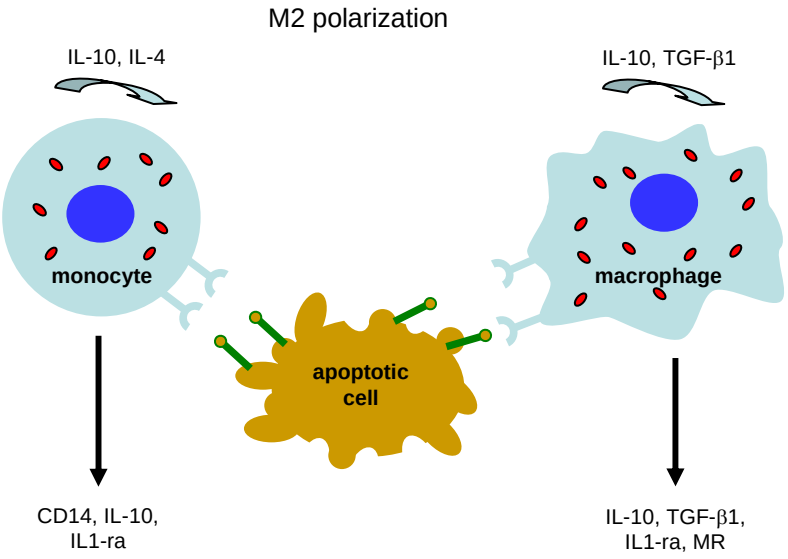
M2 polarization
IL-10, IL-4
IL-10, TGF-β1
monocyte
macrophage
apoptotic cell
CD14, IL-10, IL1-ra
IL-10, TGF-β1, IL1-ra, MR

EXPOSE

DES TRAVAUX

ARTICLE 1

Coxiella burentii, the agent of Q fever, replicates within trophoblasts and induces a unique transcriptional response

Amira Ben Amara, Eric Ghigo, Yannick Le Priol, Catherine Lépolard, Suzana P. Salcedo, Emmanuel Lemichez, Florence Bretelle, Christian Capo, Jean-Louis Mege

PLoS One, 2010, 5 : e15315

Le placenta peut être la cible de *C. burnetii* puisque l'infection des femmes enceintes se traduit notamment par de graves conséquences obstétricales. De nombreuses études effectuées sur le bétail montrent aussi que l'infection des animaux par *C. burnetii* est à l'origine d'avortements et constitue de ce fait un problème de santé vétérinaire aux conséquences économiques majeures. En outre, la voie principale de contamination humaine par *C. burnetii* est constituée des aérosols provenant des placentas infectés.

La nature des cellules placentaires cibles de *C. burnetii* reste totalement inconnue. Dans une première approche pour répondre à cette question, nous avons utilisé comme modèle de trophoblastes, le principal type de cellules constituant le placenta, les cellules de la lignée trophoblastique BeWo.

Nous avons montré que *C. burnetii* infecte les cellules BeWo et s'y réplique bien que les bactéries résident dans un compartiment de type phagolysosome. Une étude en microarray a montré que *C. burnetii* induit un profil inflammatoire « atypique » dans le sens où il diffère de celui induit par une cytokine inflammatoire classique telle que le TNF. Ce programme transcriptionnel est très particulier puisqu'il montre la surexpression de gènes impliqués dans le développement placentaire et l'angiogenèse, ce qui laisse penser que *C. burnetii* maintient l'expression des gènes qui assurent le développement du placenta afin d'assurer sa propre survie.

OPEN ACCESS Freely available online

PLoS one

Coxiella burnetii, the Agent of Q Fever, Replicates within Trophoblasts and Induces a Unique Transcriptional Response

Amira Ben Amara[1], Eric Ghigo[1], Yannick Le Priol[2], Catherine Lépolard[1], Suzana P. Salcedo[3], Emmanuel Lemichez[4], Florence Bretelle[1], Christian Capo[1], Jean-Louis Mege[1]*

1 Unité de Recherche sur les Maladies Infectieuses Tropicales et Emergentes, CNRS-IRD UMR 6236, IFR 48, Université de la Méditerranée, Marseille, France, **2** IMTSSA, Transcriptomic Platform, Parc du Pharo, Marseille, France, **3** Centre d'Immunologie de Marseille-Luminy, Université de la Méditerranée, UMR 6546, Marseille, France, **4** INSERM Unité 895, Equipe 6, C3M, Microbial Toxins in Host Pathogen Interactions, Nice, France

Abstract

Q fever is a zoonosis caused by *Coxiella burnetii*, an obligate intracellular bacterium typically found in myeloid cells. The infection is a source of severe obstetrical complications in humans and cattle and can undergo chronic evolution in a minority of pregnant women. Because *C. burnetii* is found in the placentas of aborted fetuses, we investigated the possibility that it could infect trophoblasts. Here, we show that *C. burnetii* infected and replicated in BeWo trophoblasts within phagolysosomes. Using pangenomic microarrays, we found that *C. burnetii* induced a specific transcriptomic program. This program was associated with the modulation of inflammatory responses that were shared with inflammatory agonists, such as TNF, and more specific responses involving genes related to pregnancy development, including EGR-1 and NDGR1. In addition, *C. burnetii* stimulated gene networks organized around the IL-6 and IL-13 pathways, which both modulate STAT3. Taken together, these results revealed that trophoblasts represent a protective niche for *C. burnetii*. The activation program induced by *C. burnetii* in trophoblasts may allow bacterial replication but seems unable to interfere with the development of normal pregnancy. Such pathophysiologocal processes should require the activation of immune placental cells associated with trophoblasts.

Citation: Ben Amara A, Ghigo E, Le Priol Y, Lépolard C, Salcedo SP, et al. (2010) *Coxiella burnetii*, the Agent of Q Fever, Replicates within Trophoblasts and Induces a Unique Transcriptional Response. PLoS ONE 5(12): e15315. doi:10.1371/journal.pone.0015315

Editor: Olivier Neyrolles, Institut de Pharmacologie et de Biologie Structurale, France

Received September 2, 2010; **Accepted** November 8, 2010; **Published** December 14, 2010

Funding: The work was supported by the Programme Hospitalier de Recherche Clinique 2008. The funders had no role in study design, data collection and analysis, decision to publish, or preparation of the manuscript.

Competing Interests: The authors have declared that no competing interests exist.

* E-mail: Jean-Louis.Mege@univmed.fr

Introduction

Q fever is a widespread zoonosis caused by *Coxiella burnetii*, an intracellular gram-negative bacterium recognized as a potential category-B bioweapon. Human primary infection is asymptomatic or present as isolated fever, hepatitis, or pneumonia. It spontaneously resolves but may become chronic endocarditis in patients with valve lesions, arterial aneurysm, or prosthesis or in those who are immunocompromised [1]. During pregnancy, Q fever may result in obstetric complications including spontaneous abortion, intrauterine growth retardation or fetal death, and premature delivery. In addition, pregnant women exhibit an increased risk of Q fever endocarditis even in the absence of underlying valvular lesions [2]. This phenomenon has been reproduced in C57BL/6 mice, where infection followed by repeated pregnancies was shown to result in spontaneous abortion, perinatal death and endocarditis in some animals [3]. In cattle, sheep and goats, *C. burnetii* infection is often unapparent [4,5], but there is increasing evidence that it is associated with spontaneous abortion and stillbirth [5,6]. The placentas of infected animals contain up to 10^9 organisms/g of tissue, and it is likely that heavily infected placentas contaminate the environment at the time of parturition, leading to the persistence of viable organisms in the soil for several months [7]. In addition, aerosols from the secretions and excretions of ruminants are the major source of contamination for humans [8].

C. burnetii is known to survive in the myeloid cells of humans and experimentally infected mice by resisting their natural microbicidal activity [9,10]. The cell types infected by *C. burnetii* in humans during pregnancy are unknown. Immunocytochemical studies have shown that in cows the *C. burnetii* antigen is present within trophoblasts, especially along the base of chorionic villi and in the intervillous spaces in the placentas of aborted fetuses [11]. Using in situ hybridization, it has been shown that *C. burnetii* is found both within trophoblasts and free in placenta debris from ruminant abortions [12]. Inoculation of *C. burnetii* into pregnant goats leads to an initial infection of trophoblasts of the choriallantoic membrane that precedes a massive bacterial colonization of the placenta, followed immediately by spontaneous abortion [13]. Most studies of pathogens exhibiting placental tropism, such as human cytomegalovirus [14], *Toxoplasma gondii* [15] or *Brucella abortus* [16], have used placental tissues but were unable to define the cell targets of the infection.

Although the precise mechanisms by which infection compromises pregnancy are largely undefined, it is clear that excessive inflammation at the maternal interface could play a critical role.

Placental tissue contains trophoblasts and cells with inflammatory and immunomodulatory potential that can be mobilized in response to infection. Among the inflammatory mediators produced by cells at the materno-fetal interface, Tumor Necrosis Factor (TNF) may affect both placental function and the local immune response. Studies have shown that TNF is critical for both fetal development and placental function [17]. TNF is beneficial during the pre-implantation period; it prevents development of offspring with structural anomalies, controls the differentiation of extravillous trophoblasts, balances trophoblast turnover and renewal, and stimulates uterine activity. However, exaggerated production of TNF induces apoptosis of trophoblasts, inhibits the production of human chorionic gonadotropin and the subsequent trophoblast fusion, and controls invasive trophoblast differentiation. These deleterious events that occur during bacterial and viral infections [18] may lead to obstetrical complications such as preeclampsia, premature rupture of membranes, preterm labor and spontaneous abortion.

Because the cellular distribution of *C. burnetii* in the placenta is not known, we chose to investigate if this bacterial pathogen could infect trophoblasts, which are essential for successful pregnancy. We show that *C. burnetii* infects and replicates within BeWo trophoblasts, a human trophoblastic cell line. Further, we show that *C. burnetii* stimulation induces a transcriptional activation program consisting of both *C. burnetii*-specific features and an inflammatory response similar to TNF. Such findings demonstrate that trophoblasts are a target for *C. burnetii* and respond to the bacteria with an activation program that could account for pregnancy complications resulting from Q fever.

Results

C. burnetii replication in BeWo trophoblasts

Because *C. burnetii* is found in the placenta of aborted fetuses [11,19], we investigated the ability of *C. burnetii* organisms to infect BeWo trophoblasts. We extended the previously described procedure for establishing macrophage infection by *C. burnetii* [20] to BeWo trophoblasts. Cells were infected with different doses of bacteria per cell for 4 hours and washed to remove any unbound bacteria; this time was defined as day 0. We found that BeWo cells were infected by *C. burnetii* in a dose-dependent manner (Fig. 1, inset), as demonstrated by qPCR analysis performed on the *C. burnetii com1* gene [9]. Using immunofluorescence, we determined that roughly 50% of infected cells contained one or two bacteria (data not shown), a level of infection similar to that previously described in human monocytes [21]. In subsequent experiments, an infecting dose of 200 bacteria per cell was used. We found that BeWo trophoblasts supported substantial bacterial replication (Fig. 1). At day 0, the number of bacterial DNA copies was $14\pm0.5\times10^2$; this number increased ninety fold at day 3 post-infection and steadily increased thereafter to reach $2.6\pm0.8\times10^6$ at day 9 post-infection. These results clearly demonstrated that BeWo cells were pertinent to the study of *C. burnetii* replication in trophoblasts.

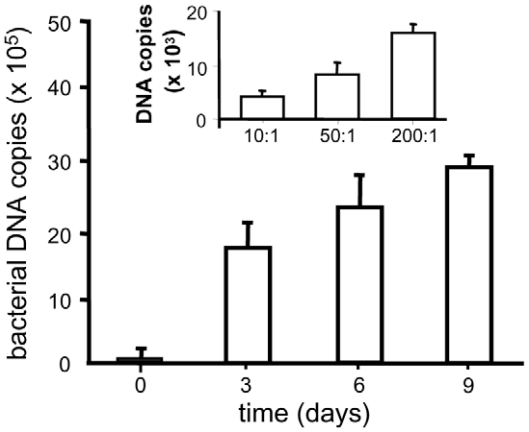

Figure 1. Intracellular fate of *C. burnetii*. BeWo trophoblasts were incubated with different concentrations of *C. burnetii* (10, 50 and 200 bacteria/cell) for 4 h and extensively washed to remove free organisms (insets). They were then cultured for 9 d. The number of bacterial DNA copies was determined using qPCR. The results represent the mean ± SEM of 3 experiments.
doi:10.1371/journal.pone.0015315.g001

Because the survival of *C. burnetii* in macrophages is based on the defective maturation of *C. burnetii*-containing phagosomes into phagolysosomes [20], we investigated the characteristics of the *C. burnetii*-containing compartment in BeWo trophoblasts using confocal microscopy (Fig. 2). At day 0, the majority of organisms co-localized with lysosomal-associated membrane protein (Lamp)-1, a marker of late endosomes and lysosomes [20]; only $27\pm8\%$ of organisms co-localized with cathepsin D, a marker of lysosomes [20]. At day 6 post-infection, more than 80% of organisms co-localized with both cathepsin D and Lamp-1. Taken together, these results showed that the replication of *C. burnetii* in BeWo trophoblasts was associated with the presence of the bacteria in phagolysosomes.

C. burnetii-induced transcriptional program

A whole-genome microarray approach was used to define the transcriptional signature of *C. burnetii* infection in BeWo trophoblasts. We found that 340 genes were significantly modulated after a 6-hour stimulation with *C. burnetii* (Fig. 3A); they consisted of 279 up-regulated genes with fold changes (FCs) ranging from 1.4 to 4.96 (Table S1) and 61 down-regulated genes with FCs ranging from -1.4 to -1.83 (Table S2). The clustering analysis of the 340 genes modulated in response to *C. burnetii* stimulation revealed a specific profile that could be organized in 6 clusters using GO terms (Fig. 3B). Cluster 1 contained 38 genes up-regulated in response to *C. burnetii* stimulation and showed enrichment for genes involved in apoptosis and kinase signaling. Cluster 1 also showed that the expression of the monocarboxylate transporter SCL16A3 (a solute carrier family 16 protein), which is known to play a role in pre-implantation [22], increased in response to *C. burnetii* stimulation. In cluster 2, 48 genes corresponding to cell motility and calcium binding GO terms were enriched in response to *C. burnetii* stimulation. These included genes encoding EGR1 (early growth response 1), IL4R (interleukin 4 receptor), MMP9 (matrix metallopeptidase 9), NDRG1 (N-myc-downstream regulated 1) and TGF-β1 (Transforming Growth Factor). The increased expression of these genes was confirmed by real-time RT-PCR (Fig. 4A). In addition, the expression level of EGR-1 protein in *C. burnetii*-stimulated BeWo cells was determined by western blot. The results showed that the amounts of EGR-1 were higher in stimulated BeWo cells than in control cells (Fig. 4B); autoradiograms quantified by scanning densitometry revealed a relative enrichment of 1.47 ± 0.23. In clusters 3 and 4, *C. burnetii* induced a moderate modulation of 18 and 24 genes, respectively (Fig. 3B). These genes showed enrichment for actin-binding and cell-cell signaling proteins. In cluster 5, 56 genes were modulated with enriched GO terms for immune and inflammatory responses. Among these genes, the expression of the genes encoding CXCR6, IFNGR2 (interferon-gamma receptor 2, also known as IFNγ transducer 1), MMP12 (also known as macrophage elastase), TNFAIP3 (tumor

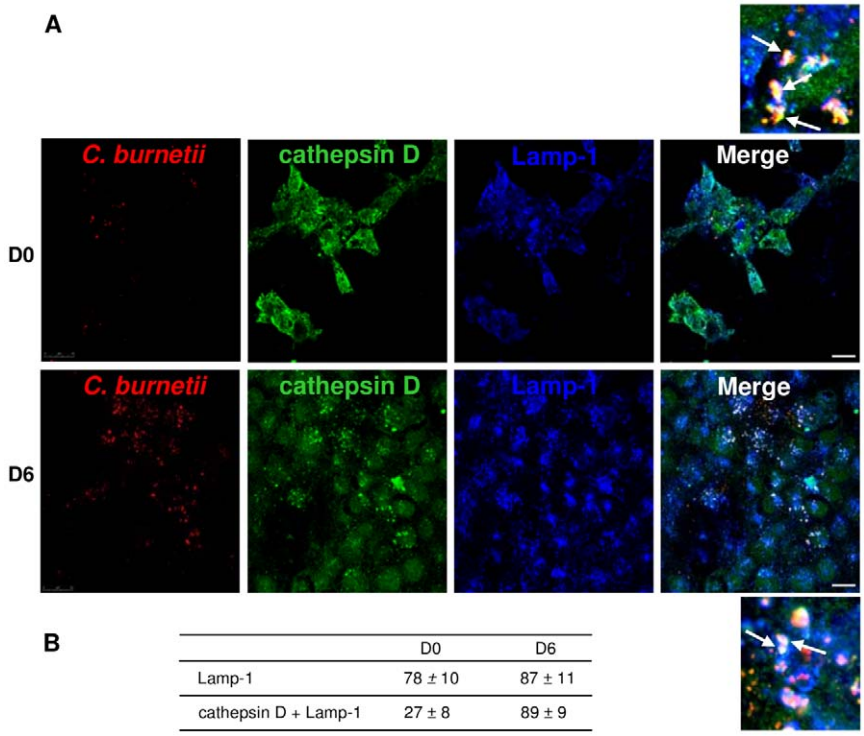

	D0	D6
Lamp-1	78 ± 10	87 ± 11
cathepsin D + Lamp-1	27 ± 8	89 ± 9

Figure 2. Intracellular localization of *C. burnetii*. Infected BeWo cells were labeled with anti-*C. burnetii* (Alexa 546), anti-cathepsin D (Alexa 488) and anti-Lamp-1 (Alexa 647) Abs and analyzed by laser scanning confocal microscopy. A, The co-localization of *C. burnetii* (red) with Lamp-1 (blue) and cathepsin D (green) is demonstrated by merging the respective fluorescent images. The co-localization of bacteria with both Lamp-1 and cathepsin D appears as white (see arrows), whereas the co-localization of bacteria with only Lamp-1 appears as yellow (see arrows). B, The percentage of bacteria that co-localized with Lamp-1 and cathepsin D was recorded. The results represent the mean ± SD of approximately 60 cells for each experimental condition. Scale bars represent 5 μm. D0 and D6 are day 0 and day 6 post-infection, respectively.
doi:10.1371/journal.pone.0015315.g002

necrosis factor alpha-induced protein 3), TNFSF10 (TNF ligand superfamily member 10), CD83, FOS (FBJ murine osteosarcoma viral oncogene homolog) and S100A9 (S100 calcium-binding protein A9) were up-regulated. This increased expression was confirmed using real-time RT-PCR (Fig. 4C). Interestingly, the analysis of cluster 6 (representing 51 modulated genes) showed that *C. burnetii* depressed the expression of the INDO gene (indoleamine-pyrrole 2,3-dioxygenase) and increased expression of CASP5 (apoptosis-related cysteine peptidase). These changes were confirmed by real time RT-PCR (Fig. 4D). Taken together, these results showed a specific transcriptional program in BeWo trophoblasts infected with *C. burnetii*.

Specific transcriptional networks stimulated by *C. burnetii*

The genes found to be modulated in response to *C. burnetii* infection were analyzed with molecular networks using pathway classification and web-based entry tools. This analysis revealed two enriched networks in the response of BeWo trophoblasts to *C. burnetii* infection. The first network consisted of 48 genes and was organized around IL6ST (IL6 signal transducer), also called gp130 (Fig. 5A). In this network, 23 genes were up-regulated in response to *C. burnetii* infection, including IL6ST, STAT3 (signal transducer and activator of transcription, also known as acute phase response factor), JUN (JUN oncogene), IL27RA (interleukin 27 receptor alpha), CCND1 (cyclin D1, also known as parathyroid adenomatosis 1 (PRAD1)) and RHO genes (rhodopsin). Among the 25 genes down-modulated in response to *C. burnetii* infection, some were specific for *C. burnetii*, including IGF2 (insulin-like growth factor 2 or somatomedin A), GFAP (glial fibrially acidic protein) and PCSK1 (proprotein cinvertase subtilisin, also known as kexin type 1). The second network that was markedly up-regulated in response to *C. burnetii* infection was organized around IL13RA2 (IL13Rα2) (Fig. 5B). The network consisted of 7 seven genes, of which five were up-regulated (TGFβ1, IL4R, ADM [adrenomedullin], STAT3, IL13RA1 [IL-13 receptor, alpha 1]) and 2 were down-regulated, including IFN-γ. Taken together, the transcriptional program stimulated by *C. burnetii* was organized in specific networks that were comparable to those induced by TNF stimulation (Fig. S1).

Transcriptional and protein patterns induced by TNF

Because *C. burnetii* infection stimulated a transcriptional program in BeWo cells in which inflammatory GO terms were enriched, we next investigated whether or not this program was similar to that induced by a typical inflammatory cytokine (TNF) known to activate trophoblast cells [23]. The transcriptional signature induced by TNF was quantitatively and qualitatively different from that induced by *C. burnetii* infection. First, TNF only induced the modulation of 166 genes (142 up-regulated and 24 down-modulated genes), less than half of the total modulated by *C. burnetii* infection (279 and 61 up- and down-regulated, respectively). Second, the majority of genes modulated by TNF were also modulated by *C. burnetii* infection (Fig. 3A), suggesting that *C. burnetii* infection induced an inflammatory response of BeWo cells. In contrast, a very large proportion of the *C. burnetii* infection-modulated genes were *C. burnetii*-specific (Fig. 3A), demonstrating that the response of BeWo cells to *C. burnetii* infection included other major functions.

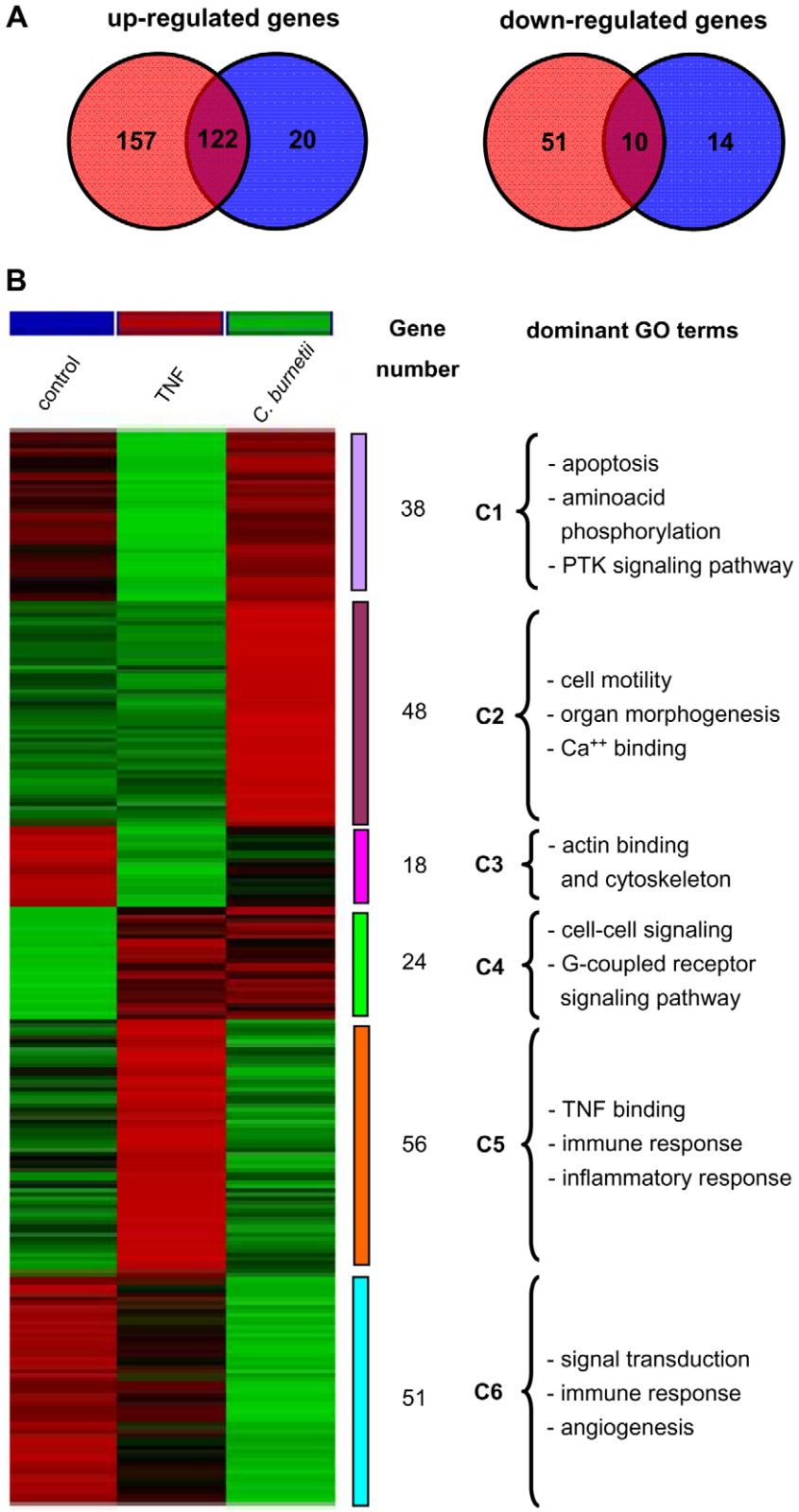

Figure 3. Venn diagram and hierarchical clustering analysis. BeWo cells were incubated with *C. burnetii* (200 bacteria/cell) or TNF (10 ng/mL) for 6 h. Total RNA was extracted and, after cyanin-3 incorporation, hybridized on chips representing 31,054 genes. Only genes that were expressed with a P value <0.05 and a confidence value >0.3 in at least one condition were included in the analysis. A, The number of genes modulated in response to *C. burnetii* (red) and TNF (blue) stimulation is indicated. Intersections showed that 122 and 10 genes were up-regulated and down-regulated, respectively, by both *C. burnetii* and TNF stimulation. B, Data were analyzed using hierarchical clustering and are represented by a color gradient (Z-score) ranging from blue (down-modulation) to yellow (up-regulation). Left: unstimulated cells (NS); middle: TNF-stimulated cells; Right: *C. burnetii*-stimulated cells. The GO analysis was performed using two filters: 1. GO term level 2$<$ gene $<$11; 2. when GO term is represented by more than 3 genes on the chip and contains more than 2 genes of the study set. The number of genes in every biological process is presented.
doi:10.1371/journal.pone.0015315.g003

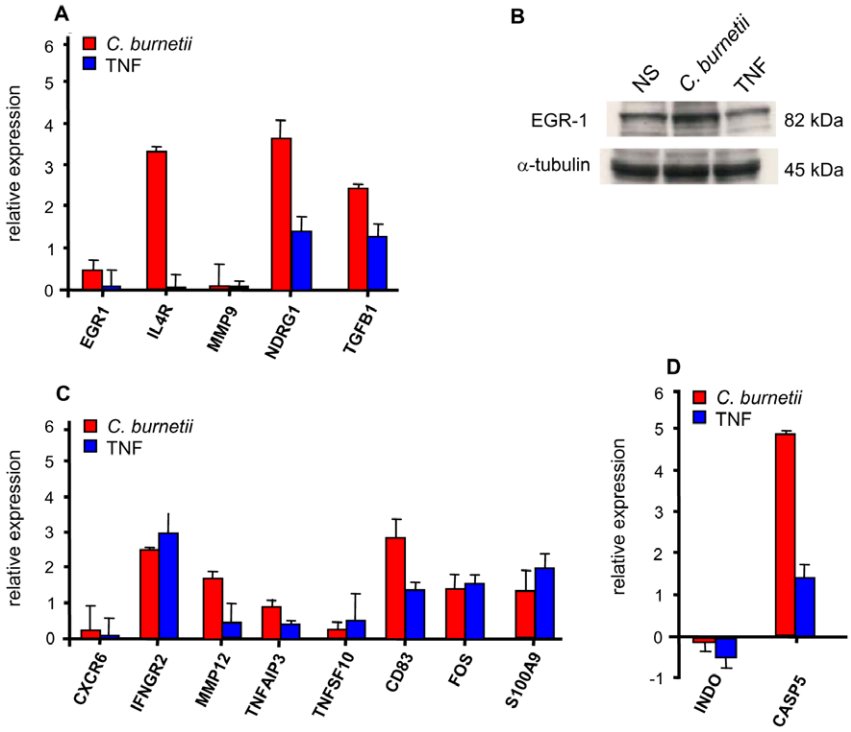

Figure 4. Real time RT-PCR and western blot analysis. BeWo cells were stimulated with *C. burnetii* for 6 h. A, C and D; RNA was extracted and real time RT-PCR was performed. Results expressed in relative expression (stimulated vs. unstimulated conditions) represent the mean ± SEM of 3 independent experiments. B, Western blot analysis was performed using specific mAbs for α-tubulin and EGR-1, and bands were revealed by chemoluminescence. Their intensity was determined by densitometry and represented the mean of three experiments.
doi:10.1371/journal.pone.0015315.g004

GO term classification showed that the genes found in clusters 5 and 6 were commonly enriched in response to TNF stimulation and *C. burnetii* infection. They included the genes encoding CXCR6, IFNGR2, MMP12, TNFAIP3, TNFSF10, CD83, FOS (FBJ murine osteosarcoma viral oncogene homolog), S100A9 and CASP5. Again, the increased expression of these genes was confirmed using real time RT-PCR (Fig. 4, C and D). Note that the INDO gene that was down-modulated in response to *C. burnetii* was also depressed in response to TNF stimulation (Fig. 4D). GO term classification also showed major differences in the transcriptional responses induced by *C. burnetii* infection and TNF treatment. Indeed, in cluster 2, the expression of the genes encoding EGR-1, IL4R, MMP9, NDRG1 and TGFβ1 was weakly modulated by TNF treatment when compared to the induction by *C. burnetii* infection (Fig. 4A). In addition, western blotting used to determine EGR-1 protein expression demonstrated that TNF stimulation was unable to up-regulate its expression (Fig. 4B). Taken together, our results showed that TNF induced transcriptional responses in BeWo trophoblasts that were not superimposable with those induced by *C. burnetii* infection.

Discussion

The aim of this study was to investigate the ability of *C. burnetii* to use trophoblastic cells as a replicative niche. We found that *C. burnetii* is able to infect and replicate within BeWo trophoblasts. The intracellular fate of *C. burnetii* in BeWo trophoblasts is dramatically different from that observed in human monocytes [21] and macrophages [24], in which *C. burnetii* survives but does not replicate. Even in the presence of potent immunoregulatory cytokines, such as IL-10, macrophages are less permissive for *C. burnetii* replication [24] than BeWo trophoblasts. The pertinence of BeWo trophoblasts as a model to study the interplay between trophoblasts and bacterial pathogens is supported by the fact that BeWo cells share several properties with human villous trophoblasts, including morphology, biochemical markers and hormone secretion [25,26]. It is likely that trophoblasts are a replicative niche for *C. burnetii*, and the results presented here may explain why these bacteria are found in abundance in infected placentas [5,6].

The intracellular life cycle of *C. burnetii* in BeWo cells was found to be based on replication in phagolysosomes. These results were markedly different from those found in macrophages, where *C. burnetii* resides and replicates within an acidic phagosome that expresses Lamp-1 but not cathepsin D [20]. These findings may be related to those found using non-microbicidal cells, in which *C. burnetii* was shown to reside in phagolysosomes or autophagosomes [27]. It is likely that the intracellular localization of *C. burnetii* is dependent on the cell type used. *Brucella*, which replicates in JEG trophoblasts, is localized within endoplasmic reticulum-derived compartments in epithelial cells [28]; however, it is unable to fuse with lysosomes in macrophages in an acidic compartment [29]. *Mycobacterium tuberculosis* localizes within early phagosomes in macrophages, [30] but in monocyte-derived dendritic cells, it escapes from phagosomes and replicates within the cytosol [31]. It has recently been suggested that the mode of bacterial entry changes the nature of the compartment where *M. tuberculosis* resides without affecting its replication [32]. We cannot rule out the possibility that *C. burnetii* uses different receptors to invade trophoblasts and myeloid cells [21]. Also, we can speculate that the molecular composition of phagolysosomes from macrophages is different from that of non-microbicidal cells. Indeed, the NADPH

A. IL-6ST pathway

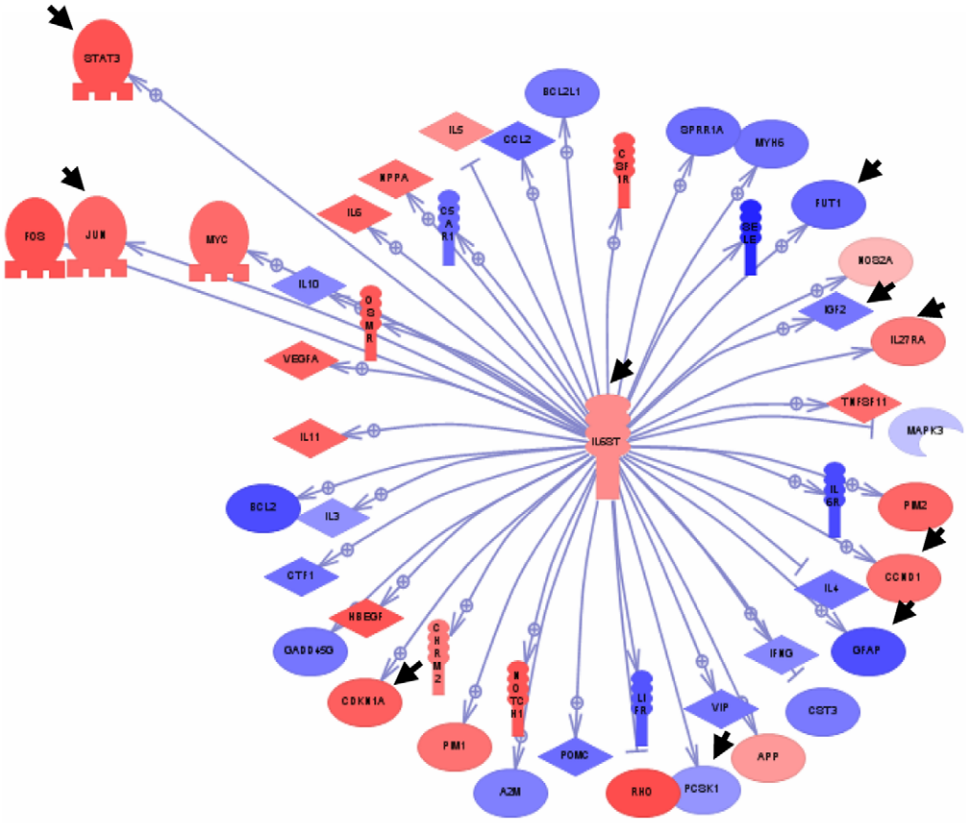

B. IL13RA2 pathway

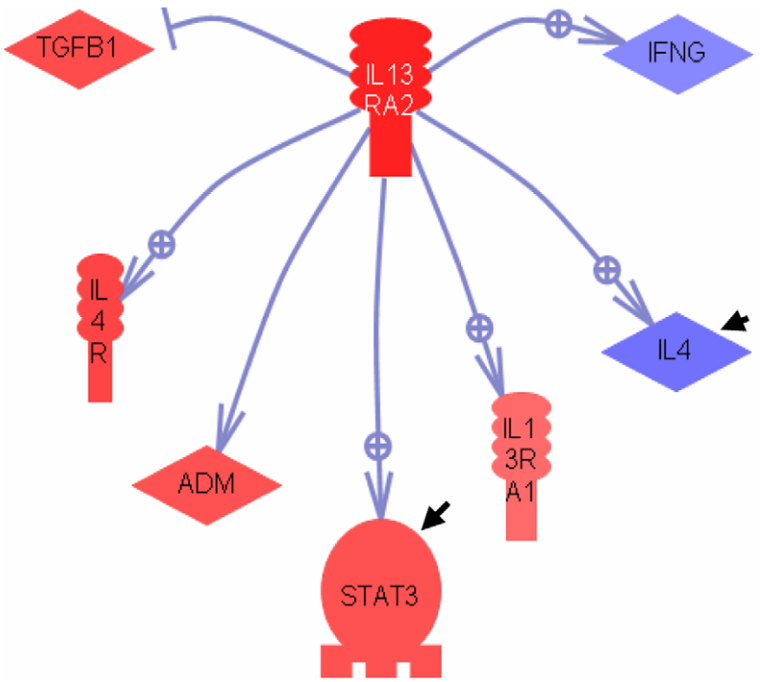

Figure 5. IL-6ST and IL-13RA2 pathways in *C. burnetii*-stimulated BeWo cells. The IL-6ST (A) and IL-13RA2 (B) pathways induced in BeWo cells by *C. burnetii* stimulation were identified using Pathway Studio© software. Up-regulated genes appeared in red and down-regulated genes in blue. Arrowheads represent the differences with TNF stimulation.
doi:10.1371/journal.pone.0015315.g005

oxidase, that is involved in the generation of reactive oxygen intermediates, is known to be highly active in stimulated phagocytic cells but is poorly active in non-microbicidal cells [33]. In addition, the inflammatory program induced in myeloid cells is dramatically higher than in non-myeloid cells. The conjunction of the lytic enzymes present in phagolysosomes with the generation of oxidative burst and the production of inflammatory mediators may inhibit *C. burnetii* replication in macrophages while the inability of trophoblast cells to mount an efficient oxidative response may favor *C. burnetii* replication.

C. burnetii induced a transcriptional program in BeWo trophoblasts that is organized in 6 clusters of genes based on GO terms. Some clusters shared by both *C. burnetii* and TNF were enriched for inflammation and immunity GO terms. They included several up-regulated genes including TNF-related genes (TNF, TNFAIP3, TNFSF10), IFN-γ-related genes (IFNγR2) and inflammatory mediators (MMP12, S100A9). This inflammatory response is strengthened by the down-modulation of INDO, which is known to exert an anti-inflammatory response that protects developing fetuses from the maternal immune response [34]. The decreased expression of INDO has been associated with cases of miscarriage [35]. These changes in inflammation and immunity GO terms suggest a type 1 cytokine response in trophoblasts. This is consistent with the results we previously obtained with monocytes in which *C. burnetii* stimulated an M1-type program [36]. This is also consistent with the response of different trophoblastic cell lines to the bacterial pathogen *Chlamydia trachomatis* [37]. Other genes organized in clusters were specifically modulated in response to *C. burnetii* but not to TNF. They included genes involved in pregnancy development; hence, *C. burnetii* modulated several genes related to apoptosis. The relationship between apoptosis and pregnancy is complex: a certain level of apoptosis is necessary for placental implantation and protects from obstetrical complications. By contrast, any further increases in the level of apoptosis may compromise normal development of pregnancy [38]. This is distinct from macrophages in which *C. burnetii* inhibits apoptosis [27]. In addition, the apoptosis of *C. burnetii*-infected macrophages by IFN-γ is associated with *C. burnetii* killing [39]. Our results suggest that the induction of apoptosis pathways favors *C. burnetii* replication in BeWo trophoblasts. They also suggest that *C. burnetii* does not interfere with the pro-implantation function of trophoblasts. This latter hypothesis is strengthened by the fact that the transporter SCL16A3, necessary for pre-implantation [40] was up-regulated in response to *C. burnetii* stimulation, whereas TNF stimulation down-modulated its expression. Two genes specifically modulated by *C. burnetii*, EGR-1 and NDRG1, likely play a major role in pregnancy. The expression level of EGR-1 is known to increase in the first trimester of pregnancy and decreases thereafter; thus, it may play a role in trophoblast transcriptional activity and growth [41]. *C. burnetii* stimulated the transcriptional expression of EGR-1, whereas TNF had no effect on the transcription and protein expression levels of EGR-1 (Fig. 4B). The ability to activate EGR-1 has been reported with other pathogens, including group B *Streptococcus* and *Chlamydia pneumoniae* [42,43]. NDRG1 is a cytoplasmic and nuclear protein involved in stress or hormone responses and cell growth and differentiation. Its expression in primary trophoblasts is stimulated by placental injury [44] and is associated with pregnancy complications [45]. Expression of the NDRG1 gene is known to be stimulated by TGF-β1 [46], and we found that both genes were up-regulated in BeWo trophoblasts stimulated with *C. burnetii*. It is tempting to relate apoptosis, which plays a critical role in the decidual regression that occurs in the end of pregnancy, to TGF-β, which is expressed in the endoterium during decidual basilis regression [46]. As TGF-β is involved in the regulation of apoptosis, we suggest that TGF-β plays an important role in the remodeling of the decidua and governs the apoptotic mechanisms observed during decidua regression [47].

We next tested if the genes modulated in response to *C. burnetii* were organized into networks. We found that *C. burnetii* stimulation induced two pathways: IL6ST and IL13RA2. The IL6 network refers to the molecules that IL6ST (gp130) helps regulate, such as IL-6, IL-11, IL-27 and STAT3. Cytotrophoblasts with an invasive phenotype express IL-6 and its receptor; IL-11 is also expressed by trophoblasts and boosts their migration [48]. IL6ST is essential for placental development because its disruption impairs placentation [49]. A critical link in the IL-6 network was the up-regulation of STAT3 in response to *C. burnetii* stimulation. STAT3 activation has been observed in human placental trophoblasts and trophoblast cell lines in response to T cell products including IL-6 [50]. The inactivation of STAT3 in mice prevents implantation [51]. A major difference between the transcriptional responses of BeWo cells to *C. burnetii* (Fig. 5) and TNF (Fig. S1) stimulation was the down-modulation of STAT3 in response to TNF that contrasted sharply with the up-regulation in response to *C. burnetii*. Our findings suggest that *C. burnetii* does not interfere with the implantation process through STAT3 whereas TNF, which down-modulates STAT3, could compromise normal pregnancy. The network organized around IL13RA2 involves a decoy receptor for IL-13 that exists in membrane, cytoplasmic and soluble forms [52]. The soluble form of IL-13 decoy receptor may interfere with IL-13 signaling, and the membrane form of IL13RA2 attenuates IL-13 responses [53,54]. The down-modulation of STAT3 is found in several networks, including that of IL13RA2. Studies using tumor cells have shown that the expression of IL13RA2 up-regulates that of STAT3, which ultimately compromises the IL-13 signal [55].

In conclusion, we report here for the first time the ability of *C. burnetii* to infect and replicate within trophoblastic cells. The analysis of the transcriptomic program induced by *C. burnetii* revealed the presence of a non-specific inflammatory response and the increased expression of genes associated with placental development. These results suggest that trophoblasts could be a niche for *C. burnetii* because their activation would not be sufficient to compromise a normal pregnancy. It is likely that the cooperation of trophoblasts and placental immune cells (which are responsive to *C. burnetii*) within the placental tissue impairs the development of pregnancy.

Materials and Methods

Ethics Statement

The mice used in our study were handled in strict accordance with the rules of Décret N° 87-848 of 10/19/1987, Paris. The experimental protocol have been reviewed and approved by the Institutional Animal Care and Use Committee of the Université de la Méditerranée (experimentation permit number C13-055-9; personal agreements 13-04 and 13-472).

Bacteria and cells

C. burnetii bacteria (RSA493 Nile Mile strain) were phenotyped [56] and cultured [21] as previously described. The dilacerated spleens of BALB/c mice infected with 10^8 *C. burnetii* organisms for 7 d were added to L929 cells. Infected cells were sonicated and centrifuged at 300×g for 10 min. Supernatants were collected and centrifuged at 10,000×g for 10 min. The concentration of organisms was determined by Gimenez staining, and the bacterial viability was assessed using the LIVE/DEAD BacLight bacterial viability kit (Molecular Probes). The BeWo (number CCL-98) cell line was obtained from ATCC. Cells were cultured in F-12 Ham medium (Invitrogen) containing 10% FCS, 2 mM L-glutamine, 100 U/ml penicillin and 50 µg/ml streptomycin. Confluent monolayers were trypsinized twice a week.

C. burnetii infection

BeWo trophoblasts (2×10^5/well) were cultured in flat-bottom 24-well plates for 48 h. They were then incubated with different doses of *C. burnetii* for 4 h. After washing to remove free bacteria (time designated as day 0), cells were cultured for 9 d. Infection was quantified using quantitative real time PCR (qPCR) as previously described [57]. In brief, DNA was extracted using a DNA Mini Kit (Qiagen) and stored in 100 µL aliquots at -20°C. qPCR was performed using 5 µL of DNA extract and the LightCycler FastStart DNA SYBR green system (Roche). The primers F *com1* (5′-GCACTATTTTTAGCCG-GAACCTT-3′) and R *com1* (5′-TTGAGGAGAAAA-ACTGGATTGAGA-3′) amplified a 225-bp fragment of the *C. burnetii com1* gene (GeneBank accession no. AF318146). The specificity of the PCR product was confirmed by sequencing. In each qPCR run, a standard curve was generated using serial dilutions ranging from 10^8 to 10^4 copies of the intergenic spacer region and calculated by the Light Cycler 5.32 software (LC-Run version 5.32, Roche).

Characterization of *C. burnetii* compartment

The compartment in which *C. burnetii* replicated was studied using immunofluorescence, as previously described [20]. BeWo trophoblasts were seeded on glass cover slips prior to infection with *C. burnetii*. After fixation in 3% paraformaldehyde, cells were permeabilized with 0.1% Triton X-100 and incubated with mouse antibodies (Abs) specific for Lamp-1 (1:1000,Abcam), rabbit Abs directed against cathepsin D (1:1000, a gift from Dr. Kornfeld, St. Louis, MO) and human Abs specific for *C. burnetii* (1:8000 dilution) obtained from patients with Q fever with their informed consent. After washing, cells were incubated with secondary fluorescent Abs (Invitrogen), washed, mounted with Mowiol, and analyzed by epifluorescence and laser scanning microscopy. Images were acquired using a confocal microscope (Leica TCS SP5) with a 63X/1.32-0.6 oil objective, an electronic magnification of 1.5× and a resolution of 1024×1024 pixels. Optical sections of fluorescent images were collected at 0.15-µm intervals using the Leica Confocal Software and processed using Adobe Photoshop© V7.0.1. At least 60 cells were examined for each experimental condition. Results were expressed as the percentage of bacteria that co-localized with fluorescent markers with the following color code: the colocalization of bacteria (in red) with Lamp-1 (green) resulted in yellow color; the colocalization of bacteria (red) with cathepsin D (blue) resulted in pink color; the colocalization of bacteria (red) with Lamp-1 (green) and cathepsin D (blue) resulted in white color.

Microarrays and data analysis

BeWo trophoblasts were stimulated with *C. burnetii* (200 bacteria/cell) or 10 ng/mL human recombinant TNF (R&D Systems) for 6 h, and total RNA was extracted using an RNeasy Mini Kit (Qiagen) and DNase treatment as previously described [58]. The quality of the RNA preparation was assessed using the 2100 Bioanalyzer and the RNA 6000 Nano LabChip kit (Agilent Technologies), and their quantity was assessed using a Nanodrop. The 4X44k Human Whole Genome microarrays (Agilent Technologies) representing 44,000 probes were used as recently described [59]. Sample labeling and hybridization were performed according to protocols specified by the manufacturer (One-Color Microarray-Based Gene Expression Analysis). Three samples per experimental condition were included in the analysis. Slides were scanned at a 5-µm resolution with a G2505B DNA microarray scanner (Agilent Technologies). Image analysis and intra-array signal correction were performed using Agilent Feature Extractor Software© A.9.1.3. Further data processing, analysis and visualization were performed using the Resolver software© (version 6.0, Rosetta Inpharmatics). The hybridized genes (about 30,000 probes) were kept for further statistical analysis. Differentially expressed gene sets consisted of genes matching for an absolute FC>1.4 and a *P*-value <0.01 as determined by the 2-tailed Student's *t* test. Results were expressed as log2 FC.

The GO viewer tool was used to calculate P-values for each GO term as recently reported [59]. In brief, the GO terms were classified by unsupervised hierarchic clustering. Data were entered in the ArrayExpress database following the MIAME procedure and can be retrieved using an accession account (username: Reviewer_E-MEXP-2800 and password: 1278523069329). Gene families were determined using the Resolver Rosetta Biosoftware (http://www.rosettabio.com/products/resolver). The genes were studied using a network generated by PathwayStudioTM© software (Ariadne Genomics).

Real time RT-PCR and western blot

Total RNA was reverse transcribed using the MMLV-RT kit according to the manufacturer's protocol (Invitrogen). Forward and reverse primers were designed with the free web software Primer3 (see Table S3 for primer sequences). Real time RT-PCR was performed using the Applied Biosystems 7900HT Fast Real-Time PCR System according to the manufacturer's recommendations. Three independent experiments were performed in triplicate. The data are expressed relative to unstimulated cells. A value of 0 indicates that the level of gene expression was similar between stimulated and unstimulated cells. A value higher than 0 indicates that the gene was up-regulated in stimulated cells, and a value less than 0 shows that the gene was down-modulated in stimulated cells.

Western blotting was performed as previously described [60]. In brief, BeWo trophoblasts were stimulated with *C. burnetii* (200 bacteria/cell) for 6 h. Roughly 40 µg of protein was loaded onto sodium dodecyl sulphate-10% polyacrylamide gels and transferred to nitrocellulose sheets. Blots were incubated with a 1:1,000 dilution of monoclonal antibody (mAb) directed against human EGR-1 (Santa Cruz Biotechnology) or mAb anti-human α-tubulin (Cell Signaling). Proteins were revealed using a 1:2000 dilution of peroxidase-conjugated $F(ab')_2$ anti-mouse immunoglobulin G (IgG; Amersham) for 60 min and enhanced chemiluminescence detection assay.

Statistical analysis

PCR results are expressed as mean values ± SEM and were compared using the non-parametric Mann-Whitney *U* test. Differences were considered significant when $P<0.05$.

Supporting Information

Figure S1 TNF-stimulated networks.
The IL-6ST (A) and IL-13RA2 (B) pathways induced in BeWo cells by TNF were identified using Pathway Studio© software. Up-regulated genes appeared in red and down-modulated genes in blue.
(TIF)

Table S1 Up-regulated genes in response to *C. burnetii*.
In tint, the modulated genes that were also analyzed by qRT-PCR. Cb: *Coxiella burnetii*.
(DOC)

Table S2 Down-modulated genes in response to *C. burnetii*.
In tint, the modulated genes that were also analyzed by qRT-PCR. Cb: *Coxiella burnetii*.
(DOC)

Table S3 Nucleotide sequences of oligonucleotide primers.
(DOC)

Author Contributions

Conceived and designed the experiments: EG CC JLM. Performed the experiments: ABA EG YLP CL SPS EL. Analyzed the data: ABA EG YLP CL FB. Contributed reagents/materials/analysis tools: SPS EL FB. Wrote the paper: ABA EG CC JLM.

References

1. Raoult D, Marrie T, Mege JL (2005) Natural history and pathophysiology of Q fever. Lancet Infect Dis 5: 219–226.
2. Carcopino X, Raoult D, Bretelle F, Boubli L, Stein A (2007) Managing Q fever during pregnancy: the benefits of long-term cotrimoxazole therapy. Clin Infect Dis 45: 548–555.
3. Stein A, Lepidi H, Mege JL, Marrie TJ, Raoult D (2000) Repeated pregnancies in BALB/c mice infected with *Coxiella burnetii* cause disseminated infection, resulting in stillbirth and endocarditis. J Infect Dis 181: 188–194.
4. Lang G, Waltner-Toews D, Menzies P (1991) The seroprevalence of coxiellosis (Q fever) in Ontario sheep flocks. Can J Vet Res 55: 139–142.
5. Arricau-Bouvery N, Rodolakis A (2005) Is Q fever an emerging or re-emerging zoonosis? Vet Res 36: 327–349.
6. Parisi A, Fraccalvieri R, Cafiero M, Miccolupo A, Padalino I, et al. (2006) Diagnosis of *Coxiella burnetii*-related abortion in Italian domestic ruminants using single-tube nested PCR. Vet Microbiol 118: 101–106.
7. Langley JM (1990) Perinatal Q fever: is *Coxiella burnetii* a human perinatal pathogen? In: Marrie TJ, ed. Q fever, Vol I: the disease. Boca Raton: CRC Press, FL. pp 201–212.
8. Tissot-Dupont H, Amadei MA, Nezri M, Raoult D (2004) Wind in november, Q fever in december. Emerg Infect Dis 10: 1264–1269.
9. Benoit M, Ghigo E, Capo C, Raoult D, Mege JL (2008) The uptake of apoptotic cells drives *Coxiella burnetii* replication and macrophage polarization: a model for Q fever endocarditis. PLoS Pathog 4: e1000066.
10. Meghari S, Bechah Y, Capo C, Lepidi H, Raoult D, et al. (2008) Persistent *Coxiella burnetii* infection in mice overexpressing IL-10: an efficient model for chronic Q fever pathogenesis. PLoS Pathog 4: e23.
11. van Moll P, Baumgartner W, Eskens U, Hanichen T (1993) Immunocytochemical demonstration of *Coxiella burnetii* antigen in the fetal placenta of naturally infected sheep and cattle. J Comp Pathol 109: 295–301.
12. Jensen TK, Montgomery DL, Jaeger PT, Lindhardt T, Agerholm JS, et al. (2007) Application of fluorescent in situ hybridisation for demonstration of *Coxiella burnetii* in placentas from ruminant abortions. Apmis 115: 347–353.
13. Sanchez J, Souriau A, Buendia AJ, Arricau-Bouvery N, Martinez CM, et al. (2006) Experimental *Coxiella burnetii* infection in pregnant goats: a histopathological and immunohistochemical study. J Comp Pathol 135: 108–115.
14. Maidji E, Genbacev O, Chang HT, Pereira L (2007) Developmental regulation of human cytomegalovirus receptors in cytotrophoblasts correlates with distinct replication sites in the placenta. J Virol 81: 4701–4712.
15. Ferro EA, Mineo JR, Ietta F, Bechi N, Romagnoli R, et al. (2008) Macrophage migration inhibitory factor is up-regulated in human first-trimester placenta stimulated by soluble antigen of *Toxoplasma gondii*, resulting in increased monocyte adhesion on villous explants. Am J Pathol 172: 50–58.
16. Carvalho Neta AV, Stynen AP, Paixao TA, Miranda KL, Silva FL, et al. (2008) Modulation of the bovine trophoblastic innate immune response by *Brucella abortus*. Infect Immun 76: 1897–1907.
17. Haider S, Knofler M (2009) Human tumour necrosis factor: physiological and pathological roles in placenta and endometrium. Placenta 30: 111–123.
18. Lee BN, Ordonez N, Popek EJ, Lu JG, Helfgott A, et al. (1997) Inflammatory cytokine expression is correlated with the level of human immunodeficiency virus (HIV) transcripts in HIV-infected placental trophoblastic cells. J Virol 71: 3628–3635.
19. Bental T, Fejgin M, Keysary A, Rzotkiewicz S, Oron C, et al. (1995) Chronic Q fever of pregnancy presenting as *Coxiella burnetii* placentitis: successful outcome following therapy with erythromycin and rifampin. Clin Infect Dis 21: 1318–1321.
20. Ghigo E, Capo C, Tung CH, Raoult D, Gorvel JP, et al. (2002) *Coxiella burnetii* survival in THP-1 monocytes involves the impairment of phagosome maturation: IFN-γ mediates its restoration and bacterial killing. J Immunol 169: 4488–4495.
21. Capo C, Lindberg FP, Meconi S, Zaffran Y, Tardei G, et al. (1999) Subversion of monocyte functions by *Coxiella burnetii*: impairment of the cross-talk between αvβ3 integrin and CR3. J Immunol 163: 6078–6085.
22. McArthur SJ, Leigh D, Marshall JT, Gee AJ, De Boer KA, et al. (2008) Blastocyst trophectoderm biopsy and preimplantation genetic diagnosis for familial monogenic disorders and chromosomal translocations. Prenat Diagn 28: 434–442.
23. Renaud SJ, Sullivan R, Graham CH (2009) Tumour necrosis factor alpha stimulates the production of monocyte chemoattractants by extravillous trophoblast cells via differential activation of MAPK pathways. Placenta 30: 313–319.
24. Ghigo E, Capo C, Raoult D, Mege JL (2001) Interleukin-10 stimulates *Coxiella burnetii* replication in human monocytes through tumor necrosis factor down-modulation: role in microbicidal defect of Q fever. Infect Immun 69: 2345–2352.
25. King A, Thomas L, Bischof P (2000) Cell culture models of trophoblast II: trophoblasts cell lines - a workshop report. Placenta 21(Suppl A): S113–119.
26. Pospechova K, Rozehnal V, Stejskalova L, Vrzal R, Pospisilova N, et al. (2009) Expression and activity of vitamin D receptor in the human placenta and in choriocarcinoma BeWo and JEG-3 cell lines. Mol Cell Endocrinol 299: 178–187.
27. Voth DE, Heinzen RA (2007) Lounging in a lysosome: the intracellular lifestyle of *Coxiella burnetii*. Cell Microbiol 9: 829–840.
28. Gorvel JP (2008) *Brucella*: a Mr "Hide" converted into Dr Jekyll. Microbes Infect 10: 1010–1013.
29. Naroeni A, Jouy N, Ouahrani-Bettache S, Liautard JP, Porte F (2001) *Brucella suis*-impaired specific recognition of phagosomes by lysosomes due to phagosomal membrane modifications. Infect Immun 69: 486–493.
30. Philips JA (2008) Mycobacterial manipulation of vacuolar sorting. Cell Microbiol 10: 2408–2415.
31. van der Wel N, Hava D, Houben D, Fluitsma D, van Zon M, et al. (2007) *M. tuberculosis* and *M. leprae* translocate from the phagolysosome to the cytosol in myeloid cells. Cell 129: 1287–1298.
32. de Chastelier C (2009) The many niches and strategies used by pathogenic mycobacteria for survival within host macrophages. Immunobiol 214: 526–42.
33. Babior BM (1999) NADPH oxidase: an update. Blood 93: 1464–1476.
34. Munn DH, Zhou M, Attwood JT, Bondarev I, Conway SJ, et al. (1998) Prevention of allogeneic fetal rejection by tryptophan catabolism. Science 281: 1191–1193.
35. Miwa N, Hayakawa S, Miyazaki S, Myojo S, Sasaki Y, et al. (2005) IDO expression on decidual and peripheral blood dendritic cells and monocytes/macrophages after treatment with CTLA-4 or interferon-γ increase in normal pregnancy but decrease in spontaneous abortion. Mol Hum Reprod 11: 865–870.
36. Benoit M, Desnues B, Mege JL (2008) Macrophage polarization in bacterial infections. J Immunol 181: 3733–3739.
37. de la Torre E, Mulla MJ, Yu AG, Lee SJ, Kavathas PB, et al. (2009) *Chlamydia trachomatis* infection modulates trophoblast cytokine/chemokine production. J Immunol 182: 3735–3745.
38. Straszewski-Chavez SL, Abrahams VM, Mor G (2005) The role of apoptosis in the regulation of trophoblast survival and differentiation during pregnancy. Endocr Rev 26: 877–897.
39. Dellacasagrande J, Ghigo E, Raoult D, Capo C, Mege JL (2002) IFN-γ-induced apoptosis and microbicidal activity in monocytes harboring the intracellular bacterium *Coxiella burnetii* require membrane TNF and homotypic cell adherence. J Immunol 169: 6309–6315.
40. McArthur SJ, Leigh D, Marshall JT, Gee AJ, De Boer KA, et al. (2008) Blastocyst trophectoderm biopsy and preimplantation genetic diagnosis for familial monogenic disorders and chromosomal translocations. Prenat Diagn 28: 434–442.
41. Akutagawa O, Nishi H, Kyo S, Higuma C, Inoue M, et al. (2007) Early growth response-1 mediates up-regulation of telomerase in placenta. Placenta 28: 920–927.
42. Kenzel S, Santos-Sierra S, Deshmukh SD, Moeller I, Ergin B, et al. (2009) Role of p38 and early growth response factor 1 in the macrophage response to group B streptococcus. Infect Immun 77: 2474–2481.

43. Jiang SJ, Kuo CC, Berry MW, Lee AW, Campbell LA (2008) Identification and characterization of *Chlamydia pneumoniae*-specific proteins that activate tumor necrosis factor alpha production in RAW 264.7 murine macrophages. Infect Immun 76: 1558–1564.
44. Xu B, Lin L, Rote NS (1999) Identification of a stress-induced protein during human trophoblast differentiation by differential display analysis. Biol Reprod 61: 681–686.
45. Chen CP, Wang KG, Chen CY, Yu C, Chuang HC, et al. (2006) Altered placental syncytin and its receptor ASCT2 expression in placental development and pre-eclampsia. Bjog 113: 152–158.
46. Jones RL, Stoikos C, Findlay JK, Salamonsen LA (2006) TGF-β superfamily expression and actions in the endometrium and placenta. Reproduction 132: 217–232.
47. Caron PL, Frechette-Frigon G, Shooner C, Leblanc V, Asselin E (2009) Transforming growth factor beta isoforms regulation of Akt activity and XIAP levels in rat endometrium during estrous cycle, in a model of pseudopregnancy and in cultured decidual cells. Reprod Biol Endocrinol 7: 80–93.
48. Fitzgerald JS, Poehlmann TG, Schleussner E, Markert UR (2008) Trophoblast invasion: the role of intracellular cytokine signalling via signal transducer and activator of transcription 3 (STAT3). Hum Reprod Update 14: 335–344.
49. Ernst M, Inglese M, Waring P, Campbell IK, Bao S, et al. (2001) Defective gp130-mediated signal transducer and activator of transcription (STAT) signaling results in degenerative joint disease, gastrointestinal ulceration, and failure of uterine implantation. J Exp Med 194: 189–203.
50. Jiang K, Chen Y, Jarvis JN (2007) Soluble factors from LPS- and PHA-activated PBMC induce MAPK, Stat1 and Stat3 phosphorylation in primary cultures of human term placental trophoblasts: implications for infection and prematurity. Placenta 28: 538–542.
51. Catalano RD, Johnson MH, Campbell EA, Charnock-Jones DS, Smith SK, et al. (2005) Inhibition of Stat3 activation in the endometrium prevents implantation: a nonsteroidal approach to contraception. Proc Natl Acad Sci U S A 102: 8585–8590.
52. Daines MO, Tabata Y, Walker BA, Chen W, Warrier MR, et al. (2006) Level of expression of IL-13Rα2 impacts receptor distribution and IL-13 signaling. J Immunol 176: 7495–7501.
53. Chiaramonte MG, Mentink-Kane M, Jacobson BA, Cheever AW, Whitters MJ, et al. (2003) Regulation and function of the interleukin 13 receptor α2 during a T helper cell type 2-dominant immune response. J Exp Med 197: 687–701.
54. Rahaman SO, Vogelbaum MA, Haque SJ (2005) Aberrant Stat3 signaling by interleukin-4 in malignant glioma cells: involvement of IL-13Rα2. Cancer Res 65: 2956–2963.
55. Andrews AL, Nasir T, Bucchieri F, Holloway JW, Holgate ST, et al. (2006) IL-13 receptor α2: a regulator of IL-13 and IL-4 signal transduction in primary human fibroblasts. J Allergy Clin Immunol 118: 858–865.
56. Glazunova O, Roux V, Freylikman O, Sekeyova Z, Fournous G, et al. (2005) *Coxiella burnetii* genotyping. Emerg Infect Dis 121: 1211–1217.
57. Meghari S, Berruyer C, Lepidi H, Galland F, Naquet P, et al. (2007) Vanin-1 controls granuloma formation and macrophage polarization in *Coxiella burnetii* infection. Eur J Immunol 37: 24–32.
58. Benoit M, Barbarat B, Bernard A, Olive D, Mege JL (2008) *Coxiella burnetii*, the agent of Q fever, stimulates an atypical M2 activation program in human macrophages. Eur J Immunol 38: 1065–1070.
59. Bastonero S, Le Priol Y, Armand M, Bernard CS, Reynaud-Gaubert M, et al. (2009) New microbicidal functions of tracheal glands: defective anti-infectious response to *Pseudomonas aeruginosa* in cystic fibrosis. PLoS ONE 4: e5357.
60. Meconi S, Capo C, Remacle-Bonnet M, Pommier G, Raoult D, et al. (2001) Activation of protein tyrosine kinases by *Coxiella burnetii*: role in actin cytoskeleton reorganization and bacterial phagocytosis. Infect Immun 69: 2520–2526.

ARTICLE 2

Coxiella burnetii infects JEG trophoblastic cell line, a model of placenta infection

Amira Ben Amara, Abdoulaye Oury Barry, Christian Capo, Jean-Louis Mege, Eric Ghigo

Soumis à publication

Nous avons utilisé dans ce travail une autre lignée de trophoblastes que la lignée BeWo, à savoir la lignée JEG. Nous avons montré que *C. burnetii* survit dans ces cellules mais sans s'y répliquer alors que *C. burnetii* se réplique de façon intense dans les celllules BeWo. *C. burnetii* semble survivre dans le même compartiment intracellulaire, à savoir dans un phagolysosome, aussi bien dans les cellules BeWo que les cellules JEG. Pour tenter de mieux comprendre ces différences de comportement à l'égard de *C. burnetii*, nous avons entrepris une étude en microarray des cellules BeWo et JEG stimulées ou non par *C. burnetii*. L'analyse en composante principale, le clustering hierarchique et des termes « Gene Ontology » montrent clairement que ces deux lignées de trophoblastes sont différentes et qu'elles se comportent à l'égard de *C. burnetii* de façon également différente. On peut supposer que ces différences reflètent la diversité in vivo des trophoblastes (villeux, extravilleux). Quoiqu'il en soit, nos résultats accréditent l'idée que les trophoblastes pourraient constituer un réservoir pour *C. burnetii*.

Coxiella burnetii infects JEG trophoblastic cell line, a model of placenta infection

Amira Ben Amara, Abdoulaye Oury Barry, Christian Capo, Eric Ghigo[#] and Jean-Louis Mege[#]*

URMITE, CNRS UMR 6236-IRD 3R198, Université de la Méditerranée, 27 Bld. Jean Moulin 13385 Marseille cedex 05, France

[#] E. Ghigo and Jean Louis Mege have contributed equally to this work

*Corresponding authors: URMITE, Faculté de Médecine, 27 Bld. Jean Moulin, 13385 Marseille Cedex 05, France. Phone: (33) 4 91 32 43 75. Fax: (33) 4 91 83 03 90.

E-mail: jean-louis.mege@univmed.fr

Abstract

Q fever is a zoonosis caused by *Coxiella burnetii*, an obligate intracellular bacterium usually found in myeloid cells. The infection is a source of severe obstetrical complications in humans and cattle, and of chronic evolution in pregnant women. As *C. burnetii* is found in the placenta of aborted foetuses in humans and ruminants, we wondered if it may infect trophoblasts. In this work, we showed that *C. burnetii*, infected JEG trophoblastic cells without replication and was localized within phagolysosomes. We analyzed gene expression programs induced by *C. burnetii* in JEG trophoblastic cell line and compared it with transcriptomic program of BeWo trophoblasts in which *C. burnetii* replicates. These transcriptomic programs induced by *C. burnetii* in JEG trophoblasts was poor and markedly different from that induced by *C. burnetii* in BeWo trophoblasts. Hence, the differences in transcriptomic programs may explain the different intracellular fate of *C. burnetii* in JEG and

BeWo cells. Our results suggest that *C. burnetii* may use trophoblastic cells as a reservoir by interfering with gene expression.

Keywords: *Coxiella burnetii*, trophoblast, phagosome, transcriptomic.

Q fever is a widespread zoonosis caused by *Coxiella burnetii*, an intracellular gram-negative bacterium. Human primary infection is asymptomatic or manifests as isolated fever, hepatitis, or pneumonia. It may become chronic endocarditis in patients with valve lesions, arterial aneurysm, or prosthesis or in immunocompromised patients (Raoult, *et al.*, 2005). During pregnancy, Q fever may result in obstetric complications including spontaneous abortion, intrauterine growth retardation or fetal death, and premature delivery. In addition, pregnant women exhibit an increased risk of Q fever endocarditis even in the absence of underlying valvular lesions (Carcopino, *et al.*, 2007). This phenomenon has been reproduced in C57BL/6 mice (Stein, *et al.*, 2000). In cattle, sheep and goats, *C. burnetii* infection is often unapparent (Lang, *et al.*, 1991, Arricau-Bouvery & Rodolakis, 2005), but there is increasing evidence that it is associated with spontaneous abortion and stillbirth (Arricau-Bouvery & Rodolakis, 2005, Parisi, *et al.*, 2006). The placentas of infected animals contain up to 10^9 organisms/g of tissue, and it is likely that heavily infected placentas contaminate the environment at the time of parturition, leading to the persistence of viable organisms in the soil for several months. In addition, aerosols from the secretions and excretions of ruminants are the major source of contamination for humans (Tissot-Dupont, *et al.*, 2004). We chose to investigate if this bacterial pathogen could infect trophoblasts, which are essential for successful pregnancy. We previously reported that *C. burnetii* replicates in BeWo trophoblastic cell line (Ben Amara, *et al.*, 2010), thus, we wondered if *C. burnetii* may infect another trophoblastic cell line JEG that shares several properties with human trophoblasts in terms of morphology, biochemical markers and hormone secretion (King, *et al.*, 2000, Pospechova, *et al.*, 2009).

We extended the classical procedure of macrophage infection by *C. burnetii* (Ghigo, *et al.*, 2002) to JEG trophoblasts. Cells were infected with different doses of *C. burnetii* Nine Mile in phase I (strain RSA493) for 4 hours and washed to remove unbound bacteria; this

time was defined as day 0. We showed that *C. burnetii* infected JEG trophoblasts in a dose-dependent manner **(Figure 1A)**, as demonstrated by qPCR performed on the *C. burnetii com1* gene (Benoit, *et al.*, 2008). Immunofluorescence staining also showed that about 60% of infected cells contained one or two bacteria, a level of infection similar to that previously found in human monocytes (Capo, *et al.*, 1999). In subsequent experiments, an infecting dose of 200 bacteria per cell was used. *C. burnetii* survived but was unable to replicate within JEG trophoblasts during 9 days **(Figure 1B)**. The intracellular fate of *C. burnetii* was completely different from that we previouly reported in the trophoblast cell line BeWo in which *C. burnetii* intensively replicated (Ben Amara, *et al.*). It has been also reported that some pathogens such as *Chlamydia abortus* (Buxton, *et al.*, 2002) and *Toxaplasma gondii* (Oliveira, *et al.*, 2006) replicate within JEG trophoblasts. In addition, the intracellular fate of *C. burnetii* in JEG trophoblasts is reminiscent of what we found in human monocytes and macrophages in which *C. burnetii* survives but does not replicate. It is likely that trophoblasts are a reservoir for *C. burnetii* and these results may explain why organisms are abundantly found in infected placentas (Arricau Bouvery, *et al.*, 2003, Parisi, *et al.*, 2006).

As the survival of *C. burnetii* in macrophages is based on the defective maturation of phagosomes containing *C. burnetii* into phagolysosomes (Ghigo, *et al.*, 2002), we investigated the nature of the *C. burnetii*-containing compartment in JEG trophoblasts by confocal microscopy. At day 0, more than 80% of organisms colocalized with LAMP (Lysosomal-associated membrane protein)-1, a marker of late endosomes and lysosomes, and cathepsin D, a marker of lysosomes (Ghigo, *et al.*, 2002). At day 9 post-infection, at least 75% of organisms colocalized with both LAMP-1 and cathepsin D (**Figure 1C**), suggesting that bacteria are localized within phagolysosomes. Although *C. burnetii* was found within phagolysosomes in JEG and also in BeWo trophoblasts (Ben Amara, *et al.*, 2010), the fate of

C. burnetii was different in JEG and BeWo cells, suggesting that other mechanisms than phagolysosome genesis are involved in *C. burnetii* fate.

We analyzed the gene expression programs of JEG trophoblasts (GSE 30330) infected with *C. burnetii* and compare it to that previously reported in BeWo trophoblasts (Ben Amara, *et al.*, 2010). Cells were stimulated with *C. burnetii* (200 bacteria per cell) for 6 hours. Total RNA was extracted and the 4X44k Human Whole Genome microarrays (Agilent Technologies) were used as previously described (Ben Amara, *et al.*, 2010). First, *C. burnetii* stimulated the expression of 304 genes ($p<0.01$, FC=2) of which 253 were downmodulated and 51 were upregulated. This was dramatically distinct from transcriptional program of BeWo cells as shown by principal component analysis: JEG and BeWo cells were clearly distinct independently of *C. burnetii* (**Figure 1D**). Hierarchical clustering confirmed that JEG and BeWo cells partitioned into two distinct branches. More than 5000 genes were modulated with a *P* value < 0.01 when unstimulated JEG cells were compared with unstimulated BeWo cells and when *C. burnetii*-stimulated JEG cells were compared with *C. burnetii*-stimulated BeWo cells, emphasizing the strong differences between the two cell types. Finally, we used Gene Ontology (GO) terms to compare JEG and BeWo trophoblasts stimulated or not with *C. burnetii*. The results demonstrated that different functional GO categories characterized JEG and BeWo trophoblasts (**Figure 1E**). These findings may be related to the paper of Burleigh et al who reported, using Affimetrix methodology, that BeWO and JEG cells exhibited different transcriptional programs in the absence of agonist (Burleigh, *et al.*, 2007). These results suggest that the depression of gene expression program in *C. burnetii*-stimulated JEG cells may account for the absence of bacterial replication in contrast to BeWO cells.

In conclusion, we reported that *C. burnetii* survived in JEG trophoblasts but replicated in BeWo trophoblasts within phagolysosomes. The gene expression programs of JEG and BeWo trophoblats stimulated or not with *C. burnetii* were dramatically different and may

account for the differences of intracellular fate of *C. burnetii* in JEG and BeWo trophoblasts. These results strengthened the idea that trophoblasts are a reservoir for *C. burnetii*.

Aknowledgments

We thanks A. El Filali for his help. A. Ben Amara is fellows of the French Research Ministry and A. Oury Barry is fellows of the Scientific Cooperation Foundation "Infectiopole Sud". The work was supported by the Programme Hospitalier de Recherche Clinique 2008. The funders had no role in study design, data collection and analysis, decision to publish, or preparation of the manuscript. The authors have no competing interests.

References

Arricau-Bouvery N & Rodolakis A (2005) Is Q fever an emerging or re-emerging zoonosis? *Vet Res* **36**: 327-349.

Arricau Bouvery N, Souriau A, Lechopier P & Rodolakis A (2003) Experimental *Coxiella burnetii* infection in pregnant goats: excretion routes. *Vet Res* **34**: 423-433.

Ben Amara A, Ghigo E, Le Priol Y, *et al.* (2010) *Coxiella burnetii*, the agent of Q fever, replicates within trophoblasts and induces a unique transcriptional response. *PLoS One* **5**: e15315.

Benoit M, Ghigo E, Capo C, Raoult D & Mege JL (2008) The uptake of apoptotic cells drives *Coxiella burnetii* replication and macrophage polarization: a model for Q fever endocarditis. *PLoS Pathog* **4**: e1000066.

Burleigh DW, Kendziorski CM, Choi YJ, Grindle KM, Grendell RL, Magness RR & Golos TG (2007) Microarray analysis of BeWo and JEG3 trophoblast cell lines: identification of differentially expressed transcripts. *Placenta* **28**: 383-389.

Buxton D, Anderson IE, Longbottom D, Livingstone M, Wattegedera S & Entrican G (2002) Ovine chlamydial abortion: characterization of the inflammatory immune response in placental tissues. *J Comp Pathol* **127**: 133-141.

Capo C, Lindberg FP, Meconi S, *et al.* (1999) Subversion of monocyte functions by *coxiella burnetii*: impairment of the cross-talk between alphavbeta3 integrin and CR3. *J Immunol* **163**: 6078-6085.

Carcopino X, Raoult D, Bretelle F, Boubli L & Stein A (2007) Managing Q fever during pregnancy: the benefits of long-term cotrimoxazole therapy. *Clin Infect Dis* **45**: 548-555.

Ghigo E, Capo C, Tung CH, Raoult D, Gorvel JP & Mege JL (2002) *Coxiella burnetii* survival in THP-1 monocytes involves the impairment of phagosome maturation: IFN-gamma mediates its restoration and bacterial killing. *J Immunol* **169**: 4488-4495.

King A, Thomas L & Bischof P (2000) Cell culture models of trophoblast II: trophoblast cell lines--a workshop report. *Placenta* **21 Suppl A**: S113-119.

Lang G, Waltner-Toews D & Menzies P (1991) The seroprevalence of coxiellosis (Q fever) in Ontario sheep flocks. *Can J Vet Res* **55**: 139-142.

Oliveira JG, Silva NM, Santos AA, Souza MA, Ferreira GL, Mineo JR & Ferro EA (2006) BeWo trophoblasts are unable to control replication of *Toxoplasma gondii*, even in the presence of exogenous IFN-gamma. *Placenta* **27**: 691-698.
Parisi A, Fraccalvieri R, Cafiero M, *et al.* (2006) Diagnosis of *Coxiella burnetii*-related abortion in Italian domestic ruminants using single-tube nested PCR. *Vet Microbiol* **118**: 101-106.
Pospechova K, Rozehnal V, Stejskalova L, *et al.* (2009) Expression and activity of vitamin D receptor in the human placenta and in choriocarcinoma BeWo and JEG-3 cell lines. *Mol Cell Endocrinol* **299**: 178-187.
Raoult D, Marrie T & Mege J (2005) Natural history and pathophysiology of Q fever. *Lancet Infect Dis* **5**: 219-226.
Stein A, Lepidi H, Mege JL, Marrie TJ & Raoult D (2000) Repeated pregnancies in BALB/c mice infected with *Coxiella burnetii* cause disseminated infection, resulting in stillbirth and endocarditis. *J Infect Dis* **181**: 188-194.
Tissot-Dupont H, Amadei MA, Nezri M & Raoult D (2004) Wind in November, Q fever in December. *Emerg Infect Dis* **10**: 1264-1269.

Figure 1. Intracellular fate of *C. burnetii* and microarray analysis

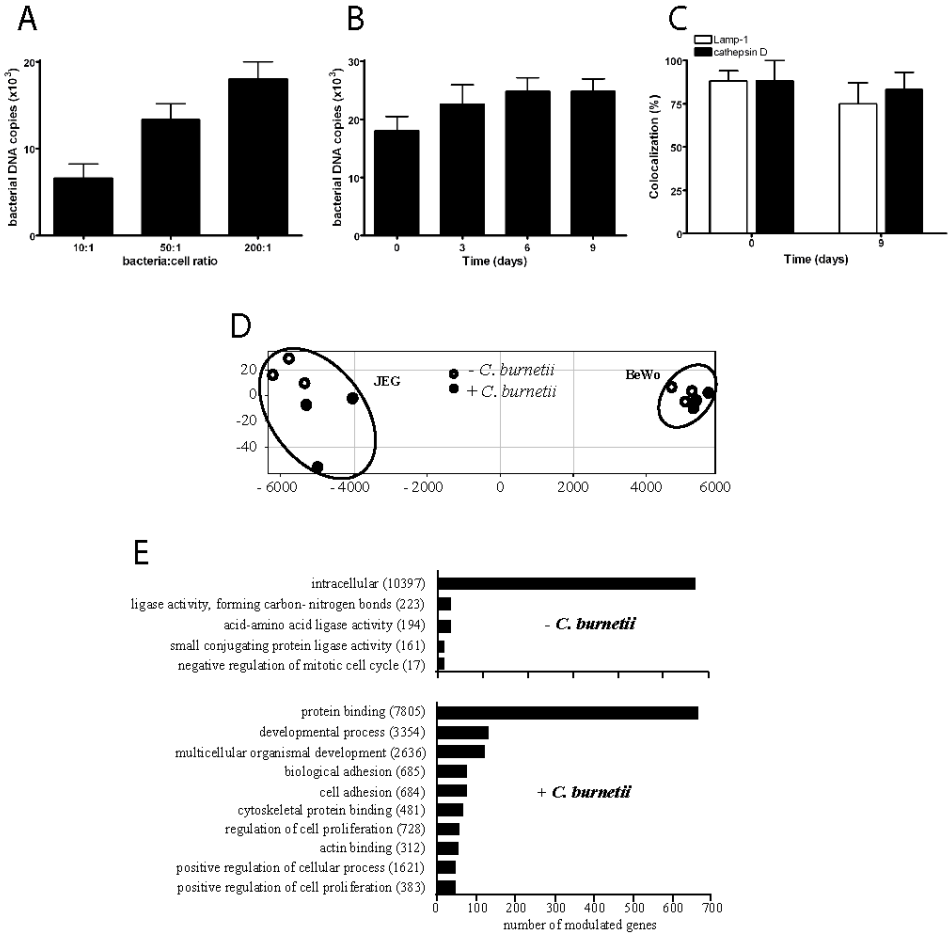

(A) JEG trophoblasts were incubated with different concentrations of *C. burnetii* for 4 hours and extensively washed to remove free organisms. **(B)** They were then cultured for 9 days. The number of bacterial DNA copies was determined using qPCR. The results represent the mean ± SEM of 3 experiments. **(C)** Infected JEG cells were labeled with anti-*C. burnetii*, anti-cathepsin D and anti-Lamp-1 and analyzed by laser scanning confocal microscopy. The percentage of co-localization of *C. burnetii* with Lamp-1 and cathepsin D was scored. The results represent the mean ± SEM of approximately 50 cells for each experimental condition. **(D-E)**, JEG and BeWo trophoblasts were stimulated with *C. burnetii* for 6 hours and microarrays were performed. Principal component analysis **(D)**. Analysis according GO terms with the number of genes that characterize the functional GO category in parentheses **(E).**

ARTICLE 3

Placenta environment induces the differentiation of macrophages into multinucleated giant cells

Amira Ben Amara, Laurent Gorvel, Christel Verollet, Vikram Mehraj, Abdoulaye Barry, Adil El-Filali, Christophe Buffat, Florence Bretelle, Eric Ghigo, Christian Capo, Isabelle Maridonneau-Parini, and Jean- Louis Mege

Soumis à publication

Les deux articles précédents suggèrent que des cellules placentaires telles que les trophoblastes pourraient être la cible de *C. burnetii*. Un autre type de cellules placentaires, les macrophages, pourraient également être infectés par *C. burnetii* puisque les macrophages se trouvent en abondance dans le placenta et que différents types de cellules myéloides, monocytes circulants ou macrophages tissulaires, sont connus pour être infectés par *C. burnetii*. L'examen de la littérature nous a montré que les macrophages placentaires sont caractérisés par un phénotype particulier puisqu'ils expriment CD14, un marqueur des monocytes et ne semblent pas exprimer, ou de façon marginale voire inconstante selon les articles, CD68, un marqueur des macrophages.

Ces caractéristiques phénotypiques différentes pourraient recouvrir des propriétés fonctionnelles différentes puisque, dans un travail précédent effectué au sein de notre laboratoire, il a été que les monocytes éliminent *T. whipplei*, l'agent de la maladie de Whipple, alors que ces mêmes bactéries se répliquent dans les macrophages dérivés de monocytes (73). C'est la raison pour laquelle nous isolé la population placentaire exprimant CD14 et que nous avons considéré cette population comme représentant les macrophages placentaires. Cette définition opératoire ne préjuge pas pour autant de l'existence ou non d'autres sous-populations macrophagiques. La culture des macrophages $CD14^+$, effectuée afin de savoir si ces macrophages placentaires éliminent *C. burnetii* ou au contraire autorisent sa réplication, nous a révélé une très grande surprise. En effet, nous avons observés qu'ils se différencient spontanément en cellules géantes multinucléées alors qu'une telle différenciation n'est classiquement observée qu'après culture en présence d'inducteurs spécifiques. Nous avons également vérifié que ces cellules géantes multinucléées placentaires correspondent bien à des cellules géantes multinucléées puisque leur taille augmente fortement, qu'elles

possèdent un nombre élevé de noyau et qu'elles les structures caractéristiques du squelette de ces cellules (podosomes, anneaux de vinculine et organisation microtubulaire).

Nous avons alors comparé les propriétés phénotypiques et fonctionnelles des macrophages placentaires $CD14^+$ et des cellules géantes multinucléées qui en sont issues. Il apparait ainsi que les propriétés phénotypiques des cellules géantes multinucléées sont quelque peu différentes de celles des macrophages placentaires $CD14^+$ puisque, en particulier, elles n'expriment CD14. Elles conservent leur pouvoir phagocytaire ainsi que la capacité de formation des dérivés actifs de l'oxygène. Elles semblent en revanche bien moins inflammatoires comme le montre le défaut d'activation de p38, une MAP kinase impliquée dans la transduction des signaux inflammatoires ou la sécrétion des cytokines en réponse au LPS. Nous nous sommes alors demandé si les macrophages placentaires $CD14^+$ et les cellules géantes multinucléées présentent un profil transcriptionnel de type M1 ou M2 après activation par l'IFN-γ ou l'IL-4. Tel n'est pas le cas, ce qui montre que les macrophages placentaires ne peuvent être assimilés aux macrophages « classiques ». Pour mieux appréhender les propriétés des macrophages placentaires $CD14^+$ et des cellules géantes multinucléées nous avons entrepris leur étude transcriptionnelle par microarray portant sur l'ensemble du génome humain. Nous avons montré par analyse en composante principale et *clustering* hierarchique que leurs propriétés sont complètement différentes de celles des monocytes et des macrophages dérivés de monocytes et qu'il est également possible de faire la distinction entre macrophages $CD14^+$ et cellules géantes multinucléées. Des analyses en termes « Gene Ontology » et en réseau de gènes confirment pleinement les différences observées entre macrophages $CD14^+$ et cellules géantes multinuclées.

Enfin, nous nous sommes demandé si le microenvironnement placentaire des macrophages $CD14^+$ pouvait expliquer leur différenciation en cellules géantes multinucléées. Pour cela, nous avons incubé des macrophages placentaires $CD14^+$ avec des trophoblastes et cette co-culture accentue leur différenciation en cellules géantes multinucléées. Cet effet des trophoblastes est probablement dû à des facteurs diffusibles. En effet, des surnageants de culture de trophoblastes induisent la formation de cellules géantes multinucléées à partir des monocytes des femmes enceintes au moment de leur délivrance mais en sont incapables lorsqu'ils sont incubés avec des monocytes de sujets contrôles. Il semble donc que le déséquilibre à la fois au niveau local et au niveau systémique observé au cours de la grossesse joue un rôle important dans la différenciation des macrophages placentaires $CD14^+$ en cellules géantes multinucléées.

Placenta environment induces the differentiation of macrophages into multinucleated giant cells

Amira Ben Amara,[1] Laurent Gorvel,[1] Christel Verollet,[2] Vikram Mehraj,[1] Abdoulaye Barry,[1] Adil El-Filali,[1] Christophe Buffat,[1] Florence Bretelle,[1] Eric Ghigo,[1] Christian Capo,[1] Isabelle Maridonneau-Parini,[2] and Jean- Louis Mege[1]

[1]Unité de Recherche sur les Maladies Infectieuses Tropicales et Emergentes, Centre National de la Recherche Scientifique, Unité Mixte de Recherche 6236, Université de la Méditerranée, Marseille, France

[2]Centre National de la Recherche Scientifique-Institut de Pharmacologie et de Biologie Structurale, Unité Mixte de Recherche 5089, Université de Toulouse, Université Paul Sabatier, 31077 Toulouse, France.

Authorship note: Amira Ben Amara and Laurent Gorvel are co–first authors and contributed equally to this work.

Corresponding author. Pr Jean-Louis Mege, URMITE, Faculté de Médecine, 27 Bld. Jean Moulin, 13385 Marseille Cedex 05, France. Tel.: (33) 4 91 32 45 86; fax: (33) 4 91 38 77 72. E-mail: Jean-Louis.Mege@univmed.fr

Conflict-of-interest: The authors have declared that no conflict of interest exists.

Abstract

Placenta macrophages play a role in the development of placenta and materno-fetal tolerance, but their properties are largely ignored. Purified $CD14^+$ macrophages from at term placentas expressed monocyte/macrophage markers and co-inhibitory molecules such as PD-L1 and PD-L2. They spontaneously matured into multinucleated giant cells (MGCs) that no more expressed CD14 and CD68 and were morphologically distinct from Langhans cells and foreign body giant cells. Placenta $CD14^+$ macrophages and MGCs were phagocytic, produced reactive oxygen intermediates and were not polarized into M1 or M2 cells. Placenta $CD14^+$ macrophages expressed genes related to pregnancy development and immune response that were down-modulated in placenta MGCs and replaced by genes related to adhesion and cytoskeleton reorganization, and metabolism. Finally, the placenta microenvironment governs MGC differentiation because placenta $CD14^+$ macrophages incubated with trophoblasts increases macrophage fusion into MGCs. In addition, co-incubating monocytes from parturient women with trophoblast supernatants resulted into MGC formation. Taken together, these results clearly demonstrated specific features of placenta $CD14^+$ macrophages likely related to the pregnancy context. We hypothesized that MGCs represent a new way to regulate the inflammatory and cytocidal activity of macrophages in a context that imposes contradictory constrains, i.e., semi-allograft acceptance, elimination of apoptotic debris and defense against aggression.

Introduction

The success of the pregnancy requires the development of an interface between the mother and the fetus that is represented by the placenta. Besides its metabolic role, the placenta supports the maternal tolerance towards the fetus (1). It is early infiltrated by maternal immune cells consisting of uterine natural killer (NK) cells, macrophages and T lymphocytes. NK cells are overrepresented at the beginning of the pregnancy and their number decreases thereafter. Macrophages represent 20-30% of decidual leukocytes at the site of implantation and their level remains high throughout pregnancy (2).

Placenta macrophages consist of distinct subpopulations. Indeed, the phenotypic characterization of placenta macrophages in the third trimester reveals that a large subset of $CD68^+$ macrophages also expresses CD14, an usual marker of monocytes whereas another subset of $CD68^+$ macrophages does not express CD14 (3). The location of these macrophages may be distinct: $CD68^+CD14^-$ macrophages are essentially present in decidua whereas $CD68^+CD14^+$ are also found in superficial myometrium (4). It has been recently shown that $CD14^+$ decidua macrophages could be discriminated according to the expression of CD11c: $CD14^+CD11c^{high}$ are more efficient antigen-presenting cells than $CD14^+CD11c^{low}$ (5). Placenta macrophages play a role in the phagocytosis of cell debris produced during the implantation (6). Decidual macrophages support the reorganization of uterine wall vasculature, which is essential to placentation and pregnancy maintenance (7), and consistently have immunosuppressive properties including suppression of mixed lymphocyte reaction, production of anti-inflammatory mediators, modulation of tryptophan catabolism and low expression of co-stimulatory molecules (4, 8).

Because of the difficulty to separate pure subsets of placenta macrophages, the analysis of their precise functions is only partial. In addition, the functions of placenta macrophages vary according pregnancy trimesters. Indeed, human macrophages in decidua of

early pregnancy express CD209 (DC-SIGN), a C-type lectin originally reported in immature dendritic cells (DCs). These macrophages are able to differentiate into mature $CD83^+$ DCs when they are stimulated with inflammatory cytokines (9). In contrast, decidua macrophages from the third trimester are unable to differentiate into DCs under the influence of interleukin (IL)-4 and granulocyte macrophage colony-stimulating factor (8). It has been shown that decidual $CD14^+$ macrophages isolated from first trimester pregnancies exhibit a M2 phenotype, which is consistent with reported immunosuppressive activities of first trimester macrophages and the Th2-dominated microenvironment of human pregnancy (10). In this study, we found that placenta $CD14^+$ macrophages from the third trimester exhibited specific membrane phenotype and were able to generate multinucleated giant cells (MGCs). While placenta $CD14^+$ macrophages expressed genes related to pregnancy development and immune response, these genes were replaced by genes related to adhesion and cytoskeleton reorganization, and metabolism in placenta MGCs. It is likely that the placenta microenvironment governs the differentiation of macrophages into MGCs. We hypothesized that MGCs represent a new way to regulate the inflammatory and cytocidal activity of macrophages in a context that imposes contradictory constrains, including semi-allograft acceptance, elimination of apoptotic debris and defense against aggression.

Results

Phenotypic characterization of placenta $CD14^+$ macrophages

We first determined the localization of $CD14^+$ macrophages in at term placenta. Clearly, $CD14^+$ macrophages were present in villi, as demonstrated by immunohistochemistry **(Figure 1A).** To characterize this population, $CD14^+$ macrophages were isolated using magnetic beads coated with anti-CD14 Abs. More than 97% of isolated cells were $CD14^+$ cells as determined by flow cytometry and did not express EGF-R and cytokeratin-7 known to characterize

trophoblasts (see **Figure S1**), demonstrating that $CD14^+$ cells were not contaminated by trophoblasts. The $CD14^+$ population consisted of small mononuclear cells in which more than 75% of them exhibited a rounded morphology and less than 25% expressed elongated extensions **(Figure 1B)**. The phenotyping of $CD14^+$ macrophages was performed using flow cytometry. The majority of them largely expressed HLA-DR, CD11b and CD11c but less than 5% of $CD14^+$ macrophages expressed CD16, CD68 and CD163. $CD14^+$ macrophages highly expressed PD-L1 and PD-L2 but only a minority of them expressed low levels of BTLA (**Figure 1C**). Placenta $CD14^+$ macrophages shared several markers with circulating monocytes such as CD14, CD11b and CD11c but did not express CD16 and CD163 that were expressed in 10% and 25% of monocytes, respectively. They were also distinct from MDMs that largely expressed CD68 (**Figure S2**). Taken together, these results demonstrated that placenta $CD14^+$ macrophages represented a population distinct from circulating monocytes and monocyte-derived macrophages.

Differentiation of placenta $CD14^+$ macrophages into MGCs

We wondered if placenta $CD14^+$ macrophages are terminally differentiated cells or if they kept maturation potential. We found that cultured $CD14^+$ macrophages spontaneously differentiated in MGCs exhibiting a size higher than 100 μm whereas the size of $CD14^+$ macrophages was comprised between 10 and 20 μm. Each MGC contained 2 to 8 nuclei that were often distributed as a ring (**Figure 2A**). After 3 days of culture, about 15% of $CD14^+$ macrophages were MGCs and this percentage steadily increased to reach about 90% of MGCs after 12 days (**Figure 2B**). The percentage of MGCs and the fusion index were related (**Figure 2B**). Thereafter, MGCs progressively disappeared and no MGC was found in cultures after 15 days. The phenotypic analysis of placenta MGCs showed that they did not originate from trophoblasts that may contaminate $CD14^+$ cells since they did not express EGF-R and

cytokeratin-7. MGCs showed marked differences with placenta $CD14^+$ macrophages. Indeed, MGCs did not express CD14 and highly expressed CD163. Nevertheless, both placenta $CD14^+$ macrophages and MGCs expressed CD11b, CD11c and HLA-DR. Nor $CD14^+$ macrophages nor MGCs expressed CD68, a marker of mature macrophages and CD16, a marker of activated macrophages. PD-L1 and PD-L2 that were highly expressed by $CD14^+$ macrophages were weakly expressed by MGCs whereas BTLA was poorly expressed by both $CD14^+$ macrophages and MGCs (**Figure S3**). Taken together, these results show that $CD14^+$ macrophages spontaneously formed MGCs that did not express CD14 and CD68, the canonical markers of monocytes and macrophages, respectively.

As MGCs obtained by other methods display a specific cytoskeleton organization (11, 12), we studied this organization in placenta MGCs. In MDMs used as controls, F-actin was concentrated in dotted structures scattered along the entire ventral surface, called podosomes (**Figure 3A, a-c**). Microtubules organized from the perinuclear centrosome and extended to cell periphery (**Figure 3A, d-f**). The cytoskeleton organization was clearly different in MGCs. Indeed, podosomes with a characteristic vinculin ring reorganized as clusters (**Figure 3B, a-c**), rosettes (**Figure 3B, d-f**) or rings at the cell periphery (**Figure 3B, g-i**). When MGCs have more than 3 nuclei, microtubules did not organize from a single point but rather from everywhere in the cell or from the nucleus envelope (**Figure 3B, d-f**). Taken together, these results show that the fusion of placental macrophages in MGCs induced a specific reorganization of both F-actin and microtubules.

Functional characterization of placenta macrophages

We then studied the functional properties of placenta $CD14^+$ macrophages and MGCs. First, $CD14^+$ macrophages and MGCs were able to ingest magnetic beads (**Figure 4A**). The percentage of positive cells was higher than 95%, demonstrating that both $CD14^+$

macrophages and MGCs were active phagocytes. Second, the percentage of ROI-producing cells was determined by NBT assay: almost all placenta $CD14^+$ macrophages and MGCs produced ROI. Third, the release of inflammatory and immunoregulatory cytokines by placenta $CD14^+$ macrophages and MGCs was studied. In the absence of stimulation, neither placenta $CD14^+$ macrophages nor MGCs released TNF or IL-10. When stimulated with LPS, placenta $CD14^+$ macrophages released TNF amounts that represented 30% of MDM response whereas placenta MGCs were unable to release TNF (**Figure 4B**). The release of IL-10 was similar in placenta $CD14^+$ macrophages and MDMs, and placenta MGCs released small amounts of IL-10 (**Figure 4C**). The low production of TNF and IL-10 by placenta MGCs in response to LPS was not due to a decreased ability to produce cytokines since the release of IL-6 was similar in MDMs, placenta $CD14^+$ macrophages and MGCs stimulated with LPS (**Figure 4D**), suggesting a specific imbalance of TNF/IL-10 ratio in placenta $CD14^+$ macrophages and MGCs compared with MDMs. Fourth, we investigated the M1/M2 polarization of placenta macrophages and MGCs by measuring the expression of nine M1 genes and ten M2 genes by qRT-PCR. We found that six M1 genes were modulated in placenta $CD14^+$ macrophages and MGCs: five were commonly modulated (*CXCL9*, *EDN1*, *IL15*, *IL15RA*, *IL2RA* genes). *INDO* gene was specifically upregulated in $CD14^+$ macrophages whereas *HESX1* gene was upregulated in MGCs. Among M2 genes, two genes (*CTSC*, *FN1*) were dramatically upregulated in both placenta $CD14^+$ macrophages and MGCs; *CCL23* gene was upregulated only in placenta $CD14^+$ macrophages (**Table 1**). Hence, placenta $CD14^+$ macrophages and MGCs did not exhibit a clearcut M1 or M2 polarization. Taken together, these results show that placenta $CD14^+$ macrophages and MGCs were phagocytic cells with a low potential to mount an inflammatory response in a way independent of M1/M2 polarization.

Transcriptional analysis of placenta macrophages

We wondered if placenta $CD14^+$ macrophages and MGCs exhibited specific gene expression profiles using full genome microarrays. Placental macrophages formed a distinct group from circulating monocytes and MDMs as determined by PCA. Among placenta macrophages, it was also possible to distinguish $CD14^+$ macrophages and MGCs (**Figure 5A**). The hierarchical clustering reveals that placenta $CD14^+$ macrophages and MGCs were present on a branch distinct from those consisting of monocytes and MDMs (**Figure 5B**). This was emphasized by the measurement of the number of genes modulated in each cell type. The number of modulated genes was high when placenta $CD14^+$ macrophages were compared with monocytes and MDMs, but was relatively similar in placenta $CD14^+$ macrophages and MGCs **(Table 2).**

The gene expression program of placenta macrophages was analyzed using GO terms. Among the upregulated genes in placenta $CD14^+$ macrophages compared with monocytes, there was an enrichment in GO terms related to development and angiogenesis (cell proliferation, organ development, cell adhesion, female pregnancy and blood vessel development) and inflammatory/immune responses (immune response, defense response, inflammatory response, regulation of apoptosis, wound healing, leukocyte activation). Among the downregulated genes, the GO terms associated with transcription/translation (RNA processing, ribosome biogenesis, translation) and metabolic activity were enriched (**Figure 6A**). Note that placenta $CD14^+$ macrophages were functionally related to pregnancy development and immune response. When the gene expression program of MGCs was compared to that of placenta $CD14^+$ macrophages, GO terms were distinct. Hence, among the upregulated genes there was an enrichment of the GO terms associated with cytoskeleton and adhesion (extracellular matrix organization, regulation of muscle contraction, biological adhesion) and metabolism (lipid biosynthetic process, monocarboxylic acid metabolic

process). Among the downregulated genes, GO terms related to immune and inflammatory responses were enriched (**Figure 6B**).

Next, the transcriptional differences between placenta $CD14^+$ macrophages and MGCs were studied by testing in qRT-PCR 28 genes found as highly modulated in microarray experiments. Only some genes (IRF2, IRF9, TIMP3) were modulated in a similar way in placenta $CD14^+$ macrophages and MGCs. Other genes were modulated in both placenta $CD14^+$ macrophages and MGCs, but their levels of expression were clearly different. The expression of the genes encoding APOC1, CCL18, FABP3, IL10, IL32, MMP12, PD-L1, TGFA and WNT5A was higher in placenta $CD14^+$ macrophages whereas that of COL1A2, LOXL2 and MMP7 genes was higher in MGCs. Other genes were upregulated in placenta $CD14^+$ macrophages and downregulated in MGCs: they included CSH1, CSH2, IDO1, IGF2, IL24, PSG6, PSG9. Only few genes (COL3A1, VEGFC) were upregulated in MGCs and downregulated in placenta $CD14^+$ macrophages (**Table 3**).

Finally, networks based on gene interactions were analyzed in MGCs compared with placenta $CD14^+$ macrophages. A major network contained two dense areas (**Figure 7**). The first area corresponded to cytoskeleton molecules with a marked enrichment with genes encoding integrin subunits, laminin and collagen. This network was connected to a group of growth factors such as platelet-derived growth factor (PDGF) and vascular endothelial growth factor (VEGF). The second area corresponded to chemokines with upregulated and downregulated genes and NF-κB/MAPK pathway with genes mainly downregulated. The modulation of signalisation pathways was confirmed at the functional level (**Figure S4**). In $CD14^+$ macrophages stimulated with LPS, the phosphorylation of p38 MAPK was maximum at 30 minutes and decreased thereafter. In contrast, p38 MAPK was not phosphorylated in LPS-stimulated MGCs. The profile of nuclear translocation of NF-κB was also different in LPS-stimulated $CD14^+$ macrophages and MGCs. While NF-kB was transiently translocated in

nuclei in $CD14^+$ macrophages, its nuclear translocation was less intense and more sustained in LPS-stimulated MGCs. In the major network of genes modulated in MGCs, we also found the interaction of the genes encoding DUSP (dual specificity phosphatase) and death-associated protein kinase (DAPK) with transforming growth factor (TGF) pathway consisting of the genes encoding TGFβ, TGFβ receptor and Smad3 (**Figure 7)**. In addition to this major network, several subnetworks were specifically associated with placenta MGCs. One was related to WNT pathway in which six *WNT* and four *FZD* genes were upregulated (**Figure 8A**). Other subnetworks were related to metabolic activities. They included cholesterol metabolism (9/11 upregulated genes) (**Figure 8B**), aminoacid metabolism (7/8 upregulated genes) and carbohydrate metabolism (6/9 upregulated genes) (**Figure S5**). Finally, small networks included genes encoding peroxisome proliferator-activated receptor (PPAR)γ/retinoic acid X receptor (RXRA) in which the former was upregulated and the latter downregulated, TNFSF4/TNFSRF4 genes in which both were upregulated and the complement network in which C1 and C2 members were upregulated and C3 was downregulated (**Figure S6**). Taken together, these results show that placenta MGCs exhibited a transcriptional program, based on interacting cytoskeleton organization and metabolism, which was completely different from that of placenta $CD14^+$ macrophages.

Effect of macrophage-trophoblast interaction on MGC differentiation

We finally wondered if the microenvironment of placenta $CD14^+$ macrophages governs their differentiation into MGCs. $CD14^+$ macrophages were incubated with trophoblasts. Resulting MGCs harbored a very high number of nuclei, sometimes higher than 20 per MGC (**Figure 9A, right bottom**), suggesting that the placenta environment was needed to drive the maturation of macrophages into MGCs. In these MGCs, podosomes were very often organized as a belt like in osteoclats and microtubules nucleated from the nuclei envelope

(**Figure 9B**). The hypothesis that the environment promotes MGC formation was verified as follows. Circulating monocytes from non-pregnant women were incubated with trophoblast supernatants: monocytes did not differentiate into MGCs. In contrast, the co-incubation of circulating monocytes from parturient women with trophoblast supernatants resulted into the formation of MGCs containing at least two nuclei (**Figure 10A**). Indeed, about 10% of cells were MGCs after three days and this percentage steadily increased to reach 72% after 12 days (**Figure 10B**). However, the number of nuclei (2-3 per MGC) and the size (about 40 to 60 μm) of these MGCs remained lower than those observed in placenta MGCs. Taken together, these data suggested that the pregnancy microenvironment was needed to induce the differentiation of macrophages into MGCs.

Discussion

In this paper, we investigated the properties of $CD14^+$ macrophages from at term placentas. They exhibited membrane-associated myeloid markers such as CD11b and markers of leukocyte activation such as HLA-DR but they poorly expressed CD68, a classical marker of macrophages. Such pattern is partly distinct from the usual phenotype of uterine macrophages that express both CD14 and CD68 in biopsies of third trimester placentas (3). The presence of high levels of CD11c on placenta $CD14^+$ macrophages may be related to the recent description of a population of $CD14^+CD11c^{high}$ decidual macrophages (5). The constitutive overexpression of HLA-DR is consistent with the presence of HLA-DR in decidua basalis from term pregnancies (9). Another phenotype feature of placenta $CD14^+$ macrophages was the expression of the co-inhibitory molecules PD-L1 and PD-L2. It is known that decidual macrophages express co-stimulatory molecules such as CD80 and CD86 (13). PD-L1 is positioned at the fetal-maternal interface and is likely expressed by trophoblasts and decidual macrophages throughout gestation. PD-L2 is localized in a more

restricted manner in mesenchymal villous cores of at term placentas (14). PD-L1 may contribute to feto-maternal tolerance since PD-L1 blockade or deficiency decreases fetal survival rates and likely acts through regulatory T cells (15). It has been recently shown that MDMs express PD-L1 and PD-L2 and that their over-expression is associated with HIV replication, confirming their role in establishing an immunosuppressive context (16). It is also likely that the co-inhibitory molecule BTLA contributes to fetal-maternal tolerance even if it expression by placenta $CD14^+$ macrophages was lower than that of PD-L1 and PD-L2 since BTLA engagement is known to transduce an inhibitory signal in target cells (17). Taken together, the phenotypic characteristics of placenta $CD14^+$ macrophages suggest that they may play a role in feto-maternal tolerance via the constitutive overexpression of PD-L1 and PD-L2.

A remarkable feature of placenta $CD14^+$ macrophages was their ability to differentiate into MGCs. The formation of giant cells has been reported in several circumstances. In tissues such as bones, giant cells are represented by osteoclasts. In the context of chronic infections, macrophages differentiate into Langhans cells and in foreign body-type giant cells in response to tissue aggression (12). In placentas of rodents, cows and humans, trophoblast giant cells are mononucleated or multinucleated and are of vital importance for embryo implantation and promoting maternal adaptation to pregnancy (18). The MGCs differentiated from placenta $CD14^+$ macrophages exhibited the reorganization of both F-actin and microtubules that is typical of giant cells. They possessed podosomes organized in clusters or as peripheral rings, which are reminiscent of osteoclast podosome belts. The number of nuclei remained low and randomly distributed throughout the cytoplasm; this distribution was also different from that found in Langhans cells in which nuclei are arranged in a circular pattern (12). Hence, placenta MGCs seem to be intermediate between Langhans cells and foreign body-type giant cells. The formation of MGCs from placenta $CD14^+$ macrophages was associated with

phenotypic changes. The decreased expression of CD14 by MGCs was not associated with the acquisition of CD68 as found in MDMs. In contrast, MGCs acquired CD163, a member of scavenger receptor superfamily that is mainly expressed by cells of monocyte/macrophage lineage (19) and may be associated with M2 macrophage polarization (20). Macrophages expressing both CD68 and CD163 are present in chorionic villi (21) and the expression of CD163 may parallel that of CD14 in preterm preeclamptic decidua basalis (22). It has been recently found that CD163 is associated with the M2 phenotype of placenta macrophages (23). If CD163 is associated with macrophage fusion remains hypothetical but MGCs obtained by the fusion of monocytes induced by interferon-γ and concanavalin A express a high level of CD163 (manuscript in preparation). While bone osteoclasts do not express CD163 (24), MGCs from papillary thyroid carcinomas express both CD68 and CD163 (25). The last phenotypic characteristics of placenta MGCs was the decreased expression of PD-L1 and PD-L2 compared with parental $CD14^+$ macrophages, suggesting that MGCs are less involved in materno-fetal tolerance than placenta $CD14^+$ macrophages. This may be related to the severe down-modulation of pregnancy-associated genes such as CSH, PSG and IDO in MGCs compared with placenta $CD14^+$ macrophages (see below).

The differentiation of placenta $CD14^+$ macrophages into MGCs did not affect the canonical features of macrophages, i.e., phagocytosis and ROI production. The maintain of phagocytosis ability by placenta macrophages is essential for the success of pregnancy since the removal of cellular debris as a result of apoptosis is necessary to keep cellular homeostasis (26). However, the activation status of placenta $CD14^+$ macrophages and MGCs was different. Placenta $CD14^+$ macrophages released high amounts of inflammatory and anti-inflammatory cytokines in response to LPS and this release was roughly similar to that of MDMs. This agrees with a recent report in which placenta $CD14^+CD11c^+$ macrophages secrete both inflammatory and anti-inflammatory cytokines (5). In contrast, the release of

MGCs of an inflammatory cytokine such as TNF was dramatically decreased and that of an immunoregulatory cytokine such as IL-10 was decreased at a lesser extent. The transition from high to low TNF/IL-10 producer was not associated with changes in macrophage polarization. We found that placenta $CD14^+$ macrophages and MGCs exhibited transcriptional programs that were dramatically distinct from those of MDMs stimulated with IFN-γ (typical M1 profile) and IL-4 (typical M2 profile) in terms of modulated genes (see **Table S1**). In addition, neither placenta $CD14^+$ macrophages nor MGCs were polarized into M1 or M2 cells. These results were consistent with a recent report in which $CD14^+CD11c^{high}$ and $CD14^+CD11c^{low}$ macrophages from first trimester placentas are not polarized (5). They did not completely agree with the initial report in which $CD14^+$ macrophages from first trimester placentas are polarized toward a M2 profile (10). It is likely that the microenvironment of first trimester placentas and term placentas differently affects the activation status of placenta $CD14^+$ macrophages. Note also that using a limited number of polarization markers may result in some over-interpretation of the data.

The transcriptomic analysis of placenta $CD14^+$ macrophages revealed the originality of their gene expression program. This program formed a group distinct from those of circulating monocytes and MDMs. The number of modulated genes in placenta $CD14^+$ macrophages was higher than those found in monocytes and MDMs. This increased transcriptional activity of placenta $CD14^+$ macrophages corresponded to the enrichment with GO terms related to development and angiogenesis and to inflammatory and immune response. To our knowledge, only two studies investigated the transcriptomic profiles of placenta macrophages and revealed common functional features with our study. In decidual $CD14^+$ macrophages, only 120 genes were specifically modulated as compared with their blood counterparts and genes involved in immune regulatory functions, tissue remodeling, cell proliferation and cell metabolism were enriched (10). In decidua $CD14^+CD11c^{high}$

macrophages, genes involved in invasion, mobility and inflammatory processes were enriched whereas the categories growth and development and extracellular matrix were enriched in $CD14^{+}CD11c^{low}$ macrophages (5). Among the modulated genes revealed by the microarray approach, we selected a list of genes that may define a minimum signature of placenta $CD14^{+}$ macrophages and we tested theses genes using real time RT-PCR. Hence, there was an increased expression of placenta hormonal molecules such as CSH1 that is critical for growth control and PSG6/9 that are increased during trophoblast differentiation preceding morphological formation of syncitia and β-chorionic gonadotropin expression (27). Growth factors such as IGF2 were upregulated, and IGF2 is known to enhance proliferation and survival of human first trimester cytotrophoblasts (28).

MGCs exhibited a transcriptional profile distinct from that of placenta $CD14^{+}$ macrophages. First, the number of modulated genes was lower in MGCs than in placenta $CD14^{+}$ macrophages. Second, the distribution of GO terms was different in MGCs and placenta $CD14^{+}$ macrophages. Among upregulated genes in MGCs, genes involved in cytoskeleton, adhesion and metabolism functions were enriched whereas genes involved in immune/inflammatory response were downregulated. The specificity of the gene pattern of MGCs was assessed by characterizing the MGC signature and building networks. The MGC signature consisted of genes upregulated in MGCs and not in placenta $CD14^{+}$ macrophages. They included the genes encoding collagen molecules such as lysyl oxidase-like 2 (LOXL2) and VEGF-C. LOXL2 is expressed in chorionic cytotrophoblasts of fetal membranes (29). Its role in the biogenesis of connective tissue makes of LOXL2 a candidate for fusion effectors. VEGF-C is a member of angiogenic factor family known to play a role in placentation in which it may control the migration of trophoblastic giant cells (30). VEGF-C is also expressed in osteoclasts, another variety of giant cells (31). Third, the analysis of gene networks amplified the GO term analysis. We identified a dense network associating different

functional groups: integrin and cytoskeleton, and TGF pathway (in which most of genes were upregulated) and inflammatory cytokines (in which most of genes were downregulated). The integrin/cytoskeleton network associated several collagen and laminin molecules and integrin subunits. It is known that β1, β2 and β3 integrins are involved in the formation of giant cells including foreign body-type giant cells and osteoclasts (32). The connection of cytoskeleton and adhesion molecules with VEGF pathway suggested that tissue reorganization and angiogenesis may be critical properties of MGCs. Network analysis also revealed the importance of different metabolic pathways including PPAR-γ and WNT pathways. PPAR-γ is involved in trophoblast invasion and differentiation including that of trophoblast giant cells (33, 34). Many WNT genes are expressed in the human endometrium during the proliferative and secretory phases of the menstrual cycle and are involved in trophoblast differentiation (35, 36). Hence, the differentiation of placenta $CD14^+$ macrophages into MGCs is associated with decreased inflammatory and immune properties and overexpression of functions that are essential for the success of pregnancy.

Finally, we found that placenta microenvironment likely played a critical role in the generation of MGCs. First, the co-incubation of placenta $CD14^+$ macrophages with trophoblasts increased the number of nuclei per MGC, suggesting that trophoblasts are involved in MGC formation. This property of trophoblasts to modulate the functions of other cells has been recently reported. Hence, the co-culture of monocyte-derived dendritic cells with placenta cytototrophoblasts induces morphological changes and decreased ability to stimulate IFN-γ production by T cells (37). Purified $CD14^+$ decidual macrophages do not express Transforming Growth Factor beta-1 unless decidual cells remain unfractionated and cultivated. Hence, the uteroplacental environment may re-program macrophage activity (38). Some soluble factors may account for this property of trophoblasts to be involved in MGC generation. Indeed, peripheral blood monocytes from pregnant women incubated with

trophoblast supernatants fuse in cells with increased size and 2-3 nuclei. In contrast, monocytes from controls incubated with trophoblast supernatants were unable to generate MGCs. Several soluble factors such as IL-4, IFN-γ, macrophage colony-stimulating factor and bacterial products have been reported to induce macrophage fusion (32). Among them, IL-4 and macrophage colony-stimulating factor are produced during pregnancy. We can suppose that these molecules are candidates to induce the formation of placenta MGCs. However, IL-4 rather induces foreign body giant cells that are rather different from placenta MGCs. Other molecules such as IL-32, a proinflammatory cytokine found in placenta $CD14^+$ macrophages, may contribute to the formation of MGCs since IL-32 causes the differentiation of osteoclast precursors in multinucleated cells (39). Finally, exosomes and HLA-G molecules may be candidates. Recently, it has been shown that exosomes isolated from trophoblastic cell lines are able to stimulate monocyte migration and activation (40). On another hand, HLA-G expressed by trophoblasts or released interacts with specific receptors on $CD14^+$ decidual macrophages leading to the secretion of proinflammatory and proangiogenic molecules by placenta macrophages (41).

In conclusion, we showed in this paper that the phenotypic, transcriptional and functional properties of placenta $CD14^+$ macrophages were specific as compared to circulating monocytes and MDMs. This may be associated to the specific role of placenta macrophages in the maintenance of pregnancy. Unexpectedly, the placenta context allowed $CD14^+$ macrophages to differentiate into MGCs that acquired a new repertoire of properties likely related to the specific environment of pregnancy. The role of these MGCs remains elusive. We hypothesize that they represent a new way to regulate the inflammatory and cytocidal activity of macrophages in a context that imposes contradictory constrains, i.e., semi-allograft acceptance, elimination of apoptotic debris and defense against aggression.

Methods

Placenta collection

At term placenta and blood were collected at Gynecology-Obstetrics Department (Hôpital de la Conception, Marseille, France). Only placentas from healthy term pregnancies and vaginal delivery were collected.

Monocytes and monocyte-derived macrophages

Blood from healthy donors (leukopacks) was provided by the Etablissement Français du Sang (Marseille). Peripheral blood mononuclear cells (PBMCs) from healthy donors and parturient women were isolated by Ficoll gradient centrifugation and suspended in DMEM-F12 containing 10% fetal calf serum (FCS), 100 U/ml penicillin and 100 µg/ml streptomycin (Invitrogen, Cergy Pointoise, France). Monocytes were isolated from PBMCs by positive selection (Miltenyi Biotec, Paris, France) using magnetic beads coated with anti-CD14 antibodies (Abs) (42). The purity of monocytes ($CD14^+$ cells) was higher than 98% as determined by flow cytometry. Monocyte-derived macrophages (MDMs) were obtained as follows (43). Monocytes were incubated in DMEM-F12 containing 10% human serum AB (Lonza, Verviers, Belgium), and antibiotics for 3 days, and FCS replaced human serum for 4 additional days. More than 95% of the cells were MDMs, as assessed by CD68 expression and CD14 down-modulation.

Placenta cells

Chorionic villi from the maternal interface were cut in the entire length without taking the membrane of the chorionic plate. They were then cut into small pieces of about 1 cm^2 and rinsed in phosphate-buffered saline (PBS). The presence of $CD14^+$ cells in villi was determined as follows. Placenta pieces were fixed in 10% neutral-buffered formalin, sectioned and embedded in paraffin. Deparaffinized placenta sections (5-µm thick) were incubated with

anti-CD14 rabbit Abs or normal rabbit serum as control. Immunodetection was performed with biotinylated anti-rabbit Abs and peroxidase-labeled streptavidin (Zymed, CliniSciences, Montrouge, France) with amino-ethylcarbazole as substrate. After washing, slides were counterstained with Mayer's hematoxylin for 5 minutes and CD14 was detected by optical observation.

Placenta samples were digested according (44, 45) with slight modifications. Briefly, placenta samples were incubated in a solution consisting of HBSS (Invitrogen), $MgSO_4$, DNase I (Sigma-Aldrich, Lyon, France), 2.5% trypsin (Invitrogen) buffered with HEPES for 45 minutes and then for 30 minutes under gentle agitation at 37°C. The digestion products were filtered through 100 µm pores, incubated in 50 ml tubes containing 2 ml FCS and centrifuged at 1,000 x *g* for 15 minutes. The cells were counted, deposited on Ficoll barriers and centrifuged at 700 x *g* for 20 minutes. Mononuclear cells were recovered and the placenta macrophages were isolated using CD14 human magnetic beads coated with anti-CD14 Abs (Miltenyi Biotech, Paris, France). The purity of $CD14^+$ cells was checked by flow cytometry and was higher than 97%. Placenta MGCs were obtained as follows. $CD14^+$ macrophages (2 x 10^5 cells per assay) were seeded in 24-well plates containing glass coverslips (time considered as day 0) and cultured in DMEM-F12 containing 10% FCS and antibiotics for 9 days. The morphology of placenta macrophages and the percentage of MGCs was determined by May-Grünwald Giemsa staining using the HemaColor kit (Merck, Martillac, France). The cell fusion index was determined as previously described (11).

For trophoblast isolation, the digestion products were deposited on Percoll barrier and centrifuged at 1200 x *g* for 20 minutes. Cells at the 25-60% Percoll interface were recovered and human magnetics beads (Miltenyi Biotech) coated with Abs specific for epidermal growth factor receptor (EGF-R, Santa Cruz, Tebu-Bio, Le Perray en Yvelines, France) were used to isolate primary trophoblasts. About 98% of isolated cells expressed EGF-R. They also

expressed cytokeratin-7, an intracellular marker of trophoblasts, as assessed by flow cytometry (**Figure S1**). Trophoblasts were cultured for about 15 days. After monolayer formation, supernatants were centrifuged at 1000 x *g* for 15 minutes to eliminate cell debris and were stored at -20°C.

Phenotyping of placenta macrophages

The phenotype of placenta $CD14^+$ macrophages was determined using flow cytometry. $CD14^+$ macrophages (10^6 cells per assay) were labeled with CD14-PC5, CD16-FITC, CD11b-FITC, HLA-DR-FITC (Beckman Coulter, Paris Nord 2, France), CD68-FITC, CD11c-FITC (Dako, Trappes, France), CD163-FITC (MBL, Montrouge, France) Abs or isotype controls). We also studied the expression of co-stimulatory molecules consisting of Programmed cell Death Ligand (PD-L)-1, PD-L2, and B and T Lymphocyte Attenuator (BTLA) using specific Abs kindly provided by D. Olive (Marseille). Abs were diluted at 1/20 in PBS containing 5% FCS for 20 minutes. After washing, $CD14^+$ macrophages were fixed with 3% paraformaldehyde, centrifuged at 400 x *g* for 5 minutes and diluted in 500 µl PBS. At least 10,000 macrophages were analyzed using the FACS Canto II cytometer (Becton Dickinson, Le Pont de Claix, France) and data were extracted with the FACS Diva version 6.1.3.software. The phenotype of MGCs was determined by immunofluorescence using a DMI 3000B microscope (Leica, Heidelberg, Germany).

Functional activity of macrophages and MGCs

The phagocytic activity of placenta $CD14^+$ macrophages and MGCs was studied as follows. Macrophages (2 x 10^5 cells per assay) were incubated with magnetic 1.31 µm beads (Kisker Biotech, Germany) at a final dilution of 1/1000 for 1 to 4 hours at 37°C. After extensive washing to discard free particles, macrophages were fixed with 3% paraformaldehyde,

permeabilized with 0.1% Triton X-100 for 5 min and labeled with bodipy phallacidin (Molecular Probes, Invitrogen). The uptake of particules by macrophages was assessed using the TCS SP5 confocal microscope (Leica Microsystems**)**. Macrophages were also incubated with opsonized 1 µm latex beads (Sigma-Aldrich, Lyon, France) and nitroblue tetrazolium to generate reactive oxygen intermediates (ROI) for two hours, as previously described (46). After washing, macrophages were observed using optical microscopy. The results are expressed as the percentage of cells that have ingested particles or generated ROI.

The ability of macrophages to release cytokines was determined by incubating macrophages (10^6 cells per assay) with 1 µg/ml *Escherichia coli* lipopolysaccharide (O55:B5 LPS, Sigma-Aldrich). After 24 hours, culture supernatants were collected and stored at -80°C before cytokine determination. The amounts of TNF, IL-10 and IL-6 in the supernatants were determined by specific immunoassays (R&D Systems, Lille, France).

Cytoskeleton determination

The cytoskeletal organization of MGCs was studied as previously described (11). Briefly, MGCs were permeabilized with 0.3% Triton X-100, incubated with mouse monoclonal anti-vinculin or anti-tubulin Abs (Sigma-Aldrich) for 1 hour and then incubated with Alexa 488-conjugated secondary Abs, phalloidin-Texas Red (Invitrogen) that specifically binds filamentous actin (F-actin) and DAPI for 30 minutes. Images were collected using a DM-RB fluorescence microscope (Leica Microsystems) and processed with Adobe Photoshop.

p38 phosphorylation and NF-κB translocation

The activation of p38 mitogen-activated protein kinase (MAPK) and the nuclear translocation of the transcription factor NF-κB, were determined as follows. Macrophages (2 x 10^5 cells per assay) were stimulated with 100 ng/mL LPS. After paraformaldehyde fixation and washing,

they were permeabilized with 0.1% Triton X-100 and incubated with rabbit Abs directed against phosphorylated p38 or NF-κB p65 (Cell Signaling, Saint Quentin en Yvelines, France) at a 1/100 dilution. After washing, Alexa Fluor 555-conjugated goat Abs directed against rabbit IgG (at a 1/100 dilution) were added to macrophages for 30 minutes. After washing, bodipy phallacidin (Invitrogen) at a dilution of 1/250 and Alexa Fluor 555-conjugated goat Abs directed against rabbit IgG (at a 1/500 dilution) were added to macrophages for 30 minutes. Macrophages were then washed and incubated with a 1/10,000 dilution of 4',6-diamidino-2-phenyl-indole (DAPI, Invitrogen) for 10 minutes. Coverslips were mounted with Mowiol, and p38 activation and NF-κB nuclear translocation were observed by epifluorescence microscopy.

Real-time RT-PCR

Real-time quantitative RT-PCR (qRT-PCR) was carried out as recently described (47). In brief, reverse transcription of 150 ng of RNA was performed with the MMLV-RT kit (Invitrogen). cDNA was obtained using oligo(dT) primers and M-MLV reverse transcriptase (Invitrogen) and qPCR experiments were performed using SYBR Green Fast Master Mix (Roche Diagnostics, Meylan, France) and a SmartCycler (Cepheid, Maurens-Scopont, France). The M1 and M2 genes were selected according a list of M1 and M2 genes elsewhere published (48, 49). The primers were designed using Primer3 (http://frodo.wi.mit.edu/primer3) (**Table S2)**. Results were normalized using the housekeeping gene β-actin and are expressed as fold change (FC) = $2^{-\Delta\Delta Ct}$, where $\Delta\Delta Ct = (CtTarget - CtActin)_{assay} - (CtTarget - CtActin)_{control}$, as recently described (47).

Microarrays

RNAs were extracted using RNeasy Mini Kit (Qiagen) with a DNase I step to eliminate DNA contaminants, as recently described (47). The quantity and the quality of RNA were assessed using Nanodrop (Thermo Science, Maurens-Scopont, France) and 2100 Bioanalyseur (Agilent Technologies, Massy, France), respectively. The microarray study was performed using the technology provided by Agilent Technologies including microarrays chips including 45,000 probes (4X44K Whole Human Genome and One Color Microarray Based Gene Expression Analysis. In brief, 400 ng of RNA were labeled with cyanine-3 CTP using low RNA Input Fluorescent Amplification kit. Three samples per experimental condition were deposited on microarray slides and the hybridization was carried out for 17 hours at 65°C using the QIamp labeling kit. The microarray slides were scanned with a pixel size of 5 µm with the DNA Microarray scanner G2505 B. The scanned images were analyzed with Feature Extraction Software 10.5.1. The data processing and analyses were carried out using R software.

Analysis of microarray results

Microarray data were pre-analyzed using Significance Analysis of Microarrays that gives a score that represents the statistical significance for each gene and analyzed using R software, version 2.11.1 and Principal Component Analysis (PCA), as recently described (49). The modulated biological processes were identified through an analysis of Gene Ontology (GO) and Kyoto Encyclopedia of Genes and Genomes (KEGG) terms using GO stats package to test GO and KEGG terms that were over- or under-represented. The data were generated in compliance with the Minimum Information About a Microarray Experiment guidelines and were deposited in the National Center for Biotechnology Information's Gene Expression Omnibus (accession number (http://www.ncbi.nlm.nih.gov/geo/query/acc.cgi?token=bxmzrwwgygmwahu&acc=GSE2957

5). Finally, network pathways of differentially expressed genes were drawn by graph package (http://www.bioconductor.org/packages/2.4/bioc/html/KEGGgraph.html) according KEGG.

Statistical analysis

The results are expressed as the mean ± SEM and were compared using the non-parametric Mann-Whitney *U* test. *P* values less than 0.05 were considered significant. Correlation analysis between microarray and qRT-PCR data was performed using Microsoft MS-Excel 2003.

Human studies

Written informed consent was received from participants prior to inclusion in the study, and the study was approved by the Ethics Committee of the Federative Research Institute 48 (agreement number: 08-012).

Acknowledgments

We would like to thank Pr D. Olive for the gift of Abs specific of co-inhibitory molecules, Dr C. Fossat for ROI determination and N. Willigenes for collecting placentas.

References

1. Trowsdale, J., and Betz, A.G. 2006. Mother's little helpers: mechanisms of maternal-fetal tolerance. *Nat Immunol* 7:241-246.

2. Munoz-Suano, A., Hamilton, A.B., and Betz, A.G. 2011. The immune system during pregnancy. *Immunol Rev* 241:20-38.

3. Kim, J.S., Romero, R., Cushenberry, E., Kim, Y.M., Erez, O., Nien, J.K., Yoon, B.H., Espinoza, J., and Kim, C.J. 2007. Distribution of $CD14^+$ and $CD68^+$ macrophages in the placental bed and basal plate of women with preeclampsia and preterm labor. *Placenta* 28:571-576.

4. Bulmer, J.N., Williams, P.J., and Lash, G.E. 2010. Immune cells in the placental bed. *Int J Dev Biol* 54:281-294.

5. Houser, B.L., Tilburgs, T., Hill, J., Nicotra, M.L., and Strominger, J.L. 2011. Two unique human decidual macrophage populations. *J Immunol* 186:2633-2642.

6. Abrahams, V.M., Kim, Y.M., Straszewski, S.L., Romero, R., and Mor, G. 2004. Macrophages and apoptotic cell clearance during pregnancy. *Am J Reprod Immunol* 51:275-282.

7. Nagamatsu, T., and Schust, D.J. 2010. The immunomodulatory roles of macrophages at the maternal-fetal interface. *Reprod Sci* 17:209-218.

8. Heikkinen, J., Mottonen, M., Komi, J., Alanen, A., and Lassila, O. 2003. Phenotypic characterization of human decidual macrophages. *Clin Exp Immunol* 131:498-505.

9. Repnik, U., Tilburgs, T., Roelen, D.L., van der Mast, B.J., Kanhai, H.H., Scherjon, S., and Claas, F.H. 2008. Comparison of macrophage phenotype between decidua basalis and decidua parietalis by flow cytometry. *Placenta* 29:405-412.

10. Gustafsson, C., Mjosberg, J., Matussek, A., Geffers, R., Matthiesen, L., Berg, G., Sharma, S., Buer, J., and Ernerudh, J. 2008. Gene expression profiling of human decidual macrophages: evidence for immunosuppressive phenotype. *PLoS One* 3:e2078.

11. Verollet, C., Zhang, Y.M., Le Cabec, V., Mazzolini, J., Charriere, G., Labrousse, A., Bouchet, J., Medina, I., Biessen, E., Niedergang, F., et al. 2010. HIV-1 Nef triggers macrophage fusion in a p61Hck- and protease-dependent manner. *J Immunol* 184:7030-7039.

12. McNally, A.K., and Anderson, J.M. 2011. Macrophage fusion and multinucleated giant cells of inflammation. *Adv Exp Med Biol* 713:97-111.

13. Petroff, M.G., Chen, L., Phillips, T.A., Azzola, D., Sedlmayr, P., and Hunt, J.S. 2003. B7 family molecules are favorably positioned at the human maternal-fetal interface. *Biol Reprod* 68:1496-1504.

14. Petroff, M.G. 2006. B7 family molecules in the placenta. In *Immunology of pregnancy*. G. Mor, editor. Georgetown: Landes Bioscience/Eurekah, Springer Science. 159-170.

15. Habicht, A., Dada, S., Jurewicz, M., Fife, B.T., Yagita, H., Azuma, M., Sayegh, M.H., and Guleria, I. 2007. A link between PDL1 and T regulatory cells in fetomaternal tolerance. *J Immunol* 179:5211-5219.

16. Rodriguez-Garcia, M., Porichis, F., de Jong, O.G., Levi, K., Diefenbach, T.J., Lifson, J.D., Freeman, G.J., Walker, B.D., Kaufmann, D.E., and Kavanagh, D.G. 2011. Expression of PD-L1 and PD-L2 on human macrophages is up-regulated by HIV-1 and differentially modulated by IL-10. *J Leukoc Biol* 89:507-515.

17. Shui, J.W., Steinberg, M.W., and Kronenberg, M. 2011. Regulation of inflammation, autoimmunity, and infection immunity by HVEM-BTLA signaling. *J Leukoc Biol* 89:517-523.

18. Hu, D., and Cross, J.C. 2010. Development and function of trophoblast giant cells in the rodent placenta. *Int J Dev Biol* 54:341-354.

19. Maniecki, M.B., Etzerodt, A., Moestrup, S.K., Moller, H.J., and Graversen, J.H. 2011. Comparative assessment of the recognition of domain-specific CD163 monoclonal antibodies in human monocytes explains wide discrepancy in reported levels of cellular surface CD163 expression. *Immunobiology*:in press.

20. Fabriek, B.O., Dijkstra, C.D., and van den Berg, T.K. 2005. The macrophage scavenger receptor CD163. *Immunobiology* 210:153-160.

21. Bockle, B.C., Solder, E., Kind, S., Romani, N., and Sepp, N.T. 2008. DC-Sign^{+} CD163^{+} macrophages expressing hyaluronan receptor LYVE-1 are located within chorion villi of the placenta. *Placenta* 29:187-192.

22. Schonkeren, D., van der Hoorn, M.L., Khedoe, P., Swings, G., van Beelen, E., Claas, F., van Kooten, C., de Heer, E., and Scherjon, S. 2011. Differential distribution and phenotype of decidual macrophages in preeclamptic versus control pregnancies. *Am J Pathol* 178:709-717.

23. Joerink, M., Rindsjo, E., van Riel, B., Alm, J., and Papadogiannakis, N. 2011. Placental macrophage (Hofbauer cell) polarization is independent of maternal allergen-sensitization and presence of chorioamnionitis. *Placenta* 32:380-385.

24. Maggiani, F., Forsyth, R., Hogendoorn, P.C., Krenacs, T., and Athanasou, N.A. 2011. The immunophenotype of osteoclasts and macrophage polykaryons. *J Clin Pathol*:in press.

25. Brooks, E., Simmons-Arnold, L., Naud, S., Evans, M.F., and Elhosseiny, A. 2009. Multinucleated giant cells' incidence, immune markers, and significance: a study of 172 cases of papillary thyroid carcinoma. *Head Neck Pathol* 3:95-99.

26. Mor, G. 2006. Macrophages and pregnancy. In *Immunology of pregnancy*. G. Mor, editor. Georgetown: Landes Bioscience/Eurekah, Springer Science. 63-72.

27. Camolotto, S., Racca, A., Rena, V., Nores, R., Patrito, L.C., Genti-Raimondi, S., and Panzetta-Dutari, G.M. 2010. Expression and transcriptional regulation of individual pregnancy-specific glycoprotein genes in differentiating trophoblast cells. *Placenta* 31:312-319.

28. Harris, L.K., Crocker, I.P., Baker, P.N., Aplin, J.D., and Westwood, M. 2011. IGF2 actions on trophoblast in human placenta are regulated by the insulin-like growth factor 2 receptor, which can function as both a signaling and clearance receptor. *Biol Reprod* 84:440-446.

29. Hein, S., Yamamoto, S.Y., Okazaki, K., Jourdan-LeSaux, C., Csiszar, K., and Bryant-Greenwood, G.D. 2001. Lysyl oxidases: expression in the fetal membranes and placenta. *Placenta* 22:49-57.

30. Pfarrer, C.D., Ruziwa, S.D., Winther, H., Callesen, H., Leiser, R., Schams, D., and Dantzer, V. 2006. Localization of vascular endothelial growth factor (VEGF) and its receptors VEGFR-1 and VEGFR-2 in bovine placentomes from implantation until term. *Placenta* 27:889-898. Erratum in: Placenta 2006, 2027:1132-1134.

31. Trebec-Reynolds, D.P., Voronov, I., Heersche, J.N., and Manolson, M.F. 2010. VEGF-A expression in osteoclasts is regulated by NF-κB induction of HIF-1α. *J Cell Biochem* 110:343-351.

32. Helming, L., and Gordon, S. 2009. Molecular mediators of macrophage fusion. *Trends Cell Biol* 19:514-522.

33. Fournier, T., Therond, P., Handschuh, K., Tsatsaris, V., and Evain-Brion, D. 2008. PPARγ and early human placental development. *Curr Med Chem* 15:3011-3024.

34. Parast, M.M., Yu, H., Ciric, A., Salata, M.W., Davis, V., and Milstone, D.S. 2009. PPARγ regulates trophoblast proliferation and promotes labyrinthine trilineage differentiation. *PLoS One* 4:e8055.

35. Pollheimer, J., Loregger, T., Sonderegger, S., Saleh, L., Bauer, S., Bilban, M., Czerwenka, K., Husslein, P., and Knofler, M. 2006. Activation of the canonical wingless/T-cell factor signaling pathway promotes invasive differentiation of human trophoblast. *Am J Pathol* 168:1134-1147.

36. Hayashi, K., Erikson, D.W., Tilford, S.A., Bany, B.M., Maclean, J.A., 2nd, Rucker, E.B., 3rd, Johnson, G.A., and Spencer, T.E. 2009. Wnt genes in the mouse uterus: potential regulation of implantation. *Biol Reprod* 80:989-1000.

37. Talayev, V.Y., Matveichev, A.V., Lomunova, M.A., Talayeva, M.V., Tsaturov, M.E., Zaichenko, I.Y., and Babaykina, O.N. 2010. The effect of human placenta cytotrophoblast cells on the maturation and T cell stimulating ability of dendritic cells in vitro. *Clin Exp Immunol* 162:91-99.

38. McIntire, R.H., Ganacias, K.G., and Hunt, J.S. 2008. Programming of human monocytes by the uteroplacental environment. *Reprod Sci* 15:437-447.

39. Felaco, P., Castellani, M.L., De Lutiis, M.A., Felaco, M., Pandolfi, F., Salini, V., De Amicis, D., Vecchiet, J., Tete, S., Ciampoli, C., et al. 2009. IL-32: a newly-discovered proinflammatory cytokine. *J Biol Regul Homeost Agents* 23:141-147.

40. Atay, S., Gercel-Taylor, C., Suttles, J., Mor, G., and Taylor, D.D. 2011. Trophoblast-derived exosomes mediate monocyte recruitment and differentiation. *Am J Reprod Immunol* 65:65-77.

41. Li, C., Houser, B.L., Nicotra, M.L., and Strominger, J.L. 2009. HLA-G homodimer-induced cytokine secretion through HLA-G receptors on human decidual macrophages and natural killer cells. *Proc Natl Acad Sci U S A* 106:5767-5772.

42. Delaby, A., Espinosa, L., Lepolard, C., Capo, C., and Mege, J.L. 2010. 3D reconstruction of granulomas from transmitted light images implemented for long-time microscope applications. *J Immunol Methods* 360:10-19.

43. Desnues, B., Raoult, D., and Mege, J.L. 2005. IL-16 is critical for *Tropheryma whipplei* replication in Whipple's disease. *J Immunol* 175:4575-4582.

44. Kliman, H.J., Nestler, J.E., Sermasi, E., Sanger, J.M., and Strauss, J.F., 3rd. 1986. Purification, characterization, and in vitro differentiation of cytotrophoblasts from human term placentae. *Endocrinology* 118:1567-1582.

45. McIntire, R.H., Petroff, M.G., Phillips, T.A., and Hunt, J.S. 2006. In vitro models for studying human uterine and placental macrophages. *Methods Mol Med* 122:123-148.

46. Stoppa, A.M., Fossat, C., Blaise, D., Viens, P., Brandely, M., Pourreau, C.N., Sainty, D., Novakovitch, G., Miquel, M., Juhan-Vague, I., et al. 1991. Interleukin-2 induces chemotactic deficiency in patients with onco hematologic malignancies and autologous bone marrow transplantation. *Eur Cytokine Netw* 2:231-237.

47. Ben Amara, A., Ghigo, E., Le Priol, Y., Lepolard, C., Salcedo, S.P., Lemichez, E., Bretelle, F., Capo, C., and Mege, J.L. 2010. *Coxiella burnetii*, the agent of Q fever, replicates within trophoblasts and induces a unique transcriptional response. *PLoS One* 5:e15315.
48. Martinez, F.O., Gordon, S., Locati, M., and Mantovani, A. 2006. Transcriptional profiling of the human monocyte-to-macrophage differentiation and polarization: new molecules and patterns of gene expression. *J Immunol* 177:7303-7311.
49. Tantibhedhyabgkul, W., Prachason, T., Waywa, D., El Filali, A., Ghigo, E., Thongnoppakhun, W., Raoult, D., Suputtamongkol, Y., Capo, C., Limwongse, C., et al. 2011. *Orientia tsutsugamushi* stimulates an original gene expression program in monocytes: relationship with gene expression in patients with scrub typhus. *PLoS Neglect Trop Dis* 5:e1028.

Table 1. Transcriptional responses of placenta cells according M1/M2 polarization

	$CD14^+$ macrophages	MGCs
M1 genes		
CXCL9	204.4	74.3
EDN1	2.35	6.89
HESX1	0.60	1.65
IL15	27.8	27.1
IL15RA	16.7	4.82
IL2RA	19.3	3.10
INDO	3.11	0.00
TNF	0.21	0.07
TRAIL	0.24	0.52
M2 genes		
ALOX15	0.15	0.03
CCL13	0.00	0.97
CCL23	3.43	0.62
CHN2	0.49	0.93
CLEC4F	0.01	0.01
CTSC	473	843
DC-SIGN	0.73	1.77
FN1	399	1992
HRH1	1.14	1.77
SLC4A7	1.75	1.57

The transcriptional response of placenta $CD14^+$ macrophages and MGCs performed on 9 M1 genes and 10 M2 genes was studied by qRT-PCR. The results, expressed as FC, are presented as the mean ± SEM of three independent experiments performed in triplicate.

Table 2. Determination of modulated genes in placenta cells

	upregulated genes	downregulated genes
$CD14^+$ macrophages vs. monocytes	2358	1282
$CD14^+$ macrophages vs. MDMs	1805	1560
MGCs vs. $CD14^+$ macrophages	548	544

The transcriptional response of placenta $CD14^+$ macrophages was studied by microarrays and compared to the transcriptional responses of monocytes or MDMs. The transcriptional response of MGCs was compared to that of placenta $CD14^+$ macrophages. The number of genes that were up- and downregulated is indicated.

Table 3. qRT-PCR determination on selected genes

Genes	FC values	
	$CD14^+$ macrophages	**MGCs**
APOC1	4040	474.4
CCL18	28329	9476
COL16A1	1.29	21.93
COL1A2	2.71	336.6
COL3A1	0.38	125.8
CSH1	1346.5	0.03
CSH2	264.1	0.37
FABP3	3743	37.5
IDO1	35.0	0.13
IGF2	1097.5	0.66
IL10	14.37	1.75
IL24	2150	0.20
IL32	389.4	4.27
IRF2	30.8	10.0
IRF4	15.8	1.29
IRF9	3.35	1.52
LOXL2	1.31	22.16
ME1	0.76	2.58
MMP12	5202	109.5
MMP7	2759	25798
PDL1	606.8	43.3
PSG6	2361	0.57
PSG9	2702	0.67
TGFA	122.4	7.89
TIMP3	159.8	96.0
VEGFC	0.11	9.8
WNT5A	306.6	4.9

qRT-PCR experiments were performed on 28 genes found to be highly regulated in microarray experiments. The results, expressed as FC, are presented as the mean ± SEM of three independent experiments performed in triplicate.

Table S1. Modulated genes in placenta cells and MDMs

	$CD14^+$ macrophages		MGCs	
	upregulated	downregulated	upregulated	downregulated
IFN-γ	9014	9119	3525	4131
IL-4	2789	3247	6662	8096

MDMs were stimulated with IFN-γ and IL-4 (20 ng/ml) for 18 hours. Their transcriptional response was studied by microarrays and compared to that of placenta $CD14^+$ macrophages and MGCs. The number of genes that were up- and downregulated in $CD14^+$ macrophages and MGCs compared with MDMs is indicated.

Table S2. Nucleotide sequences of primers

Gene symbols	Forward primers	Reverse primers
APOC1	5’-ggataagctgaaggagtttgga-3’	5’-ttcaggtcctcatgagtcaatc-3’
CCL18	5’-ctctgctgcctcgtctatacct-3’	5’-tcaggtcgctgatgtatttctg-3’
COL16A1	5’-caggaaggactcaaattggaac-3’	5’-cggtcacttgaaacagatacca-3’
COL1A2	5’-ctagacatgctcagctttgtgg-3’	5’-caagtccaactccttttccatc-3’
COL3A1	5’-gcctcattagtcctgatggttc-3’	5’-caaacgtgtttcttctcagcac-3’
CSH1	5’-gctgccctcttttagcagtaa-3’	5’-gcaaagtgaaggaagagaagga-3’
CSH2	5’-aaaggacctagaggaaggcatc-3’	5’-gcaaagtgaaggaagagaagga-3’
FABP3	5’-gcctgctctcttgtagcttctc-3’	5’-tctgtgttcttgaaggtgctgt-3’
IDO1	5’-ctgagttctggctttcaggagt-3’	5’-gtgcctcaatgttatccctagc-3’
IGF2	5’-cccacaacaaccctcttaaaac-3’	5’-ctggggtccttcttttctcttt-3’
IL10	5’-gagtccttgctggaggacttta-3’	5’-gatgcctttctcttggagctta-3’
IL24	5’-aggaggaacacgagactgagag-3’	5’-tagtgtctttcacagcccagaa-3’
IL32	5’-ggcttattatgaggagcagcac-3’	5’-tgacagagagcagcagaaactc-3’
IRF2	5’-ggaaagcatcaaccaggagtag-3’	5’-ccattactaagccccagagatg-3’
IRF4	5’-ccaagtgaccgactcatttaca-3’	5’-cctggggctagctgtatttatg-3’
IRF9	5’-tctgcagagacttggtcaggta-3’	5’-aaagaggacaggtcaatcgtgt-3’
LOXL2	5’-cccatttctcctcctcttaggt-3’	5’-cagtgggttggtttttccttag-3’
ME1	5’-attggactacggcagagaagag-3’	5’-tcgatacttgttcaggagacga-3’
MMP12	5’-acttgttcctcactgctgttca-3’	5’-ctcttttgggtctccatacagg-3’
MMP7	5’-agaagccaaactcaaggagatg-3’	5’-cgatccactgtaatatgcggta-3’
PDL1	5’-tgatacacatttggaggagacg-3’	5’-ccctcaggcatttgaaagtatc-3’
PSG6	5’-gatgggactggaggagtaactg-3’	5’-agtcatagggaggttctgacca-3’
PSG9	5’-ctccacagaggagaacacacag-3’	5’-tagaagaacatccttcccctca-3’
TGFA	5’-gtggactgtggcagatcaataa-3’	5’-gagtccgtctctttgcagttct-3’
TIMP3	5’-caaagggagtctcctctcagaa-3’	5’-tgctcctacacggcctattatt-3’
VEGFC	5’-aaacaaggagctggatgaagag-3’	5’-gtttggtggtggaacttctttc-3’
WNT5A	5’-ctgctgtgatcataccttgagc-3’	5’-gaacaagtaatgccctctccac-3’

Figure 1. Characterization of placenta CD14$^+$ macrophages

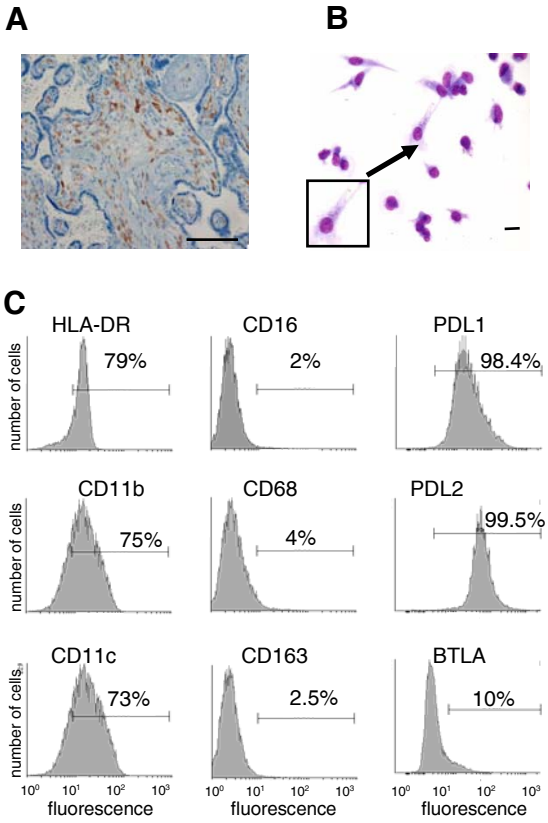

A, The presence of CD14$^+$ cells in villi was determined using immunohistochemistry revelation. Bar, 30 µm. **B**, CD14$^+$ macrophages were isolated by selective selection and were observed after May-Grünwald Giemsa staining. Bar, 10 µm. C, Immunolabeling of CD14$^+$ macrophages was performed and cell fluorescence was revealed by flow cytometry.

Figure 2. Characterization of placenta MGCs

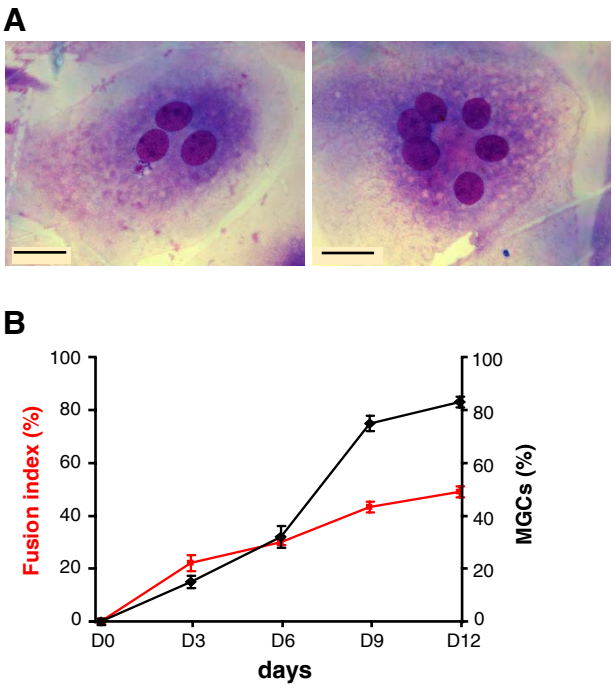

Placenta CD14^{+} macrophages were differentiated into MGCs for 12 days.

A, May-Grünwald Giemsa staining of MGCs after 9 days. Bar, 20 µm.

B, The time course of MGC differentiation was determined. The results are expressed as the percentage of cells with at least two nuclei and fusion index. They represent the mean ± SEM of four different experiments.

Figure 3. Cytoskeleton organization in placenta cells

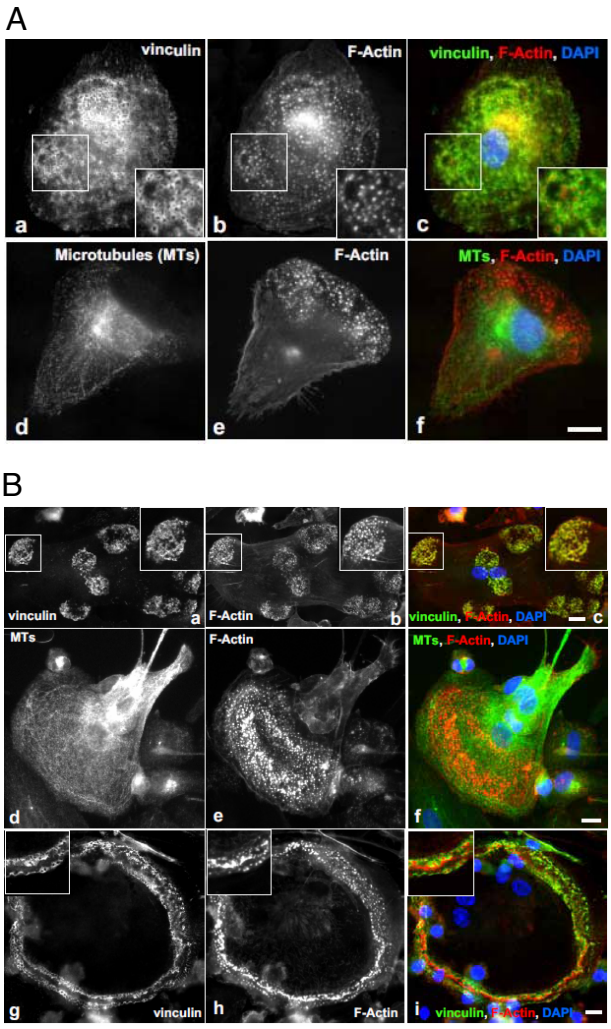

A, Placenta $CD14^+$ macrophages were isolated and the organization of podosomes and microtubules was studied using fluorescent anti-vinculin (in green, a), α-tubulin (in green, d) Abs, Texas Red-conjugated phalloidin (in red, b and e), and DAPI (in blue). Merged images in c and f. **B**, Placenta $CD14^+$ macrophages were differentiated into MGCs and the organization of podosomes and microtubules was studied using fluorescent anti-vinculin (a and g), α-tubulin (d) Abs, Texas Red-conjugated phalloidin (b, e, h), and DAPI. Merged images in c, f and i. Bar, 10 μm.

Figure 4. Functional studies of placenta cells

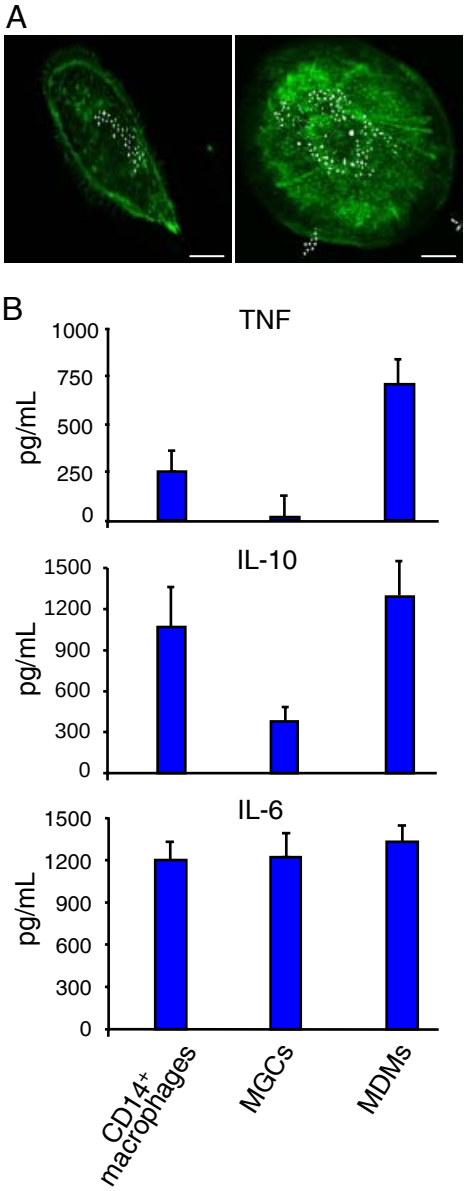

A, Placenta CD14^{+} and MGCs were incubated with magnetic beads for 1 hour, and bead phagocytosis was observed by confocal microscopy. Bars represent 5 µm (left) and 20 µm (right). **B**, Placenta cells and MDMs were incubated with 100 ng/ml LPS for 24 hours, and the amounts of cytokines released in culture supernatants were determined by immunoassays. The results are expressed as mean ± SEM of three different experiments.

Figure 5. Microarray analysis

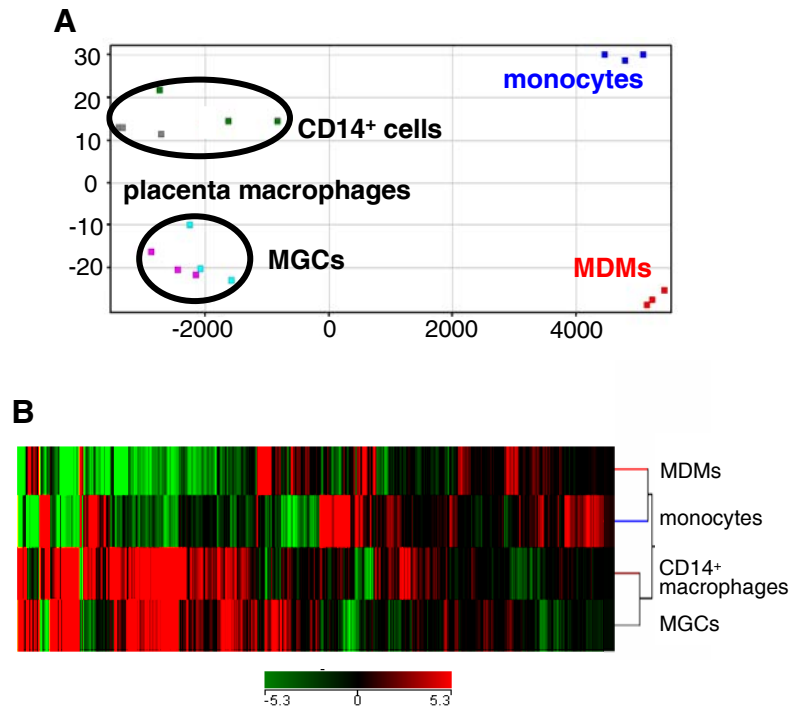

Microarrays were performed on placenta CD14+ macrophages and MGCs, monocytes and MDMs after RNA extraction. **A**, The impact of cell types on gene expression was analyzed by PCA using R. Each axis distance represents the amount of variance in gene expression. **B**, Data were analyzed using hierarchical clustering including the 300 genes that were the most modulated and are represented by a gradient ranging from green (downregulated genes) to red (upregulated genes).

Figure 6. GO annotation of regulated genes in placenta cells

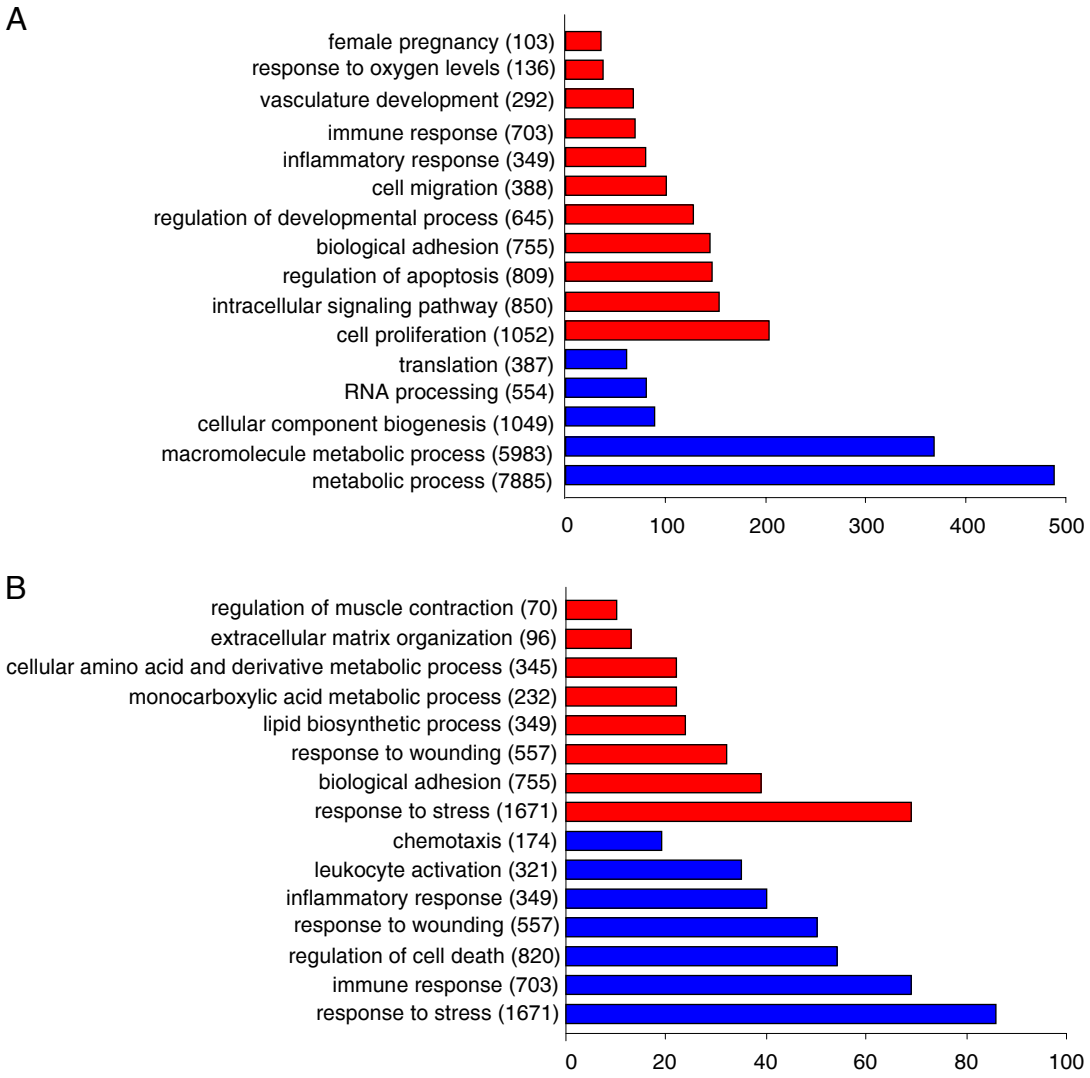

Microarrays were performed on placenta $CD14^+$ macrophages, MGCs and circulating monocytes. The genes that were differentially expressed in placenta $CD14^+$ macrophages compared with monocytes (**A**) and in MGCs compared with $CD14^+$ macrophages (**B**) were subjected to GO annotation to identify the corresponding biological process. The major biological processes are shown, including the number of regulated genes. In red, upregulated genes; in blue, downregulated genes.

Figure 7. Major gene network in MGCs

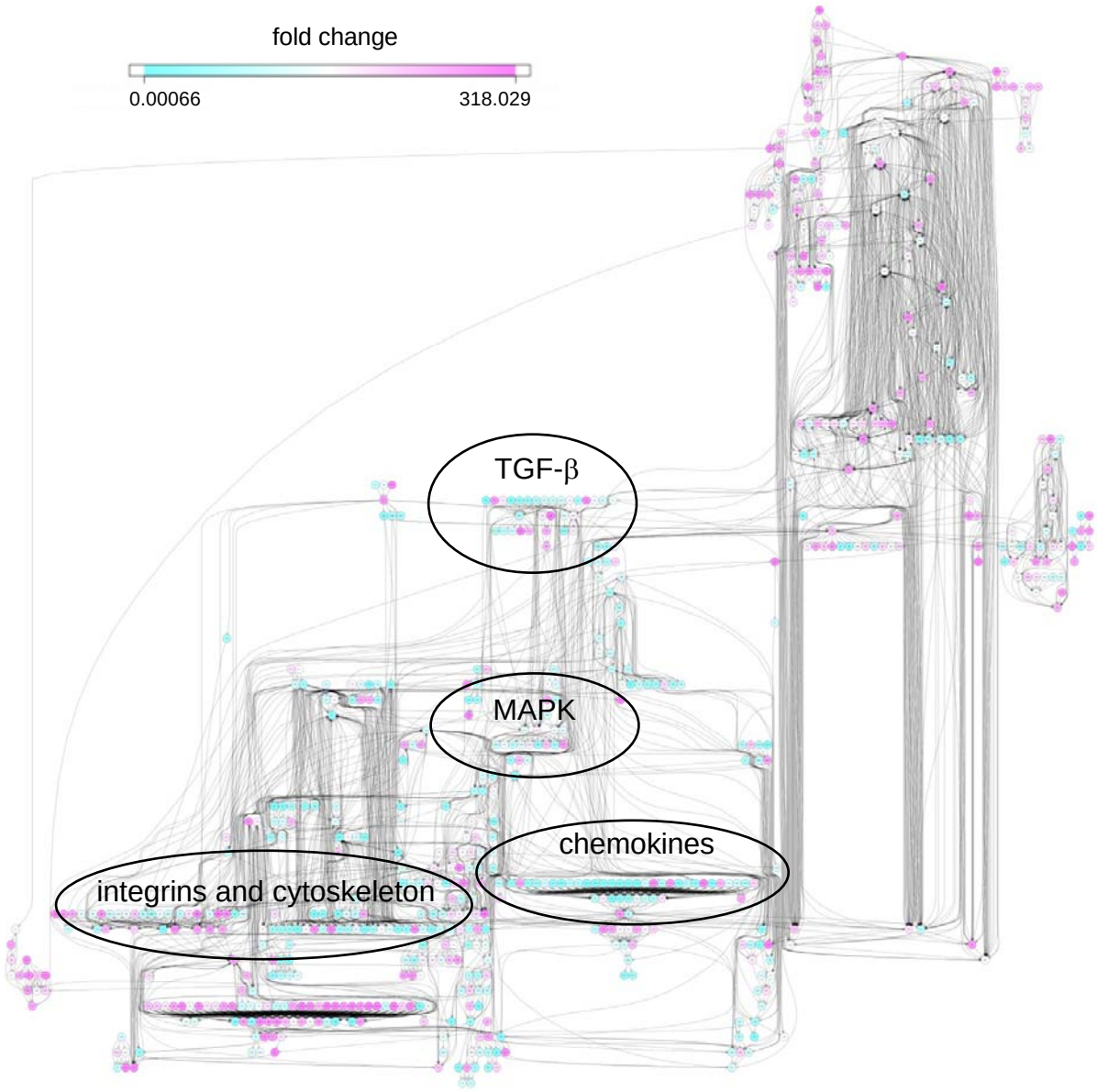

Microarray data performed on $CD14^+$ macrophages and MGCs were collected, and gene modulation was compared in MGCs vs. $CD14^+$ macrophages. The gene networks of regulated genes in MGCs with nodes controlling transcription and interaction pathways were analyzed using KEGG. The major network is represented.

Figure 8. Minor gene networks in MGCs

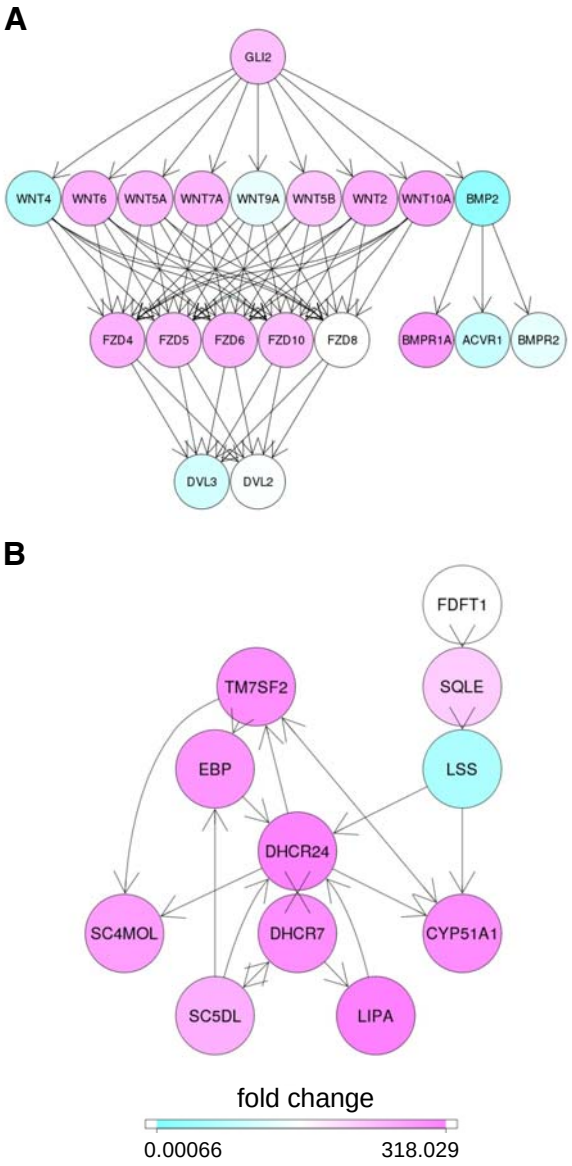

Microarray data performed on $CD14^+$ macrophages and MGCs were collected, and gene modulation was compared in MGCs vs. $CD14^+$ macrophages. The gene networks of regulated genes in MGCs with nodes controlling transcription and interaction pathways were analyzed using KEGG. Two minor networks corresponding to WNT pathway (A) and cholesterol metabolism (B) are represented.

Figure 9. Effect of trophoblats on MGC generation

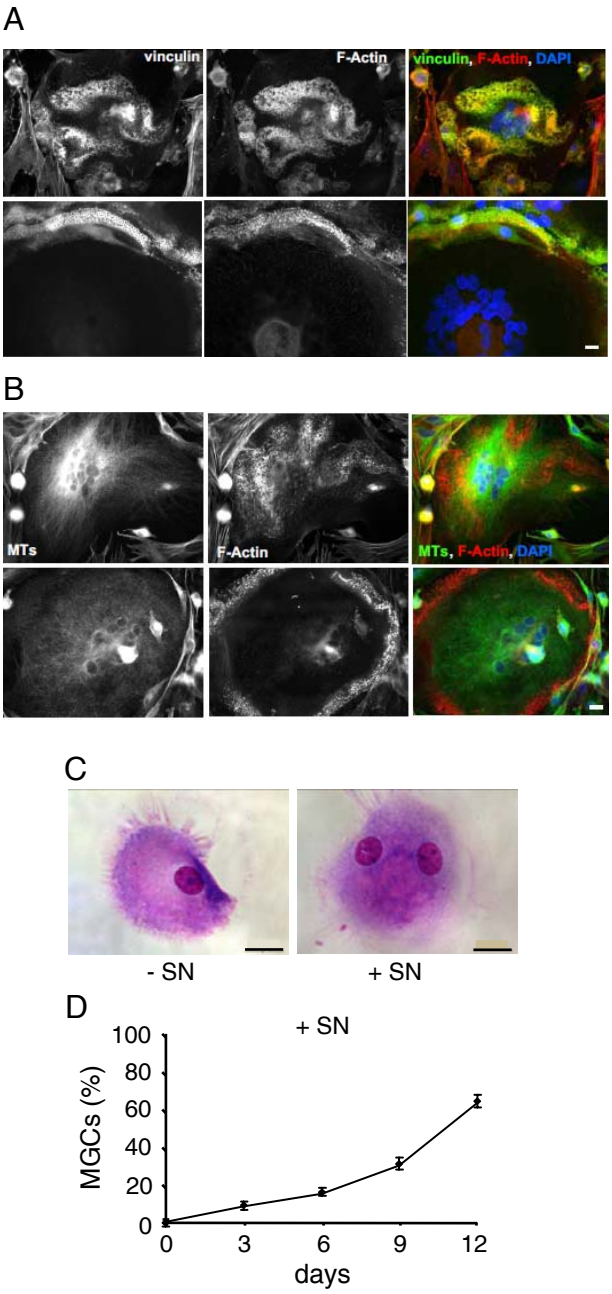

A and B, Placenta $CD14^+$ macrophages were incubated with trophoblats for 10 days. The organization of podosomes and microtubules of resulting MGCs was studied using fluorescent anti-vinculin (A), α-tubulin (B) Abs (in green), Texas Red-conjugated phalloidin (in red), and DAPI (in blue). Merged images (right). Bar, 10 µm. **C-D**, Circulating monocytes from parturient women were incubated with trophoblast supernatants for different periods. Cells were stained with May-Grünwald Giemsa. Representative micrographs after 12 days are shown (C). Bars represent 10 µm (left) and 20 µm (right). The percentage of MGCs was calculated and represents the mean ± SEM of three different experiments (D).

Figure S1. Characterization of trophoblasts

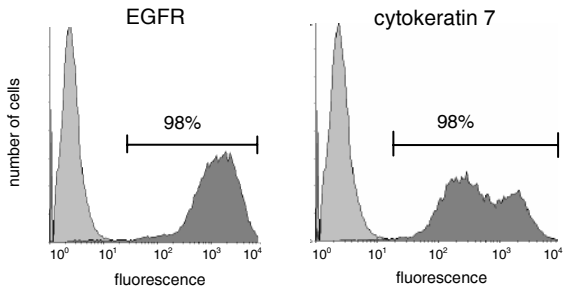

Trophoblasts were isolated on 25-60% Percoll interface and purified using magnetic beads coated with anti-EGR-R Abs. Immunolabeling of selected cells was performed and cell fluorescence was revealed by flow cytometry after permeabilization to reveal cytokertain-7. In grey, isotypic controls; in dark, specific Abs.

Figure S2. Immunophenotyping of monocytes and MDMs
Monocytes (A) and monocyte-derived macrophages (B) were labeled with different fluorochrome-conjugated Abs. Cell fluorescence was revealed by flow cytometry.

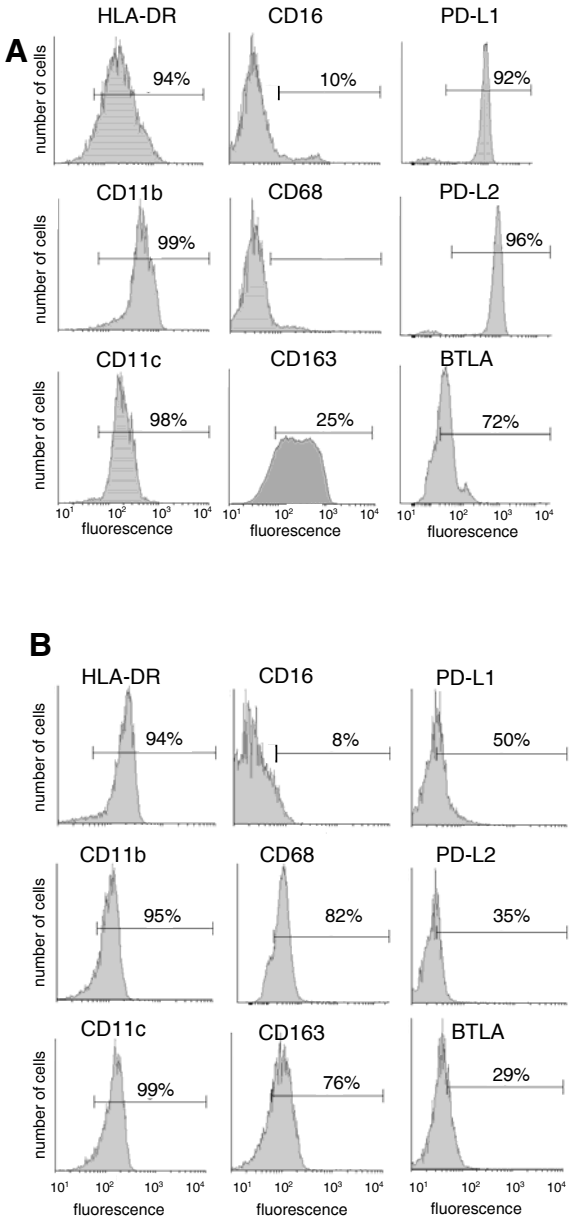

Figure S3. Marker expression of MGCs

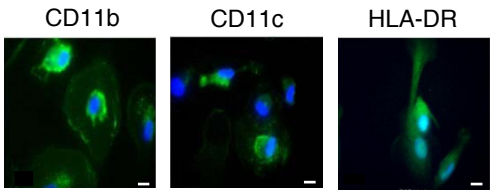

MGCs were labeled with different fluorochrome-conjugated Abs. MGC labeling was revealed by epifluorescence. Specific Abs, in green; DAPI, in blue. Bar, 5 µm.

Figure S4. Defective activation of p38 MAPK and NF-κB in MGCs

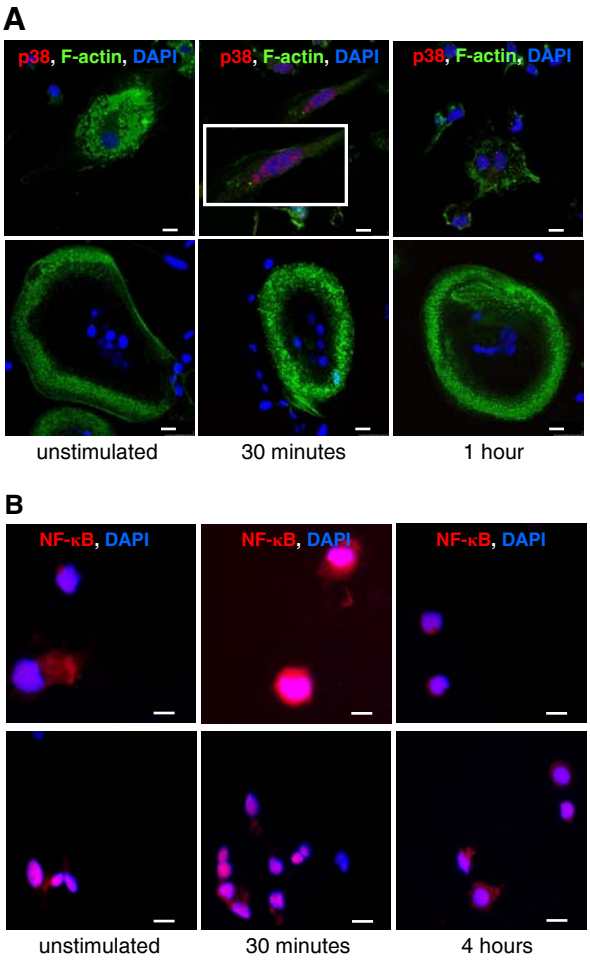

$CD14^+$ macrophages and MGCs were stimulated with 100 ng/ml LPS for different periods. **A**, $CD14^+$ macrophages (top) and MGCs (bottom) were then incubated with fluorescent anti-phosphorylated p38 Abs (in red), bodipy phallacidin (in green) and DAPI (in blue). Note that phosphorylated p38 was essentially found in perinuclear spaces. **B**, $CD14^+$ macrophages (top) and MGCs (bottom) were incubated with fluorescent anti-NF-κB p65 Abs (in red) and DAPI (in blue). Bars represent 20 µm (A and B, top) and 10 µm (A and B, bottom).

Figure S5. Metabolism gene network in MGCs
Microarray data performed on $CD14^+$ macrophages and MGCs were collected, and gene networks of regulated genes in MGCs with nodes controlling transcription and interaction pathways were analyzed using KEGG. Two subnetworks related to aminoacid (A) and carbohydrate (B) metabolism are represented.

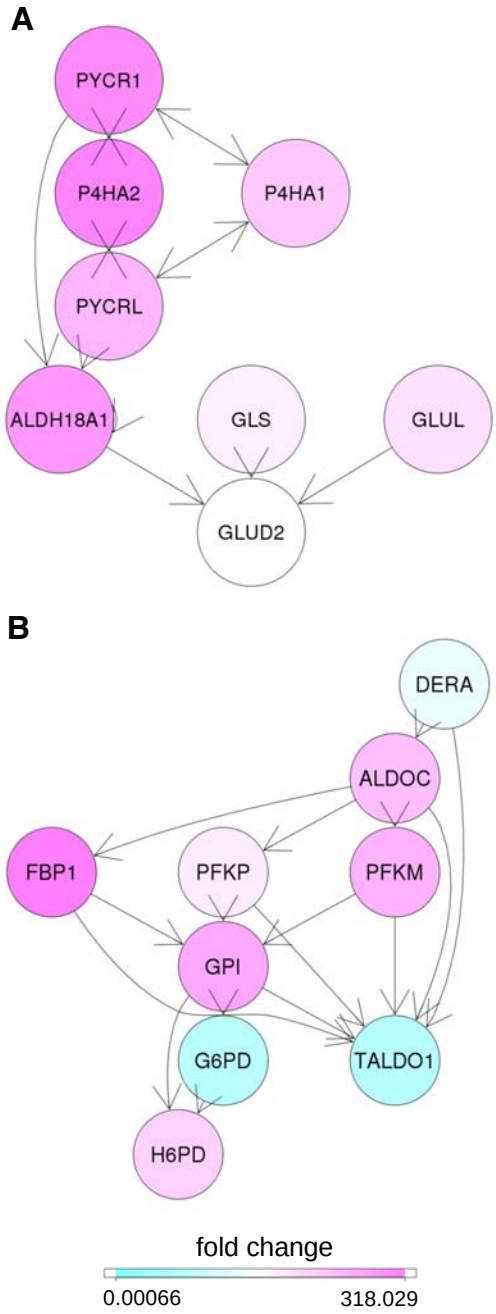

Figure S6. Small gene networks in MGCs

Microarray data performed on $CD14^{+}$ macrophages and MGCs were collected, and gene networks of regulated genes in MGCs with nodes controlling transcription and interaction pathways were analyzed using KEGG. Three subnetworks related to TNFSF4/TNFSRF4, PPARγ/RXRA and complement are represented.

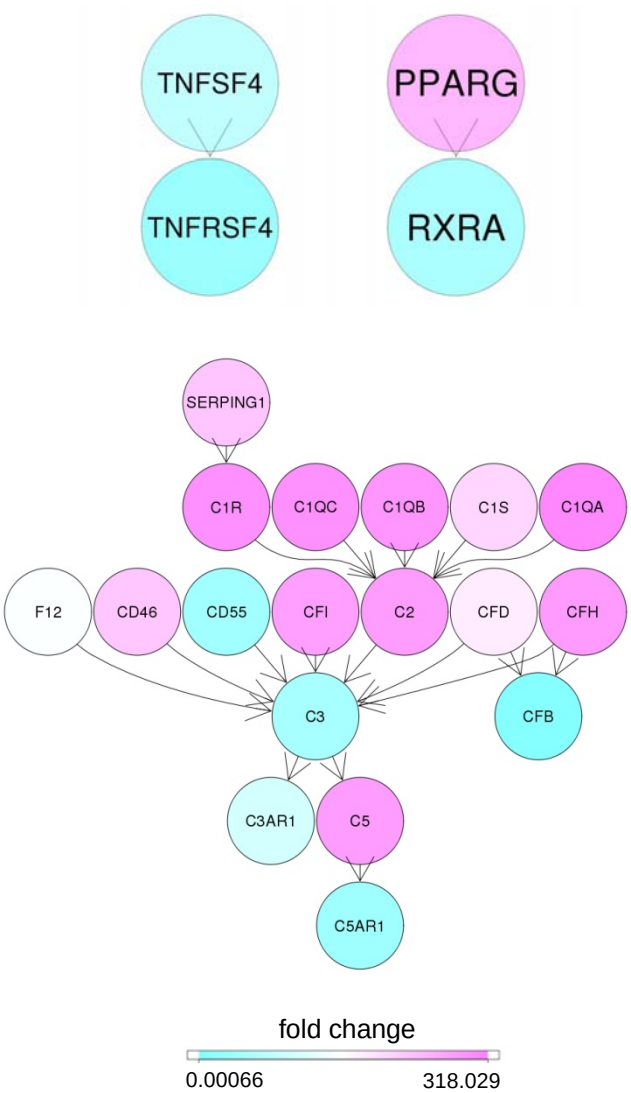

CONCLUSIONS

ET PERSPECTIVES

La fièvre Q est une maladie étonnante (*query*) à plus d'un titre. Chez l'homme, elle peut être silencieuse ou présenter diverses manifestations peu spécifiques. Elle est susceptible de se chroniciser, ce qui signifie qu'elle réside pendant des mois voire des années dans un réservoir encore inconnu. Les manifestations de la fièvre Q sont essentiellement une endocardite infectieuse, ce qui montre que *Coxiella burnetii*, l'agent de la fièvre Q, a un tropisme particulier pour les valves cardiaques sans qu'on en comprenne véritablement les raisons. *C. burnetii* présente également un tropisme pour le placenta. En effet, la fièvre Q peut se manifester chez la femme enceinte avec des conséquences pour la mère (fièvre Q chronique) et risque d'avortement ou de prématurité. L'infection du cheptel bovin, ovin et caprin par *C. burnetii* conduit également à des avortements, ce qui constitue un problème vétérinaire et économique loin d'être négligeable. Le lien entre ces différentes manifestations cliniques de l'infection par *C. burnetii* est loin d'être évident. On sait simplement que l'âge et le sexe constituent deux éléments-clés de l'infection par *C. burnetii*. En outre, même si *C. burnetii* existe sous forme sporulée qui la rend extraordinairement résistante à son environnement, son cycle réplicatif nécessite une vie intracellulaire. Il a été montré à ce jour que *C. burnetii* vit dans les monocytes/macrophages aussi bien in vitro que in vivo, ce qui n'exclut pas la possibilité que *C. burnetii* puisse vivre dans d'autres types cellulaires.

Mon projet de thèse est parti du constat que *C. burnetii* infecte le placenta, un organe constitué pour l'essentiel de trophoblastes. C'est la raison pour laquelle j'ai dans un premier temps étudié l'infection in vitro de deux lignées de cellules trophoblastiques par *C. burnetii*. J'ai montré que *C. burnetii* infecte et se réplique dans les trophoblastes de la lignée BeWo en induisant un programme transcriptionnel spécifique de type inflammatoire. De façon quelque peu surprenante, *C. burnetii* vit dans une structure de type phagolysosome puisque le compartiment contenant les bactéries est colocalisé avec Lamp-1, un marqueur des endosomes tardifs et des lysosomes et avec la cathepsine D, un marqueur des lysosomes. En revanche, *C. burnetii* ne se réplique pas dans les trophoblastes de la lignée JEG même si *C. burnetii* infecte de façon similaire les cellules BeWo et les cellules JEG. Les programmes transcriptionnels induits par *C. burnetii* sont très largement différents dans les cellules BeWo et les cellules JEG, ce qui expliquer le comportement différent de ces deux types de cellules trophoblastiques à l'égard de *C. burnetii*. Il est à noter que les cellules BeWo sont assimilées à des trophoblastes villeux alors que les cellules JEG sont plutôt assimilées à des trophoblastes extra-villeux, ce qui pourrait expliquer nos résultats. Enfin, des résultats préliminaires obtenus à partir de trophoblastes isolés à partir de placenta par sélection positive sur colonnes d'EGFR montrent que *C. burnetii* infecte ces trophoblastes, ce qui confirme les résultats obtenus sur

les deux lignées trophoblastiques. Ces résultats montrent donc la complexité de l'interaction entre *C. burnetii* et des cellules cibles qui semblent pourtant relativement proches. On ne saurait donc écarter l'hypothèse que, in vivo, *C. burnetii* infecte différemment les différentes populations de trophoblastes.

Le placenta étant un organe riche non seulement en trophoblastes mais également en macrophages, la question a donc été de savoir si les macrophages placentaires peuvent servir de réservoir à *C. burnetii*. Il nous est apparu chemin faisant qu'il était nécessaire d'approfondir la notion de macrophages placentaires. En effet, la grande majorité de ces macrophages semblent se comporter de façon très particulière puisque, sur le plan phénotypique, ils expriment CD14 tout comme les monocytes et non pas CD68, un marqueur classique des macrophages. Pour autant, ce ne sont pas des monocytes circulants de la mère infiltrant le placenta puisque leur comportement est notablement différent (voir ci-après). Une minorité de macrophages placentaires expriment CD68, mais pas CD14, ce qui en fait des macrophages « classiques ». Nous avons alors décidé de nous consacrer à l'étude des macrophages placentaires $CD14^+$. Nous avons observé que les macrophages placentaires $CD14^+$ se différencient en quelques jours en cellules géantes multinucléées, ce que ne font ni les monocytes ni les macrophages différenciés à partir de monocytes. Il est probable que l'environnement de la grossesse joue un rôle dans cette différenciation « spontanée » en cellules géantes multinucléées puisque la co-incubation des monocytes de femmes au moment de la délivrance avec des surnageants de culture de trophoblastes conduit également à la formation de cellules géantes multinucléées. L'étude comparée des macrophages placentaires $CD14^+$ et des cellules géantes multinucléées a montré que ces deux types cellulaires sont des phagocytes pourvus d'une activité microbicide. Ils varient cependant par nombre de caractéristiques phénotypiques. La réponse inflammatoire des macrophages $CD14^+$, déterminée par l'étude des cytokines produites en réponse à un inducteur tel que le LPS, est plus importante que celle des cellules géantes multinucléées. L'étude de la signalisation induite par le LPS dans les macrophages $CD14^+$ montre l'activation transitoire de la MAPK p38 et la translocation membranaire du facteur de transcription NF-κB, ce qui est en accord avec la réaction inflammatoire détectée. En revanche, dans les cellules géantes multinucléées, il n'y a ni activation de p38 ni translocation membranaire de NF-κB, ce qui pourrait expliquer leur moindre réaction inflammatoire. Ces cellules placentaires ne sont pas non plus franchement polarisables en macrophages M1/M2, ce qui montre que le concept de macrophages M1/M2 n'est pas applicable de façon universelle (cf ci-après). Enfin, l'étude transcriptionnelle en microarray montre des différences majeures entre d'une part les

macrophages placentaires et les monocytes circulants et les macrophages dérivés de monocytes et d'autre part entre les macrophages placentaires $CD14^+$ et les cellules géantes multinucléées. Des premiers résultats montrent que les macrophages placentaires $CD14^+$ peuvent être infectés par *C. burnetii* mais l'étude du devenir intracellulaire de C. burnetii dans ces cellules est rendue plus délicate du fait de leur différenciation en cellules géantes multinucléées.

Après ce détour par les macrophages placentaires et les cellules géantes multinucléées, je suis revenue à l'étude des monocytes circulants et de leur éventuelle polarisation en cellules M1 ou M2. Le concept de polarisation M1/M2 des macrophages est issu du concept Th1/Th2 de la réponse des cellules T. Il est ainsi bien montré que les macrophages murins stimulés par des agonistes tels que l'IFN-γ acquièrent de nouvelles propriétés phénotypiques et fonctionnelles: ces macrophages dits M1 deviennent inflammatoires, microbicides et tumoricides. En revanche, les mêmes macrophages stimulés par des agonistes tels que l'IL-4 acquièrent d'autres caractéristiques qui les rendent plutôt régulateurs de la réponse inflammatoire de telle sorte qu'ils perdent leurs propriétés microbicides et tumoricides. Quelques rares travaux montrent que la notion de macrophages M1/M2 acquise chez la souris s'applique également aux macrophages humains mais on ne sait rien de la capacité des monocytes circulants à se polariser en monocytes M1 ou M2. Cette question revêt une grande importance puisque seule l'étude des monocytes circulants peut être entreprise chez les patients atteints, par exemple, d'une maladie infectieuse. Savoir ainsi si un patient présente une polarisation M1 ou M2 de ses monocytes à un moment donné de son histoire clinique pourrait modifier son traitement tel qu'une augmentation de sa couverture antibiotique sans même parler de l'utilisation de cytokines ou d'anti-cytokines. C'est dans ce contexte que j'ai étudié la réponse transcriptionnelle des monocytes circulants de sujets sains à l'IFN-γ et à l'IL-4 en la comparant à celle des macrophages dont on sait qu'elle est, elle, polarisable en macrophages M1 et M2. Nous avons montré que la réponse précoce (6 heures) des monocytes à l'IFN-γ et à l'IL-4 est, pour l'essentiel, polarisable respectivement en monocytes M1 et en monocytes M2. Il est considéré classiquement que, dans leur état quiescent, les macrophages sont légèrement anti-inflammatoires, que seule une activation forte leur permet d'acquérir une puissante activité microbicide et cytotoxique et que celle-ci se doit d'être transitoire de telle sorte que succède à cette phase inflammatoire une phase résolument anti-inflammatoire. C'est la raison pour laquelle une polarisation M2 est considérée comme succédant à une polarisation M1. Notre étude transcriptionnelle à grande échelle infirme cette hypothèse, tout

au moins au niveau des monocytes. En effet, les programmes transcriptionnels des monocytes stimulés pendant 18 heures par l'IFN-γ ou par l'IL-4 n'entrent pas dans la dichotomie M1/M2 et s'avèrent être totalement originaux. Les catégories de gènes liés à la réponse immune innée et aux voies métaboliques sont enrichies en réponse à l'IFN-γ et à l'IL-4. La voie PPAR (*peroxisome proliferator-activated receptor*) est, elle, spécifiquement enrichie en réponse à l'IL-4. Les réseaux de gènes qui caractérisent les réponses tardives à l'IFN-γ et à l'IL-4 sont totalement différents de ceux observés lors des réponses précoces. Ainsi, outre des réseaux de gènes relativement attendus, deux réseaux organisés autour des gènes codant une pyruvate kinase et la kinase Lyn caractérisent la réponse tardive des monocytes à l'IFN-γ. La réponse tardive des monocytes à l'IL-4 est, elle, organisée autour d'un réseau majeur de gènes impliqués dans le maintien du cytosquelette et de gènes codant des chimiokines et de deux réseaux plus petits liés au métabolisme. Ces résultats suggèrent ainsi que l'activation des monocytes consiste en une étape précoce probablement impliquée dans les réponses effectrices de ces monocytes à laquelle succède une étape qui régule la réponse des monocytes sans pour autant être de type M2. L'établissement de banques de données relatives à la réponse des monocytes pourrait être utile à l'étude des patients par une méthode non invasive.

Je me suis enfin consacrée à une étude à l'interface de la biologie et de la clinique. L'infection à *C. burnetii*, dans sa forme chronique, se traduit essentiellement par une endocardite dont le pronostic est souvent péjoratif en dépit des traitements chirurgicaux et antibiotiques administrés. L'endocardite à *C. burnetii* ne représente cependant qu'un faible pourcentage des endocardites infectieuses dont le diagnostic n'est pas toujours assuré et que l'on ne sait pas pronostiquer. Dans un travail précédent mené au sein de notre laboratoire en liaison avec les cliniciens, il a été montré que les valves cardiaques des patients atteints d'une endocardite infectieuse à streptocoques ou à staphylocoques présentent un profil transcriptomique spécifique compatible avec l'histoire naturelle des endocardites infectieuses et qui révèle l'importance d'une molécule telle que l'aquaporine 9. Ce travail a laissé espérer qu'il serait possible de trouver une signature périphérique qui pourrait être utile au diagnostic et surtout au pronostic des endocardites infectieuses. C'est la raison pour laquelle nous avons étudié le transcriptome sur sang total des patients entrant à l'hôpital pour une suspicion d'endocardite infectieuse et dont le diagnostic a été ultérieurement confirmé ou infirmé. Les patients souffrant d'une endocardite infectieuse présentent un programme transcriptionnel spécifique, ce qui nous a permis de sélectionner un nombre restreint de gènes susceptibles de

servir de marqueurs de la maladie et les avons étudié en qRT-PCR et en dosage protéique. Il apparaît ainsi que la molécule S100A11, une protéine fixant le calcium, pourrait servir de marqueur de diagnostic des endocardites infectieuses et que l'aquaporine 9 pourrait, elle, servir de marqueur de pronostic. Ce travail demande bien entendu confirmation en augmentant le nombre de malades testés, le nombre de gènes testés puisque notre échantillon était faible eu égard à l'ensemble des gènes modulés et en développant une stratégie de dosage des molécules circulantes servant potentiellement de marqueurs des endocardites infectieuses.

Le travail que j'ai effectué au cours de cette thèse nécessite de nombreux développements. Les résultats obtenus sur les cellules des lignées trophoblastiques JEG et BeWo infectées par *C. burnetii* demandent à être étendus aux trophoblastes primaires. Cette étude pourrait être effectuée selon la même approche méthodologique que celle utilisée pour l'étude des lignées trophoblastiques. On pourrait également comparer les trophoblastes du premier trimestre et ceux du troisième trimestre. Si j'ai caractérisé la population des macrophages placentaires $CD14^+$, je n'ai pas pour autant analysé leur réponse à l'infection par *C. burnetii*. Cette étude sera prochainement réalisée et les résultats seront comparés à ceux obtenus pour les monocytes et les macrophages dérivés de monocytes et aux trophoblastes primaires. Cette comparaison effectuée en microarray pourrait permettre d'identifier un certain nombre de gènes candidats potentiellement impliqués dans la réplication ou l'élimination de *C. burnetii*. Par ailleurs, les résultats préliminaires que j'ai obtenus montrent que les trophoblastes seraient susceptibles de moduler les fonctions des macrophages placentaires. Il serait donc nécessaire d'approfondir l'étude des interactions entre les différentes populations des cellules placentaires. Parmi les populations placentaires probablement concernées par l'infection par *C. burnetii*, on ne saurait négliger les DCs. Nous avons récemment réussi à isoler des DCs placentaires par sélection positive en utilisant des anticorps anti-CD11c à partir de cellules n'exprimant pas CD14. Il semble que *C. burnetii* survive dans les DCs placentaires sans s'y répliquer tout au moins pendant quelques jours. L'étude de l'interaction entre les DCs et *C. burnetii* sera effectuée selon les mêmes critères que ceux utilisées pour l'étude des trophoblastes et des macropahges. Les résultats seront comparés à ceux obtenus avec des DCs dérivées de monocytes. L'étude de l'interaction entre les différentes cellules placentaires intègrera les DCs comme troisième partenaire. Ces études menées *in vitro* pourraient permettre d'identifier les mécanismes cellulaires et moléculaires susceptibles d'intervenir dans les défenses du placenta contre l'infection à *C. burnetii*. Par

ailleurs, il serait important d'obtenir des placentas naturellement infectés par *C. burnetii*. Une approche par microarray permettrait de définir la signature *in vivo* de l'infection et de retracer l'histoire naturelle de la fièvre Q placentaire. Des études immunohistochimiques pourraient permettre de valider les paramètres mis en évidence au cours des études *in vitro*, confirmant ainsi leur rôle de marqueurs de l'infection à *C. burnetii*. L'identification de ces biomarqueurs pourrait représenter de nouvelles cibles thérapeutiques dans la lutte contre la fièvre Q chez la femme enceinte. Enfin, on pourrait tenter de définir une signature transcriptionnelle périphérique chez la femme enceinte atteinte de fièvre Q. Si la signature périphérique et la signature tissulaire présentaient des points communs, on pourrait envisager le suivi de l'infection à *C. burnetii* chez les femmes enceintes.

REFERENCES

BIBLIOGRAPHIQUES

1. Penttila, I.A., Harris, R.J., Storm, P., Haynes, D., Worswick, D.A., and Marmion, B.P. 1998. Cytokine dysregulation in the post-Q-fever fatigue syndrome. *QJM* 91:549-560.
2. Raoult, D., Marrie, T., and Mege, J. 2005. Natural history and pathophysiology of Q fever. *Lancet Infect Dis* 5:219-226.
3. Maurin, M., and Raoult, D. 1999. Q fever. *Clin Microbiol Rev* 12:518-553.
4. Fournier, P.E., Casalta, J.P., Habib, G., Messana, T., and Raoult, D. 1996. Modification of the diagnostic criteria proposed by the Duke Endocarditis Service to permit improved diagnosis of Q fever endocarditis. *Am J Med* 100:629-633.
5. Raoult, D., Houpikian, P., Tissot Dupont, H., Riss, J.M., Arditi-Djiane, J., and Brouqui, P. 1999. Treatment of Q fever endocarditis: comparison of 2 regimens containing doxycycline and ofloxacin or hydroxychloroquine. *Arch Intern Med* 159:167-173.
6. Raoult, D., Fenollar, F., and Stein, A. 2002. Q fever during pregnancy: diagnosis, treatment, and follow-up. *Arch Intern Med* 162:701-704.
7. Leone, M., Bechah, Y., Meghari, S., Lepidi, H., Capo, C., Raoult, D., and Mege, J.L. 2007. *Coxiella burnetii* infection in C57BL/6 mice aged 1 or 14 months. *FEMS Immunol Med Microbiol* 50:396-400.
8. Maltezou, H.C., and Raoult, D. 2002. Q fever in children. *Lancet Infect Dis* 2:686-691.
9. Raoult, D., Tissot-Dupont, H., Foucault, C., Gouvernet, J., Fournier, P.E., Bernit, E., Stein, A., Nesri, M., Harle, J.R., and Weiller, P.J. 2000. Q fever 1985-1998. Clinical and epidemiologic features of 1,383 infections. *Medicine (Baltimore)* 79:109-123.
10. Leone, M., Honstettre, A., Lepidi, H., Capo, C., Bayard, F., Raoult, D., and Mege, J.L. 2004. Effect of sex on *Coxiella burnetii* infection: protective role of 17b-estradiol. *J Infect Dis* 189:339-345.
11. Textoris, J., Ban, L.H., Capo, C., Raoult, D., Leone, M., and Mege, J.L. 2010. Sex-related differences in gene expression following *Coxiella burnetii* infection in mice: potential role of circadian rhythm. *PLoS One* 5:e12190.
12. Sasaki, S., Takeshita, F., Okuda, K., and Ishii, N. 2001. *Mycobacterium leprae* and leprosy: a compendium. *Microbiol Immunol* 45:729-736.
13. Izzo, A.A., and Marmion, B.P. 1993. Variation in interferon-γ responses to *Coxiella burnetii* antigens with lymphocytes from vaccinated or naturally infected subjects. *Clin Exp Immunol* 94:507-515.
14. Sabatier, F., Dignat-George, F., Mege, J.L., Brunet, C., Raoult, D., and Sampol, J. 1997. $CD4^+$ T-cell lymphopenia in Q fever endocarditis. *Clin Diagn Lab Immunol* 4:89-92.
15. Koster, F.T., Williams, J.C., and Goodwin, J.S. 1985. Cellular immunity in Q fever: specific lymphocyte unresponsiveness in Q fever endocarditis. *J Infect Dis* 152:1283-1289.
16. Modlin, R.L., Melancon-Kaplan, J., Young, S.M., Pirmez, C., Kino, H., Convit, J., Rea, T.H., and Bloom, B.R. 1988. Learning from lesions: patterns of tissue inflammation in leprosy. *Proc Natl Acad Sci U S A* 85:1213-1217.
17. Delaby, A., Espinosa, L., Lepolard, C., Capo, C., and Mege, J.L. 2010. 3D reconstruction of granulomas from transmitted light images implemented for long-time microscope applications. *J Immunol Methods* 360:10-19.
18. Kishimoto, R.A., Rozmiarek, H., and Larson, E.W. 1978. Experimental Q fever infection in congenitally athymic nude mice. *Infect Immun* 22:69-71.

19. Andoh, M., Naganawa, T., Hotta, A., Yamaguchi, T., Fukushi, H., Masegi, T., and Hirai, K. 2003. SCID mouse model for lethal Q fever. *Infect Immun* 71:4717-4723.
20. Atzpodien, E., Baumgartner, W., Artelt, A., and Thiele, D. 1994. Valvular endocarditis occurs as a part of a disseminated *Coxiella burnetii* infection in immunocompromised BALB/cJ (H-2d) mice infected with the nine mile isolate of *C. burnetii*. *J Infect Dis* 170:223-226.
21. Kishimoto, R.A., and Burger, G.T. 1977. Appearance of cellular and humoral immunity in guinea pigs after infection with *Coxiella burnetii* administered in small-particle aerosols. *Infect Immun* 16:518-521.
22. Meghari, S., Bechah, Y., Capo, C., Lepidi, H., Raoult, D., Murray, P.J., and Mege, J.L. 2008. Persistent *Coxiella burnetii* infection in mice overexpressing IL-10: an efficient model for chronic Q fever pathogenesis. *PLoS Pathog* 4:e23.
23. Capo, C., Amirayan, N., Ghigo, E., Raoult, D., and Mege, J.L. 1999. Circulating cytokine balance and activation markers of leucocytes in Q fever. *Clin Exp Immunol* 115:120-123.
24. Armant, M., Rubio, M., Delespesse, G., and Sarfati, M. 1995. Soluble CD23 directly activates monocytes to contribute to the antigen-independent stimulation of resting T cells. *J Immunol* 155:4868-4875.
25. Capo, C., Zugun, F., Stein, A., Tardei, G., Lepidi, H., Raoult, D., and Mege, J.L. 1996. Upregulation of tumor necrosis factor alpha and interleukin-1b in Q fever endocarditis. *Infect Immun* 64:1638-1642.
26. Dellacasagrande, J., Ghigo, E., Capo, C., Raoult, D., and Mege, J.L. 2000. *Coxiella burnetii* survives in monocytes from patients with Q fever endocarditis: involvement of tumor necrosis factor. *Infect Immun* 68:160-164.
27. Capo, C., Zaffran, Y., Zugun, F., Houpikian, P., Raoult, D., and Mege, J.L. 1996. Production of interleukin-10 and transforming growth factor beta by peripheral blood mononuclear cells in Q fever endocarditis. *Infect Immun* 64:4143-4147.
28. Honstettre, A., Imbert, G., Ghigo, E., Gouriet, F., Capo, C., Raoult, D., and Mege, J.L. 2003. Dysregulation of cytokines in acute Q fever: role of interleukin-10 and tumor necrosis factor in chronic evolution of Q fever. *J Infect Dis* 187:956-962.
29. Aboudharam, G., Drancourt, M., and Raoult, D. 2004. Culture of *C. burnetii* from the dental pulp of experimentally infected guinea pigs. *Microb Pathog* 36:349-350.
30. Harris, R.J., Storm, P.A., Lloyd, A., Arens, M., and Marmion, B.P. 2000. Long-term persistence of *Coxiella burnetii* in the host after primary Q fever. *Epidemiol Infect* 124:543-549.
31. Bechah, Y., Paddock, C.D., Capo, C., Mege, J.L., and Raoult, D. 2010. Adipose tissue serves as a reservoir for recrudescent *Rickettsia prowazekii* infection in a mouse model. *PLoS One* 5:e8547.
32. Gimenez, D.F. 1964. Staining Rickettsiae in Yolk-Sac Cultures. *Stain Technol* 39:135-140.
33. McCaul, T.F., and Williams, J.C. 1981. Developmental cycle of *Coxiella burnetii*: structure and morphogenesis of vegetative and sporogenic differentiations. *J Bacteriol* 147:1063-1076.
34. Heinzen, R.A., Hackstadt, T., and Samuel, J.E. 1999. Developmental biology of *Coxiella burnettii*. *Trends Microbiol* 7:149-154.

35. Capo, C., Lindberg, F.P., Meconi, S., Zaffran, Y., Tardei, G., Brown, E.J., Raoult, D., and Mege, J.L. 1999. Subversion of monocyte functions by coxiella burnetii: impairment of the cross-talk between avb3 integrin and CR3. *J Immunol* 163:6078-6085.
36. Capo, C., Moynault, A., Collette, Y., Olive, D., Brown, E.J., Raoult, D., and Mege, J.L. 2003. *Coxiella burnetii* avoids macrophage phagocytosis by interfering with spatial distribution of complement receptor 3. *J Immunol* 170:4217-4225.
37. Meconi, S., Jacomo, V., Boquet, P., Raoult, D., Mege, J.L., and Capo, C. 1998. *Coxiella burnetii* induces reorganization of the actin cytoskeleton in human monocytes. *Infect Immun* 66:5527-5533.
38. Meconi, S., Capo, C., Remacle-Bonnet, M., Pommier, G., Raoult, D., and Mege, J.L. 2001. Activation of protein tyrosine kinases by *Coxiella burnetii*: role in actin cytoskeleton reorganization and bacterial phagocytosis. *Infect Immun* 69:2520-2526.
39. Baca, O.G., and Paretsky, D. 1983. Q fever and *Coxiella burnetii*: a model for host-parasite interactions. *Microbiol Rev* 47:127-149.
40. Hackstadt, T., and Williams, J.C. 1981. Biochemical stratagem for obligate parasitism of eukaryotic cells by *Coxiella burnetii*. *Proc Natl Acad Sci U S A* 78:3240-3244.
41. Ghigo, E., Capo, C., Tung, C.H., Raoult, D., Gorvel, J.P., and Mege, J.L. 2002. *Coxiella burnetii* survival in THP-1 monocytes involves the impairment of phagosome maturation: IFN-g mediates its restoration and bacterial killing. *J Immunol* 169:4488-4495.
42. Barry, A.O., Mege, J.L., and Ghigo, E. 2010. Hijacked phagosomes and leukocyte activation: an intimate relationship. *J Leukoc Biol* 89:373-382.
43. Holden, D.W. 2002. Trafficking of the *Salmonella* vacuole in macrophages. *Traffic* 3:161-169.
44. Guyton. 2007. Physiology og the respiratory system. In *Textbook of medical physiology*. 431-433.
45. Cros, J., Cagnard, N., Woollard, K., Patey, N., Zhang, S.Y., Senechal, B., Puel, A., Biswas, S.K., Moshous, D., Picard, C., et al. 2010. Human $CD14^{dim}$ monocytes patrol and sense nucleic acids and viruses via TLR7 and TLR8 receptors. *Immunity* 33:375-386.
46. van de Veerdonk, F.L., and Netea, M.G. 2010. Diversity: a hallmark of monocyte society. *Immunity* 33:289-291.
47. Mantovani, A., Sozzani, S., Locati, M., Allavena, P., and Sica, A. 2002. Macrophage polarization: tumor-associated macrophages as a paradigm for polarized M2 mononuclear phagocytes. *Trends Immunol* 23:549-555.
48. Gordon, S. 2003. Alternative activation of macrophages. *Nat Rev Immunol* 3:23-35.
49. Reljic, R. 2007. IFN-γ therapy of tuberculosis and related infections. *J Interferon Cytokine Res* 27:353-364.
50. Joyce, D.A., Gibbons, D.P., Green, P., Steer, J.H., Feldmann, M., and Brennan, F.M. 1994. Two inhibitors of pro-inflammatory cytokine release, interleukin-10 and interleukin-4, have contrasting effects on release of soluble p75 tumor necrosis factor receptor by cultured monocytes. *Eur J Immunol* 24:2699-2705.
51. Yoshizawa, S., Tateda, K., Matsumoto, T., Gondaira, F., Miyazaki, S., Standiford, T.J., and Yamaguchi, K. 2005. *Legionella pneumophila* evades

gamma interferon-mediated growth suppression through interleukin-10 induction in bone marrow-derived macrophages. *Infect Immun* 73:2709-2717.

52. Jones, D.E., Buxbaum, L.U., and Scott, P. 2000. IL-4-independent inhibition of IL-12 responsiveness during *Leishmania amazonensis* infection. *J Immunol* 165:364-372.
53. Hirsch, C.S., Yoneda, T., Averill, L., Ellner, J.J., and Toossi, Z. 1994. Enhancement of intracellular growth of *Mycobacterium tuberculosis* in human monocytes by transforming growth factor-b1. *J Infect Dis* 170:1229-1237.
54. Shiratsuchi, H., Hamilton, B., Toossi, Z., and Ellner, J.J. 1996. Evidence against a role for interleukin-10 in the regulation of growth of *Mycobacterium avium* in human monocytes. *J Infect Dis* 173:410-417.
55. Wilson, M., Seymour, R., and Henderson, B. 1998. Bacterial perturbation of cytokine networks. *Infect Immun* 66:2401-2409.
56. Benoit, M., Desnues, B., and Mege, J.L. 2008. Macrophage polarization in bacterial infections. *J Immunol* 181:3733-3739.
57. Biswas, S.K., Sica, A., and Lewis, C.E. 2008. Plasticity of macrophage function during tumor progression: regulation by distinct molecular mechanisms. *J Immunol* 180:2011-2017.
58. Lopez-Castejon, G., Baroja-Mazo, A., and Pelegrin, P. 2011. Novel macrophage polarization model: from gene expression to identification of new anti-inflammatory molecules. *Cell Mol Life Sci* in press.
59. Albrecht, E.D., and Pepe, G.J. 1990. Placental steroid hormone biosynthesis in primate pregnancy. *Endocr Rev* 11:124-150.
60. Ogren, L. 1994. The placental as en endocrine organ: polypeptides. In *The physiology of reproduction.* E. Knobil, and J.D. Neil, editors. New york: Raven press. 875-945.
61. Walker, W.H., Fitzpatrick, S.L., Barrera-Saldana, H.A., Resendez-Perez, D., and Saunders, G.F. 1991. The human placental lactogen genes: structure, function, evolution and transcriptional regulation. *Endocr Rev* 12:316-328.
62. Senaris, R., Garcia-Caballero, T., Casabiell, X., Gallego, R., Castro, R., Considine, R.V., Dieguez, C., and Casanueva, F.F. 1997. Synthesis of leptin in human placenta. *Endocrinology* 138:4501-4504.
63. Kaufmann, P. 1994. Anatomy and genesis of the placenta. In *The physiology of reproduction*. E. Knobil, and J.D. Neil, editors. New york: Raven press. 441-484.
64. Chaisavaneeyakorn, S., Lucchi, N., Abramowsky, C., Othoro, C., Chaiyaroj, S.C., Shi, Y.P., Nahlen, B.L., Peterson, D.S., Moore, J.M., and Udhayakumar, V. 2005. Immunohistological characterization of macrophage migration inhibitory factor expression in *Plasmodium falciparum*-infected placentas. *Infect Immun* 73:3287-3293.
65. You, H., Liu, Y., Agrawal, N., Prasad, C.K., Edwards, J.L., Osborne, A.F., Korourian, S., Lowery, C.L., and Hermonat, P.L. 2008. Multiple human papillomavirus types replicate in 3A trophoblasts. *Placenta* 29:30-38.
66. Disson, O., Grayo, S., Huillet, E., Nikitas, G., Langa-Vives, F., Dussurget, O., Ragon, M., Le Monnier, A., Babinet, C., Cossart, P., et al. 2008. Conjugated action of two species-specific invasion proteins for fetoplacental listeriosis. *Nature* 455:1114-1118.
67. Roop, R.M., 2nd, Gaines, J.M., Anderson, E.S., Caswell, C.C., and Martin, D.W. 2009. Survival of the fittest: how *Brucella* strains adapt to their intracellular niche in the host. *Med Microbiol Immunol* 198:221-238.

68. Manoussaka, M.S., Jackson, D.J., Lock, R.J., Sooranna, S.R., and Kumpel, B.M. 2005. Flow cytometric characterisation of cells of differing densities isolated from human term placentae and enrichment of villous trophoblast cells. *Placenta* 26:308-318.
69. Rey, D., Obadia, Y., Tissot-Dupont, H., and Raoult, D. 2000. Seroprevalence of antibodies to *Coxiella burnetti* among pregnant women in South Eastern France. *Eur J Obstet Gynecol Reprod Biol* 93:151-156.
70. Baumgartner, W., and Bachmann, S. 1992. Histological and immunocytochemical characterization of *Coxiella burnetii*-associated lesions in the murine uterus and placenta. *Infect Immun* 60:5232-5241.
71. Langley, J.M., Marrie, T.J., Leblanc, J.C., Almudevar, A., Resch, L., and Raoult, D. 2003. *Coxiella burnetii* seropositivity in parturient women is associated with adverse pregnancy outcomes. *Am J Obstet Gynecol* 189:228-232.
72. Fenollar, F., Fournier, P.E., Carrieri, M.P., Habib, G., Messana, T., and Raoult, D. 2001. Risks factors and prevention of Q fever endocarditis. *Clin Infect Dis* 33:312-316.
73. Lepidi, H., Houpikian, P., Liang, Z., and Raoult, D. 2003. Cardiac valves in patients with Q fever endocarditis: microbiological, molecular, and histologic studies. *J Infect Dis* 187:1097-1106.

ANNEXES

ANNEXE 1

The paradigm of macrophage polarization is not applicable per se to human circulating monocytes

Vikram Mehraj, Amira Ben Amara, Adil El Filali, Julien Textoris,
Eric Ghigo, Christian Capo, Jean-Louis Mege

Soumis à publication

Le concept de macrophages M1/M2 s'applique aux macrophages humains différenciés à partir de monocytes et aux macrophages murins péritonéaux ou différenciés à partir de moelle osseuse (55). Plus précisément, dans des conditions quelque peu caricaturales, on sait qu'une cytokine telle que l'IFN-γ induit une réponse M1 et qu'une cytokine telle l'IL-4 induit une réponse M2.

Nous nous sommes demandés si les monocytes circulants stimulés par l'IFN-γ ou l'IL-4 se polarisent respectivement en monocytes M1 et en monocytes M2 et si, compte tenu de l'extrême plasticité des macrophages, cette polarisation est stable. Cette question n'est pas triviale puisqu'on sait que les propriétés phénotypiques et fonctionnelles des monocytes et macrophages peuvent quelque peu différer. En effet, les monocytes expriment CD14 et n'expriment pas CD68 ; les macrophages dérivés de ces monocytes expriment, eux, CD68 mais pas CD14. La sensibilité des monocytes à des agents pathogènes tels que *Tropheryma whipplei*, l'agent de la maladie de Whipple, est totalement différente de celle des macrophages puisque *T. whipplei* est éliminée dans les monocytes et se réplique dans les macrophages (73). Cette question de la polarisation des monocytes en cellules M1 ou M2 est en outre de grande importance médicale puisque c'est la seule façon d'explorer les patients en pratique clinique courante.

Nous avons comparé par microarray la réponse transcriptionnelle des monocytes et des macrophages dérivés de monocytes stimulés par l'IFN-γ et de l'IL-4, deux agonistes canoniques respectifs des réponses M1 et M2. Nos résultats montrent que les monocytes ne sont polarisés que de façon transitoire et que leur réponse tardive ne correspond pas à une réponse de type M1/M2.

The Paradigm of Macrophage Polarization is not Applicable per se to Human Circulating Monocytes

Vikram Mehraj, Amira Ben Amara, Adil El Filali,

Julien Textoris, Eric Ghigo, Christian Capo and Jean-Louis Mege

Unité de Recherche sur les Maladies Infectieuses Tropicales et Emergentes, Centre National de la Recherche Scientifique Unité Mixte de Recherche 6236, Université de la Méditerranée, Marseille, France

Corresponding author. Pr J.L. Mege, URMITE, Faculté de Médecine, 27 Bld. Jean Moulin, 13385 Marseille Cedex 05, France. E-mail: Jean-Louis.Mege@univmed.fr. Tel.: (33) 4 91 32 45 86; fax: (33) 4 91 38 77 72.

Grant support

Vikram Mehraj was supported by a grant from the Higher Education Commission (HEC), Pakistan.

Abstract

Macrophage activation is required to control immune responses. The classification of M1 and M2 macrophages is operational in murine and human macrophages. However, it is not clear if this classification can be extended to monocytes. To answer this

question, human monocytes were stimulated for 6 and 18 hours with interferon-γ and interleukin-4 (two canonical agonists of M1/M2 polarization in macrophages) and gene expression programs were investigated with whole-genome microarrays. The temporal analysis of these programs showed marked differences. In 6-hour stimulated monocytes, interferon-γ- and interleukin-4-stimulated monocytes exhibited M1 and M2 polarization, respectively, similar to macrophages. Original transcriptional programs characterized 18-hour stimulated monocytes. Categories related to innate immunity and metabolic pathways were enriched in response to interferon-γ and interleukin-4, whereas the peroxisome proliferator-activated receptor pathway was specifically enriched in response to interleukin-4. In addition, the gene networks that characterized the delayed responses of monocytes to interferon-γ and interleukin-4, respectively, were markedly different from those involved in early responses. Beside expected networks, two networks organized around pyruvate kinase and Lyn genes were found in delayed response to interferon-γ. In interleukin-4-stimulated monocytes, one major network consisted of cytoskeleton and chemokine genes and two smaller networks were related to metabolism. These results suggest that monocyte activation consists of an early polarized stage that is likely involved in effector responses and a delayed stage that may regulate host responses. The establishment of databases on human monocytes using high-throughput methods may be critical for pathophysiological and clinical non-invasive studies.

Introduction

Circulating monocytes are considered to be the precursors of resident macrophages (1). Macrophages are dynamic and heterogeneous phagocytic cells that play major roles as first-line alerts, regulators of immune responses and homeostasis. Macrophages are functionally polarized and can be described as a continuum from M1 to M2 macrophages: M1 macrophages correspond to inflammatory, microbicidal and tumoricidal macrophages, and M2 macrophages to immunoregulatory and poorly inflammatory macrophages (2, 3). The polarization of macrophages requires specific stimuli. The M1 program is elicited by interferon (IFN)-γ in the presence or absence of lipopolysaccharide (LPS), whereas M2 programs are stimulated by agonists such as cytokines interleukin (IL)-4/IL-13, IL-10/Transforming Growth Factor (TGF)-β), immune complexes, apoptotic cells and corticosteroids (4, 5).

The classification of macrophages into M1 or M2 categories has been based on the expression of a limited number of membrane antigens and soluble mediators (2, 6). M1 macrophages express a panel of receptors (CCR7, CD80, Toll-like receptors (TLR)-2 and TLR-4) and produce inflammatory mediators (cytokines, chemokines and reactive oxygen and nitrogen intermediates). M2 macrophages secrete immunoregulatory molecules (IL-10, TGF-β and IL-1 receptor antagonist) and specific chemokines (CCL18), shift L-arginine metabolism toward the production of ornithine and polyamines and express membrane receptors such as the CD163, CD200 and mannose receptors (7-9).

The recent development of high-throughput microarrays has revealed the complexity of the concept of macrophage activation. Most of our current knowledge on the transcriptional activity of polarized macrophages originates from murine

macrophages (10). A meta-analysis has recently revealed that IFN-γ and IL-4 induce non-overlapping activation profiles in murine macrophages. Hence, IFN-γ induces a large cluster of interferon-responsive genes (IRGs) corresponding to immunity, host defense and cytokine- and chemokine-mediated signaling pathways, whereas IL-4 induces a gene expression pattern that includes genes associated with M2 polarization and novel genes (11). In bone marrow-derived macrophages, LPS, a typical M1 agonist, stimulates the expression of a large number of genes in clusters that belong to M1 modules (including inflammatory cytokines, ILs and IFNs), with an enrichment in M1-associated transcription factors (12). To our knowledge, only one study using high-throughput microarrays has been conducted in human macrophages. This study shows that human macrophage activation by IFN-γ and LPS affects the expression of transcripts related to M1 activation, DNA transcription and protein metabolism, whereas IL-4 stimulates the expression of a low number of transcripts with an enrichment for immune system-related molecules (9).

The M1/M2 classification has been applied to pathological conditions such as infectious diseases (5, 13), cancer (14), metabolic syndrome (15) and degenerative disorders (16). The majority of these studies have been conducted with tissue macrophages or macrophages differentiated *in vitro*. Assessing the ability of circulating monocytes to be polarized is critical because they are the sole type of myeloid cells accessible for current clinical investigations. In a murine model of *Listeria monocytogenes* infection, it has been reported that extravasated $Ly6C^+$ monocytes initiate an inflammatory M1 response whereas $Ly6C^-$ monocytes induce an M2-like program (17). In humans, the polarization of circulating monocytes is deduced from the polarization of macrophages rather than experimentally demonstrated.

Here, we aimed to determine the signatures of human monocytes stimulated with IFN-γ or IL-4 using a large-scale approach. We found that the transcriptional signature of monocytes was highly dynamic. Indeed, M1/M2 polarization was observed after 6 hours, whereas the transcriptional pattern observed after 18 hours was independent of the M1/M2 status. Gene networks also showed major differences between monocytes stimulated for 6 and 18 hours. Our data enabled the building of a database that will be used to explore monocyte responses in clinical studies.

Material and Methods

Preparation and activation of monocytes and macrophages

Leukopacks from normal blood donor buffy coats provided from the Etablissement Français du Sang (Marseille, France), as recently described (18). Peripheral blood mononuclear cells (PBMCs) were isolated from blood samples after deposition over a Ficoll density gradient, as previously described (19). PBMCs were then subjected to $CD14^+$ magnetic cell sorting using a monocyte isolation kit (Miltenyi Biotec). This procedure resulted in more than 95% monocyte purity, as assessed by flow cytometry. $CD14^+$ cells (10^6 cells per assay) were differentiated into macrophages by incubation in RPMI 1640 containing 20 mM HEPES, 10% human serum AB^+, 2 mM L-glutamine, 100 IU/ml penicillin and 100 µg/ml streptomycin (Invitrogen) for 3 days, and fetal calf serum (FCS) was substituted by human serum for 4 supplementary days. More than 95% of the cells were macrophages, as assessed by CD68 expression and CD14 down-modulation. Monocytes and macrophages were stimulated with 20 ng/ml recombinant human IFN-γ (PeproTech) or IL-4 (AbCys) for 6 or 18 hours.

RNA preparation and microarrays

RNA was extracted using an RNeasy Mini kit (Qiagen) after a DNase step. The quantity and quality of total RNAs was assessed using the Nanodrop (Thermo Scientific) and a 2100 Bioanalyzer (Agilent Technologies), and the RNA was eluted in 30 µl of water and stored at -20°C. RNA was then analyzed using microarray chips including 45,000 probes (4x44K Whole Human Genome, Agilent Technologies) and One-color Microarray Based Gene Expression Analysis, as recently described (20). In brief, 250 ng RNA was labeled with cyanine-3-CTP using a commercial kit (Low RNA Input Fluorescent Amplification Kit). After the deposition of three samples per experimental condition on slides, hybridization was performed at 65°C using the *in situ* Hybridization Plus kit (Agilent Technologies) for 17 hours. The arrays were scanned with a pixel size of 5 µm with the DNA Microarray Scanner G2505B. Image analysis and correction of intra-array signals were performed with the Feature Extraction Software A.9.1.3 (Agilent Technologies).

Analysis of microarray results

Microarray data analysis was performed using the software GeneSpring 10.01 with inter-array normalization and inter-replicate corrections using the default settings. To identify genes that were differentially expressed, we used a Student's *t* test with $P < 0.05$ with multiple testing correction by Benjamini-Hochberg test and an absolute fold change (FC) greater than 2.0. An analysis of Gene Ontology (GO) terms was performed, which identifies the modulated biological processes (21). Only the probes with the highest values of gene expression were kept in cases of multiple probes per gene. An additional data analysis was performed using R software, version 2.8.1 (22).

The raw data were pre-processed with background subtraction and quantile normalization using the bioconductor limma package Agi4x44 PreProcess (http://www.bioconductor.org/packages/2.3/bioc/html/Agi4x44PreProcess.html). To explore putative technical biases and identify major factors of gene expression variations, the dataset was also analyzed by Principal Component Analysis (PCA) (23). Datasets were pre-analyzed using Significance Analysis of Microarrays (24) that gives a score that represents the statistical significance for each gene with an estimated False Discovery Rate. Next, the microarray data were segmented into biologically significant groups. Modulated genes were associated with Kyoto Encyclopedia of Genes and Genomes (KEGG) terms using the GO stats package (25), which allows for the testing of GO and KEGG terms that were over- or under-represented, and with the hgug4112a.db annotation package (http://www.bioconductor.org/packages/2.4/data/annotation/html/hgug4112a.db.html). The IRG signature was determined by comparing our results with the interferome database (http://www.interferome.org) that identifies IRGs from multiple microarray and proteomic experiments on cells treated with IFNs (26). Our data obtained with Agilent microarrays were also compared to transcriptomic profiles of M1/M2 macrophages obtained using Illumina bead chips (9) by building a virtual Agilent microarray including both types of data, and the genes commonly identified were analyzed using R software (18). The data were generated in compliance with the Minimum Information About a Microarray Experiment guidelines. The data were deposited in the National Center for Biotechnology Information's Gene Expression Omnibus (27) and are accessible using accession number (http://www.ncbi.nlm.nih.gov/geo/query/acc.cgi?token=bxmzrwwgygmwahu&acc=GS

E27658). The differentially expressed genes that were implicated in the KEGG pathways were submitted to the KEGG graph package (http://www.bioconductor.org/packages/2.4/bioc/html/KEGGgraph.html) to draw the gene-gene interactions in the network pathways.

Real-time quantitative RT-PCR (qRT-PCR)

Microarray results were confirmed using qRT-PCR on 19 selected genes that were regulated in macrophages. They included M1 (CXCL10, IL-15, IDO1 and IRF1) and M2 genes (CCL13, CCL18 and EGR2), see below. Data obtained with both methods were highly correlated: for IFN-γ-stimulated macrophages, r = 0.783 with $P < 0.001$; for IL-4-stimulated macrophages, r = 0.929 with $P < 0.001$. qRT-PCR was performed with the MMLV RT kit (Invitrogen) using gene-specific primers and Primer3 (http://frodo.wi.mit.edu/primer3) as previously described (19). The transcriptional profiles were screened using dedicated homemade 384-well plates, targeting selected cytokines, chemokines, antigen-presenting cells membrane ligands and receptors, and transcription factors using the 7900HT Fast Real Time PCR System (Applied Biosystems). The results were normalized using the housekeeping gene β-actin and were expressed as $FC = 2^{-\Delta\Delta Ct}$, where $\Delta\Delta Ct = (CtTarget - CtActin)_{stimulated} - (CtTarget - CtActin)_{unstimulated}$ (28). Correlation analysis between microarray and qRT-PCR data was performed using Pearson's correlation coefficient method.

Statistical analysis

qRT-PCR results were expressed as mean values ± SEM and were compared using the non-parametric Mann-Whitney *U* test. Differences were considered significant when $P < 0.05$.

Results

Transcriptional responses of monocytes

Monocytes were stimulated with IFN-γ and IL-4 for 6 and 18 hour (6-h and 18-h monocytes, respectively) and compared with macrophages stimulated for 18 hours, a period known to induce the M1/M2 polarization of macrophages (9). The overall gene expression was analyzed by PCA. Most of the gene expression variance (more than 80%) was explained by the experimental protocol, principally the time of stimulation, cell type and stimulation type. Monocytes were clearly distinct from macrophages, and 6-h and 18-h monocytes were separated (**Figure 1A**). The transcriptional patterns of unstimulated cells were close and completely different from those of IFN-γ- and IL-4-stimulated cells (**Figure 1B**). As expected, IFN-γ activation led to a global transcriptional response completely different from that induced by IL-4 in 6-h monocytes and macrophages. In contrast, the responses of 18-h monocytes to IFN-γ and IL-4 were overlapping (**Figure 1B**). Hierarchical clustering performed on the most variable genes also showed that 6-h and 18-h monocytes constituted an entity separated from macrophages, which was independent of their activation state. IFN-γ and IL-4 induced specific transcriptional programs in 6-h monocytes and macrophages. In contrast, we were unable to discriminate the transcriptional profiles induced by IFN-γ and IL-4 in 18-h monocytes (**Figure 2**). We wondered if the transcriptional profiles of

monocytes were related to changes in the number of modulated genes. The number of significantly regulated genes (with a False Discovery Rate below 5%) decreased and increased in 6-h monocytes stimulated with IFN-γ and IL-4, respectively, compared to macrophages. The number of regulated genes was clearly different in 6-h and 18-h monocytes. The number of modulated genes was lower and higher in 6-h monocytes than in 18-h monocytes in response to IFN-γ and IL-4 treatments, respectively (**Table 1**). Taken together, these results suggest that IFN-γ and IL-4 induced specific transcriptional responses in monocytes in a time-dependent manner.

Functional analysis of monocyte responses to IFN-γ and IL-4

The transcriptomic responses of monocytes to IFN-γ and IL-4 were analyzed using GO terms. In 6-h monocytes, the GO terms immune system and inflammatory response were enriched in response to IFN-γ and IL-4. The GO terms Jak-STAT cascade, hydrolase activity, apoptosis and cell communication were associated with IFN-γ response, whereas the GO term signal transduction was associated to IL-4 response. Note that the GO terms were enriched in upregulated genes (**Figure 3A**). In contrast, the GO term enrichment mainly concerned downregulated genes in 18-h monocytes (**Figure 3B**). Again, different groups of GO terms, including blood coagulation, inflammatory response, receptor binding, cytokine and chemotaxis, and cellular cycle, as well as immune system-related terms, were enriched in responses to both IFN-γ and IL-4. The GO terms apoptosis and signal transduction were specifically enriched in downregulated genes in response to IFN-γ and IL-4, respectively. In upregulated genes, immune system-related terms (IFN-γ and IL-4) and membrane development (IFN-γ) GO terms were enriched (**Figure 3B**). The GO annotation in 18-h monocytes was also

distinct from that of macrophages stimulated for 18 hours. The enrichment of up- and down-regulated genes in response to IFN-γ (**Figure 4A**) and IL-4 (**Figure 4B**), respectively, was similar. Among the upregulated genes, the GO term enrichment was closer to that of 6-h monocytes than that of 18-h monocytes.

To improve the functional investigation of monocyte activation, the gene expression changes induced by IFN-γ and IL-4 were analyzed with KEGG database. We selected KEGGs in which a sufficient number of genes with low *P* values were associated with a given pathway. In 6-h monocytes, the KEGGs cell adhesion molecules, antigen processing and presentation, cytokine-cytokine receptor interaction and TLR signaling pathway were enriched in genes upregulated by both IFN-γ and IL-4 (**Table 2**). The KEGGs related to IFN-γ signaling (Jak-STAT signaling pathway) and innate immune responses (retinoic acid-inducible gene (RIG)-I-like receptor, NOD-like receptor and chemokines) were associated with IFN-γ responses. Few KEGGs were found in down-regulated genes in response to both IFN-γ and IL-4 (**Table 2**). In monocytes stimulated with IFN-γ or IL-4 for 18 hours, the KEGGs related to innate immune response, IFN-γ signaling and IFN-γ responses were enriched in down-regulated genes (**Table 3**). In contrast, there was a major enrichment in KEGGs related to metabolic pathways (including tryptophan metabolism and synthesis of unsaturated fatty acids) in response to IFN-γ and IL-4 in upregulated genes. Note that the KEGG peroxisome proliferator-activated receptor (PPAR) signaling pathway was enriched in genes upregulated by IL-4 (**Table 3**). The comparison of functional responses of monocytes with macrophages revealed that the KEGGs related to immune responses were enriched in macrophages (**Table 4**), similar to 6-h monocytes (see **Table 2**). However, the KEGG cell cycle that was absent in 6-h monocytes was significantly enriched in the downregulated genes of

both IFN-γ- and IL-4-stimulated macrophages. In addition, the KEGG metabolic pathway that was enriched in genes upregulated in IL-4-stimulated macrophages was shared with 18-h monocytes (see **Table 4** and **Table 3**, respectively). Taken together, these results indicate that the majority of KEGGs were common in 6-h monocytes and macrophages even if some pathways were found in both macrophages and 18-h monocytes.

The above analysis of transcriptomic responses of monocytes to IFN-γ revealed the modulation of genes belonging to Jak-STAT and RIG-I-like receptor signaling pathways. These pathways are known to be modulated by type II (IFN-γ) and type I (IFN-α/β) IFNs and involve a large number of IRGs (29). We used the recently established interferome database (30) to investigate the modulation of IRGs (types I and II) in monocytes and macrophages. This database contains 1,996 IRGs from 23 human datasets with currently acceptable methods and standards of statistical analysis. The numbers of IRGs modulated in response to IFN-γ and IL-4 were higher in 6-h monocytes than in macrophages. In 18-h monocytes, the number of IRGs was lower in response to IFN-γ than in macrophages, but it was similar in 18-h monocytes and macrophages in response to IL-4 (**Table 5**). Again, these results demonstrated that the early response of monocytes to IFN-γ was associated with the high level of IRG expression.

Monocytes and M1/M2 transcriptional polarization

Because IFN-γ and IL-4 are known to stimulate M1 and M2 polarization in macrophages (2, 3), we wondered if monocytes exhibited a similar transcriptional polarization. First, we retained the M1 and M2 genes that were commonly modulated in

a report by Martinez et al. (9) and our study, respectively (**Figure S1**). Only the regulated genes (measured by microarray analysis and confirmed by qRT-PCR) were finally selected: they included 34 M1 and 14 M2 genes that belong to the following categories: membrane receptors, cytokines/chemokines, apoptosis, solute carriers, enzymes, extracellular mediators and DNA binding factors (**Table 6**). In 6-h monocytes, IFN-γ induced the modulation of 23 M1 genes, and IL-4 induced the modulation of 18 M2 genes. In contrast, the transcriptional profiles of 18-h monocytes did not correspond to the M1/M2 dichotomy. Indeed, only three M1 genes and four M1 genes were modulated in response to IFN-γ and IL-4, respectively (**Table 6**). Note that *EGR2*, a M2 gene, was found in 18-h macrophages, but not in 6-h monocytes. Taken together, these results demonstrated that 6-h monocytes, but not 18-h monocytes, exhibited the same type of M1/M2 polarization as macrophages in response to IFN-γ and IL-4. Second, it has been recently shown that macrophage polarization affects the expression of genes related to iron metabolism (30). We selected 11 M1 and 21 M2 genes related to iron metabolism and we compared them with our transcriptional data (**Table 7**). In 6-h monocytes, IFN-γ stimulated the expression of four M1 genes, three of which were common with macrophages, and IL-4 stimulated the expression of 12 M2 genes, which included the four genes modulated in macrophages. The expressions of M1 and M2 genes related to iron metabolism were transient because 18-h monocytes expressed no M1 genes and only two M2 genes (**Table 7**). Taken together, these results demonstrated that the polarization of monocytes into M1 or M2 profiles was transient.

Delayed transcriptional program of monocytes

Because most modulated genes in 18-h monocytes were not related to M1/M2 polarization, we wondered if it was possible to identify a delayed signature in these 18-h monocytes. We selected six genes (*INHBA*, *cMAF*, *CCL13*, *CCL26*, *F13A1* and *WNT5A*) that were highly modulated by IFN-γ and IL-4 and for which expression by microarray and qRT-PCR was correlated (**Figure 5**). The expression of the *INHBA* gene was markedly upregulated in 18-h monocytes stimulated with IFN-γ, but not those stimulated with IL-4. The *INHBA* transcripts were almost silent in 6-h monocytes. The expression of the *cMAF* gene was dramatically increased in monocytes stimulated with IL-4, but not with IFN-γ and was higher in 18-h monocytes than in 6-h monocytes. Similarly, IL-4, but not IFN-γ, induced the upregulation of the *CCL26* gene in both 6-h and 18-h monocytes. In contrast, the expression of the *CCL13* gene, which was strongly associated with the M2 pattern in macrophages, was moderately regulated in 6-h and 18-h monocytes. Finally, the expression of *F131A1* and *WNT5A* genes was specifically associated with 18-h monocytes. The expression of the *F13A1* gene was increased in monocytes stimulated with IFN-γ for 18 hours, whereas the response of 6-h monocytes rather corresponded to the M2-type. The expression of the *WNT5A* gene was specifically upregulated in 18-h monocytes stimulated with both IFN-γ and IL-4. Taken together, these results suggest that the delayed signature of monocytes involves specific genes.

Monocyte activation networks

To understand the interaction of modulated genes in monocytes, we built networks with up- and down-regulated genes. In 6-h monocytes stimulated with IFN-γ, two networks

were prominent (**Figure S2)**. The MHC class II network contained 15 genes (14 upregulated genes). The network organized around IL-15 and the IL-15 receptor contained 18 genes (nine upregulated genes); these genes included signaling molecules such as STAT1, Jak2/3, suppressor of cytokine signaling (SOCS)-1 and IFN regulatory factor (IRF)-9. Note that the *IL12RB1* gene was downmodulated. The transcriptional response of 6-h monocytes stimulated with IL-4 was completely different from that induced by IFN-γ (**Figure S3**). A minor network consisted of MHC class II genes with 7/10 upregulated genes and the major network consisted of three subnetworks. The first subnetwork was organized around 15 chemokine genes (11 upregulated genes), and four genes (three upregulated genes) encoding chemokine receptors. The second subnetwork concerned oxygen-sensing molecules and consisted of 67 components (20 upregulated genes). The third subnetwork consisted of 21 components and was organized around the *CTNNB1* gene (encoding β1-catenin).

The gene networks that characterized the delayed responses of monocytes were different from those involved in early responses. Three networks were found in response to IFN-γ: they included an HLA network with 15 components (14 upregulated genes), a complement network with nine components (five upregulated genes) and a canonical MHC class II transactivator (CIITA) network (**Figure S4**). Interestingly, two networks were not expected: the first network was organized around pyruvate kinase and consisted of seven components (**Figure 6A**), and the second network was organized around Lyn with 17 components (seven upregulated genes) (**Figure 6B**). The latter network contained G proteins (*GNG7*), kinases (*PIK3CD*, *PI3KR1*) and FcR (*FCGR3*). In monocytes stimulated with IL-4 for 18 hours, there was one major network and two smaller networks. The major network consisted of one subnetwork associated with the

cytoskeleton and another with chemokines. The cytoskeleton subnetwork consisted of 26 genes (three upregulated genes) connected to a group of G proteins: the genes were related to integrins (*ITG* genes), extracellular matrix molecules (vinculin, fibronectin and collagen) and kinases (*PRKCA*). The chemokine subnetwork consisted of 23 genes (seven upregulated genes) connected to chemokine receptors (CXCR1, CXCR3 and CCR10) and signaling molecules (NF-κB and MAPK) (**Figure 7**). The two smaller networks were related to metabolism (**Figure 8**). The first network included nine genes, including acetyl-CoA acetyltransferase (ACAT) and molecules involved in cholesterol metabolism. The other network was organized around genes involved in glycogen storage and consisted of nine genes (five upregulated genes). Taken together, these results show that the interactions between genes in monocytes stimulated with IFN-γ or IL-4 for 6 hours were different from those found after an 18-h stimulation, demonstrating that gene interactions are highly dynamic.

Discussion

The current study was conducted to determine gene activation programs in human monocytes in the context of M1 and M2 polarization using whole-genome microarrays. This question was based on the hypothesis that distinct activation programs are induced in monocytes and macrophages. Hence, transcriptomic studies have revealed that resting monocytes exhibit a repertoire of gene expression distinct from that of macrophages (31). We confirmed that the transcriptional patterns of monocytes and monocyte-derived macrophages were markedly distinct in the absence of stimulation. This is likely the consequence of the impact of the differentiation process on gene expression. Indeed, during the first stage of monocyte differentiation,

the genes corresponding to the cell cycle are transiently modulated whereas those encoding membrane receptors, signal transducers and extracellular immune proteins are maintained and refractory to polarizing stimuli (9).

In the conditions that polarize macrophages toward the M1 and M2 status, namely, when macrophages were stimulated with IFN-γ and IL-4, respectively, the transcriptional profiles of monocytes and macrophages were dramatically different. In macrophages, a large number of genes were modulated in response to IFN-γ and IL-4. This is in agreement with previously published data (9), although some quantitative differences may be explained by the differences between Agilent (our study) and Affimetrix arrays. In monocytes, the transcriptional responses to IFN-γ and IL-4 were different after 6 hours (early activation) and 18 hours (delayed activation). Although the early responses to IFN-γ could be partitioned in clusters independent of those induced by IL-4, the dichotomy between IFN-γ and IL-4 responses was lost in 18-h monocytes. This was not related to global decreased cell activation because the quantitative response of 18-h monocytes to IFN-γ was higher than that of 6-h monocytes.

The early responses of monocytes share many features of macrophage activation. First, the GO terms related to immune and inflammatory responses and the KEGGs related to cell activation, innate immune response and pathogen-associated molecular pattern recognition were enriched in response to both IFN-γ and IL-4. Among the downregulated genes, the categories related to the cell cycle and p53 signaling were enriched, emphasizing results reported elsewhere (9). Second, the expression of a large panel of IRGs was enriched in IFN-γ-stimulated monocytes: as expected, they included type II IRGs and, more surprisingly, type I IRGs. This may be explained by the fact that several signaling partners, such as Jak1 and STAT1, are shared by the type I and type II

IFN signaling pathways (29, 32). Third, the cell polarization towards M1 and M2 types established in macrophages (3, 5, 7-9, 33-35), was also found in 6-h monocytes. The M1/M2 polarized signature was defined as a list of genes commonly modulated in our report and by Martinez et al. (9) and was confirmed by qRT-PCR. They consisted of genes classically associated with M1/M2 polarization and new candidates. Four apolipoprotein (*APOL*) genes were shared by M1 macrophages and monocytes stimulated with IFN-γ for 6 hours. These genes present on the chromosome 22q12.3 play a role in cholesterol transport: they have been associated with atherosclerosis, a disease in which macrophages exhibit a M1 profile (36). The members of the solute carrier (*SLC*) transporter family, known to play a role in the transport of divalent cations and small organic molecules, are also useful in discriminating M1 and M2 macrophages (9). The *SLC31A2* gene, associated with the M1 profile, was modulated in monocytes stimulated with IFN-γ for 6 hours, whereas *SLCA7* and *SLC21A9*, associated with the M2 profile, were found in monocytes stimulated with IL-4 for 6 hours. *SLC4A7* is expressed by osteoclasts that belong to the myeloid lineage and is regulated by CSF-1 known to shift macrophage polarization toward an M2 phenotype (37, 38). Finally, it has been shown that iron sequestration and iron release are increased in M1 and M2 macrophages, respectively (30). We also found that genes involved in iron metabolism were regulated in M1 and M2 macrophages. Taken together, these results showed that 6-h monocytes exhibited immune and inflammatory programs and could be polarized into M1- and M2-like cells. These findings may be related to murine $Gr1^{+}$/Ly-$6C^{high}$ monocytes that initiate an inflammatory program resembling the M1 macrophage program when they enter the peritoneum after challenge with *L. monocytogenes* (1).

The functional analysis of modulated genes in 18-h monocytes revealed the specificity of this delayed transcriptional pattern. First, the GO terms modulated in response to IFN-γ and IL-4 were essentially enriched in downregulated genes, in contrast to 6-h monocytes. Second, the analysis of pathways using KEGGs revealed the enrichment of metabolic pathways in response to IFN-γ and IL-4, and the PPAR signaling pathway in response to IL-4. Such patterns are distinct from 6-h monocytes and macrophages in which only IL-4 induced an enrichment of metabolic pathways. PPARγ belongs to a family of ligand-activated nuclear transcription factors expressed in human myeloid cells. The activation of PPARγ in response to IL-4 leads to the down-modulation of Th-1 type immune responses (39). The fact that the enrichment in the PPAR signaling pathway was not observed in 6-h monocytes suggests that the modulation of *PPAR* genes is related to the termination of the inflammatory response or the establishment of a regulatory response. Third, the concept of M1/M2 polarization is not valid to characterize the delayed activation of monocytes because the great majority of M1 and M2 markers are absent in 18-h monocytes. Similarly, only two iron-related genes that are characteristic of M1/M2 polarization were modulated in 18-h monocytes. It is noteworthy that IDO and CCL18, two canonical markers of M1 and M2 profiles, respectively, were still present in activated 18-h monocytes, suggesting that the early polarization of monocytes had occurred. The delayed response of monocytes to IFN-γ and IL-4 cannot be superimposed to the M2 profile that usually follows the initial M1 response to injury and contributes to the resolution of inflammation (1). In our model, we were unable to identify a sufficient number of genes to classify the delayed monocytic response as an M2 response. In addition, it may be hypothesized that LPS tolerance at least partly mimics delayed monocyte activation, but a recent report

demonstrated that LPS tolerance is associated with the initiation of a typical M2 program (40). The delayed transcriptomic signature of monocytes exhibited specific features. Some genes were specifically targeted by IFN-γ or IL-4 (*INHBA*, *cMAF* and *CCL26*) and others were indistinctly induced by IFN-γ and IL-4 (*F13A1* and *WNT5A*). The *F13A1* and *WNT5A* genes were exclusively overexpressed in the delayed responses of monocytes. In mammals, WNT signaling seems critical for stem cell homeostasis and lymphocyte differentiation (41). The expression of the *WNT5* gene is increased in macrophages stimulated with agonists, including TLR ligands, which induce M1-type responses. WNT5 ligation upregulates IL-12 and IFN-γ production and contributes to Th1-mediated responses (41). The increased expression of the *WNT5* gene in 18-h monocytes may maintain the signals necessary to activate T cells. This hypothesis is strengthened by the finding that WNT5 expression is increased in patients with sepsis who exhibit sustained inflammation (42).

The activation of macrophages has been modeled by integrating the interaction of genes, proteins and regulatory modules to build a pathway map. Hence, the construction of networks with nodes controlling transcription and interaction pathways has enabled the assessment of macrophage transcriptional responses to cytokines and microbial ligands (43). In macrophages challenged with TLR ligands, two major networks have been identified: one predominantly determined by genes from an inflammatory-like program and a second by genes from an antiviral-like program (44). IFN-γ stimulates the expression of more than 1,000 transcripts in murine bone marrow-derived macrophages, which are represented in a network with 26 clusters containing more than five members. This representation allows a dynamic view of gene interactions (45). Silencing some transcriptional factors has revealed common

mechanisms in type I and type II IFN signaling networks (46). Such findings demonstrate that 6-h monocytes express both type I and II IRGs after IFN-γ stimulation. We wondered if the building of networks would be useful to analyze the specificities of transcriptional responses in 6-h and 18-h monocytes. This network approach revealed gene interactions that were not anticipated by GO and KEGG analyses. First, the MHC network was found in 6-h and 18-h monocytes in which the expression of MHC genes was upregulated. Second, a network rich in genes encoding chemokines and chemokine receptors was found in 6-h and 18-h monocytes stimulated by IL-4. This was expected in polarized 6-h monocytes but was more surprising in 18-h monocytes in which M1/M2 polarization was blunted. Third, IFN-γ stimulated the expression of a signal transduction network around IL-15 in 6-h monocytes. The role of IL-15 in microbicidal responses of monocytes has been recently reanalyzed through the vitamin D pathway (47). Finally, the networks of 18-h monocytes exhibited a higher number of genes than in 6-h monocytes, which were differently modulated by IFN-γ and IL-4. In monocytes stimulated with IFN-γ for 18 hours, there were two unexpected networks: one linking lyn kinase to PI3 kinase and FcR, and another involved in pyruvate metabolism. In monocytes stimulated with IL-4 for 18 hours, a very dense network was found that consisted of a large number of genes encoding cytoskeleton and extracellular matrix molecules connected to integrin subunits. This network likely reflects the ability of 18-h monocytes to contribute to tissue reorganization in the cicatrisation phase of the inflammatory response. In addition, there were two networks that were related to the metabolism of cholesterol and glycogen, which strengthened the role of delayed activation of monocytes in homeostasis.

In conclusion, the activation of monocytes consisted of one early stage that involved macrophage polarizion and a delayed stage in which M1/M2 polarization was replaced by a complex network made of molecules likely required for the termination of inflammation. The lack of M1/M2 polarization in monocytes may impose a careful analysis of transcriptional responses in clinical samples. The establishment of databases of human monocytes may open a new field in pathophysiological and clinical non-invasive studies.

References

1. Geissmann F, Manz MG, Jung S, Sieweke MH, Merad M et al. (2010) Development of monocytes, macrophages, and dendritic cells. Science 327: 656-661.

2. Mantovani A, Sica A, Sozzani S, Allavena P, Vecchi A et al. (2004) The chemokine system in diverse forms of macrophage activation and polarization. Trends Immunol 25: 677-686.

3. Mosser DM, Edwards JP (2008) Exploring the full spectrum of macrophage activation. Nat. Rev. Immunol 8: 958-969.

4. Gordon, S. 2003. Alternative activation of macrophages. Nat Rev Immunol 3: 23-35.

5. Benoit M, Desnues B, Mege JL (2008) Macrophage polarization in bacterial infections. J Immunol 181: 3733-3739.

6. Martinez FO, A. Sica A, A. Mantovani A, M. Locati M (2008) Macrophage activation and polarization. Front Biosci 13: 453-461.

7. Stein M, Keshav S, Harris N, Gordon S (1992) Interleukin 4 potently enhances murine macrophage mannose receptor activity: a marker of alternative immunologic macrophage activation. J Exp Med 176: 287-292.

8. Mantovani A, Sozzani S, Locati M, Allavena P, Sica A (2002) Macrophage polarization: tumor-associated macrophages as a paradigm for polarized M2 mononuclear phagocytes. Trends Immunol 23: 549-555.

9. Martinez FO, Gordon S, Locati M, Mantovani A (2006) Transcriptional profiling of the human monocyte-to-macrophage differentiation and polarization: new molecules and patterns of gene expression. J Immunol 177: 7303-7311.

10. Martinez FO, Helming L, Gordon S (2009) Alternative activation of macrophages: an immunologic functional perspective. Annu Rev Immunol 27: 451-483.

11. Zhang S, Kim CC, Batra S, McKerrow JH, Loke P (2010) Delineation of diverse macrophage activation programs in response to intracellular parasites and cytokines. PLoS Negl Trop Dis 4: e648.

12. Ramsey SA, Klemm SL, Zak DE, Kennedy KA, Thorsson V et al. (2008) Uncovering a macrophage transcriptional program by integrating evidence from motif scanning and expression dynamics. PLoS Comput Biol 4: e1000021.

13. Mege JL, Mehraj V, Capo C (2011) Macrophage polarization and bacterial infections. Curr Op Infect Dis in press.

14. Biswas SK, Sica A, Lewis CE (2008) Plasticity of macrophage function during tumor progression: regulation by distinct molecular mechanisms. J Immunol 180: 2011-2017.

15. Odegaard JI, Ricardo-Gonzalez RR, Goforth MH, Morel CR, Subramanian V et al. (2007) Macrophage-specific PPARgamma controls alternative activation and improves insulin resistance. Nature 447: 1116-1120.

16. Arnold L, A. Henry A, F. Poron F, Y. Baba-Amer Y, N. van Rooijen N et al. (2007) Inflammatory monocytes recruited after skeletal muscle injury switch into antiinflammatory macrophages to support myogenesis. J Exp Med 204: 1057-1069.

17. Auffray C, Sieweke MH, Geissmann F (2009) Blood monocytes: development, heterogeneity, and relationship with dendritic cells. Annu Rev Immunol 27: 669-692.

18. Tantibhedhyabgkul W, Prachason T, Waywa D, El Filali A, Ghigo E et al. (2011) *Orientia tsutsugamushi* stimulates an original gene expression program in monocytes: relationship with gene expression in patients with scrub typhus. PLoS Neglect Trop Dis 5: e1028.

19. Desnues B, Raoult D, Mege JL (2005) IL-16 is critical for *Tropheryma whipplei* replication in Whipple's disease. J Immunol 175: 4575-4582.

20. Ben Amara A, Ghigo E, Le Priol Y, Lépolard C, Salcedo SP et al (2010) *Coxiella burnetii*, the agent of Q fever, replicates within trophoblasts and induces a unique transcriptional response. PLoS One 5: e15315.

21. Ashburner M, Ball CA, Blake JA, Botstein D, Butler H et al. (2000) Gene ontology: tool for the unification of biology. The Gene Ontology Consortium. Nat Genet 25: 25-29.

22. team, R. D. c. 2009. R: a language and environment for statistical computing. R foundation for statistical computing, Vienna, Austria.

23. Culhane AC, Thioulouse J, Perriere G, Higgins DG (2005) MADE4: an R package for multivariate analysis of gene expression data. Bioinformatics 21: 2789-2790.

24. Tusher VG, Tibshirani R, Chu G (2001) Significance analysis of microarrays applied to the ionizing radiation response. Proc Natl Acad Sci. U S A 98: 5116-5121.

25. Falcon S, Gentleman R (2007) Using GOstats to test gene lists for GO term association. Bioinformatics 23: 257-258.

26. Samarajiwa SA, Forster S, Auchettl K, Hertzog PJ (2009) INTERFEROME: the database of interferon regulated genes. Nucleic Acids Res 37: D852-D857.

27. Barrett T, Edgar R (2006) Gene expression omnibus: microarray data storage, submission, retrieval, and analysis. Methods Enzymol 411: 352-369.

28. Livak KJ, Schmittgen TD (2001) Analysis of relative gene expression data using real-time quantitative PCR and the $2^{-\Delta\Delta Ct}$ method. Methods 25: 402-408.

29. Platanias LC (2005) Mechanisms of type-I- and type-II-interferon-mediated signalling. Nat Rev Immunol 5: 375-386.

30. Recalcati S, Locati M, Marini A, Santambrogio P, Zaninotto F et al. (2010) Differential regulation of iron homeostasis during human macrophage polarized activation. Eur J Immunol 40: 824-835.

31. Li J, Pritchard DK, Wang X, Park DR, Bumgarner RE et al. (2007) cDNA microarray analysis reveals fundamental differences in the expression profiles of primary human monocytes, monocyte-derived macrophages, and alveolar macrophages. J Leukoc Biol 81: 328-335.

32. Rayamajhi M, Humann J, Kearney S, Hill KK, Lenz LL (2010) Antagonistic crosstalk between type I and II interferons and increased host susceptibility to bacterial infections. Virulence 1: 418-422.

33. Nathan CF, Murray HW, Wiebe ME, Rubin BY (1983) Identification of interferon-γ as the lymphokine that activates human macrophage oxidative metabolism and antimicrobial activity. J Exp Med 158: 670-689.

34. Raes G, de Baetselier P, Noel W, Beschin A, Brombacher F et al. 2002. Differential expression of FIZZ1 and Ym1 in alternatively versus classically activated macrophages. J Leukoc Biol 71: 597-602.

35. Stumpo R, Kauer M, Martin S, Kolb H (2003) IL-10 induces gene expression in macrophages: partial overlap with IL-5 but not with IL-4 induced genes. Cytokine 24: 46-56.

36. Galkina E, Ley K (2009) Immune and inflammatory mechanisms of atherosclerosis. Annu Rev Immunol 27: 165-197.

37. Bouyer P, Sakai H, Itokawa T, Kawano T, Fulton CM et al. (2007) Colony-stimulating factor-1 increases osteoclast intracellular pH and promotes survival via the electroneutral Na/HCO_3 cotransporter NBCn1. Endocrinology 148: 831-840.

38. Riihonen R, Nielsen S, Vaananen HK, Laitala-Leinonen T, Kwon TH (2010) Degradation of hydroxyapatite in vivo and in vitro requires osteoclastic sodium-bicarbonate co-transporter NBCn1. Matrix Biol 29: 287-294.

39. Daynes RA, Jones DC (2002) Emerging roles of PPARs in inflammation and immunity. Nat Rev Immunol 2: 748-759.

40. Biswas SK, Lopez-Collazo E (2009) Endotoxin tolerance: new mechanisms, molecules and clinical significance. Trends Immunol 30: 475-487.

41. Blumenthal A, Ehlers S, Lauber J, Buer J, Lange C et al. (2006) The Wingless homolog WNT5A and its receptor Frizzled-5 regulate inflammatory responses of human mononuclear cells induced by microbial stimulation. Blood 108: 965-973.

42. Pereira CP, Bachli EB, Schoedon G (2009) The wnt pathway: a macrophage effector molecule that triggers inflammation. Curr Atheroscler Rep 11: 236-242.

43. Ravasi T, Wells CA, Hume DA (2007) Systems biology of transcription control in macrophages. Bioessays 29: 1215-1226.

44. Amit I, M. Garber M, N. Chevrier N, A. P. Leite AP, Y. Donner Y et al. (2009) Unbiased reconstruction of a mammalian transcriptional network mediating pathogen responses. Science 326: 257-263.

45. Raza S, Robertson KA, Lacaze PA, Page D, Enright AJ et al. (2008) A logic-based diagram of signalling pathways central to macrophage activation. BMC Syst Biol 2: 36.

46. Lacaze P, Raza S, Sing G, Page D, Forster T et al. (2009) Combined genome-wide expression profiling and targeted RNA interference in primary mouse macrophages reveals perturbation of transcriptional networks associated with interferon signalling. BMC Genomics 10: 372.

47. Krutzik SR, Hewison M, Liu PT, J. Robles JA, Stenger S et al. (2008) IL-15 links TLR2/1-induced macrophage differentiation to the vitamin D-dependent antimicrobial pathway. J. Immunol. 181: 7115-7120.

Table 1. Number of genes modulated in response to IFN-γ and IL-4

	upregulated genes		downregulated genes	
Gene expression level	IFN-γ	IL-4	IFN-γ	IL-4
macrophages	1432	1253	2329	1377
6-h monocytes	957	2938	457	3574
	(66.8%)	(234.5%)	(19.6%)	(259.5%)
18-h monocytes	1334	990	901	1434
	(93.2%)	(79.0%)	(38.7%)	(104.1%)

Monocytes were stimulated with IFN-γ and IL-4 (20 ng/ml) for 6 and 18 hours. Their transcriptional response was studied by microarrays and compared to the transcriptional response of macrophages. The number of genes that were up- and down-regulated with a FC > 2.0 and $P < 0.05$ is indicated. In parentheses, the percentage of regulated genes in monocytes compared to macrophages.

Table 2. KEGG analysis of 6-h monocytes

KEGGID	*P* value	count	size	term
IFN-γ, KEGG terms with up-regulated genes				
04612	0.000	18	75	antigen processing and presentation
04514	0.000	23	129	cell adhesion molecules (CAMs)
04630	0.000	18	147	Jak-STAT signaling pathway
04622	0.000	10	65	RIG-I-like receptor signaling pathway
04610	0.000	10	68	complement and coagulation cascades
04060	0.001	21	248	cytokine-cytokine receptor interaction
04062	0.001	16	175	chemokine signaling pathway
04621	0.002	8	59	NOD-like receptor signaling pathway
04620	0.003	10	91	Toll-like receptor signaling pathway
IFN-γ, KEGG terms with down-regulated genes				
04210	0.001	6	84	apoptosis
04350	0.001	6	84	TGF-beta signaling pathway
IL-4, KEGG terms with up-regulated genes				
04514	0.000	17	130	cell adhesion molecules (CAMs)
04060	0.000	25	250	cytokine-cytokine receptor interaction
04620	0.001	12	96	Toll-like receptor signaling pathway
04612	0.002	10	77	antigen processing and presentation
IL-4, KEGG terms with down-regulated genes				
04115	0.002	9	68	p53 signaling pathway

Monocytes were stimulated with IFN-γ or IL-4 (20 ng/ml) for 6 hours. The genes that were up- and downregulated were analyzed according KEGG.

Table 3. KEGG analysis of 18-h monocytes

KEGGID	p value	count	size	term
IFN-γ, KEGG terms with up-regulated genes				
04612	0.000	29	78	antigen processing and presentation
01040	0.000	12	22	biosynthesis of unsaturated fatty acids
01100	0.000	170	1047	metabolic pathways
04146	0.000	21	76	peroxysome
00380	0.008	11	40	tryptophan metabolism
IFN-γ, KEGG terms with down-regulated genes				
04060	0.000	52	253	cytokine-cytokine receptor interaction
04620	0.000	23	94	Toll-like receptor signaling pathway
04062	0.000	32	180	chemokine signaling pathway
04622	0.001	14	66	RIG-I-like receptor signaling pathway
04630	0.009	22	147	Jak-STAT signaling pathway
IL-4, KEGG terms with up-regulated genes				
04612	0	23	77	antigen processing and presentation
01040	0	8	22	biosynthesis of unsaturated fatty acids
01100	0.001	121	1047	metabolic pathways
03320	0.003	12	67	PPAR signaling pathway
00380	0.01	10	59	tryptophan metabolism
IL-4, KEGG terms with down-regulated genes				
04620	0,000	24	94	Toll-like receptor signaling pathway
04060	0,000	45	253	cytokine-cytokine receptor interaction
04062	0,000	32	180	chemokine signaling pathway
04622	0,001	15	66	RIG-I-like receptor signaling pathway
04210	0.002	17	85	apoptosis

Monocytes were stimulated with IFN-γ or IL- 4 (20 ng/ml) for 18 hours. The genes that were up- and downregulated were analyzed according KEGG.

Table 4. KEGG analysis of macrophages

KEGGID	p	count	size	term
IFN-γ, KEGG terms with up-regulated genes				
04620	0.000	11	96	Toll-like receptor signaling pathway
04622	0.000	18	66	RIG-I like receptor signalling pathway
04062	0.000	31	180	chemokine signalling pathway
04621	0.001	14	62	NOD-like receptor signalling pathway
03050	0.001	11	43	proteasome
04666	0.002	17	90	Fc gamma R-mediated phagocytosis
04630	0.002	24	147	Jak-STAT signaling pathway
04670	0 .010	18	113	Leukocyte transendothelial migration
IFN-γ, KEGG terms with down-regulated genes				
00330	0.002	15	54	arginine and proline metabolism
04110	0.003	26	123	cell cycle
04115	0.007	16	68	p53 signaling pathway
IL-4, KEGG terms with up-regulated genes				
04612	0.000	23	78	antigen processing and presentation
01040	0.000	8	22	biosynthesis of unsaturated fatty acids
01100	0.001	121	1047	metabolic pathways
04060	0.004	23	250	cytokine-cytokine receptor interaction
03010	0.010	9	72	ribosome
IL-4, KEGG terms with down-regulated genes				
04610	0.001	15	68	complement and coagulation cascades
04110	0.001	22	123	cell cycle
00100	0.002	6	17	steroid biosynthesis
04115	0.005	16	68	p53 signaling pathway

Macrophages were stimulated with IFN-γ or IL-4 (20 ng/ml) for 18 hours. The genes that were up- and downregulated were analyzed according KEGG.

Table 5. IRGs regulated by IFN-γ and IL-4

	Number of IRGs (type II)	**Number of IRGs (type I)**
IFN-γ		
6-h monocytes	82	83
18-h monocytes	27	25
macrophages	54	51
IL-4		
6-h monocytes	29	30
18-h monocytes	27	20
macrophages	18	18

The IRG response of monocytes and macrophages stimulated with IFN-γ and IL-4 was determined by microarray. The 300 genes that were the most regulated in each experimental condition were compared with the 1,996 genes contained in the interferome database (25). The number of common genes is showed.

Table 6. Regulated genes according M1 and M2 profiles

	Membrane receptors	Cytokines/ Chemokines	Apoptosis	Solute carriers	Enzymes	Extracellular mediators	DNA-binding factors
macrophages							
IFN-γ 34 M1 genes	IL2RA IL15RA	CCL5 CCL19 CCL20 CXCL9 CXCL10 CXCL11 ECGF1 IL15 PBEF1 TNF TRAIL	GADD45G XIAP-AF1	SLC2A6 SLC31A2	HSD11B1 IDO OASL OAS2 PLA1A PSMA2 PSMB9	APOL1 APOL2 APOL3 APOL6 EDN1 IGFBP4 INHBA	HESX1 IRF1 IRF7
IL-4 14 M2 genes	DCSIGN DECTIN1 HRH1	CCL13 CCL18 CCL23		SLC4A7	ALOX15 CERK CTSC	CHN2 FN1 SEPP1	EGR2
6-h monocytes							
IFN-γ 23 M1 genes	IL15RA	CXCL9 CXCL10 CXCL11 IL15 PBEF1 TNF TRAIL	BCL2A1 GADD45G XIAP-AF1	SLC31A2	IDO OAS2 PSMB9	APOL1 APOL2 APOL3 APOL6 INHBA PDGFA	IRF1 IRF7
IL-4 18 M2 genes	CLECSF13 CXCR4 DCSIGN DECTIN1 MS4A4A MS4A6A TLR5	CCL13 CCL18 CCL23		SLC4A7 SLC21A9	ALOX15 CERK CTSC HNMT HS3ST2	CHN2	
18-h monocytes							
IFN-γ 3 M1 genes				SLC21A15	IDO		HESX1
IL-4 4 M2 genes		CCL18 CCL23 IGF1					EGR2

Macrophages were stimulated with IFN-γ and IL-4 (20 ng/ml) for 18 hours and monocytes for 6 and 18 hours. Their transcriptional responses were studied by microarrays. The genes belonging to M1 and M2 classifications that were regulated are shown.

Table 7. Regulated genes according iron metabolism

M1 macrophages	ALAS1, BCL2, CP, FTH1, HAMP, HIF1A, HPX, NFE2L1, SFXN1, SR1, TF
macrophages + IFN-γ	ALAS1, CP, NFE2L1, SR1
6-h monocytes + IFN-γ	ALAS1, CP, HAMP, SR1
18-h monocytes + IFN-γ	none
M2 macrophages	ALAD, CPOX, CYBRD1, FECH, FTL, FXN, ISCU, HFE, HMOX1, JMJD1A, LRP1, MYC, NFS1, PPOX, SFXN2, SFXN3, SFXN4, SLC11A1, SLC40A1, TSPO, UROD
macrophages + IL-4	ALAD, CYBRD1, MYC, NFS1
6-h monocytes + IL-4	ALAD, CYBRD1, FTL, FXN, HFE, JMJD1A, LRP1, MYC, NFS1, SFXN2, SFXN3, SLC11A1
18-h monocytes + IL-4	ISCU, MYC

The transcriptional signatures of macrophages and monocytes stimulated with IFN-γ and IL-4 were determined by comparing our microarray data with the expression of M1/M2 genes related to iron metabolism in macrophages (30). The genes belonging to M1 and M2 classifications that were regulated are shown. CP: ceruloplasmin ferroxidase; TF: transferrin.

Figure 1. PCA analysis

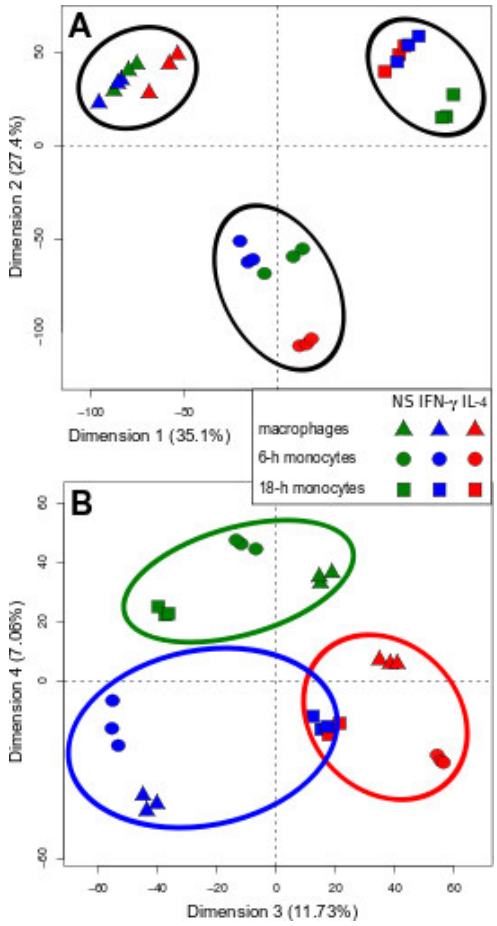

Macrophages and monocytes were stimulated with IFN-γ or IL-4 (20 ng/ml), and microarrays were performed after RNA extraction. A-B**,** The impact of cell type (A) and cell stimulation by IFN-γ and IL-4 (B) on gene expression was analyzed by PCA using R. Each axis distance represents the amount of variance in gene expression explained by the corresponding factor (cell type or stimulation).

Figure 2. Hierarchical clustering of macrophages and monocytes

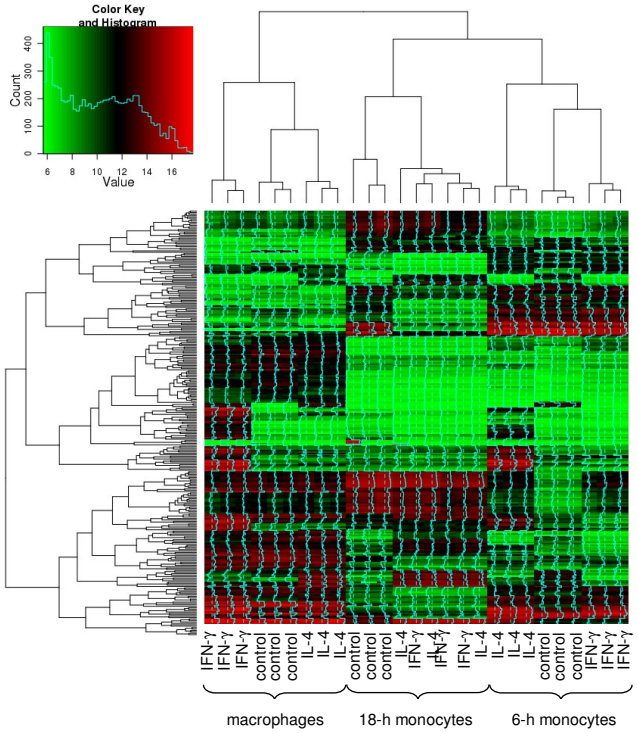

Macrophages and monocytes were stimulated with IFN-γ or IL-4 (20 ng/ml), and microarrays were performed after RNA extraction. Data were analyzed using hierarchical clustering including the 300 genes with the highest variation and are represented by a color gradient ranging from green (downregulation) to red (upregulation). The transcriptional programs of macrophages and monocytes stimulated with or without IFN-γ or IL-4 were organized into three clusters corresponding to macrophages and monocytes incubated for 6 and 18 hours, respectively. Note that IFN-γ and IL-4 induced the polarization of macrophages and 6-h monocytes, but not 18-h monocytes.

Figure 3. GO annotation of regulated genes in monocytes

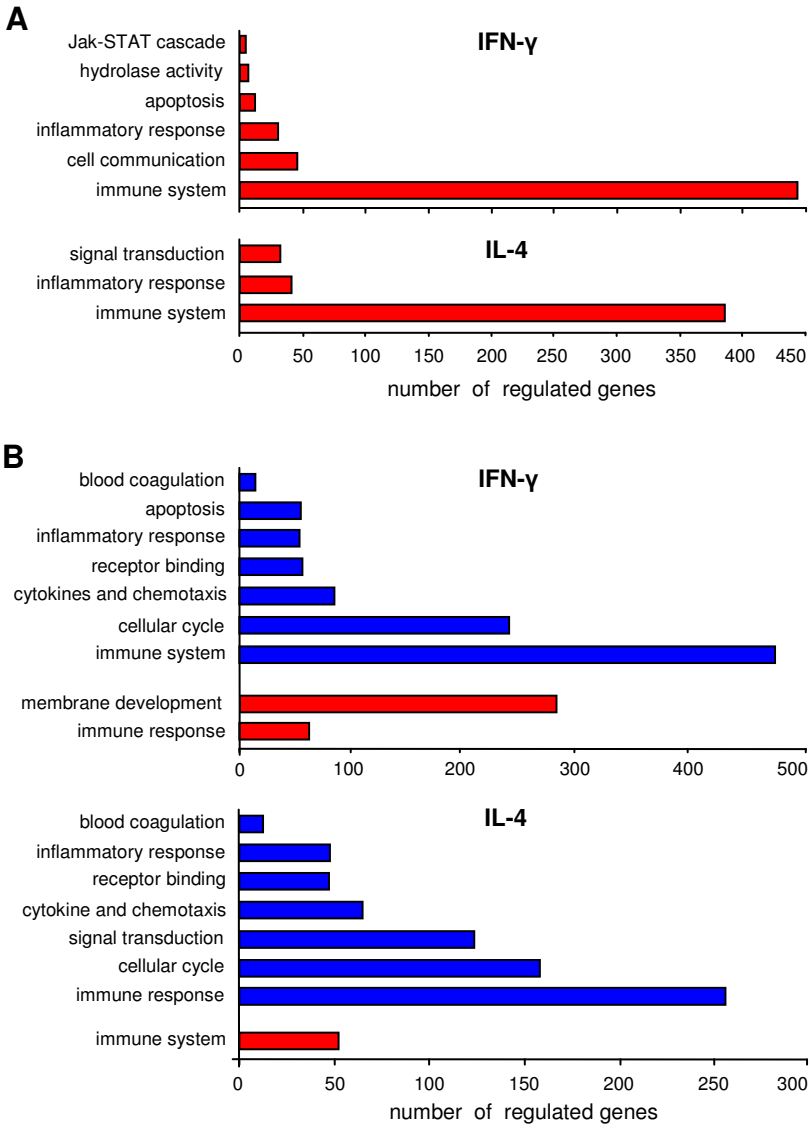

Monocytes were stimulated with IFN-γ or IL-4 (20 ng/ml) for 6 (A) and 18 hours (B). The genes that were differentially expressed in stimulated cells were subjected to GO annotation to identify the corresponding biological process. The major biological processes are shown, including the number of regulated genes. GO redundancy is due to the involvement of individual genes in multiple biological processes. In red, up-regulated genes; in blue, down-regulated genes.

Figure 4. GO annotation of regulated genes in macrophages

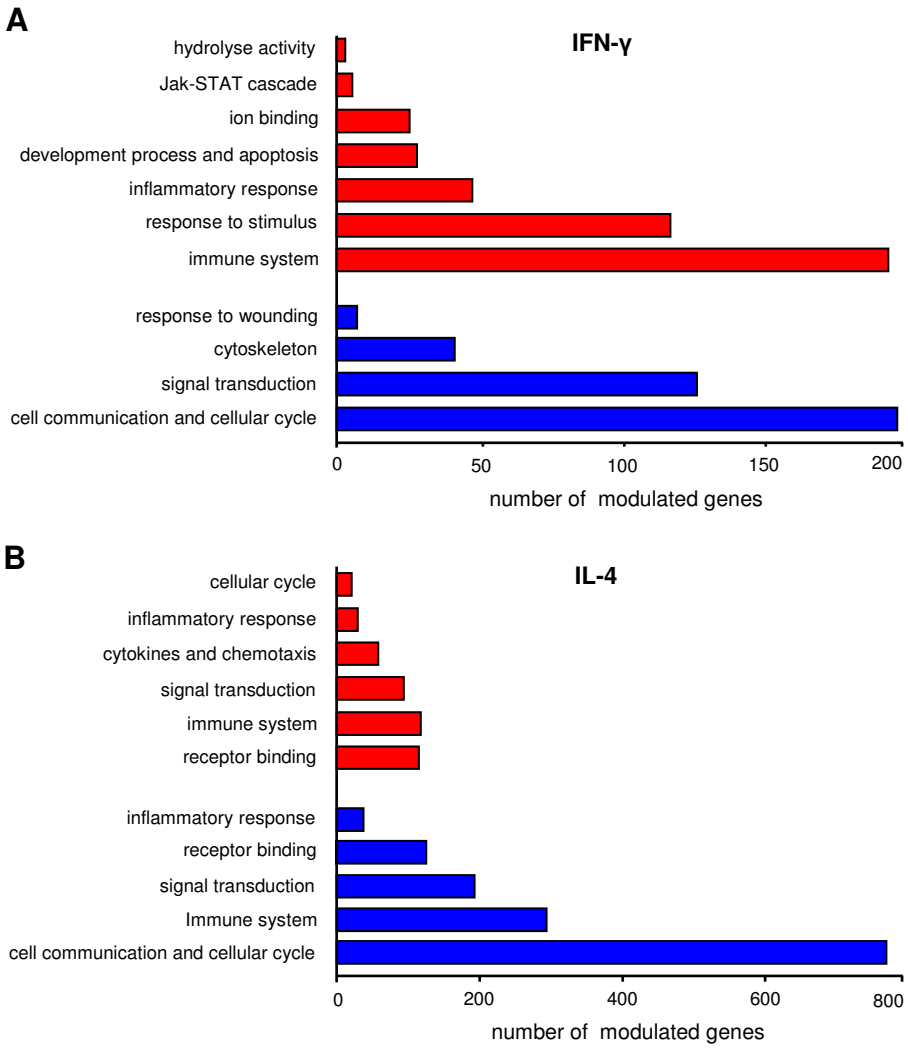

Macrophages were stimulated with IFN-γ (A) and IL-4 (B) for 18 hours. The genes that were differentially expressed in stimulated cells were subjected to GO annotation to identify the corresponding biological process. The major biological processes are shown, including the number of regulated genes. GO redundancy is due to the involvement of individual genes in multiple biological processes. In red, upregulated genes; in blue, downregulated genes.

Figure 5. qRT-PCR of selected genes in 18-h monocytes

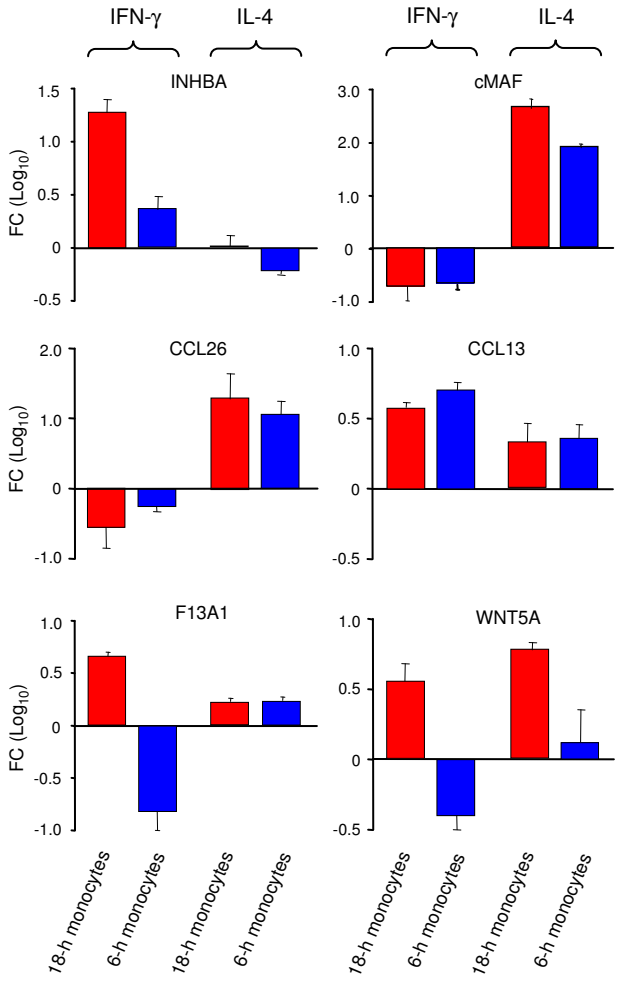

Monocytes were stimulated with IFN-γ or IL-4 (20 ng/ml) for 18 hours and RNA was extracted. qRT-PCR was performed on 6 genes found to be regulated in microarray experiments. The results, expressed as FC (Log10), are presented as the mean ± SEM of three independent experiments performed in triplicate.

Figure 6. Lyn/PI3K and pyruvate kinase networks

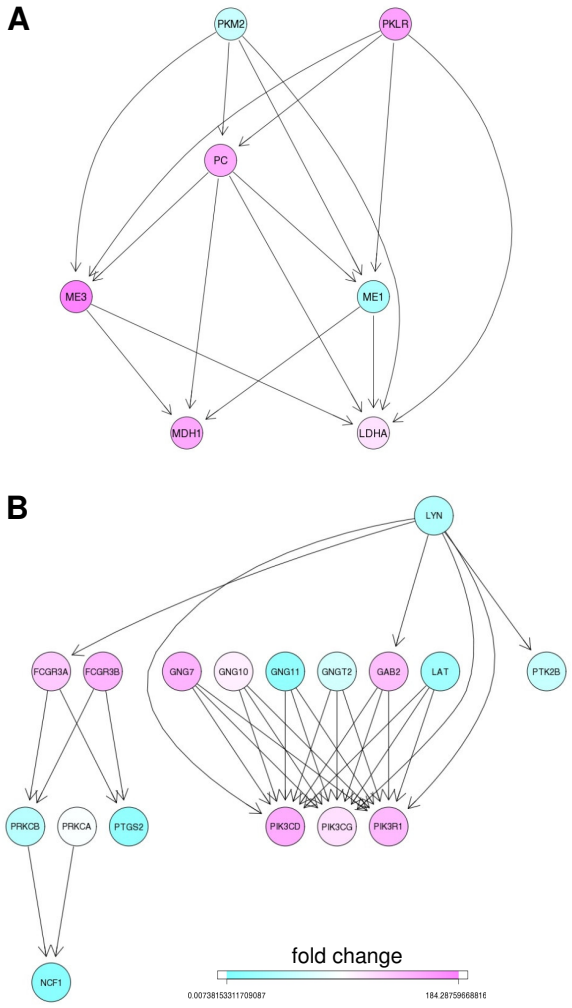

Monocytes were stimulated with IFN-γ (20 ng/ml) for 18 hours and RNA was extracted. Microarray data were collected, and pyruvate kinase (A) and lyn/PI3K (B) networks of regulated genes with nodes controlling transcription and interaction pathways are represented.

Figure 7. Cytoskeleton and chemokine network

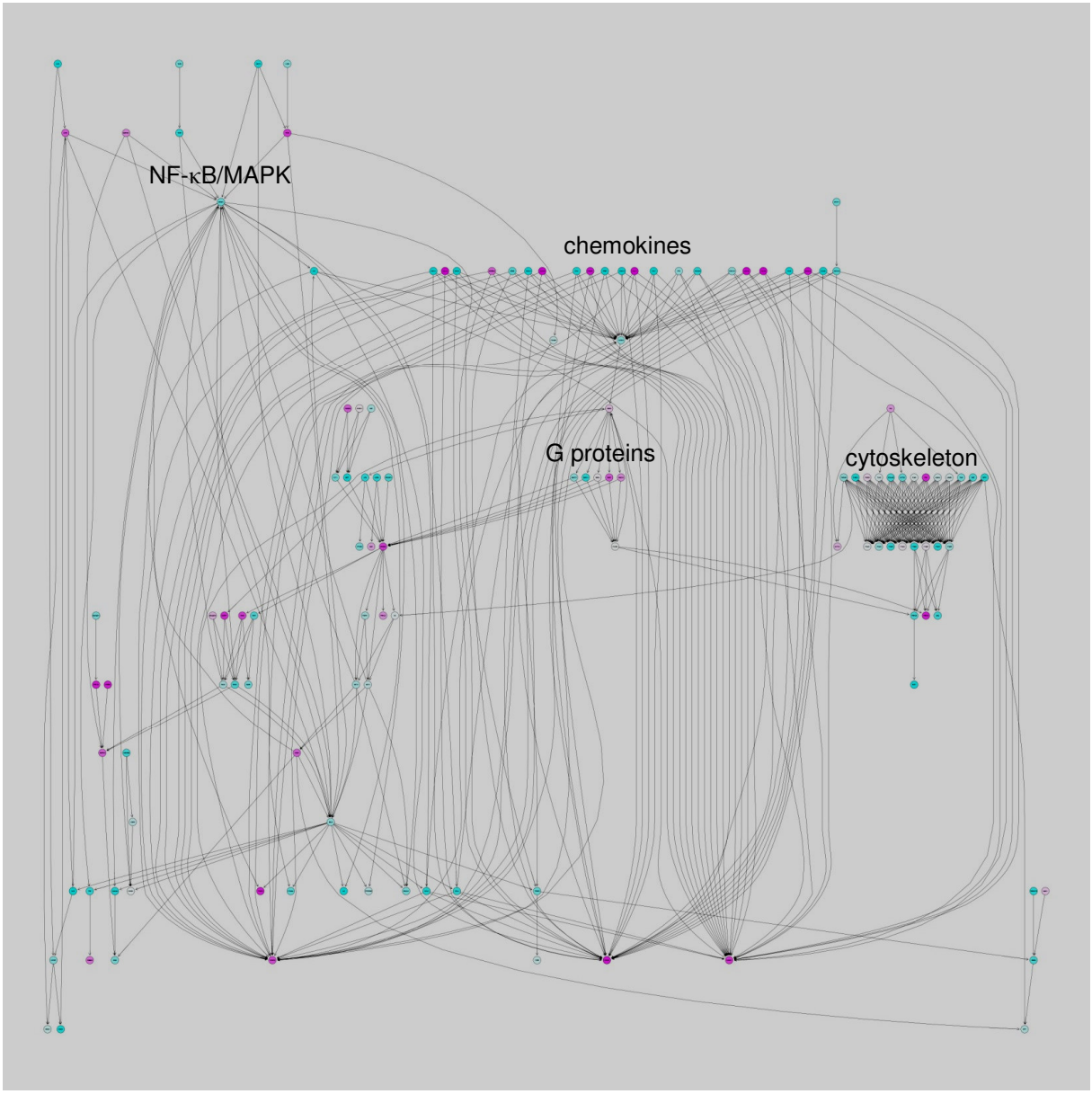

Monocytes were stimulated with IL-4 (20 ng/ml) for 18 hours and RNA was extracted. Microarray data were collected, and the major network of regulated genes with nodes controlling transcription and interaction pathways are represented as cytoskeleton and chemokine subnetworks.

Figure 8. Metabolism-related networks

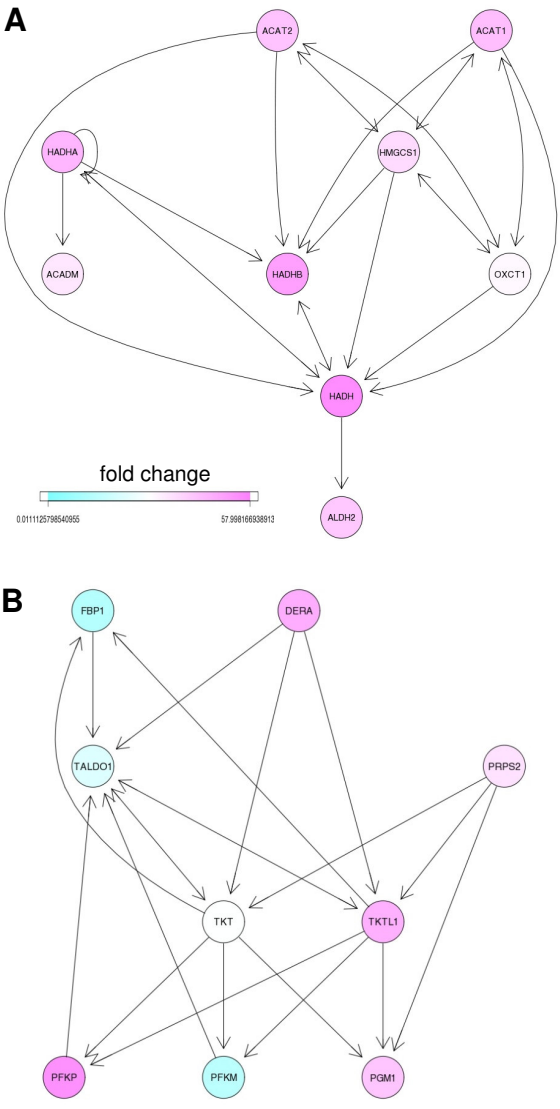

Monocytes were stimulated with IL-4 (20 ng/ml) for 18 hours and RNA was extracted. Microarray data were collected, and the cholesterol (A) and glycogen (B) networks of regulated genes with nodes controlling transcription and interaction pathways are represented.

Figure S1. Comparative hierarchical clustering of macrophages

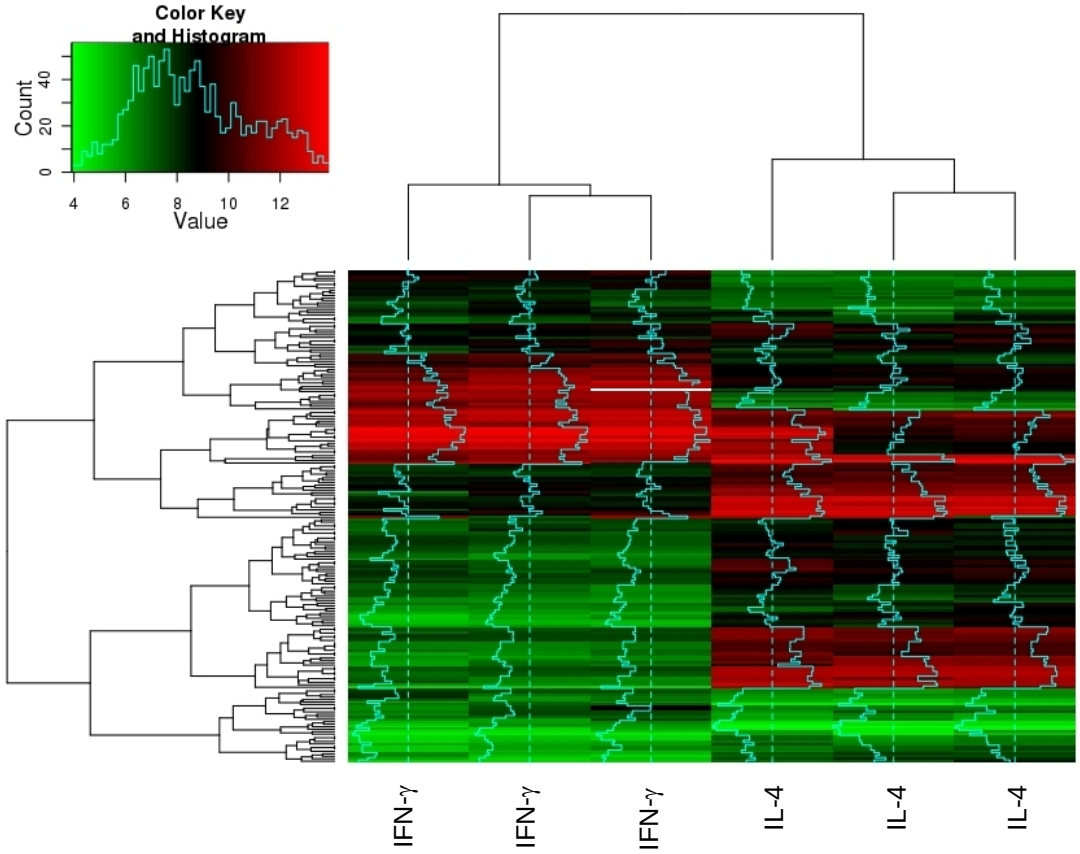

Macrophages were stimulated with IFN-γ or IL-4 for 18 h. After RNA extraction, Agilent microarrays were performed. Data were compared with transcriptomic profiles of M1 and M2 macrophages described in (9) obtained using Illumina bead chips by building a virtual Agilent microarray including both types of data. Hierarchical clustering included the 125 genes with the highest variation. These genes are represented by a color gradient ranging from green (down-regulation) to red (up-regulation).

Figure S2. Gene networks in monocytes stimulated with IFN-γ for 6 h
Microarray data were collected, and the networks of regulated genes with nodes controlling transcription and interaction pathways were represented.

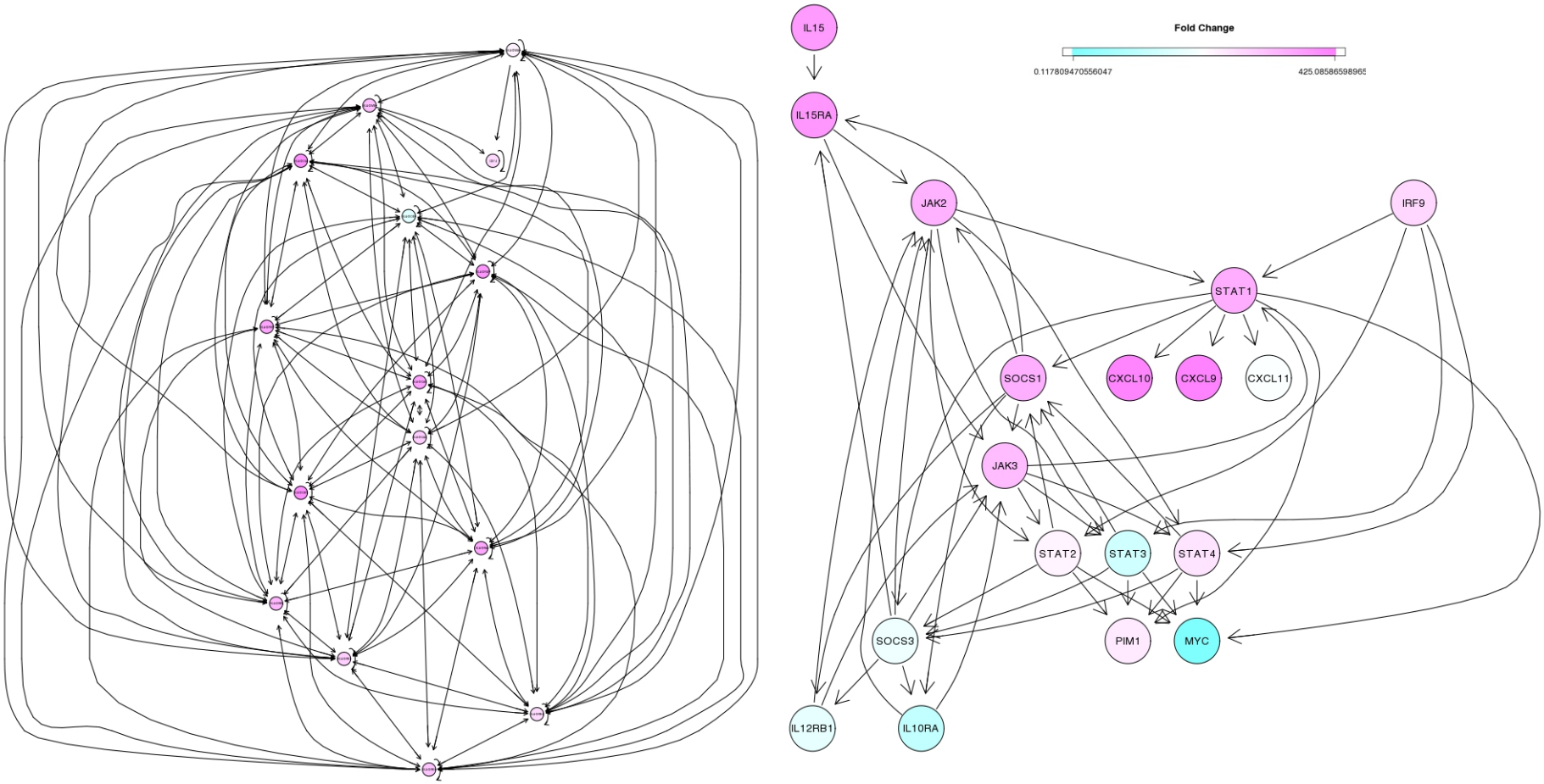

class II MHC network **IL-15 network**

Figure S3. Gene networks in monocytes stimulated with IL-4 for 6 h
Microarray data were collected, and the networks of regulated genes with nodes controlling transcription and interaction pathways were represented.

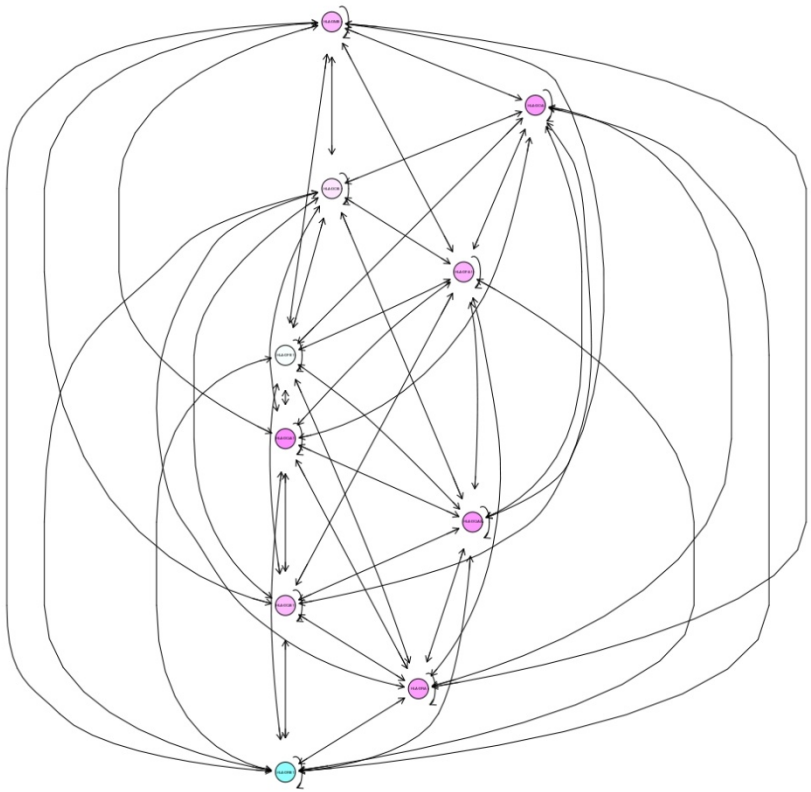

class II MHC network

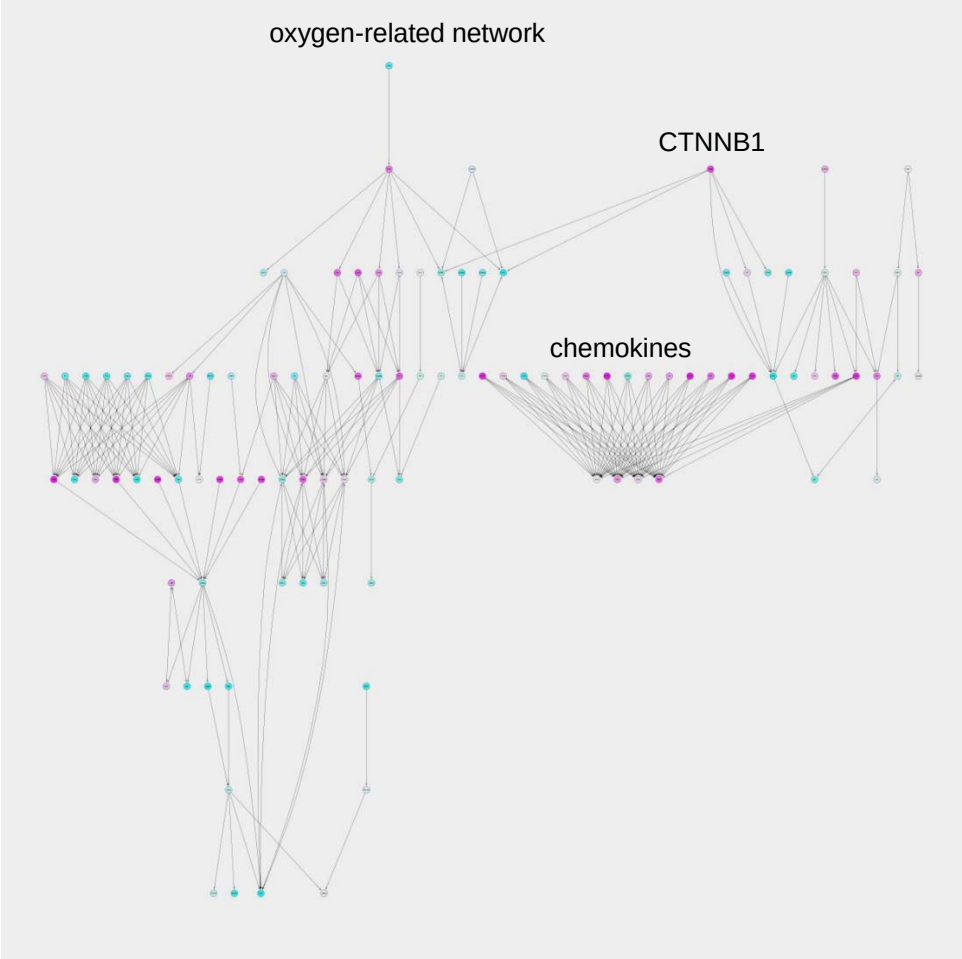

Figure S4. Networks in monocytes stimulated with IFN-γ for 18 h
Microarray data were collected, and networks of regulated genes with nodes controlling transcription and interaction pathways were represented.

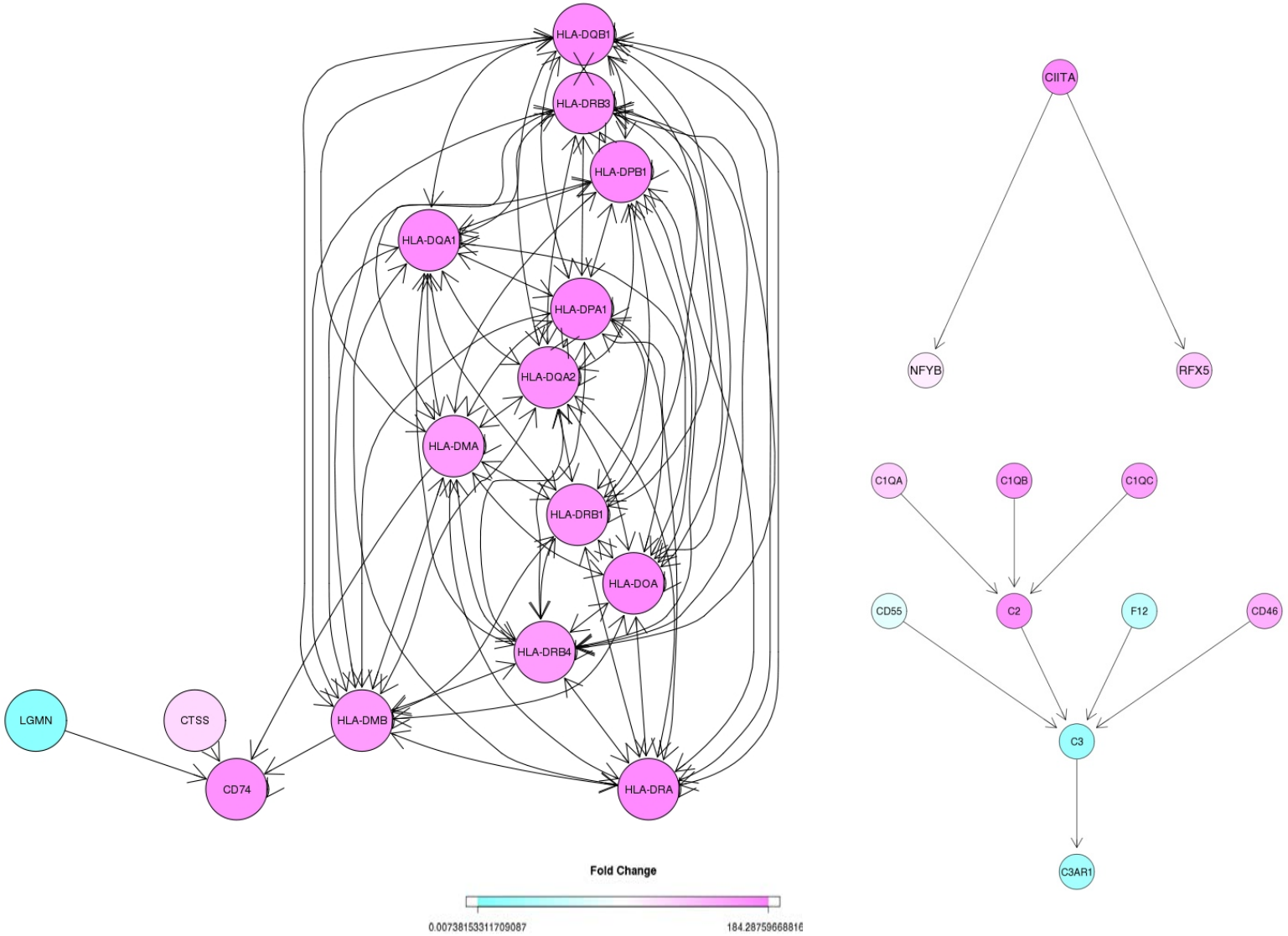

ANNEXE 2

The Gene expression analysis of blood reveals *S100A11* and *AQP9* as potential biomarkers of infective endocarditis

Franck Thuny, Amira Ben Amara, Adil El Filali, Christian Capo, Gilbert Habib, Didier Raoult, Jean-Louis Mege, soumis à publication

La principale conséquence clinique de la fièvre Q chronique est une endocardite même si *C. burnetii* n'est à l'origine que d'une faible part des endocardites infectieuses. En effet, la grande majorité des endocardites infectieuses sont dues aux staphylocoques et aux streptocoques. Par ailleurs, malgré des progrès récents dans les domaines de l'imagerie médicale et de la microbiologie, le diagnostic d'endocardite infectieuse reste difficile à établir. En outre, le risque de complications cardiaques et emboliques dues aux endocardites infectieuses demeure élevé, ce qui explique une morbidité et une mortalité importante des patients. En d'autres termes, il n'existe pas à ce jour de marqueurs biologiques satisfaisants de diagnostic et de pronostic des endocardites infectieuses.

C'est la raison pour laquelle les profils transcriptionnels des valves cardiaques de patients atteints d'une endocardite infectieuse ont été comparés à ceux de valves prélevées sur des patients atteints d'une pathologie cardiaque non infectieuse (116). Un clustering hiérarchique a révélé une signature des endocardites infectieuses composée de 146 gènes. Parmi les 89 gènes dont l'expression est augmentée, la plupart d'entre eux sont impliqués dans le recrutement des cellules inflammatoires dans les végétations, l'angiogénèse et le remodelage de l'endocarde. D'autres sont associés à la voie apoptotique intrinsèque et aux caspases. Deux gènes semblent particulièrement associés aux endocardites infectieuses, le gène codant la métalloprotéinase (MMP)-12 et le gène codant l'aquaporine-9. En outre, la protéine MMP-12 est exprimée par les macrophages infiltrant les valves des patients atteints d'une endocardite infectieuse. De même,

l'aquaporine-9 est exprimée dans l'endothélium présent au niveau des valves infectées, ce qui suggère qu'elle pourrait être associée à la néo-vascularisation de ces valves.

Si intéressants ces résultats soient-ils, ils ne peuvent servir directement de marqueurs de diagnostic ou de pronostic des endocardites infectieuses puisqu'ils procèdent d'un acte chirurgical lourd. C'est ainsi que nous avons décidé d'étendre cette approche transcriptomique à grande échelle (microarray) à l'étude de la réponse périphérique des patients atteints d'une endocardite infectieuse. Nous avons à cet effet sélectionné 39 patients admis dans le Service de Cardiologie de l'Hôpital de la Timone à Marseille pour endocardite infectieuse et dont l'endocardite infectieuse a été confirmée, 10 patients présentant une suspicion initiale d'endocardite infectieuse mais qui a été ultérieurement infirmée et 10 sujets contrôles.

Les patients atteints d'une endocardite infectieuse présentent un programme transcriptionnel spécifique avec la modulation d'environ 6.000 gènes et prédominance de catégories de gènes associés à l'activation cellulaire, la réponse immune innée et la réponse inflammatoire. Ces catégories de gènes sont organisées dans un réseau constitué lui-même de sous-réseaux incluant le complexe majeur d'histocompatibilité, les cellules *Natural Killer*, la voie de l'IFN de type 1 et le trafic intracellulaire. Quelques gènes particulièrement modulés et potentiellement impliqués dans l'histoire naturelle des endocardites infectieuses ont été étudiés en RT-PCR en temps réel. L'expression du gène codant la protéine S100A11 fixant le calcium est spécifiquement augmentée chez les patients avec endocardite infectieuse et plus particulièrement chez les patients avec une endocardite due à une infection par staphylocoques. Les concentrations sériques de la protéine S100A11 confirment ces résultats, ce qui suggère que le dosage de la molécule S100A11 pourrait servir de marqueur de diagnostic des endocardites infectieuses. Nous avons également montré que la régulation du gène codant l'aquaporine-9 est associée aux événements aigus de défaillance cardiaque (*acute heart failure*), ce qui pourrait améliorer le pronostic des endocardites infectieuses.

Ces résultats ouvrent la voie à trois axes de recherche. Le premier consisterait à étendre l'étude à un plus grand nombre de malades atteints d'une endocardite infectieuse, le deuxième à explorer un plus grand nombre de gènes modulés au cours des endocardites infectieuses et le troisième à effectuer un suivi longitudinal des patients atteints d'une endocardite infectieuse afin d'associer paramètres cliniques et paramètres biologiques.

The Gene Expression Analysis of Blood Reveals *S100A11* and *AQP9* as Potential Biomarkers of Infective Endocarditis

Franck Thuny, MD,[1,2] Amira Ben Amara, MSc,[2] Adil El Filali,[2] Christian Capo, PhD,[2] Gilbert Habib, MD,[1,2] Didier Raoult, MD, PhD,[2] Jean-Louis Mege, MD, PhD[2]

[1] Département de Cardiologie, Hôpital de la Timone, Marseille, France.

[2] Unité de Recherche sur les Maladies Infectieuses Transmissibles et Emergentes, Centre National de la Recherche Scientifique (CNRS) Unité Mixte de Recherche 6236, Université de la Méditerranée, Faculté de Médecine, Marseille, France.

Short title: Peripheral gene expression in endocarditis

Word count: 3320

Journal subject codes: 111, 19, 141, 142, 143, 155

Address for correspondence:

Pr Jean-Louis Mege

URMITE, Faculté de Médecine, 27 Bld. Jean Moulin 13385 Marseille Cedex 5, France.

Tel: +33 (0)4 91 32 43 75.

Fax: +33 (0)4 91 38 77 72.

E-mail: jean-louis.mege@univmed.fr

ABSTRACT

Background—Diagnosis and pronostic assessment are challenging in infective endocarditis (IE). To investigate the host response during IE and identify potential biomarkers, we determined the circulating gene expression profile through a whole genome microarray analysis.

Methods and Results—A transcriptomic case-control study was performed on blood samples from patients with native valve IE (n=39), excluded IE after an initial suspicion (n=10) at patient's admission, and age-matched healthy controls (n=10). The whole genome microarray analysis showed that patients with IE exhibited a specific transcriptional program with a predominance of gene categories associated with cell activation, innate immune and inflammatory responses. These categories were organized in a dense network from which arose numerous subnetworks including major histocompatibily complex and natural killer cell network, type 1 interferon pathway and intracellular traffic. Quantitative real-time RT-PCR performed on a selection of highly modulated genes showed that the expression of the gene encoding S100 calcium binding protein A11 (*S100A11*) was significantly increased in patients with IE in comparison with controls ($P<0.001$) and patients with excluded IE ($P<0.05$). Interestingly, the upregulated expression of *S100A11* gene was more pronounced in staphylococcal IE than in streptococcal IE ($P<0.01$). These results were confirmed by serum concentrations of the S100A11 protein. Finally, we showed that, in patients with IE, the upregulation of aquaporin-9 gene (*AQP9*) was significantly associated to the occurrence of acute heart failure ($P=0.02$).

Conclusions— Using transcriptional signatures of blood samples, we identified *S100A11* as a potential diagnostic marker of IE. In addition, the determination of *AQP9* may improve the prognostic assessment of IE.

Key Words: gene microarray, biomarker, endocarditis, diagnosis, pathogenesis

INTRODUCTION

Infective endocarditis (IE) is a severe disease with an incidence ranging from 30 to 100 episodes per million person-years.[1, 2] Mortality is high, and more than one-third of patients will die within the first year of their diagnosis.[3-6] Despite developments of microbiological and imaging techniques, diagnosis of IE remains challenging. Indeed, etiologic diagnoses may not be obtained in 2.5% to 31% of cases[1, 7] and echocardiography is negative in around 10% of cases.[8] Otherwise, morbidity and mortality remain high and strategies fail to detect and predict substantial number of events such as heart failure and embolic events. One of the reasons of these issues is the complex pathogenesis of the disease involving many host-pathogen interactions. Indeed, previous endocardial lesions can lead to exposure of the underlying extracellular matrix proteins, local inflammation with interleukin-1 release, and then thrombus formation termed "non-bacterial vegetation". In case of bacteremia, valves with those pre-existing sterile vegetations or minimal lesions tissue can be colonized because of crucial interactions between bacteria, platelets and endothelial cells via several bacterial surface proteins or plasma-bridging molecules. This process leads to the recruitment of circulating cells, including neutrophils and monocytes, the release of cytokines and procoagulant factors that contribute to the enlargement of vegetations and thus the protection of bacterial pathogens from host defenses.[9]

This complex situation highlights the need for methods that improve the management of IE. Especially, the identification of new biomarkers for diagnosis and risk stratification will be useful. Molecular signatures of IE represent promising means for addressing this challenge. In particular, microarray-based transcriptomes can identify specific signatures of the disease that might ultimately be translated into clinically useful molecular biomarkers.[10] Recently, we identified a transcriptional signature of IE from valvular tissue,[11] but this approach is difficult to be used by physicians in their dayly practice. Peripheral blood is an

alternative to tissue sample for molecular profiling of human diseases[10] because it interacts with every tissue in the body and has a crucial role in many IE pathophysiological processes such as immunity, inflammation and coagulation.

To investigate the host response during IE and identify potential biomarkers, we determined the circulating gene expression profile through a unique whole genome microarray analysis. We show that patients with IE exhibited a specific transcriptional program with a predominance of gene categories associated with cell activation, innate immune and inflammatory responses. We demonstrate that the gene encoding S100 Calcium Binding Protein A11 (*S100A11*) and the serum concentration of S100A11 protein are significantly increased in IE patients, especially in case of staphylococcal etiology. Moreover, in IE patients, the upregulation of aquaporin-9 gene (*AQP9*) is associated with occurrence of acute heart failure.

METHODS

Study Population

All the participants to the study were prospectively enrolled, from January 2009 to December 2010, at the Cardiology Department of La Timone Hospital (Marseille, France), a teaching tertiary care adult's hospital. The patients were eligible for the study entry if they had a clinical suspicion of IE. The exclusion criteria were age <18 years, pregnancy, history of previous IE, intracardiac material (prosthetic valve, pacemaker or implantable cardioverter defibrillator) and an antibiotic treatment for more than one week.

The transcriptomic case-control study was performed in 39 consecutive patients with native valve IE (IE group) diagnosed by a multidisciplinary team who applied the modified Duke criteria,[12] 10 patients admitted for a suspicion of IE but with a final excluded IE diagnosis (excluded IE group) (Table 1), and 10 age-matched healthy volunteers (control

group). Ten IE patients and five controls were arbitrary selected and investigated with microarrays, and all the patients were finally analyzed by quantitative real-time reverse transcriptase-polymerase chain reaction (qRT-PCR).

For each case, the following data were collected: age, sex, comorbidity,[13] signs and symptoms, duration of symptoms, biological results, history of antimicrobial therapy for the current illness that prompted the patient to seek medical attention, antecedent disease, predisposing factors for IE including systemic disease, intravenous drug use, treatment received during the course of hospitalization and complications (acute heart failure, embolic event, and cardiac abscess). Echocardiography was performed by a systematic transthoracic and trans-esophageal approach.[5] For the microbiological diagnosis, a diagnostic kit including blood cultures and serologies was used as previously described.[14] When cardiac surgery was required, valvular surgical samples were analyzed using cultures and PCR amplification.

The study was performed according to the principles of the Declaration of Helsinki. Informed and written consent was obtained from each subject and the study was approved by the Ethics Committee of the Université de la Méditerranée.

RNA Preparation and Microarrays

Peripheral blood was drawn at the admission of patients in PAXgene tubes (Qiagen). RNA was extracted using according to the manufacturer's recommendations, which included a DNase step. The quality and quantity of isolated RNAs were assessed using the Nanodrop (Thermo Scientific) and 2100 Bioanalyzer (Agilent Technologies), and the RNAs were eluted in 80 µL of water and stored at -20°C. RNAs were then analyzed using microarray chips (Agilent Technologies) including 45,000 probes (4x44K Whole Human Genome, Agilent Technologies) and One-color Microarray Based Gene Expression Analysis, as recently described.[15] In brief, 400 ng RNAs were labeled with cyanine-3 CTP using a commercial kit

(Low RNA Input Fluorescent Amplification Kit, Perkin Elmer). After the deposition of samples on the slide, hybridization was performed at 65°C using the In situ Hybridation Plus kit (Agilent Technologies) for 17 hours. The arrays were scanned with a pixel size of five microns with the DNA Microarray Scanner G2505B (Agilent Technologies). Image analysis and correction of intra-array signals were performed with the Feature Extraction Software A.9.1.3 (Agilent Technologies). Differentially expressed gene sets consisted of genes matching for a *P*-value <0.01 as determined by the 2-tailed Student's *t* test. The modulated genes were functionally analyzed using Gene Ontology (GO) and Kyoto Encyclopedia of Genes and Genomes (KEGG) databases.[15, 16] The modulated genes that were implicated in KEGG pathways were submitted to the KEGG graph package (http://www.bioconductor.org/packages/2.4/bioc/html/KEGGgraph.html) to draw gene-gene interactions in the network pathways. The data were generated according the Minimum Information About a Microarray Experiment guidelines and were deposited in the National Center for Biotechnology Information's Gene Expression Omnibus.[17] The data are accessible using accession number (http://www.ncbi.nlm.nih.gov/geo/query/acc.cgi?token=bxmzrwwgygmwahu&acc=GSE29161).

qRT-PCR Analyses

Reverse transcription of 150 ng of total RNAs per reaction was performed with the MMLV-RT kit (Invitrogen), as previously described.[15] Quantitative real-time PCR was performed using gene-specific primers designed using Primer3 (http://frodo.wi.mit.edu/primer3). The list of primers with their sequences is provided in the Data supplement file 1. The transcriptional profiles of selected genes were screened in dedicated homemade 384-well plates using the 7900HT Fast Real Time PCR System, and qRT-PCR data were extracted using the SDS 2.2

software (Applied Biosystems). Results were normalized using the housekeeping gene β-actin and are expressed as $FC = 2^{-\Delta\Delta Ct}$, where $\Delta\Delta Ct = (CtTarget - CtActin)_{assay} - (CtTarget - CtActin)_{control}$, as previously described.[15]

S100A11 Assay

Serum concentrations of S100A11 protein were assessed by enzyme-linked immuno-sorbent assay kit (USCN, Life Science Inc.) according to the manufacturer's protocol. The sensitiviy of the test is 0.37 ng/mL.

Statistical Analysis

Categorical data were reported as frequencies and percentages, and were compared using the Fischer exact two tailed test. Continuous data are expressed as mean ±SEM or median and interquartile range. Comparisons between two groups were performed using the Mann-Whitney *U* test and comparisons between the three groups of individuals were performed by Kruskal-Wallis test with post-hoc Dunn's multiple comparison test. This statistical analysis was conducted using SPSS for Windows, version 16.0 (SPSS Inc., Chicago, Illinois). Values of $P<0.05$ were considered statistically significant.

RESULTS

Microarray Analysis of Patients with IE

A whole-genome microarray approach was used to define the peripheral transcriptional signature of IE. For that purpose, we arbitraly selected ten IE patients and five controls. The principal components analysis of overall gene expression showed that IE patients and controls were organized in two different groups (Figure 1, Panel A). The Euclidean clustering (Figure

1, Panel B) and hierarchical clustering of the 300 most variable genes (Figure 1, Panel C) also showed that the modulated genes in IE patients and controls were distributed in two different clusters. Finally, we found that 3,819 probes were upregulated and 2,164 downregulated with a *P* value less than 0.01 in IE patients compared to controls. Taken together, these different analyses of gene expression demonstrated that patients with IE exhibited a specific transcriptional program.

Functional Analysis of Modulated Genes in Patients with IE

The genes that were differentially expressed in IE patients were classified into different categories based on GO database (Table 2). In upregulated genes, there was an enrichment with biological processes related to cell activation, inflammation and immune response. They corresponded to the following GO terms: macromolecule localization, intracellular signaling pathway, protein ubiquitination, post-translational protein modification, I-κB kinase, NF-κB cascade, immune response, innate immune response and response to virus. In downregulated genes, the GO terms such as regulation of RNA stability, gene expression, regulation of cell proliferation, were enriched. The KEGG analysis emphasized GO analysis (Table 3). Indeed, the categories related to innate immune activation (Toll-Like Receptor [TLR] signaling pathway) and cell activation (endocytosis) were also enriched. The enrichment of the calcium-signaling pathway observed in KEGG is likely related to the GO term calcium ion transport (Table 2).

The functional interactions between modulated genes were assessed by constructing gene networks. A complex and dense network consisted of pathways related to innate immune and inflammatory responses (Figure 2). Among these pathways, we could identify the TLR pathway (5 upregulated genes), the IRF7 and type 1 interferon (IFN) pathways (with only upregulated genes), MAP kinase and NF-κB pathways. Interestingly, *HLAC* and *KIR2DL4*

genes were associated with a subnetwork of inflammatory genes, suggesting the involvement of natural killer (NK) cells in IE. Besides this complex network, we found 13 small networks including endocytosis (5 SEC-related genes), ubiquitination (4 genes encoding ubiquitin-conjugating enzymes and 2 related genes) and intracellular traffic (5 Rab11-related genes, 2 genes encoding Rab5 isoforms and 3 related genes) (Data supplement file 2). Taken together, the analysis of gene networks revealed the enrichment with gene categories associated with cell activation, inflammatory and immune response. These categories were organized in a dense network from which arose numerous subnetworks including major histocompatibility comples and NK cell network, type 1 interferon pathway and intracellular traffic.

Validation of Modulated Genes in Patients with IE

Because of the large number of modulated genes and the density of transcriptomic networks, the following procedure was used to validate microarray data. Seven upregulated genes were selected from the list of the 300 most modulated genes according to their putative role in IE pathophysiology. Their expression was determined by qRT-PCR in an enlarged cohort of IE patients (n=39) and controls (n=10). The genes encoding aquaporin-9 (AQP9), S100A11, plasminogen activator urokinase receptor (PLAUR), solute carrier family 16, member 3 (SLC16A3), transforming growth factor beta 1 (TGFβ1), interferon gamma-inducible protein 16 (IFI16), and apolipoprotein B mRNA editing enzyme, catalytic polypeptide-like 3B (APOBEC3B) were significantly upregulated in IE patients (P<0.001 for all, Figure 3).

As these results may be due to the underlying valvular abnormality or the global inflammatory response, they were compared with those obtained in the group of excluded IE after an initial suspicion (n=10). It clearly appeared that the *S100A11* gene was significantly upregulated in IE patients compared with patients with excluded IE (P<0.05, Figure 3). The upregulated expression of the *S100A11* gene had functional consequences. Indeed, the serum

concentration of S100A11 protein was higher in patients with IE than in patients with excluded IE (5.0 ± 1.0 versus 2.1 ± 0.5 ng/mL, $P<0.05$).

Finally, we tested whether the bacterial etiology of IE plays a role in the modulated expression of *S100A11* gene. In our series, 23 patients were infected with staphylococci (*Staphylococcus aureus* in nine patients) and 16 patients with streptococci. The expression of *S100A11* gene was significantly higher in staphylococcal IE than in streptococcal IE and patients with excluded IE ($P<0.01$ and $P<0.001$, respectively) (Figure 4, Panel A). Similarly, the serum concentration of S100A11 protein was slightly increased in staphyloccocal IE compared with streptococcal IE and was significantly ($P<0.05$) increased compared to patients with excluded IE (Figure 4, Panel B). Taken together, these results suggested that the determination of S100A11 at both the transcriptional and the protein levels was potentially predictive of IE. S100A11 determination also discriminated between staphylococcal and streptococcal IE.

IE Transcriptional Signature and Major IE-Related Complications

We finally analyzed the modulation of the seven genes determined by qRT-PCR in admission according to IE-related complications including acute heart failure (n=17), embolic events (n=14), and cardiac abscess (n=10). The expression of *AQP9* gene was increased only in patients who experienced acute heart failure ($P<0.05$). The expression of *S100A11*, *PLAUR*, *SLC16A3*, *TGFβ1*, *IFI16*, and *APOBEC3B* genes was not related to acute heart failure, embolic events, and abscess (Figure 5). Taken together, these results suggested that the *AQP9* gene might be a marker of prognosis in IE.

DISCUSSION

The aim of the present study was to characterize the peripheral transcriptional profile of patients with IE and to identify potential biomarkers. The clinical history of IE is dependent on the causative microorganism, the presence or absence of pre-existing cardiac disease, and the mode of presentation. The modified Duke criteria for IE diagnostic have been validated,[12] but they have clear limitations especially when blood cultures and/or echocardiography are negative. Other parameters have been proposed to increase the yield of the diagnostic process, but none has definitely implemented the diagnostic criteria. A small study suggests that serum procalcitonin may be a valuable diagnostic marker in patients with suspected IE.[18] New imaging techniques such as computed tomography (CT),[19] positron emission tomography/CT scan,[20] three-dimensional echocardiography,[21] or systematic cerebral MRI[22] are emerging to improve IE diagnostic but their final place has to be defined. Transcriptional analysis of a disease is a promising method to identify novel biomarkers that might ultimately be translated into clinical practice.[10] In the present study we found that blood transcriptome may be used to characterize IE. We have recently described the valvular transcriptional signature of IE[11] but, to our knowledge, it is the first time that the host response in IE was studied at the blood level, which is more accessible and relevant than valvular tissue in the clinical practice.

The peripheral signature we reported was enriched with cell activation and immune response gene categories as demonstrated by GO and KEGG analyses. In particular, this signature likely reflects the response of circulating monocytes to infectious challenge. First, monocytes are known to play a critical role of in the pathogenesis of IE.[23-26] Indeed, endocardial vegetations have procoagulant monocyte-dependent activity.[27] After thrombus formation on a previously damaged endocardium (non-bacterial vegetation), pathogens that cause IE can colonize endocardium through their ability to bind fibrin, fibronectin and platelet proteins. The subsequent activation of monocytes leads to increased production of tissue

factor and cytokines and thus to the enlargement of vegetations.[27] Second, the functional interactions between modulated genes we found suggest that monocytes acted on IE pathogenesis through the modulation of the TLR signaling pathway. TLRs are membrane-bound receptors that are expressed on monocytes-macrophages and recognize ubiquitous components of Gram-positive or Gram-negative bacteria.[28] TLR ligation induces the production of inflammatory cytokines and the upregulation of costimulatory molecules needed to trigger the adaptative immune response. TLR signals include a MyD88-dependent pathway that leads to the production of inflammatory cytokines with intense activation of NF-κB and MAP kinases and a MyD88-independent pathway that is associated with the regulation of IFN-β and IFN-inducible genes with delayed activation of NF-κB and MAP kinases.[29] Our analysis in functional pathways clearly show that TLR-associated molecules such as NF-κB and MAP kinases were involved in IE as well as inflammatory molecules such as TNF. The inflammatory pathway revealed by blood transcriptomic signature of IE suggest that monocytes from IE samples were close to M1 macrophages.[30]

The transcriptomic signature of IE included the increased expression of *PLAUR* gene, suggesting the role of fibrinolysis in IE pathophysiology. The activation of the host fibrinolytic and proteolytic system by pathogens likely plays an important role in the endocardial damages related to IE.[31] Indeed, we recently demonstrated that the transcriptional signature of valves from patients with IE includes matrix metalloproteinases upregulation,[11] and that increased serum level of matrix metalloproteinase-9 is associated with risk of embolism.[32] Unexpectedly, the network analysis showed that genes involved in endocytosis and intracellular traffic were regulated in IE. Note that, among these genes, Rab5 and Rab11-related genes were upregulated. A recent study demonstrated that Rab5 and Rab11 are required for cell survival in response to toxins secreted by bacteria including *Staphylococcus aureus* and group A and B streptococci.[33]

The present analysis of the peripheral signature of IE also allowed identification of potential candidates for diagnostic and prognostic assessment of IE. We showed that the expression of *S100A11* gene was increased in patients with a final diagnosis of IE compared to patients with an excluded IE diagnosis after an initial suspicion. The increased expression of *S100A11* gene was essentially related to *Staphylococcus* infection. These transcriptional results were in accordance with higher serum concentrations of the S100A11 protein in IE patients. S100A11 is a member of the family of S100 proteins that are localized in the cytoplasm and/or nucleus of a wide range of cells. S100A11 proteins would be involved in endocytosis and exocytosis,[34] regulation of enzyme activity, cell growth regulation, apoptosis and inflammation.[35] Note that endocytosis and inflammation were two hallmarks of the peripheral signature of IE we determined. We suggest that the increased expression of *S100A11* gene offered new perspectives in the diagnostic of IE. This marker should be tested in future prospective studies that will specifically address the question of the role of S100A11 in the diagnosis of IE.

In addition, the expression of *AQP9* gene was clearly increased in IE patients who experienced acute heart failure, suggesting that its determination may be useful to the prognostic of IE. The detection of predictors of acute heart failure is of crucial importance because it can lead to indicate valvular surgery at an early stage of the disease.[36] Despite the identification of echocardiography and biological factors that are associated acute heart failure,[2] this complication remains the first cause of death during IE.[5] This highlights the need of additional markers. AQPs are cell membrane-embedded proteins that facilitate water movements by increasing membrane water permeability and water flux in response to osmotic gradients.[37] AQPs are involved in multiple different pathological process including abnormalities of renal function,[37] myocardial,[38] and brain[39] edema. Interestingly, we previously reported that the *AQP9* gene is overexpressed in valvular tissue of IE patients and

that AQP9 protein is expressed in endothelial cells lining the lumen of neo-vessels.[11] The association between the modulation of *AQP9* gene and acute heart failure may be due to the upregulation of *AQP9* gene in patients with the most severe valvular damages. Patients with fluid retention may also differently express the *AQP9* gene in organs such as lungs and kidneys. These hypotheses offer new perspectives in the prognostic assessment of patients with IE and could have therapeutic implications since patients at high risk of hemodynamic instability are candidates for an early surgical management.[36] It may be useful to extent our results to a large cohort of patients to confirm the clinical relevance of the use of both biomarkers for diagnosis and pronostic of IE.

In summary, we reported for the first time the circulating gene expression profile of IE patients. This peripheral signature enabled to address at least in part the complex pathogenesis of IE. It revealed an enrichment with processes related to cell activation and inflammatory and immune response. The identification of novel candidates such as S100A11 and AQP9 for diagnostic and prognostic assessment likely opened new perpectives for future clinical studies.

FUNDING SOURCES

Franck Thuny was recipient of a grant from the Fédération Francaise de Cardiologie.

DISCLOSURES

None

REFERENCES

1. Hoen B, Alla F, Selton-Suty C, Beguinot I, Bouvet A, Briancon S, Casalta JP, Danchin N, Delahaye F, Etienne J, Le Moing V, Leport C, Mainardi JL, Ruimy R, Vandenesch F. Changing profile of infective endocarditis: results of a 1-year survey in France. *JAMA.* 2002;288:75-81.

2. Habib G, Hoen B, Tornos P, Thuny F, Prendergast B, Vilacosta I, Moreillon P, de Jesus Antunes M, Thilen U, Lekakis J, Lengyel M, Muller L, Naber CK, Nihoyannopoulos P, Moritz A, Zamorano JL, Vahanian A, Auricchio A, Bax J, Ceconi C, Dean V, Filippatos G, Funck-Brentano C, Hobbs R, Kearney P, McDonagh T, McGregor K, Popescu BA, Reiner Z, Sechtem U, Sirnes PA, Tendera M, Vardas P, Widimsky P. Guidelines on the prevention, diagnosis, and treatment of infective endocarditis (new version 2009): the Task Force on the Prevention, Diagnosis, and Treatment of Infective Endocarditis of the European Society of Cardiology (ESC). *Eur Heart J.* 2009;30:2369-2413.

3. Hasbun R, Vikram HR, Barakat LA, Buenconsejo J, Quagliarello VJ. Complicated left-sided native valve endocarditis in adults: risk classification for mortality. *JAMA.* 2003;289:1933-1940.

4. Chu VH, Cabell CH, Benjamin DK, Jr., Kuniholm EF, Fowler VG, Jr., Engemann J, Sexton DJ, Corey GR, Wang A. Early predictors of in-hospital death in infective endocarditis. *Circulation.* 2004;109:1745-1749.

5. Thuny F, Di Salvo G, Belliard O, Avierinos JF, Pergola V, Rosenberg V, Casalta JP, Gouvernet J, Derumeaux G, Iarussi D, Ambrosi P, Calabro R, Riberi A, Collart F, Metras D, Lepidi H, Raoult D, Harle JR, Weiller PJ, Cohen A, Habib G. Risk of embolism and death in infective endocarditis: prognostic value of echocardiography: a prospective multicenter study. *Circulation.* 2005;112:69-75.

6. San Roman JA, Lopez J, Vilacosta I, Luaces M, Sarria C, Revilla A, Ronderos R, Stoermann W, Gomez I, Fernandez-Aviles F. Prognostic stratification of patients with left-sided endocarditis determined at admission. *Am J Med.* 2007;120:369 e361-367.

7. Werner M, Andersson R, Olaison L, Hogevik H. A clinical study of culture-negative endocarditis. *Medicine (Baltimore).* 2003;82:263-273.

8. Evangelista A, Gonzalez-Alujas MT. Echocardiography in infective endocarditis. *Heart.* 2004;90:614-617.

9. Widmer E, Que YA, Entenza JM, Moreillon P. New concepts in the pathophysiology of infective endocarditis. *Curr Infect Dis Rep.* 2006;8:271-279.

10. Mohr S, Liew CC. The peripheral-blood transcriptome: new insights into disease and risk assessment. *Trends Mol Med.* 2007;13:422-432.

11. Benoit M, Thuny F, Le Priol Y, Lepidi H, Bastonero S, Casalta JP, Collart F, Capo C, Raoult D, Mege JL. The transcriptional programme of human heart valves reveals the natural history of infective endocarditis. *PLoS One.* 2010;5:e8939.

12. Li JS, Sexton DJ, Mick N, Nettles R, Fowler VG, Jr., Ryan T, Bashore T, Corey GR. Proposed modifications to the Duke criteria for the diagnosis of infective endocarditis. *Clin Infect Dis.* 2000;30:633-638.

13. Charlson ME, Pompei P, Ales KL, MacKenzie CR. A new method of classifying prognostic comorbidity in longitudinal studies: development and validation. *J Chronic Dis.* 1987;40:373-383.

14. Raoult D, Casalta JP, Richet H, Khan M, Bernit E, Rovery C, Branger S, Gouriet F, Imbert G, Bothello E, Collart F, Habib G. Contribution of systematic serological testing in diagnosis of infective endocarditis. *J Clin Microbiol.* 2005;43:5238-5242.

15. Ben Amara A, Ghigo E, Le Priol Y, Lepolard C, Salcedo SP, Lemichez E, Bretelle F, Capo C, Mege JL. Coxiella burnetii, the agent of Q fever, replicates within trophoblasts and induces a unique transcriptional response. *PLoS One.*5:e15315.

16. Tantibhedhyangkul W, Prachason T, Waywa D, El Filali A, Ghigo E, Thongnoppakhun W, Raoult D, Suputtamongkol Y, Capo C, Chanin Limwongse C, Mege JL. Orientia tsutsugamushi stimulates an original gene expression program in monocytes: relationship with gene expression in patients with scrub typhus. *PLoS Neglect. Trop. Dis.* 2011;in press.

17. Barrett T, Edgar R. Gene expression omnibus: microarray data storage, submission, retrieval, and analysis. *Methods Enzymol.* 2006;411:352-369.

18. Mueller C, Huber P, Laifer G, Mueller B, Perruchoud AP. Procalcitonin and the early diagnosis of infective endocarditis. *Circulation.* 2004;109:1707-1710.

19. Feuchtner GM, Stolzmann P, Dichtl W, Schertler T, Bonatti J, Scheffel H, Mueller S, Plass A, Mueller L, Bartel T, Wolf F, Alkadhi H. Multislice computed tomography in infective endocarditis: comparison with transesophageal echocardiography and intraoperative findings. *J Am Coll Cardiol.* 2009;53:436-444.

20. Van Riet J, Hill EE, Gheysens O, Dymarkowski S, Herregods MC, Herijgers P, Peetermans WE, Mortelmans L. (18)F-FDG PET/CT for early detection of embolism

and metastatic infection in patients with infective endocarditis. *Eur J Nucl Med Mol Imaging.*37:1189-1197.

21. Liu YW, Tsai WC, Lin CC, Hsu CH, Li WT, Lin LJ, Chen JH. Usefulness of real-time three-dimensional echocardiography for diagnosis of infective endocarditis. *Scand Cardiovasc J.* 2009;43:318-323.

22. Duval X, Iung B, Klein I, Brochet E, Thabut G, Arnoult F, Lepage L, Laissy JP, Wolff M, Leport C. Effect of early cerebral magnetic resonance imaging on clinical decisions in infective endocarditis: a prospective study. *Ann Intern Med.*152:497-504.

23. Bancsi MJ, Thompson J, Bertina RM. Stimulation of monocyte tissue factor expression in an in vitro model of bacterial endocarditis. *Infect Immun.* 1994;62:5669-5672.

24. Bancsi MJ, Veltrop MH, Bertina RM, Thompson J. Role of monocytes and bacteria in Staphylococcus epidermidis endocarditis. *Infect Immun.* 1998;66:448-450.

25. Veltrop MH, Beekhuizen H, Thompson J. Bacterial species- and strain-dependent induction of tissue factor in human vascular endothelial cells. *Infect Immun.* 1999;67:6130-6138.

26. Veltrop MH, Bancsi MJ, Bertina RM, Thompson J. Role of monocytes in experimental Staphylococcus aureus endocarditis. *Infect Immun.* 2000;68:4818-4821.

27. Bancsi MJ, Veltrop MH, Bertina RM, Thompson J. Role of phagocytosis in activation of the coagulation system in Streptococcus sanguis endocarditis. *Infect Immun.* 1996;64:5166-5170.

28. Qureshi ST, Medzhitov R. Toll-like receptors and their role in experimental models of microbial infection. *Genes Immun.* 2003;4:87-94.

29. O'Neill LA, Bowie AG. The family of five: TIR-domain-containing adaptors in Toll-like receptor signalling. *Nat Rev Immunol.* 2007;7:353-364.

30. Benoit M, Desnues B, Mege JL. Macrophage polarization in bacterial infections. *J Immunol.* 2008;181:3733-3739.

31. Wong AP, Cortez SL, Baricos WH. Role of plasmin and gelatinase in extracellular matrix degradation by cultured rat mesangial cells. *Am J Physiol.* 1992;263:F1112-1118.

32. Thuny F, Habib G, Le Dolley Y, Canault M, Casalta J, Verdier M, Avierinos J, Raoult D, Mege J, Morange P, Alessi M. Circulating matrix metalloproteinases in infective endocarditis: a possible marker of the embolic risk. *PLoS One.* 2011;6:e18830.

33. Los FC, Kao CY, Smitham J, McDonald KL, Ha C, Peixoto CA, Aroian RV. RAB-5- and RAB-11-dependent vesicle-trafficking pathways are required for plasma membrane repair after attack by bacterial pore-forming toxin. *Cell Host Microbe.* 2011;9:147-157.

34. Seemann J, Weber K, Gerke V. Annexin I targets S100C to early endosomes. *FEBS Lett.* 1997;413:185-190.

35. He H, Li J, Weng S, Li M, Yu Y. S100A11: diverse function and pathology corresponding to different target proteins. *Cell Biochem Biophys.* 2009;55:117-126.

36. Thuny F, Beurtheret S, Mancini J, Gariboldi V, Casalta JP, Riberi A, Giorgi R, Gouriet F, Tafanelli L, Avierinos JF, Renard S, Collart F, Raoult D, Habib G. The timing of surgery influences mortality and morbidity in adults with severe complicated infective endocarditis: a propensity analysis. *Eur Heart J.* 2009. *doi: 10.1093/eurheartj/ehp089*

37. Agre P, Kozono D. Aquaporin water channels: molecular mechanisms for human diseases. *FEBS Lett.* 2003;555:72-78.

38. King LS, Kozono D, Agre P. From structure to disease: the evolving tale of aquaporin biology. *Nat Rev Mol Cell Biol.* 2004;5:687-698.

39. Badaut J. Aquaglyceroporin 9 in brain pathologies. *Neuroscience.* 2010;168:1047-1057.

TABLES

Table 1. Characteristics of patients according to the final diagnosis

	IE group (n=39)	Excluded IE group (n=10)	*P* Value
Age, mean ±SD, years	58 ±18	63 ±15	0.42
Sex ratio (M/F)	30/9	7/3	0.65
Intravenous drug user	5 (13%)	0 (0%)	0.57
Cancer	3 (8%)	1 (10%)	1.0
Diabete	5 (13%)	1 (10%)	1.0
Comorbidity index >2	15 (38%)	3 (30%)	0.72
Fever, temperature >38°C	38 (97%)	7 (70%)	0.02
Vascular phenomena*	14 (36%)	1 (10%)	0.15
Immunologic phenomena†	0 (0%)	0 (0%)	NA
Heart failure	16 (41%)	5 (50%)	0.72
Serum creatinine >20mg/L	3 (8%)	1 (10%)	1.0
Valve localization of abnormality			1.0
Aortic	17 (44%)	4 (40%)	
Mitral	23 (59%)	6 (60%)	
Right valves	3 (8%)	0 (0%)	
Severe valvular regurgitation	32 (82%)	7 (70%)	0.41
Vegetation	32 (82%)	0 (0%)	<0.001
Abscess	10 (26%)	0 (0%)	<0.001
Blood cultures			<0.001
Streptococci‡	27 (69%)	0 (0%)	
Staphylococci§	12 (31%)	1 (10%)	
Negative	0 (0%)	9 (90%)	
C reactive protein, mean ±SD, $x10^9$/L	147 ±102	9 ±9	<0.001

NA=not applicable
*Including arterial emboli, septic pulmonary infarcts, mycotic aneurysms, intracranial hemorrhages, conjunctival hemorrhages, and Janeway's lesions.
†Including glomerulonephritis, Osler's nodes, Roth's spots, and rheumatoid factor
‡Including three enterococci
§Including nine *Staphylococcus aureus*

Table 2: Gene Ontology (GO) Analysis of Genes in IE

	GOBP identity	*P* value	Odds Ratio	Exp Count	Count	Size	Term
Upregulated							
	GO:0033036	<0.0001	1.78	181	276	1219	macromolecule localization
	GO:0043687	<0.0001	1.65	219	314	1472	post-translational protein modification
	GO:0023034	<0.0001	1.65	219	314	1473	intracellular signaling pathway
	GO:0007249	<0.0001	3.07	26	60	174	I-kappaB kinase/NF-kappaB cascade
	GO:0016567	<0.0001	2.14	42	76	283	protein ubiquitination
	GO:0030163	<0.0001	1.89	57	93	381	protein catabolic process
	GO:0006955	<0.0001	1.55	102	143	685	immune response
	GO:0006897	<0.0001	1.86	40	65	268	endocytosis
	GO:0045087	<0.0001	1.95	31	52	206	innate immune response
	GO:0016570	<0.0001	2.09	24	42	158	histone modification
	GO:0009615	<0.0001	2.09	23	41	154	response to virus
Downregulated							
	GO:0043487	0.001	5.12	2	8	27	regulation of RNA stability
	GO:0010467	0.001	1.26	273	317	3570	gene expression
	GO:0006816	0.001	2.00	15	27	192	calcium ion transport
	GO:0031327	0.002	1.50	47	66	610	negative regulation of cellular biosynthetic process
	GO:0042127	0.003	1.42	64	86	837	regulation of cell proliferation
	GO:0048731	0.004	1.24	189	221	2470	system development

GOPB = gene ontology biological process

Table 3: KEGG Analysis of Genes in IE

	KEGG identity	*P* value	Odds Ratio	Exp Count	Count	Size	Term
Upregulated							
	4666	<0.0001	3.34	14	34	88	Fc gamma R-mediated phagocytosis
	4144	<0.0001	1.84	32	51	198	Endocytosis
	4650	0.001	2.01	20	34	123	Natural killer cell mediated cytotoxicity
	4920	0.001	2.39	11	21	67	Adipocytokine signaling pathway
	4115	0.002	2.34	11	21	68	p53 signaling pathway
	4620	0.008	1.87	15	25	95	Toll-like receptor signaling pathway
Downregulated							
	790	0.005	7.58	1	4	11	Folate biosynthesis
	3040	0.006	2.14	9	17	124	Spliceosome
	4020	0.006	1.92	13	22	177	Calcium signaling pathway

GOPB = gene ontology biological process

Figure 1. Microarray analysis of patients with IE

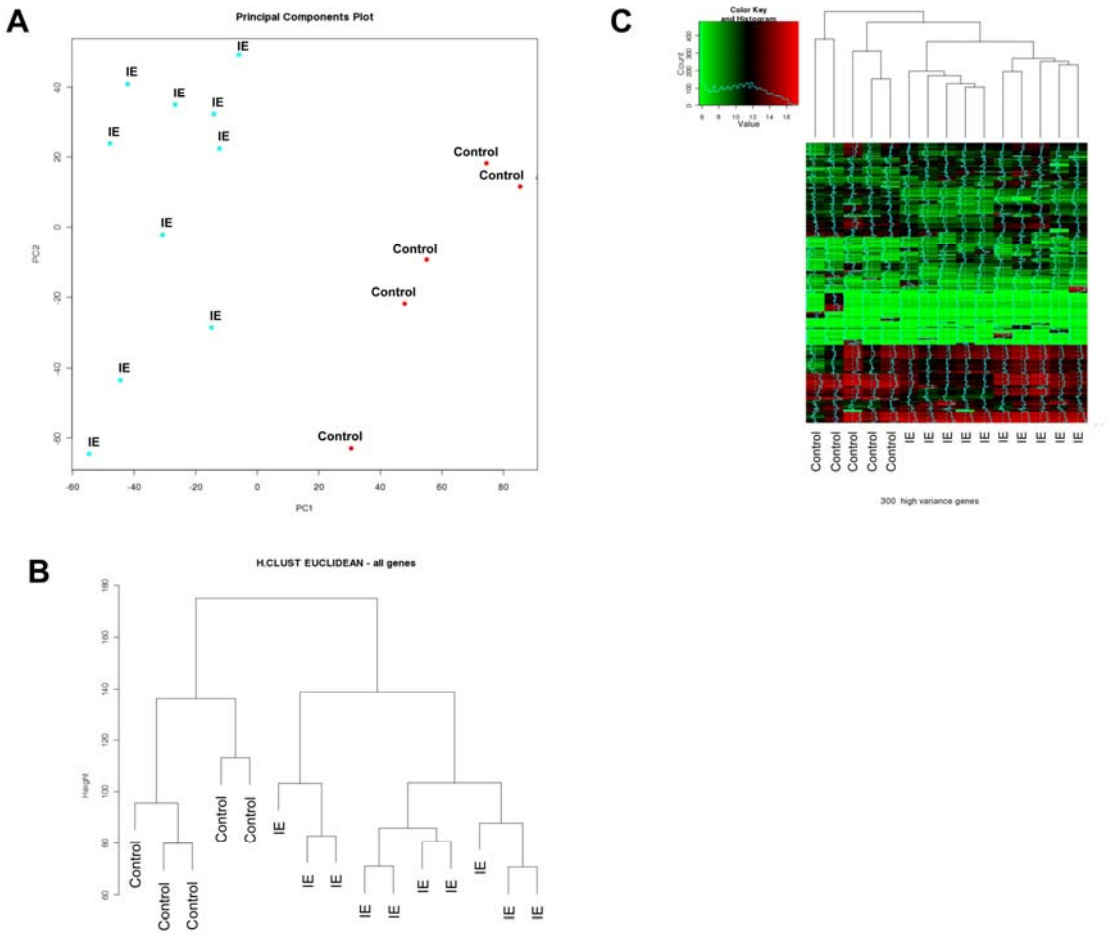

A, Principal component analysis of patients with IE. A scatterplot of the first two principal components demonstrated a general separation of IE patients and controls along the first principal component (PC1). **B,** Euclidean clustering from all gene probes. The modulated genes in IE patients and controls were distributed on two different clusters. **C,** Hierarchical clustering analysis of transcriptional profile of patients. The hierarchical clustering of the 300 genes the most modulated is shown, with a color gradient (Z-score) from green (downregulation) to red (upregulation). The transcriptional profiles of IE patients were organized in a common cluster placed on a branch distinct from that of healthy controls.

Figure 2. Gene networks

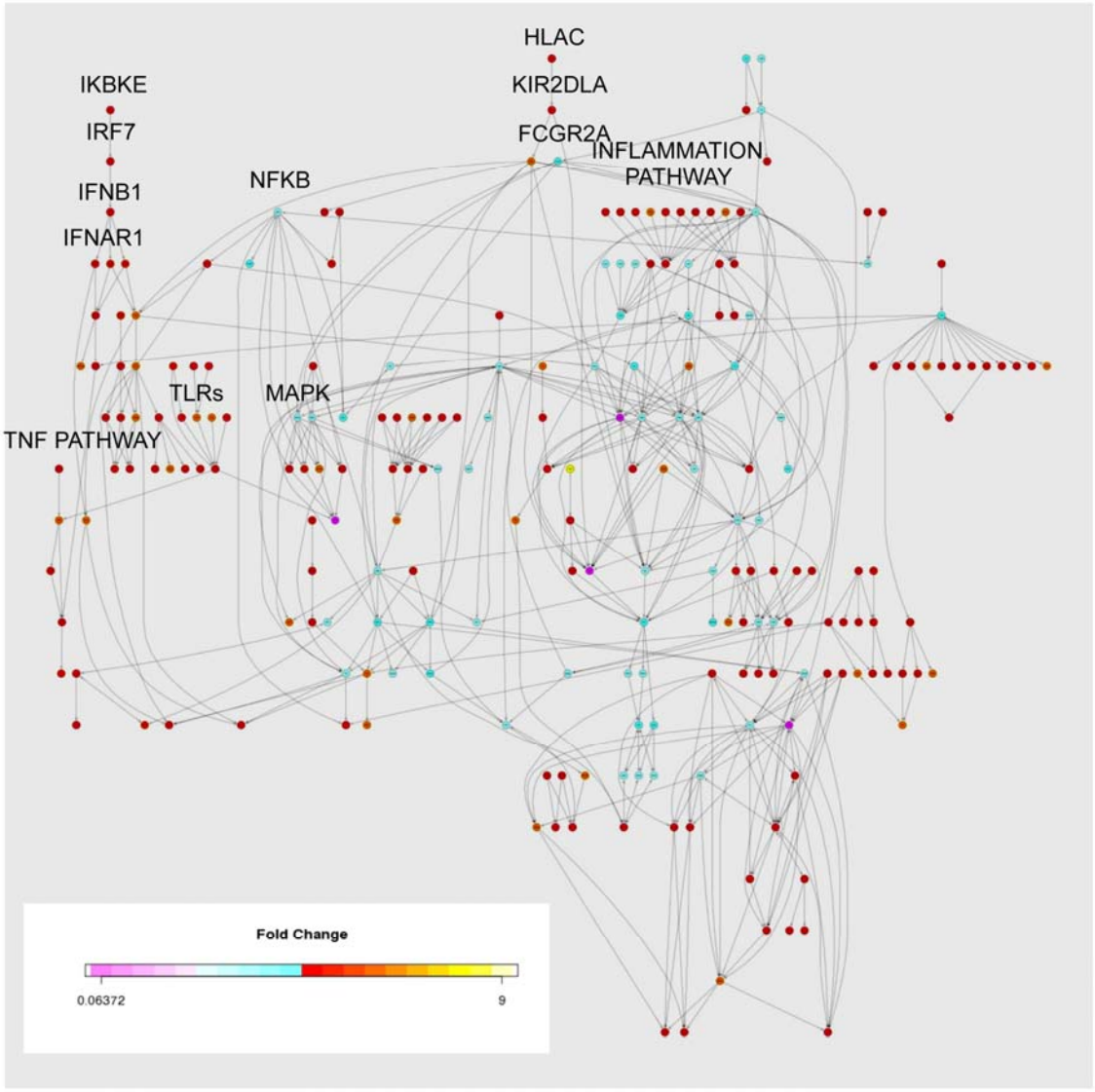

The peripheral signatures of IE patients and healthy controls were analyzed according gene networks. In IE, a complex and dense network consisted of pathways related to innate immune and inflammatory responses. These pathways consisted of TLR, IRF7 and type 1 interferon, MAP kinase and NF-κB pathways. HLAC and KIR2DL4 genes were associated with a subnetwork of inflammatory genes, suggesting the involvement of natural killer cells in IE.

Figure 3. Analysis of genes modulation using qRT-PCR

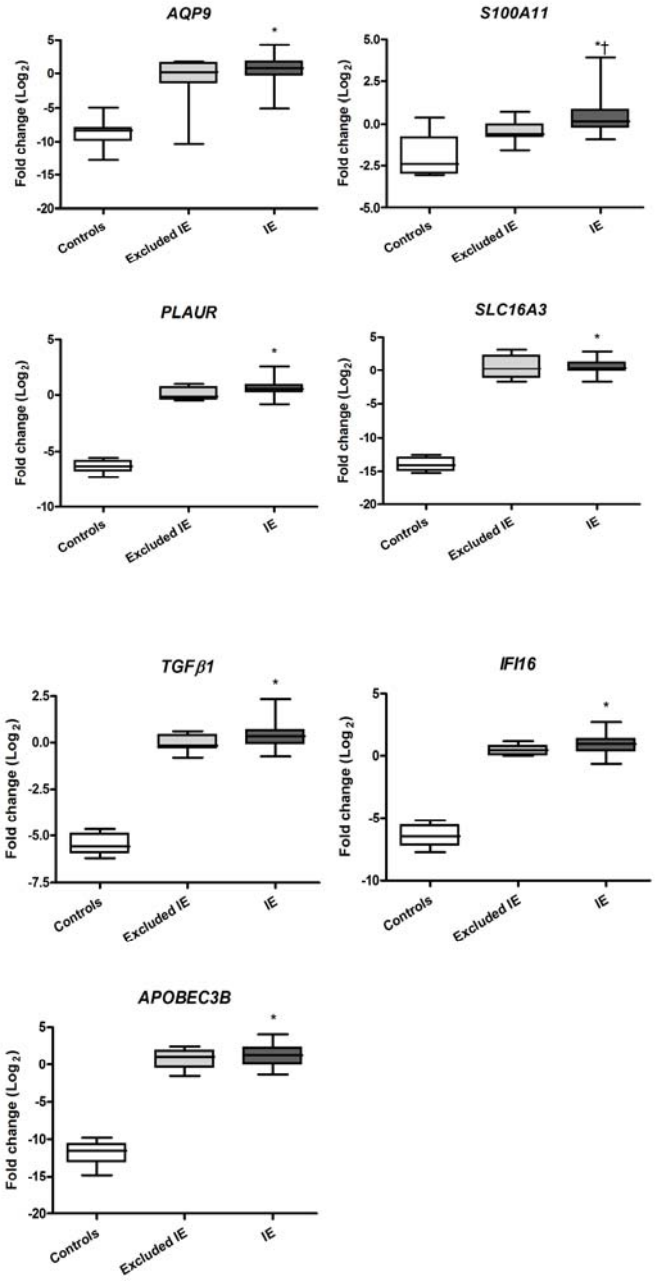

Blood samples from 39 patients with IE, 10 patients with excluded IE after an initial suspicion, and 10 controls were analyzed by qRT-PCR for the expression of seven genes found upregulated by microarray. Results were normalized with the β-actin gene.

**P*<0.001 for the comparison between IE patients and controls.

†*P*<0.05 for the comparison between IE patients and patients with excluded IE.

Figure 4. Expression of *S100A11* gene and S100A11 protein

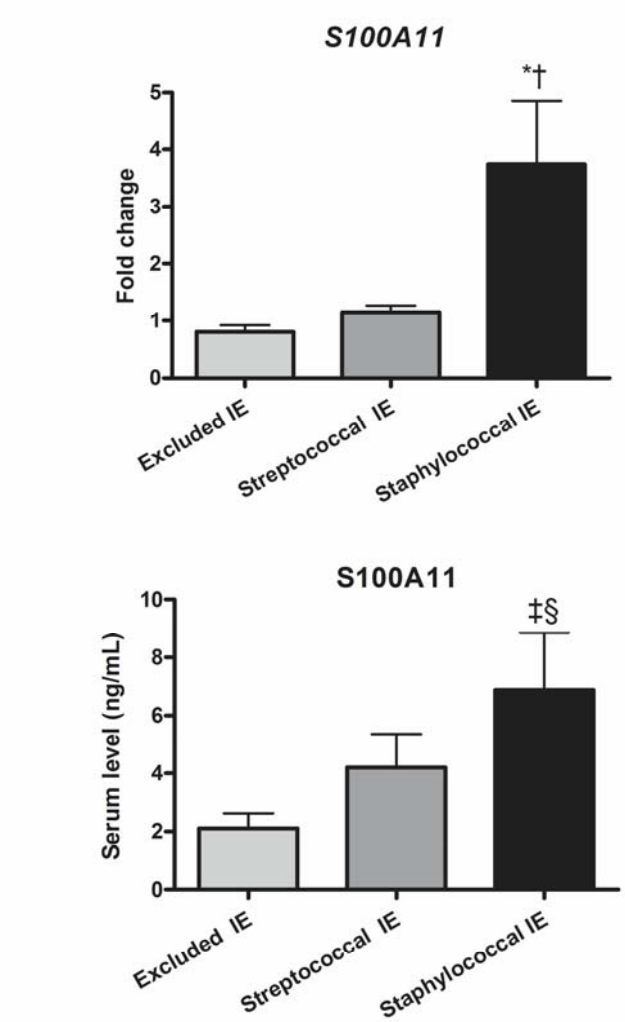

A, *S100A11* gene was significantly overexpressed in the group of IE patients compared with the group of excluded IE patients ($P<0.05$).

*$P<0.001$ for the comparison between staphylococcal IE and excluded IE.

†$P<0.01$ for the comparison between staphylococcal IE and streptococcal IE.

B, S100A11 serum level was higher in staphylococcal IE (6.9 ± 2.0 ng/mL) than in excluded IE (2.1 ± 0.5 μg/mL) and staphylococcal IE (4.2 ± 1.2 ng/mL).

‡$P<0.05$ for the comparison between staphylococcal IE and excluded IE.

§$P=0.17$ for the comparison between staphylococcal IE and streptococcal IE.

Figure 5. Genes expression according to the major IE-related complications

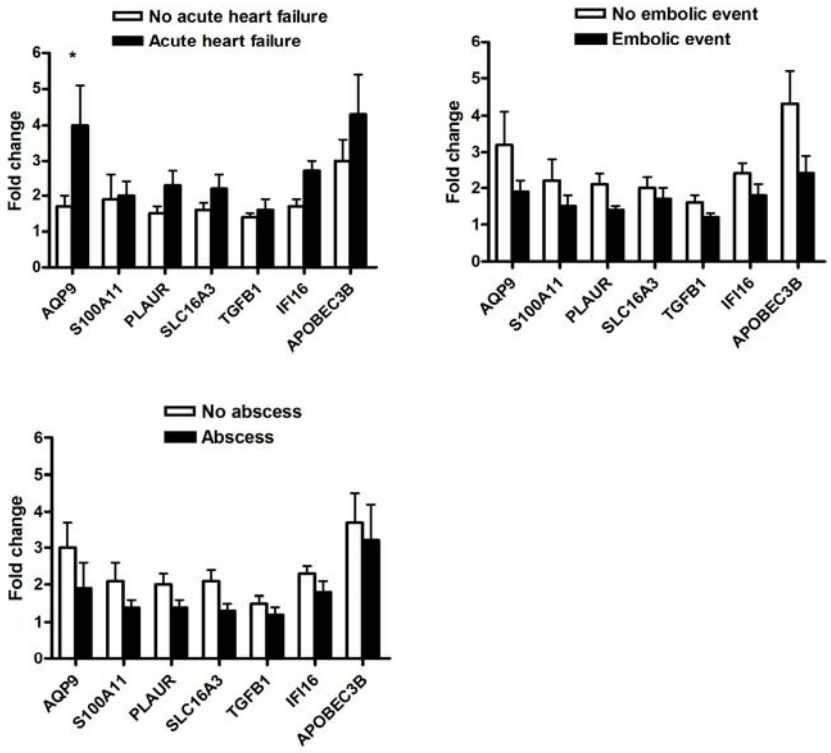

A, The expression of *AQP9* gene was significantly increased only in patients who experienced acute heart failure.

B and C, The expression of *S100A11*, *PLAUR*, *SLC16A3*, *TGFβ1*, *IFI16*, and *APOBEC3B* genes was not related to acute heart failure, embolic events, and abscess.

*$P<0.05$.

DATA SUPPLEMENT.

Data supplement file 1. List of primers

Primers	Sequences
AQP9 left	agaccctcattgtctgggtcta
AQP9 right	gaaaagactgagccagaggaaa
S100A11 left	tgaagaaactggacaccaacag
S100A11 right	tgtggagatgatgacagaaagg
APOBEC3B left	acttggctgtgctatgaagtga
APOBEC3B right	aaccaggtgatctggaaacact
PLAUR V2 right	ctgaaacatctggggctctatc
PLAUR V1 right	gggtggttacagccacttttag
PLAUR V1 left	tgctcctctgaagagactttcc
PLAUR V2 left	tgctcctctgaagagactttcc
PLAUR V3 right	gggtggttacagccacttttag
PLAUR V3 left	gaagaagtcctggagcttgaaa
IFI16 left	gctgaccgaaacatggagat
IFI16 right	tcaaacaccccattcacaaa
SLC16A3 V1 left	ctatgctcaaggacctggaaac
SLC16A3 V1 right	gaaaccgttggtcctaacactc
SLC16A3 V2 left	ctatgctcaaggacctggaaac
SLC16A3 V2 right	gaaaccgttggtcctaacactc
SLC16A3 V3 left	ctatgctcaaggacctggaaac
SLC16A3 V3 right	gaaaccgttggtcctaacactc
TGFβ1 left	ctcgccagagtggttatctttt
TGFβ1 right	tgaagcaatagttggtgtccag

Data supplement file 2. Additional gene networks involved in infective endocarditis.

These networks include endocytosis (5 SEC-related genes), ubiquitination (4 ubiquitin-conjugating enzymes and 2 related genes) and intracellular traffic (5 Rab11-related genes, 2 Rab5 isoforms and 3 related genes)

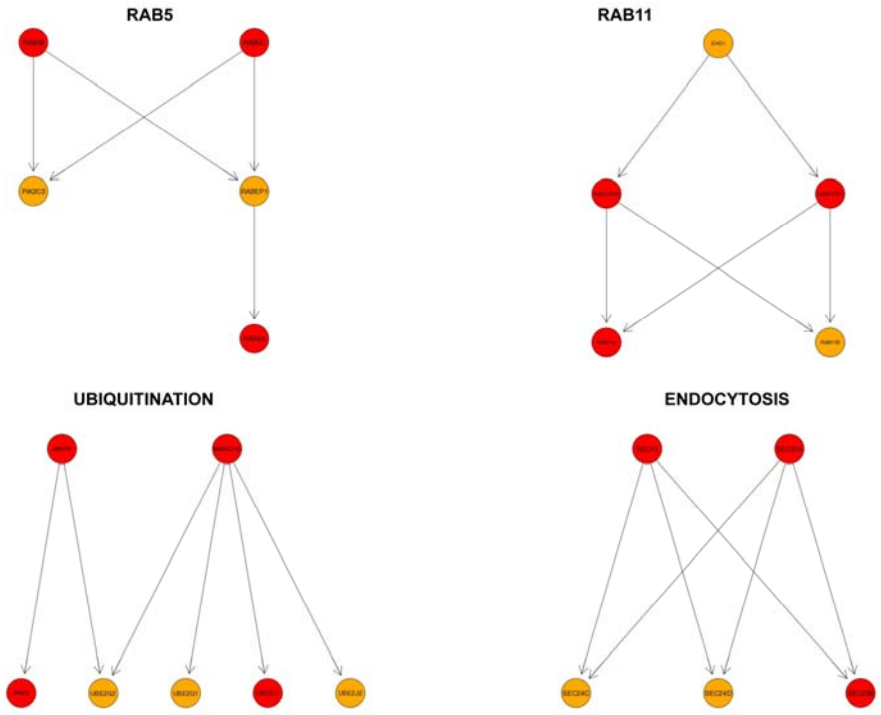

ANNEXE 3

Global analysis of circulating immune cells by matrix-assisted laser desorption ionization time-of-flight mass spectrometry

Richard Ouedraogo, Christophe Flaudrops, Amira Ben Amara,

Christian Capo, Didier Raoult, Jean-Louis Mege

PLoS One 2010, 5: e13691

La spectrométrie de masse est une technique physique d'analyse permettant de détecter et d'identifier des molécules d'intérêt par mesure de leur masse. Son consiste en la séparation en phase gazeuse de molécules chargées (ions) en fonction de leur rapport masse/charge (*m/z*). En fragmentant les molécules elle permet en outre de caractériser leur structure chimique. Son utilisation, facile, rapide et peu coûteuse, s'est largement répandue dans de nombreux domaines, y compris en biologie. C'est ainsi que, associée à d'autres approches, la spectrométrie de masse permet l'étude du protéome. Etendue récemment à la médecine, elle permet d'étudier des mélanges complexes de protéines tels qu'on les trouve dans le sérum des malades, ce qui pourrait être utile au diagnostic de différentes maladies. La spectrométrie de masse sous sa variante MALDI-TOF (*matrix-assisted laser desorption ionization-time-of-flight*) est récemment entrée dans les laboratoires de microbiologie puisqu'elle permet la détection des toxines bactériennes, d'identifier et de classifier différents types bactériens en utilisant des bactéries intactes. C'est ainsi que la comparaison de leurs spectres permet d'identifier différentes espèces et sous-espèces bactériennes. Enfin, il est devenu possible d'identifier un grand nombre d'espèces bactériennes dans des prélèvements cliniques en utilisant des banques de données fabriquées à partir de chacune de ces espèces.

C'est essentiellement le constat qu'il est possible d'identifier des espèces bactériennes en spectrométrie de masse MALDI-TOF qui a inspiré notre démarche consistant à utiliser cette approche pour identifier différents types de cellules eucaryotes, en particulier les cellules de la réponse immune. Différentes tentatives avaient été effectuées dans le passé mais la plupart partaient d'extraits cellulaires obtenus après extraction par divers solvents organiques (Karger *et al.*, J Virol Methods 2010, 164:116-121). C'est dans le même esprit qu'un article avait comparé trois lignées

cellulaires (K562, BHK et GM15226) après extraction des protéines par différents bains dans la solution de MALDI (Zhang et al., J Am Soc Mass Spectrom 2006, 17:490-499 et ce n'est que de façon incidente que l'on pouvait penser que la méthode de spectrométrie de masse MALDI-TOF pouvait être utilisée sur cellules entières. Enfin, il semble possible de caractériser grâce à cette technique de spectrométrie de masse MALDI-TOF des spores de différentes espèces de *Penicillium* (Chen & Chen, Rapid Commun Mass Spectrom 2005, 19 :3564-3568).

Dans ce papier, nous avons montré que les spectres de monocytes vivants ou congelés pendant 48 heures sont identiques en dehors de toute préparation ou extraction, ce qui a permis d'utiliser dans la suite du travail des cellules congelées. Les spectres en spectrométrie de masse MALDI-TOF des monocytes, des lymphocytes et des polynucléaires présents dans le sang sont spécifiques de ces trois types de cellules. Nous avons étendu à une vingtaine de types cellulaires cette observation que les spectres sont spécifiques de chaque type cellulaire. Ces types cellulaires incluaient des cellules primaires et des cellules en lignée, différents types de macrophages ou de cellules différenciées à partir des mêmes cellules d'origine (macrophages et cellules dendritiques différenciées à partir de monocytes). Il est à signaler que nous avons inclus à titre de contrôles des cellules d'amibes et de xénope et que celles-ci ont des spectres très largement différents de ceux des cellules eucaryotes. Notre approche permet ainsi d'établir une banque de données qu'il est possible d'étendre à un grand nombre de types cellulaires. Nous avons alors testé la fiabilité de notre banque de données en mesurant la reproductibilité des spectres considérés comme spécifiques d'une population cellulaire donnée (ici, les monocytes, les lymphocytes et les polynucléaires) au sein d'une population contenant en proportion variable ces types cellulaires. C'est ainsi qu'il est possible d'identifier la signature des monocytes et des lymphocytes T au sein des PBMCs.

En résumé, la méthode que nous avons mise au point est facile d'utilisation ; elle est également rapide et ne demande aucun apport extérieur (de type anticorps), ce qui lui permet d'être utilisable hors tout présupposé. C'est la raison pour laquelle elle fait l'objet d'un dépôt de brevet. Elle pourrait être étendue à l'étude de la composition cellulaire des tissus et elle est en cours d'évaluation pour l'étude de l'état d'activation des cellules immunes (stimulation des macrophages par différents agonistes tels que ceux induisant une polarisation M1 ou M2).

OPEN ACCESS Freely available online

PLoS one

Global Analysis of Circulating Immune Cells by Matrix-Assisted Laser Desorption Ionization Time-of-Flight Mass Spectrometry

Richard Ouedraogo, Christophe Flaudrops, Amira Ben Amara, Christian Capo, Didier Raoult, Jean-Louis Mege*

Unité de Recherche sur les Maladies Infectieuses Tropicales et Emergentes, Centre National de la Recherche Scientifique - Institut de Recherche pour le Développement Unité Mixte de Recherche 6236, Université de la Méditerranée, Faculté de Médecine, Marseille, France

Abstract

Background: MALDI-TOF mass spectrometry is currently used in microbiological diagnosis to characterize bacterial populations. Our aim was to determine whether this technique could be applied to intact eukaryotic cells, and in particular, to cells involved in the immune response.

Methodology/Principal Findings: A comparison of frozen monocytes, T lymphocytes and polymorphonuclear leukocytes revealed specific peak profiles. We also found that twenty cell types had specific profiles, permitting the establishment of a cell database. The circulating immune cells, namely monocytes, T lymphocytes and polymorphonuclear cells, were distinct from tissue immune cells such as monocyte-derived macrophages and dendritic cells. In addition, MALDI-TOF mass spectrometry was valuable to easily identify the signatures of monocytes and T lymphocytes in peripheral mononuclear cells.

Conclusions/Significance: This method was rapid and easy to perform, and unlike flow cytometry, it did not require any additional components such as specific antibodies. The MALDI-TOF mass spectrometry approach could be extended to analyze the cell composition of tissues and the activation state of immune cells.

Citation: Ouedraogo R, Flaudrops C, Ben Amara A, Capo C, Raoult D, et al. (2010) Global Analysis of Circulating Immune Cells by Matrix-Assisted Laser Desorption Ionization Time-of-Flight Mass Spectrometry. PLoS ONE 5(10): e13691. doi:10.1371/journal.pone.0013691

Editor: Laurent Rénia, BMSI-A*STAR, Singapore

Received July 15, 2010; **Accepted** September 30, 2010; **Published** October 27, 2010

Funding: This work was supported by the Centre National de la Recherche Scientifique and Assistance Publique - Hôpitaux de Marseille. The funders had no role in study design, data collection and analysis, decision to publish or preparation of the manuscript.

Competing Interests: The authors have declared that no competing interests exist.

* E-mail: Jean-Louis.Mege@univmed.fr

Introduction

Immune cells are characterized by specific morphologies and functions, which can be used to identify different immune cell types. This is illustrated by the use of flow cytometry to identify immune cell populations based on the recognition of increasing numbers of membrane antigens by specific antibodies. This method has been widely applied in the fields of immunology and hematology. The development of systems biology approaches (such as transcriptomics) has enabled cell subsets to be identified through their characteristic transcriptional signatures. For example, it has been recently reported that circulating lymphocytes and polymorphonuclear cells (PMNs) exhibit gene expression signatures reflecting the enrichment of genes encoding specific surface proteins that can be used as biomarkers for estimating the abundance of these cell types within complex tissues [1]. This approach enables discrimination between cells in the same lineage but at different stages and between cells that have differentiated, such as the differentiation of human monocytes into macrophages or dendritic cells (DCs) [2]. However, changes in mRNA levels do not necessarily reflect the altered expression of proteins [3]. A proteomic approach that analyzes signatures based on protein expression would provide a robust method with power similar to that of the transcriptomic approach.

Mass spectrometry (MS) is a key tool in cell proteomics [4–6]. This technique, based on mass determination [7], is currently used to identify proteins, their amino-acid sequences and their post-translational modifications [8,9]. This method can also be used for the identification and sequencing of DNA, RNA and sugars [9,10]. MALDI-TOF (matrix-associated laser desorption ionization/time of flight) MS is used to identify unknown protein or peptide sequences in fractionated cells [9]. Coupled with two-dimensional gels, MALDI-TOF MS can be used to create proteomic maps of cell types such as macrophages [4] and of intracellular compartments [11]. MALDI-TOF MS has been recently introduced into microbiology laboratories to identify [12,13] and classify bacterial species using intact bacteria [14,15]. In 2008 a large number of bacterial species present in clinical specimens were identified using databases established from isolated species [16,17]. In 2006, MALDI-TOF MS has been applied to mammalian cells from three cell lines after lysis in 2,5-dihydroxybenzoic acid matrix solution. In these conditions, it has been possible to discriminate the different mammalian lines [18]. Recently, MALDI-TOF MS has been applied to eukaryotic cell

lines to provide rapid characterization of cultured cells. However, the method used to analyze these cultured cells involved two steps of ethanol inactivation and formic acid/acetonitrile extraction [19]. To our knowledge, MALDI-TOF MS has not yet been directly applied to intact eukaryotic cells.

Our objective was to determine whether intact immune cells exhibited reproducible and specific signatures in MALDI-TOF MS. We found that this approach was useful for discriminating between immune cells. For example, circulating T lymphocytes, monocytes and PMNs as well as monocyte-derived macrophages and DCs all exhibited distinct spectra. We describe the first elements of a database that will be useful for studying cell subsets in tissues and possibly their activation state.

Methods

Ethics Statement

Healthy human placentas were collected after informed and written consent obtained from each subject, and the study was approved by the Ethics Committee of the Université de la Méditerranée, Marseille, France.

Human primary cells

Peripheral blood mononuclear cells (PBMCs) from healthy donors were isolated from leukopacks (Etablissement Français du Sang) by Ficoll gradient (MSL, Eurobio) and suspended in RPMI 1640 containing 20 mM HEPES (Invitrogen), as previously described [20]. Monocytes and T lymphocytes were isolated using CD14 and CD3 MicroBeads, respectively, and the MACS separation system (Miltenyi Biotec) according to the manufacturer's protocol. Monocytes were cultured for seven days in RPMI 1640 containing 10% human AB serum, 2 mM L-glutamine, 100 UI/mL penicillin and 100 µg/mL streptomycin to obtain monocyte-derived macrophages (MDMs), as previously described [21]. More than 90% of cells were macrophages as assessed by flow cytometry using CD68 as a specific marker. To obtain dendritic cells (DCs), monocytes were treated with 1,000 U/ml of human recombinant granulocyte macrophage-colony stimulating factor (Peprotech Inc.) and 500 U/ml of human recombinant interleukin 4 (Tebu-Bio) in RPMI 1640 containing 10% fetal calf serum (FCS), L-glutamine and antibiotics for seven days. The cells obtained expressed high levels of CD11c and CD1a, and low levels of CD14 and CD68. PMNs obtained after Ficoll gradient were prepared by sedimentation of red blood cells (RBCs) with 1.5% (w/v) dextran T500 (Pharmacosmos), as previously described [22]. Cell supernatants were centrifuged at 700× *g*, and a hypotonic shock of 30 s was applied to cell pellets to remove contaminating RBCs; more than 98% of the cells were PMNs. RBCs were diluted and suspended in RPMI 1640 containing 20 mM HEPES before use.

Human placentas were collected, and small pieces were rinsed several times and digested in Hank's balanced salt solution containing DNase I (Sigma-Aldrich, 300 units/mL) and 2.5% trypsin (Invitrogen) for 2×45 min, as previously described [23]. Isolated cells were filtered and centrifuged at 1,200× *g* on 25–60% Percoll gradients (GE Healthcare). Cells present at the interface were subjected to positive selection using MicroBeads coupled with rat anti-mouse IgG2 antibodies (Miltenyi Biotec) and mouse antibodies directed against epidermal growth factor receptor (Santa Cruz Biotechnology), a specific marker of trophoblasts. Primary trophoblasts were cultured in Dulbecco's Minimum Eagle's Medium (DMEM)-F12-Ham containing 10% FCS and antibiotics.

Mouse primary cells

Bone marrow-derived macrophages (BMDMs) were generated from six- to eight-week-old C57BL/6 mice killed by cervical dislocation, as previously described [24]. In brief, the bone marrow was flushed out from femurs and tibias in DMEM supplemented with 10% FCS, 2 mM L-glutamine and antibiotics. Cells were cultured in DMEM supplemented with 10% FCS, L-glutamine, antibiotics and 15% L929 cell supernatant rich in granulocyte macrophage-colony stimulating factor for seven days.

Cell lines

The human monocytic leukemia cell line THP1 (ATCC N° TIB-202) and the murine J774 (ATCC N° TIB-67) and canine DH82 (ATCC N° CRL-10389) macrophage cell lines were cultured in RPMI 1640 containing 10% FCS, L-glutamine and antibiotics. The human T cell leukemia cell line C8166 that stably expresses the CCR5 chemokine receptor [25] was kindly provided by Dr. G. Querat (Marseille). Murine L929 (ATCC N° CCL-1) is a fibroblastic-like cell line. The epithelial cells used were human HeLa (ATCC N° CCL-2) cells and 293T cells (ATCC N° CRL-1573). Fibroblast-like cells and epithelial cells were cultured in DMEM containing 10% FCS, L-glutamine and antibiotics. The human BeWo and JEG trophoblast cell lines were obtained from ATCC (N° CCL-98 and HTB-36, respectively) and were cultured in DMEM F-12 Ham medium in the same way as primary trophoblasts (Invitrogen). Confluent monolayers were trypsinized twice a week and used for a maximum of five passages.

Non-mammalian cells

The XTC-2 cell line, derived from *Xenopus laevis*, was cultured in Leibowitz-15 medium containing L-glutamine, amino-acids, 5% FCS and 2% tryptose phosphate (Invitrogen) at 28°C, as previously described [26]. Amoebae including *Acanthamoeba polyphaga* (ATCC N° 30461), *Acanthamoeba castellanii* (ATCC N° 30234), *Hartmannella vermiformis* (ATCC N° 50237) and *Poteriochromonas melhamensis* (ATCC N° 11532) were grown in peptone yeast-extract glucose (PYG) medium consisting of 20 g/L roteosepeptone, 1 g/L yeast extract, 1 g/L sodium citrate, 4 µM $MgSO_4$, 0.4 µM $CaCl_2$, 2.5 µM Na_2HPO_4, 2.5 µM KH_2PO_4, 5 µM $(NH_4)_2FeII(SO_4)_2$, and 0.1 M glucose for three days at 32°C, as previously described [27]. Harvested amoebae were washed twice in Page's amoeba saline (PAS) to remove most nutrients and diluted in sterile PBS.

MALDI-TOF MS

Primary cells and cell lines were obtained from at least ten different isolation procedures, and MALDI-TOF MS was performed at least in duplicate on each cell isolate. Isolated cells (10^6 cells per assay) were centrifuged at 300× *g* for 5 min, washed in sterile PBS without Ca^{2+} or Mg^{2+}, and again centrifuged to remove medium traces. Cell pellets were collected in 10 µL of sterile PBS without Ca^{2+} or Mg^{2+} and were frozen at −80°C for 2–3 days before analysis. When monocytes (10^6 cells) and T lymphocytes (10^6 cells) were mixed, cell pellets were collected in 20 µL of PBS. In some experiments, human monocytes were lysed with a RIPA buffer containing 25 mM Tris, 750 mM NaCl, 5% TritonX-100 (Sigma-Aldrich), 25 mM $MgCl_2$, 5 mM EDTA and 0.5% sodium dodecyl sulfate, or they were sonicated in the presence of complete protease inhibitor cocktail tablets (Roche Applied Science). MALDI-TOF MS was performed using an AutoflexII mass spectrometer and FlexControl software (Bruker Daltonics), as previously described [13,28]. In brief, after samples

were thawed, 1 µl was deposited on the MALDI target in which 1 µl of acid-α-cyano-4 hydroxy-cynnamic (HCCA) matrix was added. This matrix consisted of a 10 mg/mL solution of HCCA diluted in 50% acetonitrile and 25% Milli-Q grade water containing 10% trifluoroacetic acid. The evaporation that gradually took place at room temperature allowed the formation of HCCA crystals containing the dispersed samples. The crystals were illuminated with a nitrogen laser (337 nm, 3 ns pulse width), and released ions were extracted with an accelerating voltage of 20 kV in linear mode, and extraction delay times varied from 280 to 320 ns depending on the chosen mass range (m/z range of 2000–20,000). Each spectrum resulted from the sum of positive ions obtained after 525 laser shots performed in seven different regions of the analyzed sample. A signal-to-noise ratio of 3 was selected to define peaks, with a maximum of 100 peaks per spectrum.

Spectrum analysis and database acquisition

The ClinProTools version 2.2 software (Bruker Daltonics) was used to analyze the variability between samples from different blood donors. The Gel View representation displays two types of spectra arranged in a pseudo-gel format. The 2D Peak Distribution View automatically selects two peaks, and their relative intensities are expressed as a 2D representation. The Biotyper version 2.0 (Bruker Daltonics) software was used to create an averaged spectrum for each cell type corresponding to at least 20 individual spectra obtained from at least ten different cell cultures tested in duplicate. Baselines were automatically subtracted from spectra, and the background noise was smoothed during acquisition through the FlexControl software. This reference was validated by other samples from the same cell type. The Biotyper software realigns acquired spectra from each cell type and automatically creates an average spectrum using default Biotyper software settings provided by the manufacturer. These settings were the same than those used in routine bacteriology [13]. Briefly, the sensitivity or the maximum tolerated error on the values of mass spectra and spectrum shift was 8000 particles per million. The minimum frequency to benchmark selection of peaks was 25%, and only peaks with a signal/noise intensity above background were selected by the software. The cell-type reference consisting of 70 peaks was added to the database. The Biotyper software was also used to identify unknown spectra by comparison with reference spectra, as recently described for the identification and classification of microorganisms [13]. We used the score values proposed by the manufacturer for microorganisms: values between 0.000 and 1.699 did not allow reliable cell identification; values between 1.700 and 1.999 allowed probable cell identification; scores higher than 2.0 were considered statistically significant and allowed the confident identification of different cell species. Finally, we used Multiexperiment Viewer (MeV) version 4.3 software (http://www.tm4.org/) to perform hierarchical clustering with dendrogram representations of collected MALDI-TOF MS data. The mass values of peaks (with an area equal or greater than to 20) of the reference spectrum of each cell type were selected

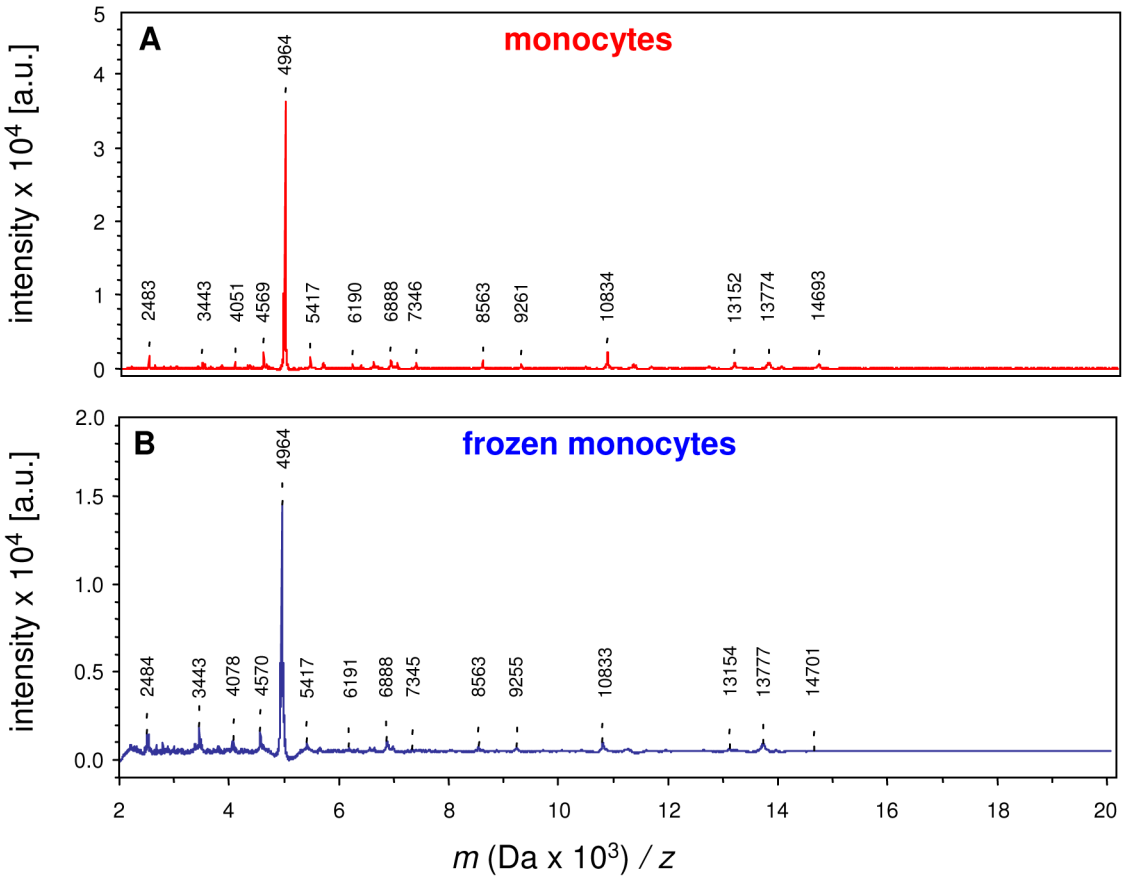

Figure 1. MALDI-TOF MS spectra of monocytes. Human monocytes (10^6 cells per assay) were collected in 10 µl of PBS, and 1 µl was deposited on the MALDI target. Representative MALDI-TOF MS spectra are shown for A, freshly isolated and B, frozen monocytes.
doi:10.1371/journal.pone.0013691.g001

after treatment of these spectra (smoothing and subtraction of background noise) by the FlexAnalysis software. For a given spectrum, only the weight values with a gap strictly greater than 3 were selected; for spectra of different cell types, the gap must be greater than or equal to 3. The m/z values of peaks from given spectra were transferred into an Excel file with a value of +1. The value of −1 was assigned to m/z positions without a peak, and conventional color code was applied to hierarchical clustering representation.

Results

MALDI-TOF MS analysis of monocytes

In the first series of experiments, the MALDI-TOF MS signature of monocytes isolated with CD14 microbeads was analyzed. When 10^6 monocytes per assay were used, several peaks with different intensities were detected (Fig. 1A), whereas no peak was observed in the control matrix (supplementary Fig. S1A). A major peak was observed at 4964 m/z, and several minor peaks were detected between 2,000 and 15,000 m/z. Note that the software identified more than 100 peaks per spectrum. In a second series of experiments, monocytes were either frozen at −80°C for two days, lysed using a lysis buffer or sonicated. The freezing procedure did not alter the monocyte signature (Fig. 1B). In contrast, when the monocytes were lysed, diffuse spectra were obtained (supplementary Fig. S1B). When the monocytes were sonicated, the spectra showed peaks that did not correspond to those observed with viable monocytes (supplementary Fig. S1C). Consequently, only frozen samples were used in subsequent experiments.

The effect of monocyte concentration on the presence and positions of peaks was then assessed. Increasing the initial cell concentration (10^6 cells) by 5- or 10-fold did not modify the position or the intensity of detected peaks, but it did increase the background. Using 10^5 monocytes was insufficient to detect the full range of peaks that were detected with 5×10^5 or 10^6 monocytes. As a consequence, further experiments were performed using 10^6 frozen cells per assay. Taken together, these results showed that monocyte freezing was a very simple method that permitted delayed handling of samples.

MS analysis of circulating cells

We then compared the profiles of circulating cells isolated from a healthy blood donor. The MALDI-TOF MS signature of T lymphocytes was distinct from that of monocytes (compare Fig. 2A with Fig. 1B). The gel view representation created by the ClinProTools version 2.2 software allowed the comparison of individual spectra (Fig. 3). Peaks at 5418, 6577, 7345 and 10.836 m/z were present in monocytes but not in T lymphocytes. Conversely, a peak at 8412 m/z present in T lymphocytes was lacking in monocytes. Some peaks were common to both monocytes and T lymphocytes (e.g., the peak at 11360 m/z). Similarly, the MALDI-TOF MS spectrum of PMNs (Fig. 2B) differed from those of both monocytes and T lymphocytes. Indeed, the intensity (see the peak at 3445 m/z) and presence (see the peak at 4329 m/z) of certain peaks distinguished PMNs from both monocytes and T lymphocytes. Finally, the MALDI-TOF MS spectrum of RBCs (Fig. 2C) differed dramatically from those of monocytes, T lymphocytes and PMNs. First, the intensity of the detected peaks was lower by 1000-fold in RBCs. Second, the great

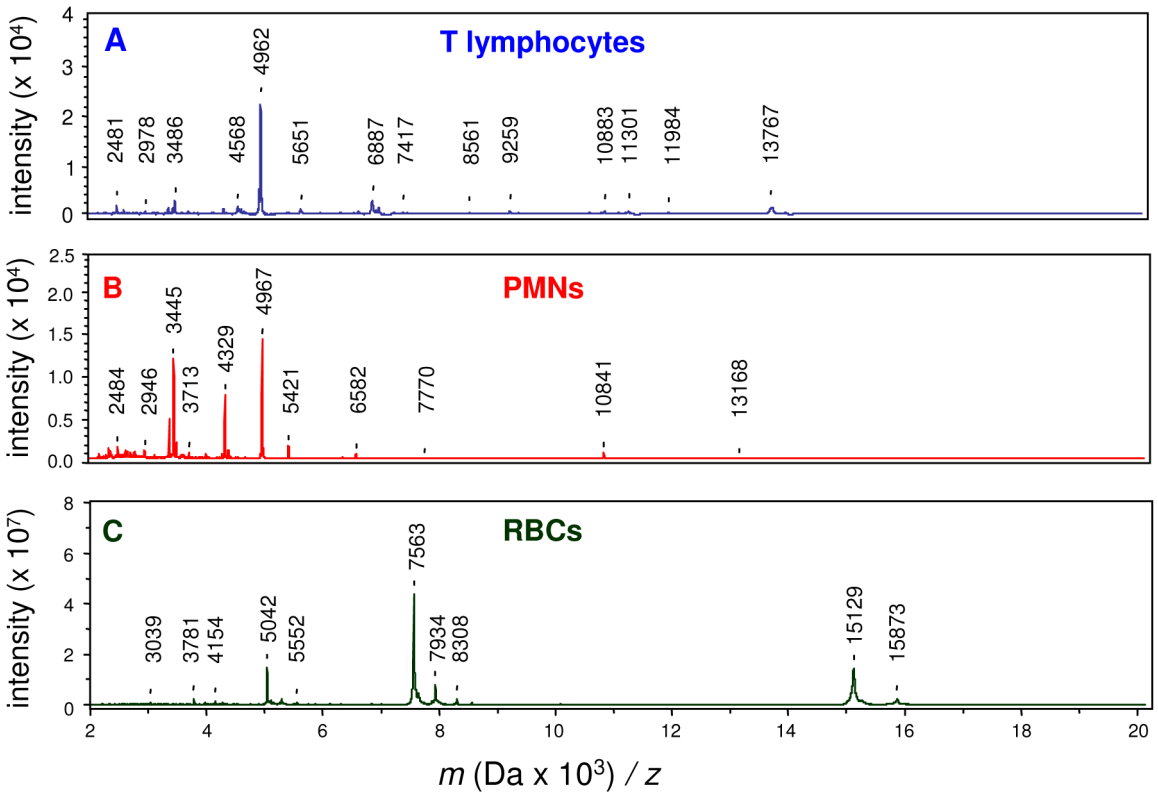

Figure 2. MALDI-TOF MS spectra of circulating cells. T lymphocytes (A), PMNs (B) and RBCs (C) were isolated from a healthy blood donor. Representative MALDI-TOF MS spectra are shown.
doi:10.1371/journal.pone.0013691.g002

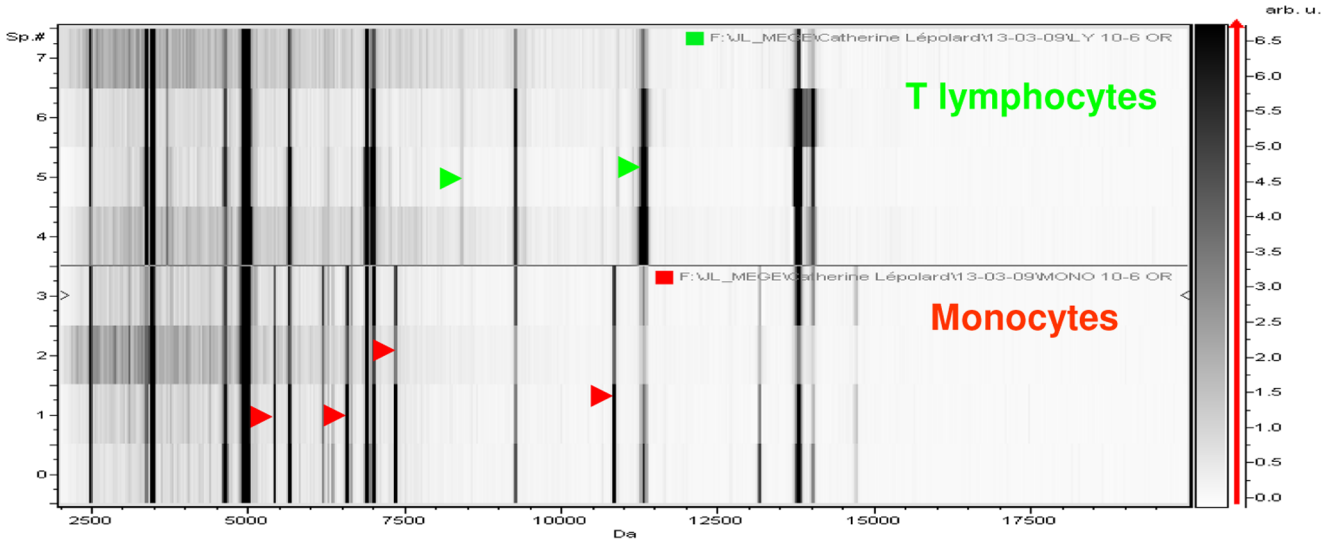

Figure 3. Gel view representation of monocytes and T lymphocytes. Monocytes and T lymphocytes were isolated from a healthy blood donor. MALDI-TOF MS spectra were analyzed using the ClinProTools software, and the spectra are presented in Gel View representation. Representative spectra are shown with *m/z* values on the x-axis and the peak intensity (in arbitrary units) on the y-axis. Major differences between monocytes and T lymphocytes are indicated by arrowheads.
doi:10.1371/journal.pone.0013691.g003

majority of peaks (see, for example, the peaks at 5042, 7563, 11129 and 15873 *m/z*) were present only in RBCs, whereas other peaks common to monocytes, T lymphocytes and PMNs, such as the peaks at 2484, 4964 m/z, were lacking in RBCs.

The reproducibility of the signatures of monocytes, T lymphocytes and PMNs was tested using ten different donors. The 2D representation provided by the ClinProTools version 2.2 software illustrates the differences between monocytes, T lymphocytes and PMNs, and it shows that their signatures are remarkably homogenous (Fig. 4). The MALDI-TOF MS data was then clustered hierarchically using the MeV software. The presence of peaks is represented in red (Fig. 5). Clearly, RBCs did not cluster with the other circulating cells. Monocytes clustered with PMNs while T lymphocytes were nearer to monocytes than PMNs. These results suggest that MALDI-TOF MS profiles of circulating cells are reproducible and specific.

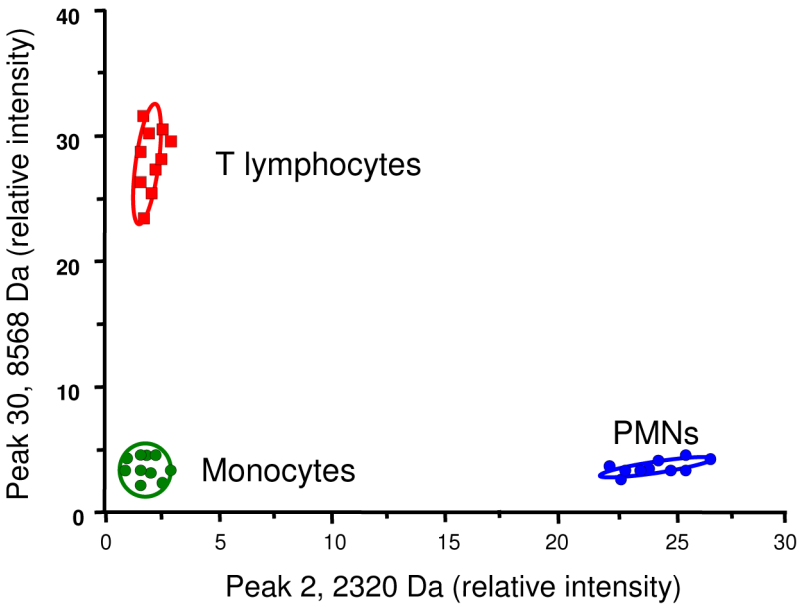

Figure 4. Reproducibility of MALDI-TOF MS signatures. Monocytes (in green), T lymphocytes (in red) and PMNs (in blue) were isolated from ten healthy blood donors. MALDI-TOF MS spectra were analyzed using the ClinProTools software and 2D Peak Distribution View. The relative intensities of the two peaks automatically selected were homogenous among blood donors, and the ellipses represent the standard deviation within each cell population (monocytes, T lymphocytes and PMNs, respectively).
doi:10.1371/journal.pone.0013691.g004

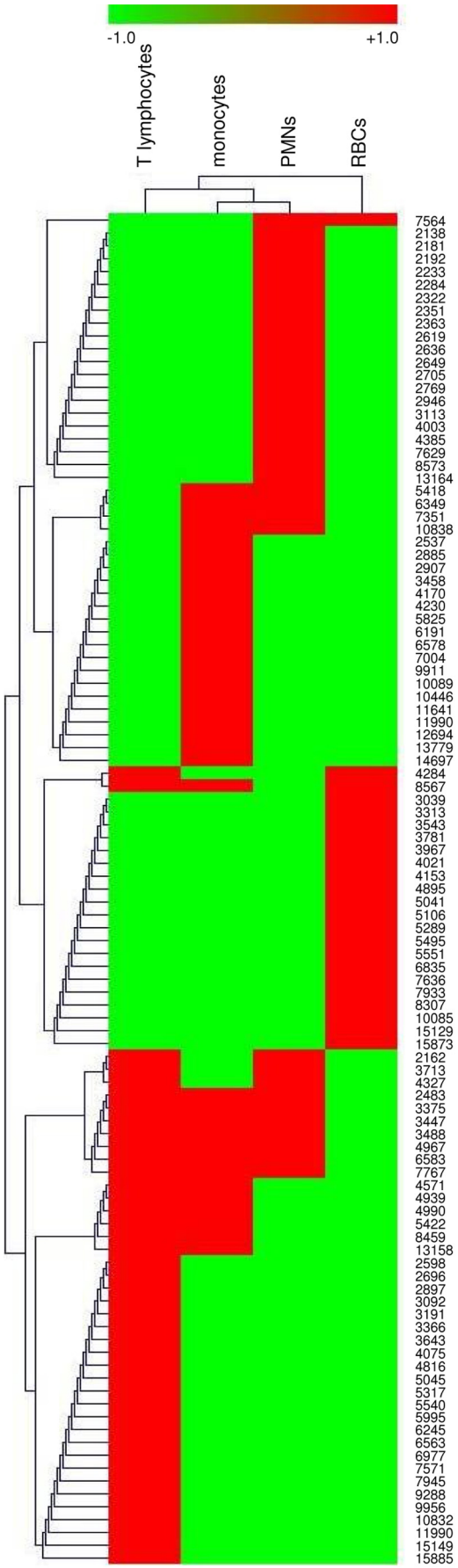

Figure 5. Hierarchical clustering of circulating cells. Monocytes, T lymphocytes, PMNs and RBCs were isolated from a healthy blood donor. MALDI-TOF MS spectra were analyzed using MeV software. A conventional value of +1 was assigned to the m/z values of spectra (in red) and −1 to m/z positions without peaks (in green).
doi:10.1371/journal.pone.0013691.g005

Development of a cell database

Because MALDI-TOF MS profiles seemed to be specific for different types of circulating cells, we created a cell database using the BioTyper version 2.0 software. We included primary myeloid cells such as human MDMs and murine BMDMs in the database. We also included human THP-1 myelomonocytic cells and the murine J774 and canine DH82 macrophage cell lines. Because circulating monocytes differentiate into MDMs or DCs depending on culture conditions, we also assessed the ability of MALDI-TOF MS to discriminate between MDMs, monocyte-derived DCs, and circulating monocytes. Similarly, circulating CD3 T cells were compared to a human CCR5-transfected leukemia cell line. We also analyzed one fibroblast-like cell line, murine L929 cells, and two epithelial cell lines, consisting of human HeLa and 293T cells. Additionally, we compared human placenta trophoblasts with the human BeWo and JEG trophoblast cell lines. Finally, we selected non-mammalian cells such as a *Xenopus* cell line and different types of amoebae for analysis.

The mean spectra of the 22 different cell types were introduced into the database, allowing for an accurate comparison. The cell database was then used to classify and clusterize the various primary cells and cell lines (Fig. 6). Two major clusters were found. The first one contained an invertebrate cell line, several amoebae and (surprisingly) human RBCs. The second cluster included mammalian immune cells and cell types. Among this latter cluster, several branches were identified. The branch that included circulating immune cells could be divided into three specific branches: T lymphocytes, monocytes and PMNs. It is noteworthy that monocyte-derived macrophages and DCs were present in distinct branches, along with several macrophage cell lines (J774, DH82, THP-1) and a T cell line (C8166 cells). Two trophoblast cell lines (i.e., JEG and BeWo cells) clustered together but were distant from primary trophoblasts. Epithelial cells also clustered together (HeLa and 293T cells). Finally, non-immune cell lines including epithelial, fibroblastic and trophoblast cells were located in a branch distinct from immune cells. These results show that MS profiles discriminated immune cells from other eukaryotic cells, and it positioned circulating immune cells (monocytes, T lymphocytes and PMNs) distantly from other immune cells.

An MS database as a tool for cell identification

We tested the efficiency of the database in three different ways. First, we compared a new monocyte sample with the mean spectrum of monocytes generated within the database (Fig. 7). The resulting score of 2.65 was highly significant and authenticated the tested cell population as monocytes. Second, we determined whether it is possible to identify cell populations within a cell mixture. Circulating monocytes and T lymphocytes (10^6 each cell type) were mixed and the spectra obtained were compared to the database. Monocytes and T lymphocytes were respectively identified with a correct score of 2.25 for both monocytes and T lymphocytes. Third, the MALDI-TOF MS profile of PBMCs was analyzed according to the same procedure. Although the proportion of monocytes was small compared to T lymphocytes (about 1/7), we identified both T lymphocytes (with a score of 2.22) and monocytes (with a score of 2.21). Taken together, these results demonstrate that we were able to identify monocytes and T lymphocytes in a complex

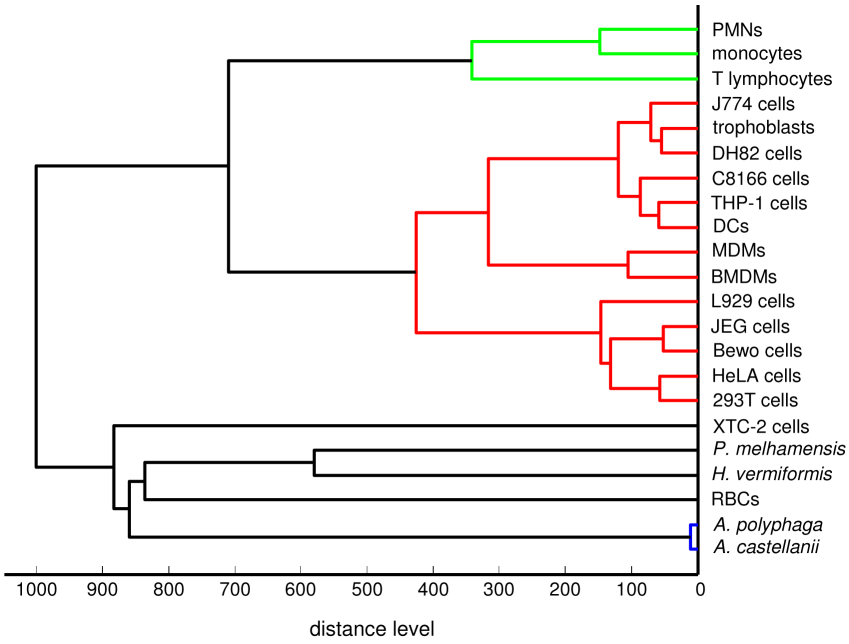

Figure 6. Dendrogram of 22 eukaryotic cell types. MALDI-TOF MS was performed on 22 cell types with at least 20 spectra per cell type. An averaged spectrum for each cell type was added to the database using the BioTyper software and the dendrogram creation method.
doi:10.1371/journal.pone.0013691.g006

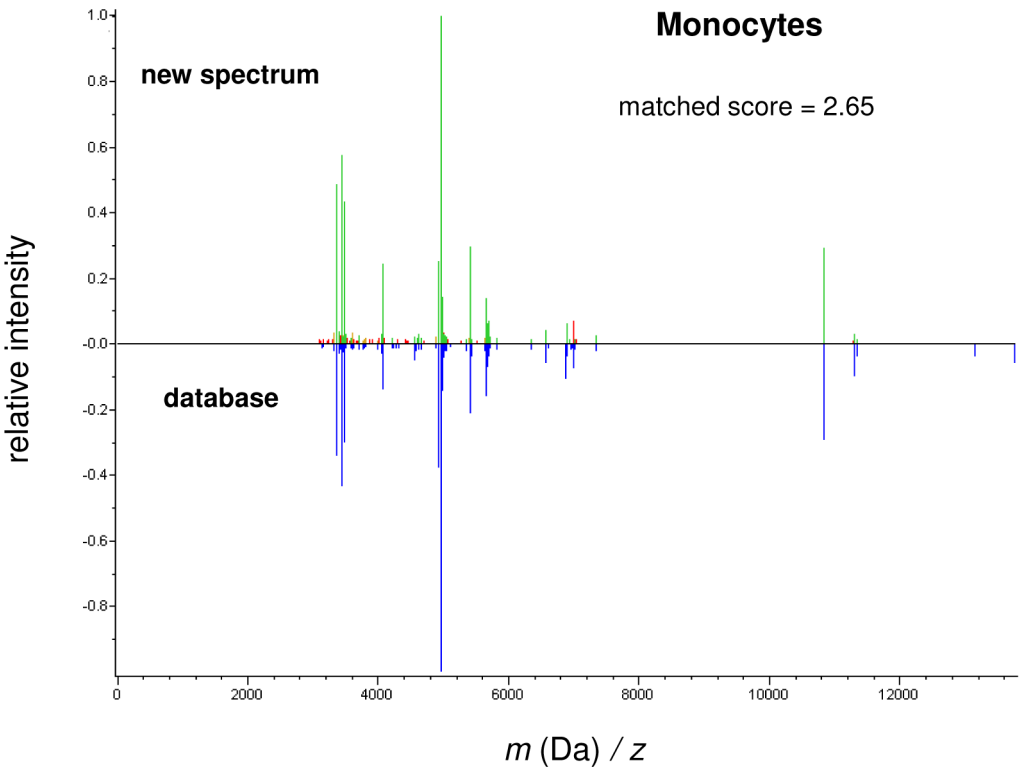

Figure 7. Efficiency of the database. A MALDI-TOF MS spectrum of unknown cells (here, monocytes from a blood donor) was compared to the averaged spectrum of monocytes generated from the database using the BioTyper software. The score indicates the identification of the tested cell population as monocytes.
doi:10.1371/journal.pone.0013691.g007

mixture, and they suggest that MALDI-TOF MS allows the confident identification of cell subsets in tissues.

Discussion

In this report, we showed that a MALDI-TOF MS approach was able to identify intact immune cells. This method was rapid and easy to perform and did not require any additional components (such as specific antibodies), in contrast to flow cytometry. In addition, the repertoire of analyzed molecules is different between MALDI-TOF MS and flow cytometry because MALDI-TOF MS is applicable to soluble molecules with a molecular weight ranging from 2 to 20 kDa, whereas flow cytometry detects surface markers or intracellular proteins through permeabilization procedures. Our MALDI-TOF MS approach extended to eukaryotic cells an approach previously used for bacterial identification [12–17,28]. In this study, intact primary or cultured cells were washed in saline to eliminate contamination by components such as cytokines or albumin contained in FCS, and thawed samples were deposited on the MALDI target in which HCCA matrix was added. Clearly, spectra were constituted by a collection of peaks, and their masses and relative intensities varied according cell origin. Other attempts have been performed to analyze MALDI-TOF MS profiles of whole eukaryotic cells. A recent report shows that MALDI-TOF MS typing is efficient to characterize 66 cell culture samples representing 34 species from insects to primates. Spectra of each cell type were composed of a variety of peaks with different masses and intensities, demonstrating the feasibility of our approach. However, as cell samples are treated by ethanol and formic acid/acetonitrile before assay [19], the two methods are not superimposable. Another report describes MALDI-TOF MS spectra from K562, BHK21 and GM15226 cell lines after lysis in 2,5-dihydroxybenzoic acid matrix solution. Again, obtained spectra show common peaks among the three cell types and specific peaks [18], demonstrating that MALDI-TOF MS performed on crude extracts of mammalian cell types may be useful to easily identify different cell types. In addition, we demonstrated that freezing cells at $-80^{\circ}C$ was sufficient to obtain high quality spectra, whereas cell lysis increased background noise in a non-interpretable way. Cell sonication led to spectra that were non-reproducible and peaks that were not entirely superimposable with those found in viable and frozen cells. The cell concentrations used to obtain significant spectra were relatively high, but were still less than those required for transcriptomics, another type of global method. In a prior study employing MALDI-TOF MS to analyze human macrophages, the extraction of membrane proteins requires specific protocols and a large quantity of cells [4].

We demonstrated that the spectra of immune cells were specific since they were markedly distinct from those of unrelated cell lines and differed between related immune cells. This specificity was supported by a set of peaks that represent the MS signature of each cell type. In addition, this study enabled us to develop a cell database comprised of 22 cell types representing diverse lineages of eukaryotic cells [29]. The database relies on the creation of a specific reference spectrum for each cell type and a score that validates the identification. These data have two major applications: first the establishment of a dendrogram of eukaryotic cells, and second, the analysis of mixed cell populations. The dendrogram revealed two major branches: one cluster of insect cells, amoebas and RBCs, and another cluster with immune cells and cell lines. Among the circulating leukocytes, the distance was smaller between monocytes and T lymphocytes, which are functionally distinct, than between monocytes and PMNs, although both are phagocytic cells. Monocytes, T lymphocytes and PMNs were in branches distinct from tissue immune cells such as macrophages and DCs. The divergence between monocytes and MDMs is consistent with previous transcriptomic studies in which each cell type had a specific program [30]. In addition, maturation from monocytes is a common feature of MDMs and DCs, and this accounts for the clustering of these two cell types. MDMs and DCs remained markedly distant in the dendrogram, which underlines their functional divergence. Interestingly, the clustering between cell types seemed independent of species origin. Indeed, human MDMs and murine BMDMs were close in the dendrogram. Similarly, the distance between the human THP-1, murine J774 and canine DH82 monocytic cells was low. We found that the position of primary trophoblasts was surprising: close to macrophage cell lines and distant from trophoblast cell lines (JEG and BeWo cells).

The use of the database enabled us to identify different cell populations among cell mixtures. The common signature of monocytes among individual donors was robust. Additionally, monocytes and T lymphocytes were accurately identified when they were mixed. Furthermore, the specific signatures of monocytes and T lymphocytes were found when PBMCs were studied. We suggest that the MALDI-TOF MS approach can be used to identify different cell types among tissue infiltrates. In addition, it is likely that its discriminative power is similar to that of genomic [29], proteomic and transcriptomic approaches [30]. Recent proteomic and transcriptomic approaches allow the discrimination between $CD14^{+}CD16^{-}$ and $CD14^{+}CD16^{+}$ monocyte subsets. Similarly, we preliminarily found that the activation of monocytes and macrophages resulted in specific spectra that correlated with their transcriptomic patterns (manuscript in preparation).

In conclusion, we developed a new method for identifying immune cells based on a MALDI-TOF MS approach. A major advantage of this method compared to the usual techniques is the lack of purification steps and staining procedures, which often lead to cell activation. The cell database we constructed was useful for identifying a cell type within a cell mixture, and it could potentially be used to identify different functional states of a cell population such as monocytes or macrophages.

Supporting Information

Figure S1 MALDI-TOF MS spectra of monocyte preparations. Human monocytes (106 cells per assay) were collected in 10 µl of PBS, and 1 µl was deposited on the MALDI target. Representative MALDI-TOF MS spectra are shown: A, in the absence of monocytes; B, lysed monocytes; C, sonicated monocytes.
Found at: doi:10.1371/journal.pone.0013691.s001 (0.30 MB TIF)

Acknowledgments

The authors are grateful to Pr B. La Scola for providing amoebae, and to Philippe Decolpman and Carine Couderc for helpful assistance with MALDI-TOF MS.

Author Contributions

Conceived and designed the experiments: CC DR JLM. Performed the experiments: RO CF ABA. Analyzed the data: RO CF ABA CC DR JLM. Contributed reagents/materials/analysis tools: RO CF ABA. Wrote the paper: CC DR JLM.

References

1. Palmer C, Diehn M, Alizadeh AA, Brown PO (2006) Cell-type specific gene expression profiles of leukocytes in human peripheral blood. BMC Genomics 7: 115.
2. Lehtonen A, Ahlfors H, Veckman V, Miettinen M, Lahesmaa R, et al. (2007) Gene expression profiling during differentiation of human monocytes to macrophages or dendritic cells. J Leukoc Biol 82: 710–720.
3. Consortium, C. H. L. P. P. (2010) First insight into the human liver proteome from PROTEOME(SKY)-LIVER(Hu) 1.0, a Publicly available database. J Proteome Res 9: 79–94.
4. Dupont A, Tokarski C, Dekeyzer O, Guihot AL, et al. (2004) Two-dimensional maps and databases of the human macrophage proteome and secretome. Proteomics 2004 4: 1761–1778.
5. Srisomsap C, Sawangareetrakul P, Subhasitanont P, Panichakul T, Keeratichamroen S, et al. (2004) Proteomic analysis of cholangiocarcinoma cell line. Proteomics 4: 1135–1144.
6. Horlock C, Shakib F, Mahdavi J, Jones NS, Sewell HF, et al. (2007) Analysis of proteomic profiles and functional properties of human peripheral blood myeloid dendritic cells, monocyte-derived dendritic cells and the dendritic cell-like KG-1 cells reveals distinct characteristics. Genome Biol 8: R30.
7. Robertson JW, Rodrigues CG, Stanford VM, Rubinson KA, Krasilnikov OV, et al. (2007) Single-molecule mass spectrometry in solution using a solitary nanopore. Proc Natl Acad Sci U S A 104: 8207–8211.
8. Johnson RP, El-Yazbi AF, Hughes MF, Schriemer DC, Walsh EJ, et al. (2009) Identification and functional characterization of protein kinase A-catalyzed phosphorylation of potassium channel Kv1.2 at serine 449. J Biol Chem 284: 16562–16574.
9. Li X, Cowles EA, Cowles RS, Gaugler R, Cox-Foster DL (2009) Characterization of immunosuppressive surface coat proteins from *Steinernema glaseri* that selectively kill blood cells in susceptible hosts. Mol Biochem Parasitol 165: 162–169.
10. Mellmann A, Cloud J, Maier T, Keckevoet U, Ramminger I, et al. (2008) Evaluation of matrix-assisted laser desorption ionization-time-of-flight mass spectrometry in comparison to 16S rRNA gene sequencing for species identification of nonfermenting bacteria. J Clin Microbiol 46: 1946–1954.
11. Trost M, English L, Lemieux S, Courcelles M, Desjardins M, et al. (2009) The phagosomal proteome in interferon-γ-activated macrophages. Immunity 30: 143–154.
12. Lay JO, Jr., Holland RD (2000) Rapid identification of bacteria based on spectral patterns using MALDI-TOF MS. Methods Mol Biol 146: 461–487.
13. Seng P, Drancourt M, Gouriet F, La Scola B, Fournier PE, et al. (2009) Ongoing revolution in bacteriology: routine identification of bacteria by matrix-assisted laser desorption ionization time-of-flight mass spectrometry. Clin Infect Dis 49: 543–551.
14. Dieckmann R, Helmuth R, Erhard M, Malorny B (2008) Rapid classification and identification of salmonellae at the species and subspecies levels by whole-cell matrix-assisted laser desorption ionization-time of flight mass spectrometry. Appl Environ Microbiol 74: 7767–7778.
15. Petersen CE, Valentine NB, Wahl KL (2009) Characterization of microorganisms by MALDI mass spectrometry. Methods Mol Biol 492: 367–379.
16. Majcherczyk PA, McKenna T, Moreillon P, Vaudaux P (2006) The discriminatory power of MALDI-TOF mass spectrometry to differentiate between isogenic teicoplanin-susceptible and teicoplanin-resistant strains of methicillin-resistant *Staphylococcus aureus*. FEMS Microbiol Lett 255: 233–239.
17. Degand N, Carbonnelle E, Dauphin B, Beretti JL, Le Bourgeois M, et al. (2008) Matrix-assisted laser desorption ionization-time of flight mass spectrometry for identification of nonfermenting gram-negative bacilli isolated from cystic fibrosis patients. J Clin Microbiol 46: 3361–3367.
18. Zhang X, Scalf M, Berggren TW, Westphall, Smith LM (2006) Identification of mammalian cell lines using MALDI-TOF and LC-ESI-MS/MS mass spectrometry. J Am Soc Mass Spectrom 17: 490–499.
19. Karger A, Bettin B, Lenk M, Mettenleiter TC (2010) Rapid characterisation of cell cultures by matrix-assisted laser desorption/ionisation mass spectrometric typing. J Virol Methods 164: 116–121.
20. Benoit M, Ghigo E, Capo C, Raoult D, Mege JL (2008) The uptake of apoptotic cells drives *Coxiella burnetii* replication and macrophage polarization: a model for Q fever endocarditis. PLoS Pathog 4: e1000066.
21. Desnues B, Raoult D, Mege JL (2005) IL-16 is critical for *Tropheryma whipplei* replication in Whipple's disease. J Immunol 175: 4575–4582.
22. Lepidi H, Benoliel AM, Mege JL, Bongrand P, Capo C (1992) Double localization of F-actin in chemoattractant-stimulated polymorphonuclear leucocytes. J Cell Sci 103: 145–156.
23. Kliman HJ, Nestler JE, Sermasi E, Sanger JM, Strauss JF, 3rd (1986) Purification, characterization, and in vitro differentiation of cytotrophoblasts from human term placentae. Endocrinology 118: 1567–1582.
24. Meghari S, Bechah Y, Capo C, Lepidi H, Raoult D, et al. (2008) Persistent *Coxiella burnetii* infection in mice overexpressing IL-10: an efficient model for chronic Q fever pathogenesis. PLoS Pathog 4: e23.
25. Fouchier RA, Meyer BE, Simon JH, Fischer U, Malim MH (1997) HIV-1 infection of non-dividing cells: evidence that the amino-terminal basic region of the viral matrix protein is important for Gag processing but not for post-entry nuclear import. EMBO J 16: 4531–4539.
26. Drancourt M, Jarlier V, Raoult D (2002) The environmental pathogen *Mycobacterium ulcerans* grows in amphibian cells at low temperatures. Appl Environ Microbiol 68: 6403–6404.
27. Greub G, Raoult D (2002) Crescent bodies of *Parachlamydia acanthamoeba* and its life cycle within *Acanthamoeba polyphaga*: an electron micrograph study. Appl Environ Microbiol 68: 3076–3084.
28. Fournier PE, Couderc C, Buffet S, Flaudrops C, Raoult D (2009) Rapid and cost-effective identification of *Bartonella* species using mass spectrometry. J Med Microbiol 58: 1154–1159.
29. Hartman H, Fedorov A (2002) The origin of the eukaryotic cell: a genomic investigation. Proc Natl Acad Sci U S A 99: 1420–1425.
30. Zhao C, Zhang H, Wong WC, Sem X, Han H, et al. (2009) Identification of novel functional differences in monocyte subsets using proteomic and transcriptomic methods. J Proteome Res 8: 4028–4038.

Résumé

La fièvre Q se traduit par de graves conséquences obstétricales chez la femme enceinte. La voie principale de la contamination humaine par *Coxiella burnetii*, l'agent de la fièvre Q, est constituée des aérosols provenant des placentas d'animaux infectés. La nature des cellules placentaires cibles de *C. burnetii* reste totalement inconnue. J'ai montré que *C. burnetii* infecte les trophoblastes des lignées BeWo et JEG et que les bactéries se répliquent fortement dans les cellules BeWo et survivent dans les cellules JEG. Une analyse par microarray montre que *C. burnetii* induit une réponse inflammatoire dans les cellules BeWo qui lui est spécifique. Ces résultats suggèrent que les trophoblastes pourraient constituer une niche pour *C. burnetii*. Les macrophages placentaires pourraient également servir de réservoir pour *C. burnetii*. J'ai montré que les macrophages placentaires $CD14^+$ sont des macrophages qui présentent des caractéristiques phénotypiques, transcriptionnelles et fonctionnelles différentes de celles des monocytes circulants et des macrophages dérivés de monocytes. Ils forment en outre des cellules géantes multinucléées qui pourraient réguler l'activité cytolytique des macrophages dans le contexte placentaire puisque les macrophages placentaires $CD14^+$ ne sont ni de type M1 ni de type M2. Si la polarisation des macrophages est établie, il n'en est pas de même pour les monocytes. Nous avons activé les monocytes par des cytokines connues pour induire respectivement une réponse M1 et M2 et étudié leur réponse par microarray: la réponse précoce, 6 heures, des monocytes correspond à une réponse de type M1/M2 mais la réponse tardive, 18 heures, n'est pas de type M1/M2, ce qui montre un nouveau degré d'hétérogénéité des cellules myéloïdes. L'endocardite est la principale manifestation clinique de la fièvre Q chronique mais l'endocardite à *C. burnetii* ne représente qu'une faible proportion des endocardites infectieuses. Il n'existe pas de marqueurs satisfaisants de pronostic des endocardites infectieuses. C'est la raison pour laquelle nous avons étudié le profil transcriptionnel périphérique des patients atteints d'une endocardite infectieuse. Nous avons montré que S100A11 constitue un marqueur de diagnostic et l'aquaporine 9 un marqueur de pronostic des endocardites infectieuses.

Mots-clés : macrophages, fièvre Q, *C. burnetii*, trophoblastes, microarray

Abstract

In pregnant women Q fever presents obstetrical complications. The principal way of human contamination by *Coxiella burnetii*, the agent of Q fever, is due to aerosols from placentas of infected animals. The nature of placenta cells that are targeted by *C. burnetii* remains unknown. I showed that *C. burnetii* infects BeWo and JEG trophoblastic cells and that organisms intensively replicated in BeWo cells and survived in JEG cells. A microarray analysis showed that *C. burnetii* induced a specific inflammatory response in BeWo cells. These results suggest that trophoblasts may serve as a reservoir for *C. burnetii*. Placenta macrophages placentaires may also targeted by *C. burnetii*. I showed that placenta $CD14^+$ macrophages were characterized by phenotypic, transcriptional and functional properties different from those of circulating monocytes and monocyte-derived macrophages. In addition, placenta $CD14^+$ macrophages differentiate into multinucleated giant cells that may regulate the cytolytic activity of macrophages in the placenta context since placenta $CD14^+$ macrophages were not polarized in M1 or M2 macrophages. While M1/M2 polarization of macrophages is well established, that of monocytes remains an important question. We activated monocytes with canonical agonists of M1 and M2 profiles in macrophages using microarrays. The early response, 6 hours, of monocytes corresponded to a type M1/M2 response but the delayed response, 18 hours, did not correspond to the M1/M2 dichotomy, demonstrating a new level of heterogeneity of myeloid cells. Endocarditis is the main clinical manifestation of chronic Q fever but *C. burnetii* endocarditis represents a small proportion of infective endocarditis. To date there is no robust biomarkers of pronostic of infective endocarditis. We studied the peripheral transcriptional profiles of patients with infective endocarditis. We proposed S100A11 as a diagnostic marker and aquaporine 9 as a pronostic marker of infective endocarditis.

Mots-clés : macrophages, Q fever, *C. burnetii*, trophoblasts, microarray